

Winter 2003

Chemical sensors based on swellable molecularly imprinted polymer microspheres in a hydrogel

Wenzhe Fan

University of New Hampshire, Durham

Follow this and additional works at: <https://scholars.unh.edu/dissertation>

Recommended Citation

Fan, Wenzhe, "Chemical sensors based on swellable molecularly imprinted polymer microspheres in a hydrogel" (2003). *Doctoral Dissertations*. 191.

<https://scholars.unh.edu/dissertation/191>

This Dissertation is brought to you for free and open access by the Student Scholarship at University of New Hampshire Scholars' Repository. It has been accepted for inclusion in Doctoral Dissertations by an authorized administrator of University of New Hampshire Scholars' Repository. For more information, please contact nicole.hentz@unh.edu.

**CHEMICAL SENSORS BASED ON SWELLABLE MOLECULARLY
IMPRINTED POLYMER MICROSPHERES IN A HYDROGEL**

By

WENZHE FAN

B.S., Shaanxi Normal University, P. R. China, 1990

M.S., Shaanxi Normal University, P. R. China, 1993

DISSERTATION

Submitted to the University of New Hampshire
in Partial Fulfillment of
the Requirements for the Degree of

Doctor of Philosophy

in

Chemistry

December, 2003

UMI Number: 3111504

INFORMATION TO USERS

The quality of this reproduction is dependent upon the quality of the copy submitted. Broken or indistinct print, colored or poor quality illustrations and photographs, print bleed-through, substandard margins, and improper alignment can adversely affect reproduction.

In the unlikely event that the author did not send a complete manuscript and there are missing pages, these will be noted. Also, if unauthorized copyright material had to be removed, a note will indicate the deletion.

UMI[®]


UMI Microform 3111504

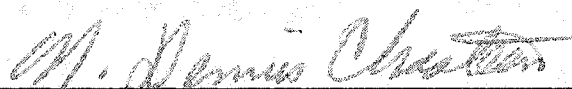
Copyright 2004 by ProQuest Information and Learning Company.

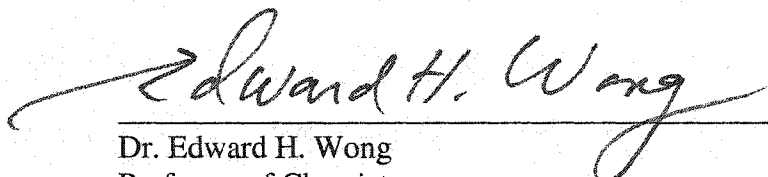
All rights reserved. This microform edition is protected against unauthorized copying under Title 17, United States Code.


ProQuest Information and Learning Company
300 North Zeeb Road
P.O. Box 1346
Ann Arbor, MI 48106-1346

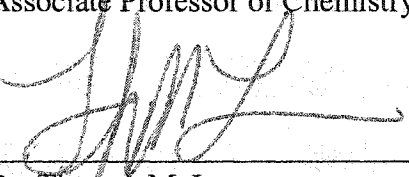
This dissertation has been examined and approved.



Dissertation Director, Dr. W. Rudolf Seitz
Professor of Chemistry


Dr. N. Dennis Chasteen
Professor of Chemistry


Dr. Edward H. Wong
Professor of Chemistry


Dr. Roy P. Planalp
Associate Professor of Chemistry


Dr. Thomas M. Laue
Professor of Biochemistry & Molecular Biology


Date

DEDICATION

This dissertation is dedicated
to my parents, Huqian Fan and Guaifeng Qu,
My brother, Wenxin Fan and my sister, Zijuan Fan,
and especially to my wife, Jie Li,
for their love, support and encouragement.

ACKNOWLEDGMENTS

First, I would like to express my sincere gratitude to my research advisor, Professor W. Rudolf Seitz, for all of the support, encouragement and guidance over my five years.

I also wish to thank my committee members and all other faculty members for their time, assistance, and encouragement.

I want to thank Nancy Cherim, UNH Instrument Center, for her help with Scanning Electron Microscopy.

I thank Dr. Barry Lavine of Clarkson University for his support and guidance during his sabbatical at the University of New Hampshire.

Many thanks to Cindi Rohwer, Peggy Torch, Amy Lindsay, Kathy Gallagher, Sabrina Kirwan, Bob Constantine for their help and friendship.

Thanks to my graduate fellows, past and present, and my friends at UNH for their help and making my stay enjoyable.

Finally, a special thank to my wife for her love, encouragement, and support.

TABLE OF CONTENTS

DEDICATION	iii
ACKNOWLEDGMENTS	iv
LIST OF TABLES	viii
LIST OF FIGURES	ix
ABSTRACT	xvi
CHAPTER	Page
1 INTRODUCTION	1
1.1 Background of Chemical Sensors	1
1.2 Classification of Chemical Sensors	4
1.3 Chemical sensors based on swellable polymer microspheres	12
1.4 Chemical sensors based on molecularly imprinted polymers	16
1.5 Summary of this dissertation research	23
2 THEORY	25
2.1 Polymer Background	25
2.2 Free Radical Polymerization	30
2.3 Suspension Polymerization	31
2.4 Dispersion Polymerization	33
2.5 Theory of Polymer Swelling	38
2.6 Swelling Behavior of Thermosensitive Poly N-Isopropylacrylamide Polymers	41
2.7 Optical Measurements of Microspheres Embedded in Hydrogel Membranes	44
2.8 Molecularly Imprinted Polymers	46
3 EXPERIMENTAL	54
3.1 Reagents	54
3.2 Apparatus	58
3.3 Procedures	58
3.4 Characterization	70
4 PRELIMINARY DATA AND PREPARATION OF SWELLABLE MOLECULAR IMPRINTED POLYMER PARTICLES FOR CHEMICAL	75

SENSING	
4.1 Introduction	75
4.2 Molecular Specific Swelling of Molecular Imprinted Polymer	76
4.3 Sensor Design Based on Swellable MIP Microspheres in a Hydrogel	82
4.4 Preparation of Swellable MIP Particles Using Suspension Polymerization	84
4.5 Preparation of Swellable MIP Microspheres Using Dispersion Polymerization	96
4.6 Conclusion	97
5 HYDROGEL MEMBRANES CONTAINING SUSPENSION POLYMERIZED MOLECULARLY IMPRINTED POLYMER PARTICLES FOR NOREPHEDRINE SENSING	104
5.1 Introduction	104
5.2 Results and Discussion	108
5.2.1 Preparation of norephedrine imprinted poly NIPA-AAc particles	108
5.2.2 Turbidity of norephedrine imprinted poly NIPA-AAc particles in hydrogels	111
5.2.3 Turbidity changes as a function of temperature and phase transition	114
5.2.4 pH effect on turbidity measurements and transition temperature	117
5.2.5 Heating rate effect on transition temperature	120
5.2.6 Buffer composite effect on turbidity measurements and phase transition	120
5.2.7 Norephedrine measurements	123
5.2.8 Specificity	126
5.2.9 Response time and reversibility	127
5.2.10 Norephedrine response in buffer medium	127
5.3 Conclusion	130
6 HYDROGEL MEMBRANES CONTAINING SUSPENSION POLYMERIZED SWELLABLE MOLECULARLY IMPRINTED POLYMER MICROSPHERES FOR THEOPHYLLINE SENSING	132
6.1 Introduction	132
6.2 Results and Discussion	134
6.2.1 Preparation of theophylline templated poly NIPA-MAA microspheres	134
6.2.2 Effect of formulation variables on polymer properties	137
6.2.3 Effect of formulation variables on sensor response and specificity	145
6.2.4 THO response and selectivity of templated poly NIPA-MAA in water	147
6.2.5 pH effect on turbidity and transition of poly NIPA-MAA microspheres	154

6.2.6	Response and selectivity of poly NIPA-MAA in buffer	156
6.2.7	Varying the temperature transition	161
6.2.8	Response and specificity of poly NIPA-NTBA-MAA microspheres	167
6.2.9	THO Response and specificity of poly NNPA-MAA microspheres	175
6.3	Conclusion	187
7	PRILEMINARY EVALUATION OF POLY NIPA MICROSPHERES FOR TEMPERATURE SENSING	189
7.1	Introduction	189
7.2	Synthesis of Poly NIPA Microspheres by Dispersion Polymerization	191
7.3	pH Effect	194
7.4	Ionic Strength Effect	195
7.5	Thermal Response	196
7.6	Conclusion	198
8	CONCLUSIONS AND FUTURE WORK	199
8.1	Conclusions	199
8.2	Future Work	201
	LIST OF REFERENCES	202

LIST OF TABLES

	Page
Table 1-1 Comparison of natural biomolecules with MIPs	18
Table 2-1 Comparison of heterogeneous polymerization systems	31
Table 3-1 A typical formulation of synthesis of norephedrine templated	60
Table 3-2 Formulation for suspension polymerization of norephedrine templated poly NIPA-AAc MIP particles	63
Table 3-3 A typical formulation for dispersion polymerization for THO templated poly NIPA-MAA microspheres	65
Table 3-4 Recipe for preparation of poly NIPA thermosensitive microspheres	66
Table 3-5 Fractional Design for Reaction Variables for THO templated poly NIPA-MAA Dispersion Polymerization	74
Table 4-1 Surfactant effect on suspension polymerization	86
Table 4-2 The requirements of medium properties for SPG Emulsification	88
Table 4-3 Immiscibility of dioxane with salt solutions	91
Table 4-4 Compatibility of dispersion and continuous phase with SPG membranes	92
Table 4-5 Surfactant selection for oil phase or dioxane phase in SPG	93
Table 5-1 Surfactant effect on polymer size and distribution by suspension polymerization in perfluorocarbon in sonicator	109
Table 6-1 Results of Fractional Experiment for Reaction Variables	139
Table 6-2 Results of analysis of variance for turbidity contrast	139
Table 6-3 Effect of alkyl side group on transition temperature of N-alkylacrylamide hydrogel	162

LIST OF FIGURES

	Page
Figure 1-1 General model for chemical sensors, differentiating between recognition phase, transduction mode and data processing	2
Figure 1-2 Basic designs of FOCS: (a). direct spectroscopic sensors; (b). reagent-mediated sensors.	9
Figure 1-3 Two principle designs of reagent-mediated FOCS	11
Figure 1-4 Schematic of sensing response mechanism. Microspheres are diethanolamine-derivatized polystyrene.	14
Figure 1-5 A schematic representation of research area in MIP technology in 2002	17
Figure 1-6 Publications of MIPs in last decade	17
Figure 1-7 Publications of MIP-based sensors in the last decade	19
Figure 2-1 Presentation of copolymer types: (a) alternating, (b) random, (c) block, and (d) graft.	26
Figure 2-2 Schematic representation of different types of polymers. (a) linear, (b) branched, and (c) network	27
Figure 2-3 Free radical polymerization of VBC using benzoyl peroxide as initiator	29
Figure 2-4 Schematic of particle growth in dispersion polymerization. (a) Homogeneous polymer solution.	37
Figure 2-5 Publications of poly NIPA from Scifinder search results	43
Figure 2-6 Schematic representation of the molecular imprinting principle	47
Figure 2-7 Common functional monomers for MIP production	51

Figure 3-1	Structures of monomers, crosslinkers, initiators and polymers used for preparation of microspheres and hydrogel membranes	57
Figure 3-2	Polymerization reaction used to prepare MIPs selective for norephedrine	60
Figure 3-3	Structure of polymeric surfactant poly(acryloyl PFA-1) and the structure of acrylate precursors	61
Figure 3-4	The structure of PFPS and its precursor monomer	62
Figure 3-5	Polymerization reaction used to prepare MIPs selective for THO	65
Figure 3-6	Membrane holder for turbidity measurements	72
Figure 4-1	The swelling ratio (relative volume of gels, V/V_0) as a function of temperature for untemplated and templated gels in 0.1 M norephedrine solution	78
Figure 4-2	Structures of templates, norephedrine, adrenaline	79
Figure 4-3	The swelling ratio for norephedrine templated gels as a function of concentration of either norephedrine or adrenaline at 30 °C	80
Figure 4-4	The swelling ratio for norephedrine templated gels as a function of concentration of either norephedrine or adrenaline at 50 °C	80
Figure 4-5	Swelling ratio for norephedrine templated gels at different pH as a function of temperature	81
Figure 4-6	Model of chemical sensing based on swellable MIP microspheres in a hydrogel	83
Figure 4-7	SPG Membrane emulsification apparatus	87
Figure 4-8	Relationship between the applied pressure and droplet formation	89
Figure 4-9	Micrographs of norephedrine imprinted poly NIPA-AAc-MBA particles prepared by perfluorocarbon suspension polymerization in ultrasonic bath	95

Figure 4-10	Scanning electron micrographs of untemplated poly NIPA-MAA-TRIM (12%) microspheres prepared by dispersion polymerization	99
Figure 4-11	Scanning electron micrographs of theophylline templated poly NIPA-MAA-TRIM (12%) microspheres prepared by dispersion polymerization	100
Figure 4-12	Scanning electron micrographs of theophylline templated poly NIPA-MAA-TRIM (5%) microspheres prepared by dispersion polymerization	101
Figure 4-13	Scanning electron micrographs of theophylline templated poly NIPA-MAA-MBA (5%) microspheres prepared by dispersion polymerization	102
Figure 4-14	Microscope picture of untemplated poly NIPA-NTBA-MAA microspheres prepared by dispersion polymerization	103
Figure 5-1	Chemical structures of sympathomimetic drugs	106
Figure 5-2	Untemplated poly NIPA-AAc particles prepared by perfluorocarbon suspension polymerization	110
Figure 5-3	Turbidity spectra for norephedrine imprinted poly NIPA-AAc particles embedded in HYPAN membranes	112
Figure 5-4	Dependence of turbidity on particles concentration (w/w) in HYPAN membranes	113
Figure 5-5	Turbidity changes of poly NIIA-AAc particles embedded PVA membrane as a function of temperature and the determination of transition temperature	115
Figure 5-6	Comparison of swelling properties and transition temperatures of poly NIIA-AAc particle embedded in HYPAN80 and PVA membranes in water	116
Figure 5-7	Deprotonation of the poly NIPA-AAc particles	118
Figure 5-8	pH effect on turbidity of poly NIPA-AAc particles in a PVA membrane as a function of temperature	118

Figure 5-9	pH effect on turbidity of poly NIPA-AAc particles in a HYPAN80 membrane as a function of temperature	119
Figure 5-10	Heating rate effect on transition temperature of poly NIPA-AAc particles in a PVA membrane in pH 4.0 acetate buffer	121
Figure 5-11	Buffer composite effect on turbidity and transition temperature of poly NIPA-AAc particles in a PVA membrane at pH 4.0	122
Figure 5-12	Turbidity of norephedrine templated poly NIPA-AAc particles in PVA membrane as a function of temperature and concentration of norephedrine	124
Figure 5-13	Norephedrine (NE) response of templated poly NIPA-AAc particles in PVA membrane at 55C	125
Figure 5-14	Turbidity of untemplated poly NIPA-AAc particles in a PVA membrane as a function of temperature and concentration of norephedrine	126
Figure 5-15	Response vs. time for templated poly NIPA-AAc particles in a PVA membrane upon adding 1.0×10^{-6} M norephedrine at 50°C	128
Figure 5-16	Turbidity of norephedrine templated poly NIPA-AAc particles in a PVA membrane as a function of temperature and concentration of norephedrine in pH4.0	128
Figure 5-17	Turbidity vs. log norephedrine concentration for a PVA membrane containing templated poly NIPA-AAc microspheres at pH 4.0 and 45° C	129
Figure 6-1	The structure of theophylline and caffeine	134
Figure 6-2	Turbidity changes as a function of temperature of poly NIPA-MAA microspheres with 5% MBA or TRIM as a crosslinker	136
Figure 6-3	Turbidity change of poly NIPA-MAA formulation #7-12 as a function of temperature	140
Figure 6-4	The average effect on turbidity contrast upon changing the level of the main variables	141

Figure 6-5	The effect of the NIPA*MAA/THO interaction on turbidity contrast	144
Figure 6-6	The effect of the Crosslinker*MAA interaction on turbidity contrast	145
Figure 6-7	Turbidity of templated poly NIPA-MAA microspheres as a function of temperature and THO concentration	148~ 150
Figure 6-8	Turbidity of templated poly NIPA-MAA microspheres as a function of temperature and CAF concentration	151~ 153
Figure 6-9	Deprotonation of the poly NIPA-MAA microspheres	154
Figure 6-10	pH effect on transition temperature and turbidity change as a function of temperature	155
Figure 6-11	Turbidity of templated poly NIPA-MAA microspheres in a PVA membrane as function of temperature and pH in the presence of 1.0×10^{-3} M THO	157
Figure 6-12	Turbidity of templated poly NIPA-MAA microspheres as function of temperature and concentration of theophylline in pH 7.0 buffer	158
Figure 6-13	THO response of templated poly NIPA-MAA in pH 7.0 buffer at 37° C	158
Figure 6-14	Turbidity of untemplated poly NIPA-MAA microspheres as a function of temperature and concentration of theophylline in pH 7.0 buffer	159
Figure 6-15	Turbidity of THO templated poly NIPA-MAA microspheres as a function of temperature and concentration of caffeine in pH 7.0 buffer	160
Figure 6-16	Turbidity of poly NIPA-NTBA-MAA microspheres as a function of temperature and percentage of NTBA	163~ 165
Figure 6-17	Transition temperature of poly NIPA-NTBA-MAA microspheres as a function of percentage of NTBA	166
Figure 6-18	Micrograph and size distribution of untemplated poly NIPA-NTBA (30%)-MAA microspheres prepared by dispersion polymerization	168

Figure 6-19	Micrograph and size distribution of untemplated poly NIPA-NTBA(20%)-MAA microspheres prepared by dispersion polymerization.	169
Figure 6-20	Turbidity changes and phase transition of poly NIPA-NTBA-MAA microspheres containing different percentage of NTBA	170
Figure 6-21	Micrograph and size distribution of THO templated poly NIPA-NTBA-MAA microspheres prepared by dispersion polymerization	171
Figure 6-22	THO response of templated NIPA-NTBA-MAA microspheres in PVA membrane at 30° C	172
Figure 6-23	THO response of untemplated NIPA-NTBA-MAA microspheres in PVA membrane at 30° C	173
Figure 2-24	CAF response of THO templated NIPA-NTBA-MAA microspheres in PVA membrane at 30° C	173
Figure 6-25	Turbidity of templated poly NIPA-NTBA-MAA microspheres in PVA membrane as a function of temperature and pH	174
Figure 6-26	Micrograph and size distribution of untemplated poly NNPA-MAA microspheres prepared by dispersion polymerization	176
Figure 6-27	Micrograph and size distribution of templated poly NNPA-MAA microspheres prepared by dispersion polymerization	177
Figure 6-28	Phase transition of untemplated and templated poly NIPA-MAA microspheres as a function of temperature	178
Figure 6-29	Turbidity change of PVA membrane containing templated poly NNPA-MAA microspheres as a function of theophylline concentration at 25° C	180
Figure 6-30	Turbidity vs. log THO concentration for a PVA membrane containing templated poly NNPA-MAA microspheres at 25° C	181
Figure 6-31	Turbidity vs. log THO concentration for PVA membrane containing untemplated poly NNPA-MAA microspheres	182

Figure 6-32	Response vs. time for templated poly NNPA-MAA polymers responding to theophylline and caffeine at 25° C	183
Figure 6-33	Turbidity vs. log caffeine concentration for a PVA membrane containing THO templated poly NNPA-MAA microspheres at 25° C	183
Figure 6-34	Turbidity vs. time for a membrane containing templated poly NNPA-MAA microspheres in 1.0×10^{-5} M THO solution and water at 25° C	184
Figure 6-35	Turbidity of THO templated poly NNPA-MAA microspheres as function of temperature and pH	185
Figure 6-36	Turbidity of THO templated poly NNPA-MAA microspheres as function of temperature and pH for 1×10^{-3} M THO solutions	186
Figure 6-37	Turbidity of THO templated poly NNA-MAA microspheres as a function of temperature in 1.0×10^{-3} M THO buffer solution	186
Figure 7-1	Micrograph and size distribution of poly NIPA microspheres prepared by dispersion polymerization in aqueous medium	192
Figure 7-2	Turbidity spectra of poly NIPA-MBA microspheres embedded in polyurethane hydrogel	193
Figure 7-3	Turbidity of poly NIPA-MBA microspheres as a function of temperature in pH 7.0 and water	194
Figure 7-4	Turbidity of poly NIPA-MBA microspheres as a function of temperature in water and 0.1M NaCl	195
Figure 7-5	Turbidity of a polyurethane membrane containing poly NIPA-MBA microspheres as a function of temperature in water	196
Figure 7-6	Turbidity of a polyurethane membrane containing poly NIPA-MBA microspheres as a function of temperature in pH 7.0	197

ABSTRACT

CHEMICAL SENSORS BASED ON SWELLABLE MOLECULARLY IMPRINTED POLYMER MICROSPHERES IN A HYDROGEL

By

Wenzhe Fan

University of New Hampshire, December 2003

A novel design of chemical sensors based on swellable molecularly imprinted polymer microspheres is presented. These sensors were successfully used to measure norephedrine and theophylline in water and in buffer at neutral pH.

A new method was developed for preparing swellable norephedrine templated poly (N-isopropylacrylamide-acrylic acid) (poly NIPA-AAc) particles by suspension polymerization in a perfluorocarbon solvent using ultrasonic emulsion technique. The particles were crosslinked with 5% of N, N'-methylene-bis-acrylamide (MBA) using 20% fluorinated surfactant as a stabilizer. The resulting particles were around 6 μm in diameter. HYPAN and poly (vinyl alcohol) (PVA) hydrogels were used to make hydrogel membranes containing norephedrine templated poly NIPA-AAc particles. The PVA membrane has higher response at high temperature. The phase transition of poly NIPA-AAc is affected by heating rate and pH. The sensor responds to norephedrine in water with high sensitivity (1.0×10^{-7} M) and specificity. The response time is ~5 minutes.

A dispersion polymerization method was developed to prepare swellable theophylline (THO) templated poly(N-isopropylacrylamide-methacrylic acid) (poly NIPA-MAA) microspheres in acetonitrile with 5% MBA as the crosslinker. MAA was used as a functional monomer to form recognition sites with the template during polymerization. Poly (styrene-co-acrylonitrile) (20% w/w) was used as a stabilizer resulting in uniform, spherical microspheres with diameter $\sim 1.0 \mu\text{m}$. The percentages of NIPA and crosslinker are critical variables affecting polymer properties including the magnitude of swelling and shrinking, sensitivity, and selectivity. The response of PVA membranes containing templated microspheres in water and buffer were investigated. These microspheres were successfully used for theophylline sensing in water and phosphate buffer with high sensitivity ($1.0 \times 10^{-8} \text{ M}$) and selectivity (no response to caffeine up to $1.0 \times 10^{-3} \text{ M}$).

Poly (NIPA-N-t-butylacrylamide-MAA) (poly NIPA-NTBA-MAA) and poly (N-n-propylacrylamide-MAA) (poly NNPA-MAA) microspheres were prepared by the same method. The resulting microspheres were uniform, spherical, and $\sim 1.0 \mu\text{m}$ in diameter. The lower transition temperatures (12 and 15 °C) of these polymers enable them to be used at room temperature. They were sensitive to theophylline concentration as low as $1.0 \times 10^{-7} \text{ M}$ and did not respond to caffeine as high as $1.0 \times 10^{-3} \text{ M}$.

CHAPTER 1

INTRODUCTION

1.1. Background of Chemical Sensors

A chemical sensor is a device that transforms chemical information into an analytically useful signal [1]. The chemical information can range from the concentration or activity of a chemical species in solution to total chemical composition of the system. Ideally, the device is capable of operating in a continuous and reversible manner directly in the sample matrix and obtaining information about a particular chemical species in real time [1, 2]. However, some non-continuous (immunoassay) and irreversible (enzymatic catalysis) probes are also considered as chemical sensors [3].

In general, a chemical sensor consists of two basic components [3] (Figure 1-1). One is the recognition phase where a specific interaction with the analyte of interest enables it to be recognized. The second component, the transducer, transforms this interaction into an electrical signal to be amplified and detected. This electrical signal is correlated to the concentration of target analyte. The interaction of analyte with the sensor can be a surface interaction where the analyte is adsorbed at the surface, or a bulk interaction where it partitions between the sample and a recognition bulk phase. The target analyte may be any organic, inorganic ion or any uncharged molecule present in gaseous, or liquid sample. Chemical sensors involve a broad spectrum of transduction including optical and electrical process, and various other ways as shown in Figure 1-1.

As a subgroup of chemical sensors, biosensors involve biological host molecules, such as natural or artificial antibodies, enzymes, or receptors, which provide chemical recognition. Chemical sensors have been widely used in industry process control, pharmaceutical therapy, and environmental and security monitoring.

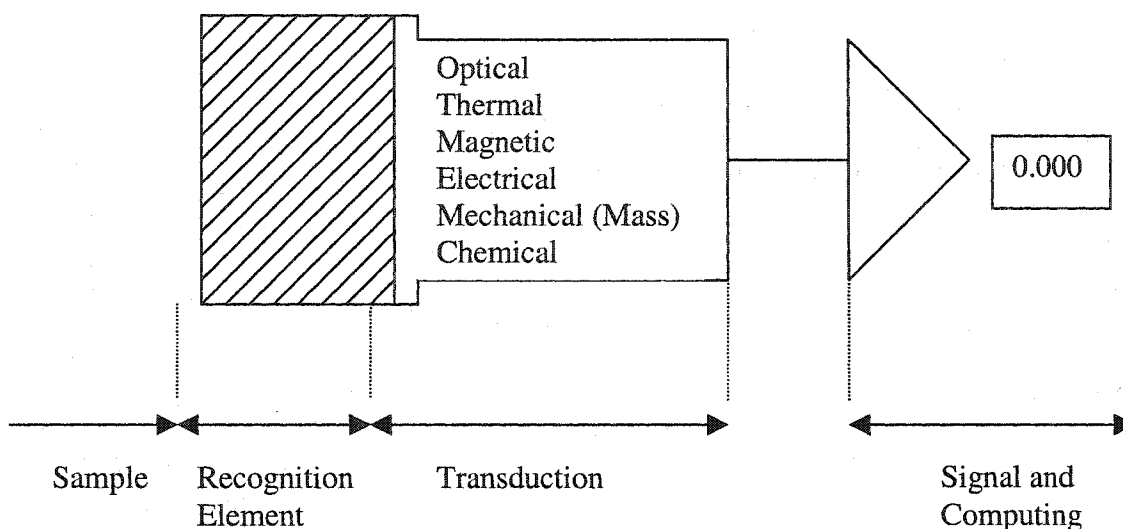


Figure 1-1. General model for chemical sensors, differentiating between recognition phase, transduction mode and data processing

One of the first sensors was built by Wilhelm von Siemens in 1860 [3]. Copper wire was used as a thermoelement of a resistor to measure temperature. The first successfully commercialized chemical sensor, the well known glass electrode, was developed by Arnold Beckman in 1932 [4]. It led to one of the most successful analytical instrument companies-Beckman Instruments. From then on, a variety of chemical sensors have been developed and applied. Several journals specialize in chemical sensors including *Sensors and Actuators B*, *Biosensors and Bioelectronics*, *Chemical Sensors*, *Chemical Sensor Technology*, *Sensors*, *Chemical Senses*, etc.; a number of reviews [5-8] and books [1-3, 9, 10] have been published covering the development of theory,

technology, and application of chemical sensors; More than 2000 sensor-related papers are published each year, and the rate of publication has kept increasing over the past decade [7]; Sensor divisions have been established in almost all large professional societies; and several series of international conferences on sensor are held regularly, such as *The International Meeting on Chemical Sensors* (already took place 9 times since the first meeting in 1983), and *World Congress on Biosensors*, etc. Chemical sensors constitute an accepted part of analytical chemistry.

The key features of chemical sensors are selectivity, detection limit, accuracy, sensitivity, dynamic response range, stability, response time, reliability and lifetime, etc. To operate successfully, output from a chemical sensor ideally should depend only on the presence and concentration of analyte of interest. Thus, the sensor should be specific for a single target molecule or ion. However, in reality, most sensors respond to a single chemical species, but also exhibit minor responses to other species that act as interferents. Achieving a better selectivity has been a major objective of chemical sensor research for the past 50 years [5]. Many sensors have been developed with improved selective recognitions, such as ionophore carrier-based chemical sensors for ion detection [1, 10], “lock and key mechanism”, in which only the target molecule fits the “lock” (enzyme, antibody, synthetic ligands, or molecularly imprinted polymer, etc) within the sensor to generate an output [3].

The transducer, actuators, or amplifiers have been improved considerably and their development is more advanced than that of the chemical recognition components used in sensors. Depending on the application need, the development of transducers has been concentrated on miniaturizing sensor devices [9, 11] to enhance the application in a

small scale (e.g. a single cell [11]) or preparing sensor arrays to enhance the information acquisition process. Optical fiber and waveguides allow chemical sensors to be used for remote measurements [12]. With the growing power of computers, new materials, processing tools, new optical components, information transmission technology, chemical sensor will be developed by coupling new chemistry and biochemistry.

1.2. Classification of Chemical Sensors

There are several alternative ways to classify chemical sensors. These involve the type of transducer, the type of the recognition process (chemical sensor in strict sense, oxide semiconductor sensors, enzymatic sensors, immunochemical sensors, receptrodes, etc.), the type of sensing layer (surface active sensors, bulk-phase sensors, etc.), the application (clinical sensors, environmental sensors), the size of sensor device (micro, nano, macro, bench-type, etc.). According to the type of transducer and the primary physical quantity analyzed, chemical sensor can be classified in four major subclasses: electrochemical, thermal, mass, and optical sensors.

1.2.1. Electrochemical Sensors

Electrochemical sensors are the largest and oldest group of chemical sensors. Many members of this group have reached commercial maturity while others are still in various stages of development. They are divided by their mode of measurement into three subgroups: potentiometric, amperometric, and conductometric sensors [2, 13].

Ion-selective electrodes (ISEs) are typical potentiometric sensors for ions as analytes with liquid internal contact while ion-selective field effect transistors (ISFETs)

are potentiometric sensors with a solid internal contact material. For amperometric sensors, the analytes are redox-active compounds. These sensors often incorporate a biochemical recognition element, such as an enzyme. The amperometric sensing reaction follows steady-state kinetics. The rate-determining step of the overall electrolytic process is controlled by the experimental conditions. Ideally, the sensor's response current should depend on the turnover rate of the substrate. Conductometric sensors are based on measurement of chemically-induced conductivity changes.

1.2.2. Thermal Sensors

Thermal sensor is a device that acquires the analytical information from heat evolved or absorbed by a specific chemical reaction. A typical thermal sensor consists of a chemically sensitive layer is applied on top of a thermal probe. The temperature change or heat flux is measured when a specific reaction takes place in the chemical layer. Only about 23 papers were published on average per year in the last decade showing that thermal sensors have been typically the smallest subclass of chemical sensors [13]. Most research have been focused on the development and improvement of sensing arrays based on the dioxide, pyroelectric effect, and catalytic thermistors. New materials for the fabrication of pyroelectric sensors have been reported.

1.2.3. Mass Sensors

Mass can be measured by a refractive index change, by the local conductivity, or by frequency modulation of an oscillating crystal. Since piezoelectric crystals can very

accurately measure small changes in mass, they are attractive platforms to build chemical mass sensors [2].

There are two types of piezoelectric mass sensor, bulk acoustic wave (BAW) devices and surface acoustic wave (SAW) devices [2, 9]. Both of these approaches are based on mechanical deformation of piezoelectric crystals that results from applying a potential in a controlled manner. By applying a potential or voltage, acoustic waves are generated and travel either through the bulk of crystal, or along its surface. These devices are useful for chemical sensing because the velocity of the waves and their frequency strongly depend on the mass of the crystal. The performance of these mass sensors is not limited by instrumentation but depends strongly on the properties of the chemically sensitive film immobilized on the crystal.

To make these piezoelectric sensors sensitive to specific species of chemical, biological, or environmental interest, they must first be modified with a layer that selectively interacts with the species of interest. The sensor can be modified with either synthetic (such as polymers, inorganic complexes, etc.) or biological materials (such as enzymes, antibodies, etc.).

Due to their advantages such as, low weight, low power required, high sensitivity, low expense and readily availability, mass sensors are used and will continue to be used as the basic transduction mechanism for a wide variety of chemical sensors [9].

1.2.4. Optical Sensors

There are two terms for optical sensor: “optrode”, based on the name ‘electrode’ and the name “optode” from “optical” or “optics”. They have a history of 35 years [3]. In

contrast to electrochemical sensors, optical chemical sensors can detect not only charged analytes but also a broader spectrum of analytes. A typical fiber optical sensor (FOCS) consists of a light source, an optical detector, optical fibers and other spectral filtering devices. Light is transmitted between these components by cylindrical optical fibers or by planar waveguides.

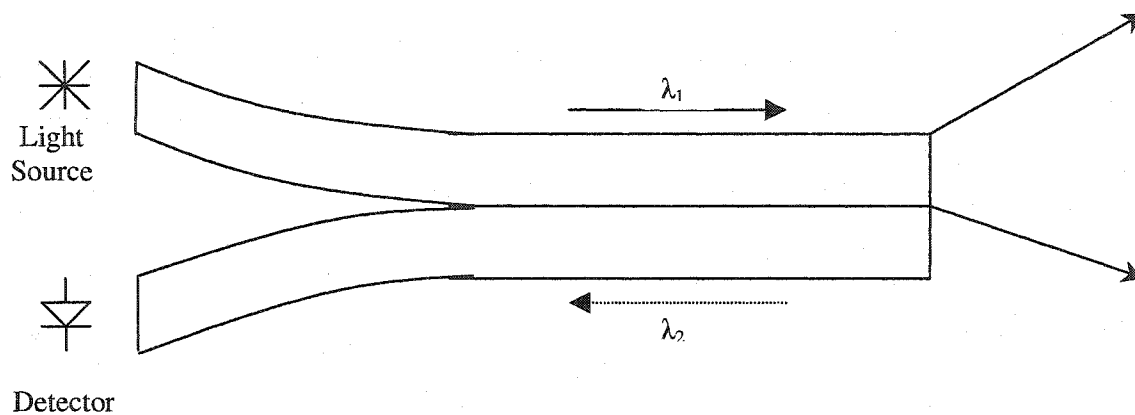
In 1968, Bergman reported the first type of optical oxygen sensor based on fluorescence quenching [14]. The fluorescent dye was incorporated into a 25-50 μm thick film made from polyethylene, silicon rubber, or porous glass. A portable instrument was used to measure the atmospheric oxygen partial pressure by luminescence quenching. The first chemiluminescence based fiber optical H_2O_2 sensor was constructed and fully described by Seitz in 1978 [15]. Horseradish peroxidase was immobilized in a polyacrylamide gel on the end of optical fiber. Chemiluminescence was generated as H_2O_2 diffuses into the peroxidase phase in the presence of the excess of luminal. The first detailed description of the construction and performance of a pH fiber optical sensor was from Peterson in 1980 [16]. Microspheres of polyacrylamide containing a dye indicator, phenol red, and smaller polystyrene microspheres for light scattering were packed in cellulosic dialysis tubing at the end of plastic optical fibers. The sensor was based on the absorbance of the reflected light. The sensor could be used to measure blood pH over the range 7.0-7.4 to the nearest 0.01 pH unit. In 1983, Seitz developed a fluorescence-based aluminum (III) sensor [17], which is the first fiber optic chemical sensor (FOCS) for the detection of an ion other than hydrogen. Morin was immobilized on cellulose powder and attached to the end of a bifurcated fiber optic bundle. The reaction between aluminum and morin generates a highly fluorescent complex that can be monitored by a simple

fluorescence measurement. Successful fiber optical sensors that can provide simultaneous measurements have been developed for pH, CO₂, and O₂. These sensors have been used to monitor in vitro blood gases [18] and the pH, CO₂, and O₂ changes during beer fermentation [19]. Kopelman and his group have demonstrated a miniaturized fluorescence glucose sensor using fibers pulled to the tip size on the order of 1 μm [11]. This work provides the possibility of using fiber optic sensors for in situ measurements in single cells.

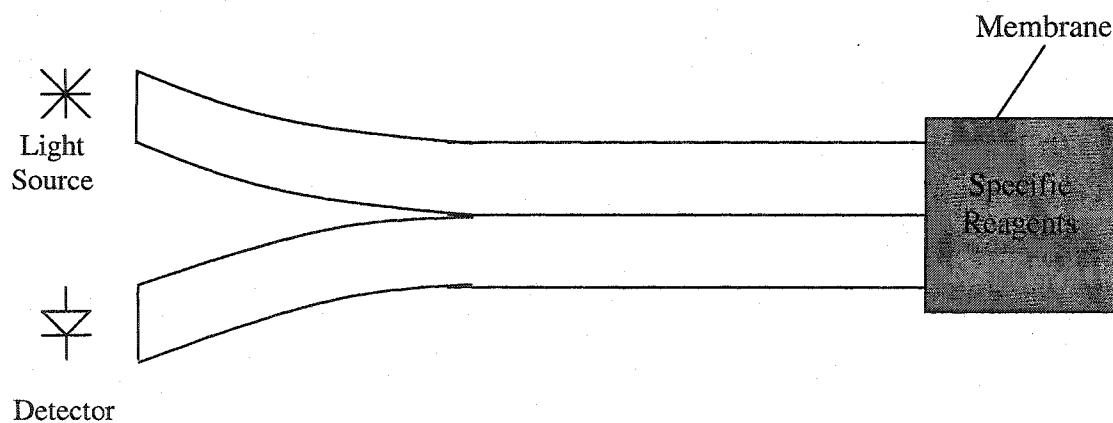
There are a variety of applications of optical sensor in industry process control, biomedical, and environmental monitoring [7, 12]. A comprehensive study and review of the broad range of issues affecting FOCS is presented in the two-volume book edited by Wolfbeis [10]. More recent updates on developments in the field are reported in special editions of Sensors and Actuators B [20]. In addition, the proceedings of the annual SPIE meeting on Chemical, Biochemical and Environmental Fiber Sensors provide a useful overview of research activity in this area [21, 22]. A series of review papers written by Wolfbeis [23, 24] has closely traced the recent development and application of optical chemical sensors.

Fiber optical chemical sensors are classified in two categories: direct spectroscopic sensors and reagent-mediated sensors [9]. The fundamental FOCS designs are shown in Figure 1-2. In the case of direct spectroscopic sensors, the fiber is only used as a simple lightguide that separates the sensing site from the monitoring instrumentation (light source, detector, spectral filtering, etc.). Direct spectral analysis (such as fluorescence, absorption, Raman scattering) of a sample can be easily obtained through

fibers. A typical example is the remote detection of naturally fluorescent contaminants in groundwater using far-ultraviolet laser-induced fluorescence [25].



(a) Direct Spectroscopic Sensors

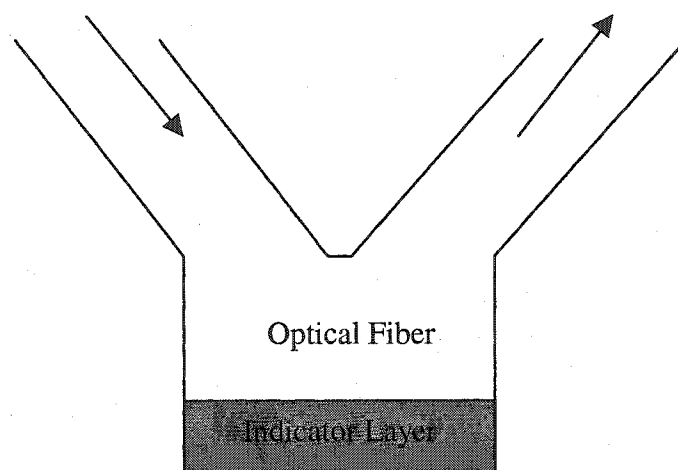


(b) Reagent-Mediated Sensors

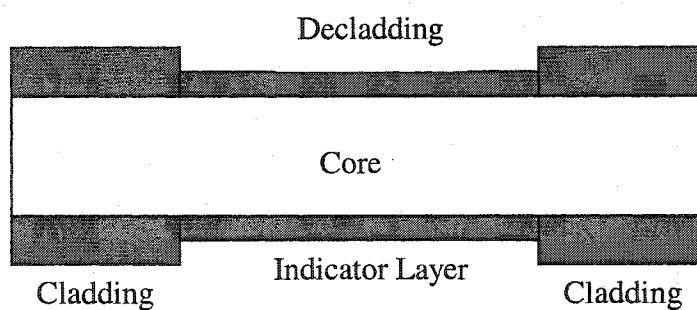
Figure 1-2. Basic designs of FOCS: (a). direct spectroscopic sensors; (b). reagent-mediated sensors.

In the case of reagent-mediated sensors, the optical fiber is combined with a chemical reagent which is chosen to react sensitively and specifically with the target analyte. The change of reagent's optical properties, such as fluorescence or absorption, can be used to directly measure the analyte concentration. A number of configurations have been developed. For example, reagents can be contained in a reservoir attached to the fiber tip and separated from the sample by an appropriate membrane [15]; reagents can also be entrapped or immobilized in a synthetic polymer [1] or sol-gel membrane [26], which is coupled to optical fiber. There are two types of reagent-mediated sensors: distal-type FOCS, the most common design, in which the specific reagent is immobilized at the tip of either a bifurcated fiber bundle or a single optical fiber; field-type in which the reagent is immobilized along the core of a clad optical fiber to make evanescent wave FOCSs. The FOCS for chemical and biological species based on evanescent wave interactions have attracted considerable research interest [27]. Figure 1-3 shows these two designs for reagent-mediated sensors.

Fiber optical chemical sensors have many advantages. The low attenuation of optical fibers which enables remote in situ monitoring of species; geometric versatility; electrical noise immunity of optical fibers; allow sensing in difficult or hazardous locations, such as groundwater monitoring or monitoring of process streams in nuclear fuel reprocessing plants; No reference signal is required; Different type of signals can be monitored, such as wavelength, phase, time, and intensity; Fiber optic sensors are easily miniaturized (e.g., nanoscale) and used for small volume samples or in vivo applications; fiber bundle may be coupled for imaging sensors and sensor arrays to simultaneously monitor multiple analytes [28].



(a). Tip-Type



(b). Field-Type

Figure 1-3. Two principle designs of reagent-mediated FOCS.

1.3. Chemical Sensors Based on Swellable Polymer Microspheres

In 1978, Tanaka first described how lightly cross-linked polymers swell and shrink with changes in their environment [29]. There are two forces when a cross-linked polymer is placed in a compatible solvent: swelling forces arising from polymer solvation and retractive forces from the cross-linked polymer network. These two forces reach equilibrium when the polymer absorbs solvent. If the polymer is uncharged, the more affinity of polymer backbone for the external solvent, the more it swells. If there are charged sites on the polymer backbone, additional swelling caused by electrostatic charge repulsion or osmotic pressure effect must be considered [30]. This property of polymers has been widely and successfully used for controlled drug release systems [31], but its use in chemical sensing is a relatively new concept and not mature enough for commercial applications. Swelling of a hydrophilic polymer has been used in some humidity sensors [32, 33].

Our group has been developing chemical sensors based on swellable polymers for over a decade [30]. First a porous derivatized polystyrene membrane was prepared and bonded to a substrate for pH sensing [34]. This membrane could undergo large numbers of swelling and shrinking cycles without cracking. When the membrane swells and shrinks, the density of reflected or scattered light changes because of the change of membrane refractive index. There are mechanical problems associated with this kind of membrane, such as the delamination of membranes from the surface of substrates during swelling and shrinking, and cracking when the membrane dried out. However, it was observed that the optical properties of these membranes changed upon swelling in aqueous solutions. They appeared clear in swollen state when the pores in the membranes

were filled with water. When they shrank they became white [35]. This observation encouraged a new idea to prepare polymer microspheres in a hydrogel membrane instead of using a polymer membrane with water filled pores. From then on, much of our research and efforts have been concentrated on synthesis of polymer microspheres and exploiting of this advantage. Our chemically-derivatized lightly cross-linked polymer microspheres are designed to swell and shrink as a function of analyte concentration. These microspheres are then embedded into hydrogel membranes. Swelling leads the microsphere refractive index to decrease and become closer to the hydrogel refractive index, which reduces the turbidity of membranes. Either transmission or reflection can be used to measure the turbidity changes of membranes.

Different methods, such as dispersion polymerization, suspension polymerization, and seeded emulsion polymerization, have been tested and used to prepare microspheres with diameters on the order of 0.3-3.0 micrometers [30]. Three different hydrogels, poly vinyl alcohol (PVA), poly(hydroxyethylmethacrylate) (poly HEMA), and HYPAN (a commercial poly acrylonitrile-acrylate block copolymer) have been used for our membranes of ~75 micrometer. Several different types of polymer microspheres have been prepared. Most of these microspheres have been developed for pH sensing [36-42]. Figure 1-4 shows the principle for pH sensing [30]. For example, diethanolamine derivatized poly(vinylbenzyl chloride) (poly VBC) microspheres have been prepared and suspended in PVA hydrogel membrane. When this membrane is placed in acid solution, protonation of the amine group introduces a positive charge onto the polymer backbone. The charge repulsion causes the polymer to swell resulting in the decrease of microsphere refractive index to 1.43, which is closer to PVA refractive index (1.34). The turbidity

decrease of the membrane can be used to measure pH in the range from 6.5 to 7.8, which is relevant for many applications, such as biological measurements.

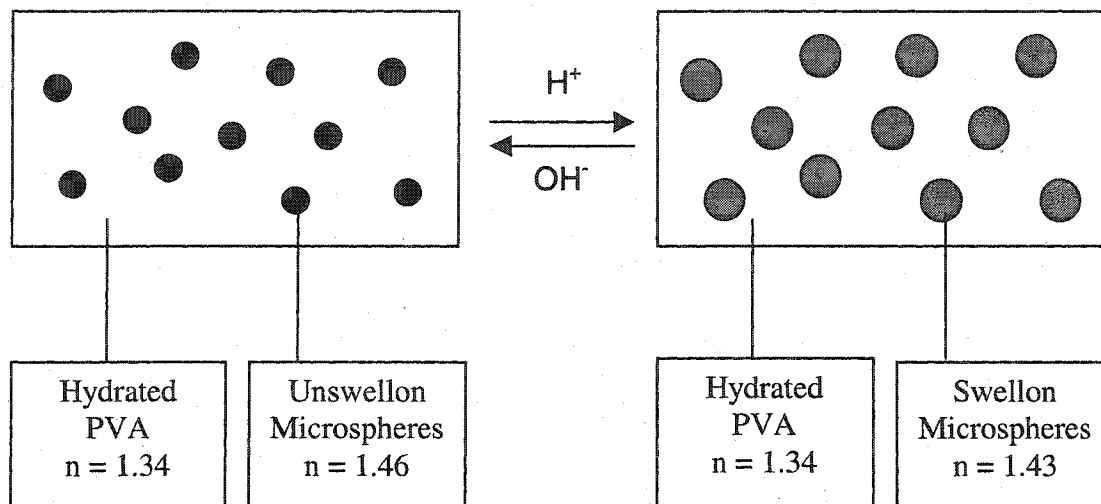


Figure 1-4. Schematic of sensing response mechanism. Microspheres are diethanolamine derivatized polystyrene. n is estimated refractive index of microspheres and membranes.

Several other types of porous polymer microspheres have been prepared to improve the sensor response. For example, poly (4-acetoxystyrene) was prepared by two-step seeded emulsion polymerization and were then mono- or binitro-derivatized for pH sensing [40]. These microspheres swell and shrink in seconds when introduced to pH buffers. This is because derivatization removes the acetoxy group which leaves some microporosity within the polymer and also increases the polymer backbone hydrophilicity. Both cause the microspheres to swell slightly and allow protons to easily partition into the microspheres. Co-polymers of 2,4,5-trichlorophenyl-acrylate (TCPA) with VBC have been prepared by dispersion polymerization [41]. The resulting copolymers can be easily derivatized to introduce a hydrophilic functional group because 2,4,5-trichlorophenol group is an excellent leaving group. Poly (VBC-co-TCPA) microspheres were aminated

to convert the chloromethyl group of VBC to amine for sensing pH and also to convert the TCPA to amide which is hydrophilic. This causes the polymer to swell slightly in aqueous media introducing microporosity. Additional microporosity can be obtained if the reagent used to introduce the hydrophilic functional group is smaller than the 2,4,5-trichlorophenol leaving group. These microspheres are sufficiently porous to respond to pH with response times on the order of 10 seconds.

A metal ion optical sensor based on polymer swelling has been developed by Wang [40]. Membranes consisting of ionophore modified poly(4-hydroxy, 3-nitrostyrene) microspheres in a hydrogel were prepared for potassium sensing. When the membrane is immersed in a solution of potassium ions, the neutral ionophore, dibenzo-18-crown-6, in the polymer will selectively bind the potassium ion to form an ion-pair complex. The ion binding is accompanied by release of a proton to maintain electroneutrality. This introduces charged sites into the polymer backbone causing it to swell. The higher the potassium concentration, the more swelling. Turbidity was used to determine the concentration of potassium ion. This indicates that ion-pairing chemistry can be used in our sensing approach based on polymer swelling. A family of ion-selective optical sensors can be developed based on this approach.

In addition to optical sensors, Liu [42] investigated a new type of magnetoacoustic chemical sensors based on polymer swelling in our group. A magnetic strip coated with a layer of hydrogel membrane containing aminated poly VBC-TCPA or dicarboxylated poly VBC microspheres was used for pH sensing. The characteristic frequency shifts as the microspheres swell or shrink due to the changes of pH. These magnetoacoustic sensors do not require an external power source and any physical

connections to the sensing elements. They are ideally suitable for applications where physical connections are undesired or impossible.

1.4. Chemical Sensors Based on Molecularly Imprinted Polymers

Selectivity is one of the essential features of a chemical sensor, because it determines if a reliable measurement in the sample is feasible. At this point, the recognition phase is the most important component of chemical sensor so that the development of new recognition principles or the improvement of known ones is a major task for sensor chemists. The long-term goal of sensor research is making chemical sensors with the typical high selectivity of biomolecules while having robustness to operate in harsh environments such as high temperature, acid, base, organic solvent, etc.

Molecularly imprinted polymers (MIPs) have attracted much attention in various fields because of their high stability and selectivity for target molecules [43]. Molecular imprinting is a technique for providing synthetic polymers with specific binding properties. This method is based on prearrangement of template molecules and functional monomers before initiation of polymerization. A polymer is formed with sites complementary to the template molecule both in the shape and in functional group positions. The molecularly-specific sites will remain after removing the template molecule by extraction. Molecular imprinting has been recognized as a promising technique for the development of materials for such areas as separation [44, 45], material science (e.g. drug delivery [46, 47]), sensing [48-52], etc. (see Figure 1-5) and has developed very fast in the last decade (Figure 1-6).

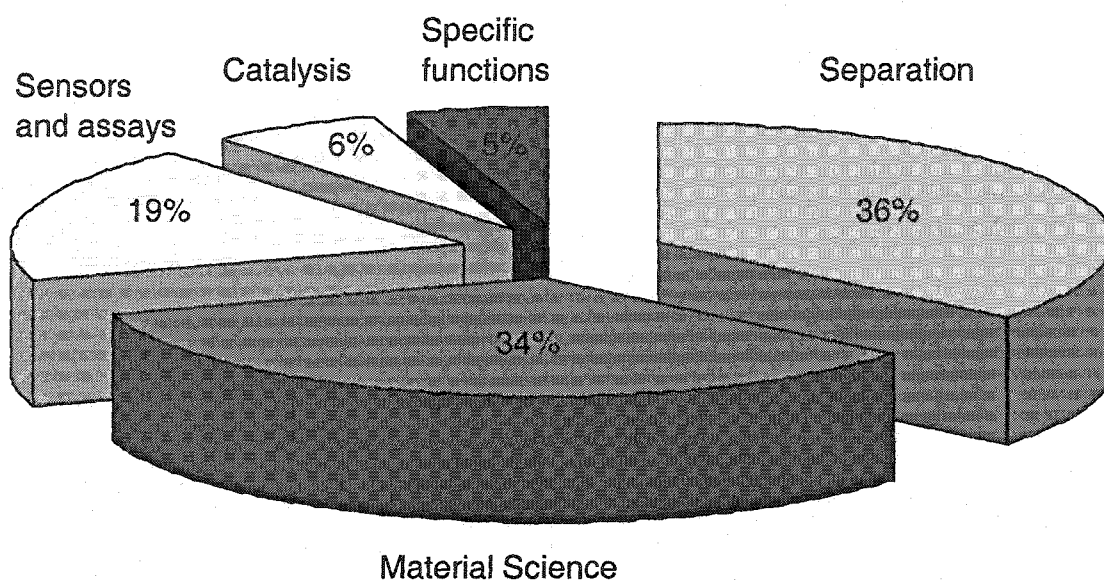


Figure 1-5. A schematic representation of research area in MIP technology in 2002

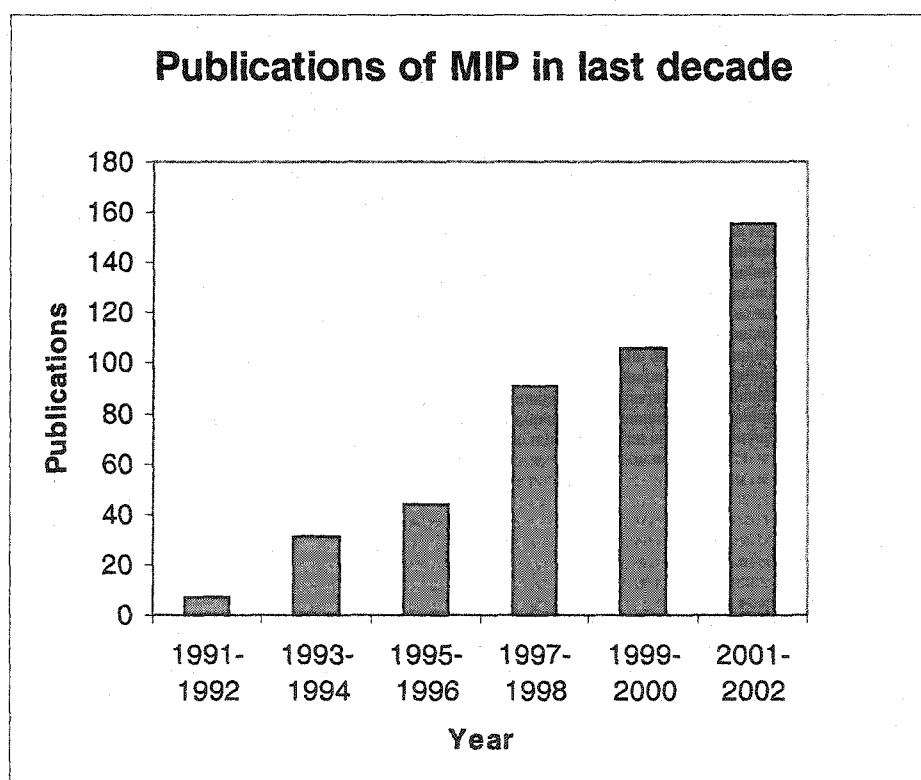


Figure 1-6. Publications of MIPs in last decade.

So far, MIPs have been used primarily for separations and material science. Recently, however, they have been used in sensors due to their unique properties that make them suitable for sensor technology. They have the affinity and selectivity required for a sensing device. They exhibit good specificity for various analytes of medical, environmental, and industrial interest. They are also highly robust and have excellent operational stability. Also the performance of sensors based on MIPs is not affected by acid, base, heat, or organic solvent treatment [48]. MIPs are an attractive alternative if natural recognition elements are not available (Table 1-1). Because of these exciting advantages, MIP-based sensors have attracted increased interest recently. Figure 1-7 shows how publications about MIP-based sensors have increased in last decade.

Table 1-1. Comparison of natural biomolecules with MIPs

Property	Natural Biomolecules	MIPs
Stability	Low	Stable at low/high pHs, pressure and temperature
Cost	High	Inexpensive and easy preparation
Integration into multisensor unit	Difficult due to different operational requirements of these molecules (pH, ionic strength, temperature, substrate)	Flexible MIP design allows preparation of MIPs against many combinations of analytes
Compatibility with micromatching technology/miniaturization	Poor	Fully compatible
Spectrum of analytes	Limited	Practically unlimited

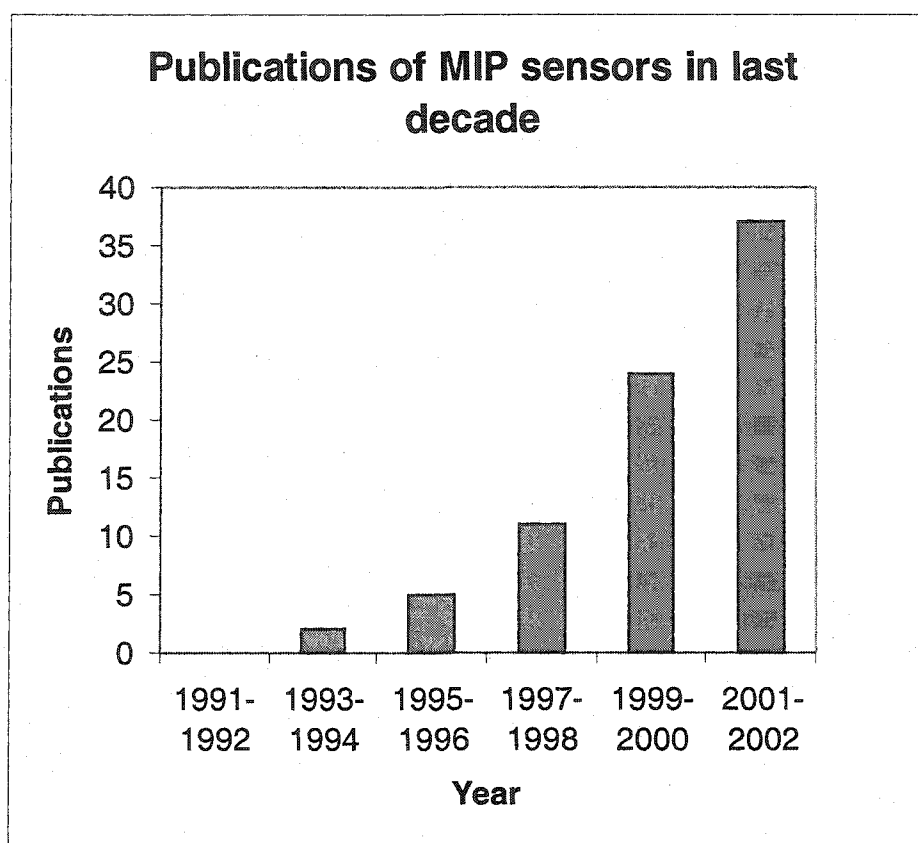


Figure 1-7. Publications of MIP-based sensors in the last decade.

In 1993, the first reported attempt was to make a biomimetic sensor based on measuring capacitance changes for a field-effect transistor coated with a phenylalanine anilide imprinted polymer [53]. However, the results were qualitative. A competitive amperometric morphine sensor was constructed by coating morphine-imprinted polymer on a platinum electrode and showed more quantitative results [54]. Membrane-based conductometric sensors for several compounds including nucleotides and amino acids [55], atrazine [56-58] were reported. A direct signal is obtained on binding of the positively-charged species to the negatively-charged MIPs placed on the conductometric

transducer. The difference in signal between the sensor and a reference sensor correlated well with the concentration of the analyte.

So far, the majority of published papers related to MIP sensors deal with electrochemical [51] or piezoelectric devices [59, 60], but there is a long way to go in the field of optical sensing. There are many possibilities for the design of optical sensors based on MIPs.

(a). Analytes with native optical properties [50, 61]

In this situation, the MIP acts as an adsorbent/extractant material to preconcentrate an optically detectable analyte. Measurement is based on the native optical properties of the analyte. Although sensing based on this concept is straightforward and has increased sensitivity by concentrating the analyte, the application potential is limited to those species which can be detected directly.

(b). Analytes with nonnative optical properties

MIP sensor elements developed for applications involving these analytes are designed to change color or fluorescence after interacting with the analyte. Approaches include indirect sensing [62, 63]; direct sensing [64, 65]; and competitive assays [66-68]. Powell and co-workers [63] have developed a fluorescent chemosensor for adenosine 3',5'-cyclic monophosphate (cAMP) based on molecular imprints containing a fluorescent dye, trans-4-[p-(N,N-dimethylamin)styryl]-N-vinylbenzylpyridinium chloride, as an integral part of the recognition cavity. This fluorescent MIP serves as both the recognition element and the measuring element for the fluorescent detection of cAMP in aqueous media. When cAMP was bound to polymer, the fluorescence of the polymer was quenched, and was proportional to the amount of cAMP added. Metal ions such as Al

(III) can be directly sensed based on the formation of fluorescent complexes using polymers imprinted with the corresponding morin-metal chelate [65]. The idea is that MIPs are prepared with a fluorescent complex as the template which is formed from a nonfluorescent ligand and the metal ion. After removal of the metal ion from MIP, the recognition cavity for the metal ion is arranged at the suitable position for the selective sensing of the metal ion. The idea of competitive assays using MIPs as antibody mimics was first proposed by Kriz et al. in 1995 [61]. Piletsky and co-workers developed fluorescent sensing assays for triazine herbicide [67]. This method is based on the competition between fluorescent-labeled and the unlabeled substance-analyte for the specific binding sites which were formed in polymer by the imprinting of the template. They also demonstrated competitive sensing assays for the antibiotic chloramphenicol using methyl-red as colorimetric marker[68].

To date, almost all MIPs in sensor system have been prepared by bulk polymerization methods. This process is simple, and optimization of imprinting conditions is relatively straightforward. However, the grinding and sieving process is tedious and may also be detrimental to some of the binding sites. Hence, beaded polymers would be preferable. Another problem for MIP sensors is the long response time (15-60 min) [48] because of very slow mass transfer in the extremely rigid polymer. Using smaller polymer particles with appropriate levels of cross-linker should improve diffusion rates giving shorter response times.

Two constraints have been considered for making swellable MIP microspheres. Usually a high level of cross-linker (e.g. >12 mole %) is required to make MIPs so that polymer is rigid enough to retain the cavity shape after removal of the template. However,

if the polymer is too rigid, the mass transfer of template into and out of the polymer is very slow resulting in a longer response time. Also if the polymer is too rigid, it is difficult to swell and shrink so that it is unsuitable for our sensing scheme based on polymer swelling and shrinking. So, cross-linker level was optimized to reach a compromise between rigidity and flexibility to maintain high selectivity with acceptable response time.

A second constraint is that the template must be surrounded by functional monomers and stay in the polymer during polymerization so that the resulting polymer has high specificity. In self-assembly imprinting protocols using only noncovalent interactions, which have been predominantly used to produce MIPs, the specificity is usually exerted via ionic interactions and hydrogen bonding between the templates and the functional monomers. So common approaches to polymer synthesis in aqueous medium are not suitable for preparing MIPs because water-soluble template molecules would be lost due to partitioning into the aqueous phase instead of staying in polymer.

Almost all molecular imprinted polymers can not undergo a significant swelling when they interact with template due to the very high crosslinking. However, a recent study of swellable MIPs has been reported by Watanabe [69]. Copolymer gels consisting N-isopropylacrylamide (NIPA) and acrylic acid (AAc) have been prepared in dioxane in the presence of two templates, norephedrine and adrenaline. They have similar structures. The polymer was prepared in capillary tubes to obtain a thin polymer thread. Medium level of crosslinker causes these MIPs to undergo swelling changes and at the same time have their molecular specificity. The swelling is based on the thermal properties of poly NIPA which is solvated by water at low temperature and shrinks at high temperature [70].

It was observed that the volume at high temperature varied with template concentration for the templated polymer but not for the untemplated polymer. The norephedrine-templated polymer also did not respond to adrenaline and vice versa which indicated the high specificity of this MIPs. This kind of template-induced polymer swelling phenomenon encouraged us to investigate the possibility of using these materials for chemical sensing. The goal of this dissertation was to prepare swellable MIP microspheres, cast them into hydrogel membranes, measure the changes accompanying swelling, and finally develop new chemical sensors based on swellable MIP microspheres.

1.5. Summary of This Dissertation Research

The primary objective of my research was to develop new chemical sensors based on swellable MIPs for drugs, such as norephedrine, theophylline (THO). The most important part of this research is to synthesize and characterize swellable MIP microspheres that can swell or shrink when they interact with template-analyte. Thermal sensitive poly(N-isopropylacrylamide) (poly NIPA) MIP microspheres have been prepared by either dispersion or suspension polymerization.

Many efforts have been made to find a nonpolar system and stabilizer to reach our goals. Suspension polymerization using a perfluorocarbon solvent as the suspending medium has been developed to prepare norephedrine-templated poly NIPA-acrylic acid (AAc) microparticles. Theophylline templated poly NIPA-methacrylic acid (MAA) microspheres have been prepared by dispersion polymerization in acetonitrile with polyacrylonitrile-co-styrene as a stabilizer. Several formulation variables, such as percent cross-linker, ratio of NIPA to functional monomer, template concentration, etc., have

been studied and optimized to obtain swellable, uniform with size of ca. 1 micron microspheres with high sensitivity and specificity.

In order to make these sensors work conveniently at room temperature, poly NIPA-NTBA (N-t-butylacrylamide) and poly NNPA (N-n-propylacrylamide) microspheres have also been prepared and evaluated. The working temperature of these microspheres was decreased to room temperature.

In this dissertation, Chapter 2 describes the background and theory on molecular imprinting. Background material on polymer chemistry, swellable polymers, and hydrogel membranes are also discussed. Chapter 3 describes experimental methods to make and characterize the MIP microspheres for sensing norephedrine, theophylline and temperature. Chapter 4 describes the preliminary results and attempts to make swellable, uniform MIP microspheres sensing for norephedrine, theophylline and temperature. Chapter 5 describes the MIP-based microspheres sensing for norephedrine. The effects of formulation variables on MIPs using suspension polymerization in perfluorocarbon were investigated. The effects of variables on sensor performance for the determination of norephedrine were also studied. Chapter 6 describes the MIP-based microspheres sensing for theophylline. Systematic study and a factorial experiment have been used to extensively study the effects of formulation variables on swelling properties, sensitivity and specificity of MIP microspheres for THO. Chapter 7 describes a temperature sensor based on thermal-sensitive poly NIPA. The effects of variables (pH, ionic strength) on the performance of sensor were studied. Chapter 8 summarizes the work of this dissertation.

CHAPTER 2

THEORY

2.1 Polymer Background

The word “Polymer” is derived from the Greek *poly* and *mer*, meaning “many” and “parts”, respectively [71]. *Macromolecule* or large molecule is also used as a term synonymous with polymer. A polymer is a large molecule which has a chain of atoms held together by covalent bonds. It is synthesized through a process known as *polymerization* where simple molecules called *monomers* react together to form linear chains or a three-dimensional network of polymer. The main characteristic which separates polymers apart from other materials is that polymer samples are made up of long molecules. A typical sample of polyethylene may have molecules which contain an average 50,000 atoms and would be 25,000Å long [72]. Many material are polymers including biological polymers (such as protein), and nonbiological polymers (such as the fibers for clothing, automotive tires, paints, plastics, and so on). Thus, polymers are the basis for both plant and animal life and play an extremely role in our everyday life.

The structure of a polymer depends on the monomer or monomers used in its preparation. A *homopolymer* is formed from one type of monomer while a *copolymer* is synthesized from more than one type of monomers. There are four different copolymer types: alternating copolymer, random copolymer, block copolymer, and graft copolymer corresponding to four possible arrangements of monomers: alternating, random, block,

and graft. Figure 2-1 illustrates these four types of copolymers (A, B are used as two different monomers) [71]. Polymers can also be described as linear, branched, and three-dimensional as shown in Figure 2-2. Linear or branched polymers are prepared without crosslinker and can be usually dissolve in compatible solvent. Network polymers are crosslinked with a high degree of mechanical stability.

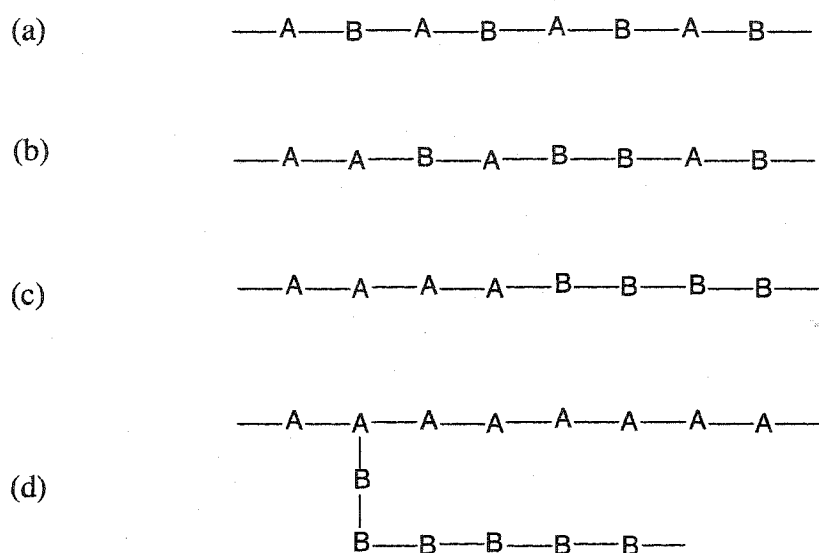


Figure 2-1. Presentation of copolymer types: (a) alternating, (b) random, (c) block, and (d) graft.

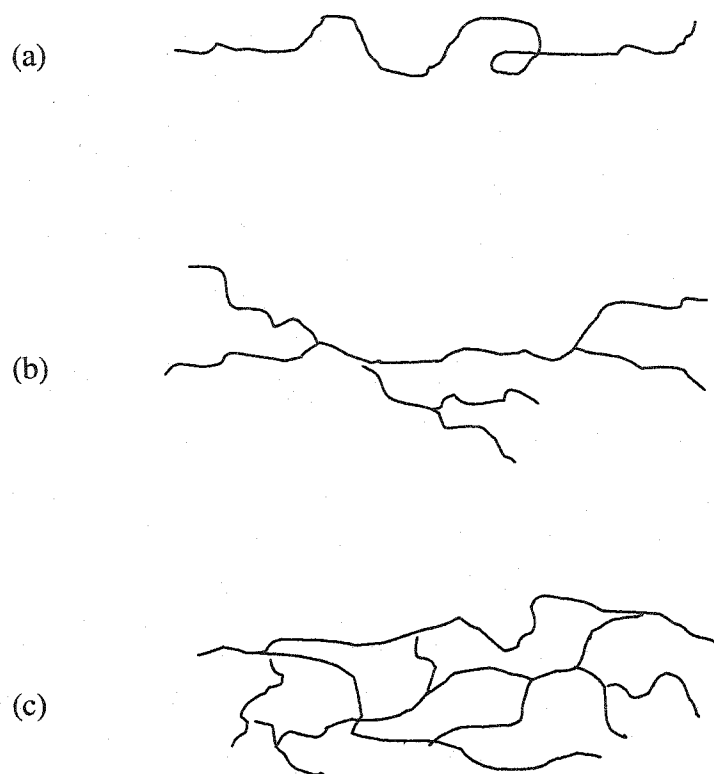


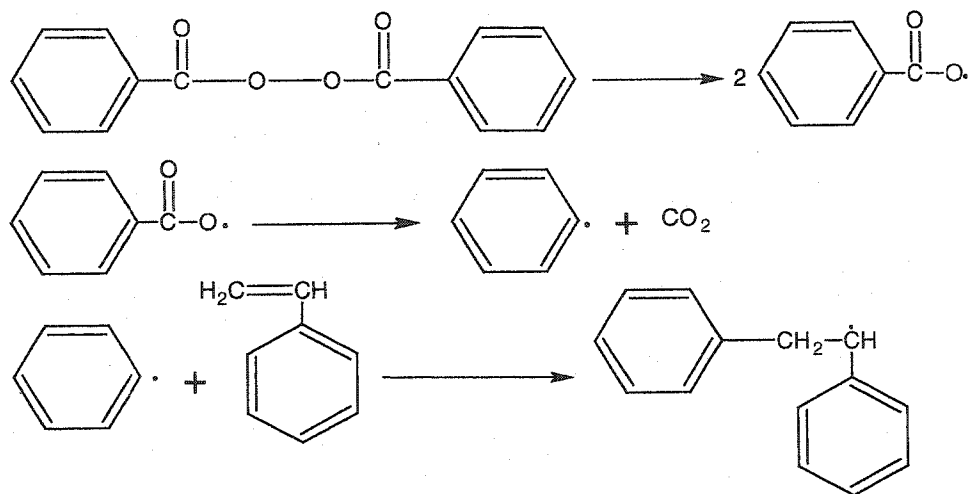
Figure 2-2. Schematic representation of different types of polymers.
(a) linear, (b) branched, and (c) network

The synthesis of polymers can be conventionally classified into two main categories, condensation and addition polymerization [72]. Condensation polymerization, also called step-growth polymerization, involves a condensation reaction between multifunctional monomers in which a small molecule like water is condensed out. Monomer molecules react with each other in a step-growth fashion. Bi-functional monomers can be used to form a linear polymer. Monomers with a functionality of greater than two can form network polymers.

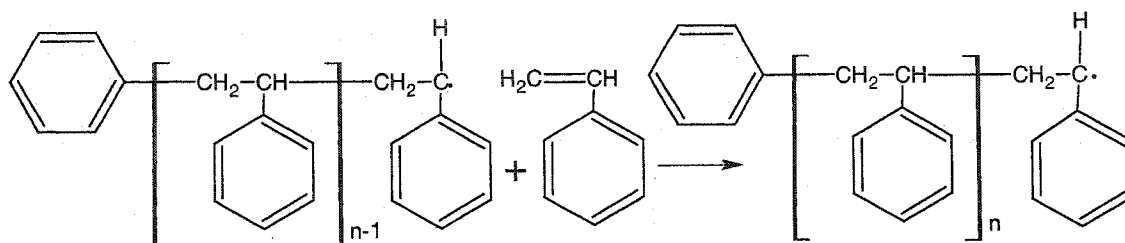
The principal mechanism of addition polymerization, or chain-growth polymerization, is by addition of monomer molecules to a growing chain. Monomers for addition polymerization usually contain double bonds that can be attacked by initiators. According to the nature of initiators, addition polymerization can be further classified as free radical or ionic. The polymers in this work were prepared by free radical addition polymerization which involves three distinct steps: initiation, propagation, and termination. Figure 2-3 shows a typical example of a free radical chain reaction polymerization process.

In initiation step, the initiator is first activated to form free radicals. These radicals then subsequently react with the vinyl double bond of the monomer to form an active center or chain carrier. Initiators can be peroxides ($-O-O-$) or azo ($-N=N-$) compounds which can be activated by thermolysis or photolysis. The rate of decomposition of peroxides such as benzoyl peroxide (BP) may be increased by the addition of small amounts of tertiary amines such as N,N-dimethylaniline. Azobisisobutyronitrile (AIBN) can be activated by either thermolysis or photolysis. Both AIBN and BP have been investigated in this work. The second step is chain propagation which involves the rapid addition of monomer molecules to the growing chain. This reaction is so fast that several thousands of additions can take place within a few seconds. There are two possibilities for addition during propagation: head-to-head and head-to-tail. For vinyl polymers, the predominant reaction is head-to-tail addition because of steric repulsion. The resulting polymer has functional groups on alternate carbons. The rapid chain propagation can be terminated by several mechanisms. One of these mechanisms is called combination where two growing chains react with each other to form inert polymer

(1) Initiation



(2) Propagation



(3) Termination

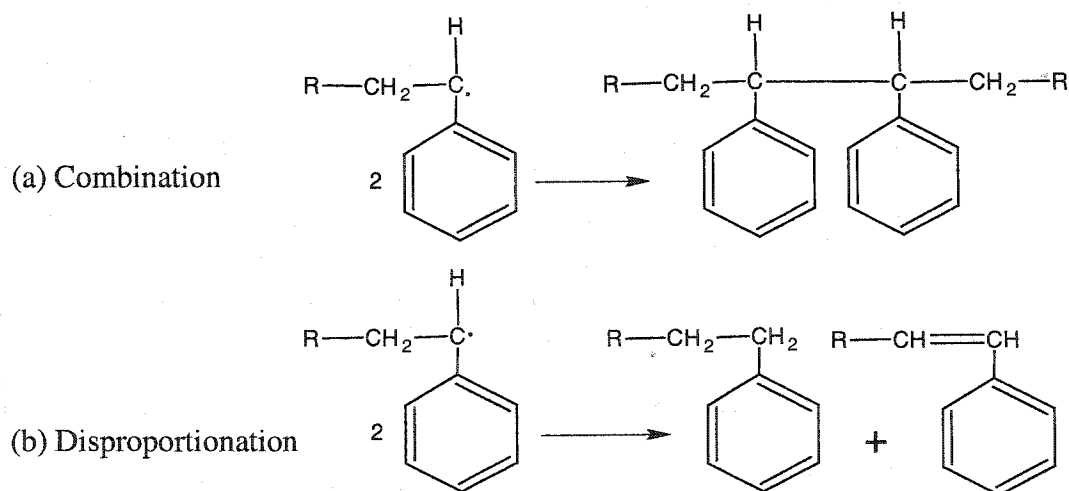


Figure 2-3. Free radical polymerization of VBC using benzoyl peroxide as initiator.

molecules in a head-to-head reaction. The resulting polymer has initiator fragments at both ends. Another termination is called disproportionation where a hydrogen atom can be alternatively transferred from one chain to the other resulting in two polymer chains with initiator fragment at one end. One polymer chain has a saturated group at the end while the other has unsaturated group at its end (Figure 2-3).

2.2 Free Radical Polymerization

Free radical polymerization can be divided conveniently into homogeneous and heterogeneous systems [72]. In homogeneous systems, the initiator, monomer and polymer are all mutually soluble in a single phase. In heterogeneous systems, the initiator, monomer and polymer are not mutually soluble and the polymer forms as a discrete phase which is dispersed in droplets.

Homogeneous polymerization includes bulk polymerization and solution polymerization. In the case of bulk polymerization, solution containing initiator, monomer without solvent is polymerized to form a block of polymer. This is the simplest technique and is usually used to produce small amounts of polymer. Bulk polymerization suffers from several difficulties: (a). the necessity to remove unreacted monomer; (b). poor heat transfer due to the viscosity increase as polymer is formed, which can cause an explosion; and (c). the possible necessity to change the polymer's physical state (e.g. putting it in a solution or making a powder). Solution polymerization can overcome these difficulties by using an inert solvent. The addition of solvent can decrease the viscosity of the system so that heat can be easily removed from the vessel, but solvent cost is an added factor, and solvent removal is often difficult and expensive. The hydrogel

membranes and swellable molecular imprinting polymer fiber described in this dissertation have been prepared using bulk polymerization, and solution polymerization, respectively.

In contrast to homogeneous polymerization used to produce a block of polymer, heterogeneous polymerization is used to produce smaller polymer particles, and has a wide range of application in industry, such as the paint, surface coating, chromatographic stationary phases, immunoassay sorbent, drug delivery, etc. Techniques of heterogeneous polymerization include suspension, dispersion and emulsion polymerization. They have different general characteristics and produce particles with different sizes (Table 2-1) [72]. The polymer particles used in this dissertation have been prepared by suspension and dispersion polymerization.

Table 2-1. Comparison of heterogeneous polymerization systems

Process	Suspension	Dispersion	Emulsion
Continuous Phase	Aqueous	Organic	Aqueous
Particle Size	10 μm -10mm	0.1-15 μm	0.05-5 μm

2.3 Suspension Polymerization

Suspension polymerization is a process in which the monomer or mixture of monomers is dispersed as fine droplets by mechanical agitation in a continuous aqueous phase (usually water). The monomer droplets are polymerized while they are dispersed

by continuous agitation. Equilibrium between breakup and coalescence/coagulation of droplets/particles is established using strong agitation and dispersing agents. This process is also known as pearl polymerization, bead polymerization, and granular polymerization. A free radical initiator is dissolved in the monomer droplets and polymerization is carried out by heating it to a certain temperature. Since the initiator is usually insoluble in water and soluble in the monomer droplets, each individual droplet acts as a small bulk polymerization system and the kinetics of polymerization usually follows bulk polymerization kinetics.

In addition to mechanical agitation, a combination of a dispersing agent and stabilizing agents is required to stabilize the resulting suspension and also control the size of monomer droplets. Agitation provides (a) the shear stress needed for the droplet/particle breakup and (b) the flow needed for homogeneous distribution of droplets/particles in the polymerization mixture. Dispersing agents and stabilizer have two functions: (a) reduce the interfacial tension at the droplet surface, and (b) create a protective layer around the droplet/particle to protect it against coalescence/coagulation. Several types of dispersing agents are used, including poly (vinyl alcohol), gelatin, hydroxyethyl cellulose, and sodium poly (acrylic acid), etc.

The particle sizes of the final product from suspension polymerization are from 10 to 1000 μm diameter [72]. The particle size is determined by numerous parameters like addition of colloids, stirring conditions, reactor geometry and so on. The product of the polymerization can be uniform spherical beads of polymer if the conditions are optimized, otherwise large lumps of polymer can be formed if coalescence takes place. Suspension polymerization has been used for large-scale industrial free-radical polymerization of

many olefinic monomers. Both homopolymers and copolymers of monomers such as methyl methacrylate, styrene, vinyl acetate and vinyl chloride can be readily made by this technique [72].

2.4 Dispersion Polymerization

Dispersion polymerization is a newer polymerization method. This method involves monomer, stabilizer and initiator dissolved in organic solvent to polymerize, followed by the formation of insoluble polymer particles dispersed in the oil media by the stabilizer. The resulting polymer particles are in the size range of 0.01-10 μm . In this process the polymerization begins as solution polymerization but become to heterogeneous polymerization upon stabilization of the polymer particles.

Dispersion polymerization was invented by Osmond and coworkers at ICI [73] and is really a modified precipitation polymerization. The critical condition for such a reaction is that the monomer to be polymerized must be soluble in the dispersion medium while its polymer must be insoluble.

2.4.1 Components of Dispersion Polymerization

The main components of a typical dispersion polymerization include the monomers, initiator, stabilizer, and dispersion solvent. Initially, all of the components are soluble in the dispersion solvent to obtain a homogeneous solution. After initiation of the reaction, the solution remains transparent for around 5 minutes. After that, the reaction mixture becomes cloudy as the nuclei formed. These nuclei are well stabilized against

coagulation so the particles continue to grow as discrete mature particles until the reaction is terminated.

Monomers

A wide range of monomers can be used in dispersion polymerization. They can be water-soluble or oil-soluble but must satisfy the critical requirement that monomer is soluble in the dispersion medium while its polymer is not. Monomers such as styrene, vinyl chloride, methyl methacrylate, vinyl acetate, acrylonitrile, acrylamide, and acrylic acid, etc have been used [73]. In principle, dispersion copolymerization is also possible with two or more monomers; however, few studies have been reported [73]. In this dissertation dispersion copolymerization of propylacrylamides and methacrylic acid has been investigated.

Steric Stabilizer

The stabilizer is a very important component for forming polymer particles that are not coagulated. Three types of stabilizers have been used successfully in dispersion polymerization: block and graft copolymers, homopolymers, and macromonomers [73]. Block and graft copolymers are amphipathic and very effective as steric stabilizers. Usually one portion or one block of the polymer stabilizer is insoluble in the dispersion medium so it will form an anchor to the surface of the growing particle while the other portion or block of stabilizer is soluble in the dispersion medium. The ratio of soluble block to the anchor block is an important variable. If the anchor/soluble block ratio is larger than a critical number, stable particles can not be obtained, even though the

stabilizer is soluble in the dispersion medium. Poly (styrene-co-acrylonitrile) is an example of block copolymer that has been used and investigated in this dissertation. 30% styrene is the suitable anchor percentage ratio for our dispersion polymerization using acetonitrile as a dispersion medium.

Homopolymers usually contain labile hydrogen atoms. The hydrogen abstraction of these polymers leads to the grafting of monomer in solution to produce an amphiphathic copolymer which can be used as a steric stabilizer. Macromonomers are relatively low molecular weight polymers and actually are stabilizer precursors.

Initiators

The most important requirement of initiator is that it is soluble in the dispersion medium and monomer so that it can initiate the polymerization. Different initiators produce significant differences in the final product because of their different solubility in the dispersion medium. Two types of free radical initiators, peroxide (e.g. benzyl peroxide, potassium persulfate), or azo (e.g. azobisisobutyronitrile) have been used in this work.

Dispersion medium

The dispersion medium must satisfy the requirement that it dissolves the monomers but not the final polymer. It also must dissolve initiator and the steric stabilizer. Early studies involved aliphatic hydrocarbon fluids as dispersion media while more recently polar solvents, such as alcohol, water, or water-alcohol mixtures [40], have

been used. In this work acetonitrile was used for acrylate / acrylamide based monomers, such as N-isopropylacrylamide (NIPA) and methacrylic acid (MAA).

2.4.2 Particle Formation and Growth in Dispersion Polymerization

Figure 2-4 shows the main steps of particle formation and growth in a dispersion polymerization [74]. At the beginning, all components including monomers, initiator, stabilizer and solvent are mixed in a homogeneous solution. Once the temperature is increased, the initiator decomposes to give free radicals which then add to the vinyl group of the monomers resulting in oligomeric radicals. When oligomers grow to a critical chain length, they precipitate from solution and begin to graft with stabilizer to form particle nuclei. These nuclei then collide with each other via homocoagulation, self-nucleation, or aggregation to form a large polymer species. The polymer species continue to grow by further polymerization giving mature particles when enough stabilizers have been grafted and adsorbed to the particles. Continued growth may occur by accretion of dead polymer to give the final particles.

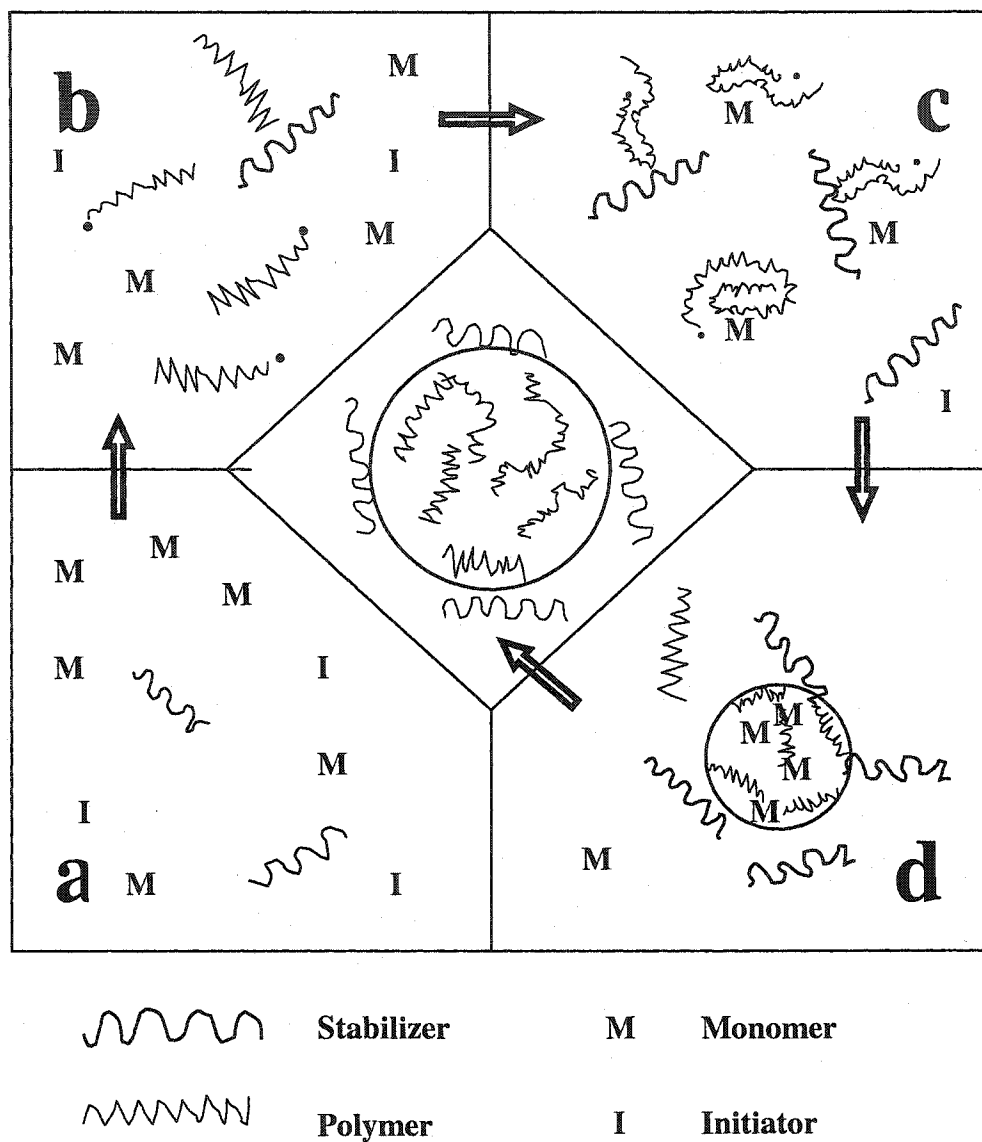


Figure 2-4. Schematic of particle growth in dispersion polymerization. (a) Homogeneous polymer solution. (b) Oligomeric radicals. (c) Self-nucleation and aggregation. (d) Particle growth. (e) Continued growth

2.5 Theory of Polymer Swelling

When slightly crosslinked polymer is placed in a compatible solvent, it will absorb solvent swelling instead of dissolving in the solvent. As mentioned in the introduction, there are two types of polymer swelling: nonionic polymer swelling and ionic polymer swelling [36, 75]. The swelling extent depends on the balance of solvation and retractive forces, and the charge density on the polymer compared to the charge density in the external solvent. Swelling phenomenon is a critical problem when polymers are used as the stationary phase for column chromatography. Unwanted polymer swelling leads to very low column efficiency. Polymer swelling, however, is an advantage for sensors based on refractive index changes. Good sensor response can be obtained if there is a large degree of swelling accompanying the changes of analyte concentration.

2.5.1 Swelling of Nonionic Polymer

There are two main factors that affects swelling of a nonionic polymer network: the degree of crosslinking and polymer-solvent interaction. Nonionic polymers swell because of the absorption of solvent into the polymer network with a resulting increase in volume. In the mean time, this solvation is counterbalanced by the retractive forces of crosslinking to reach an equilibrium state. Flory [75] described the swelling equilibrium of nonionic polymer gels by the following equation:

$$q_m^{5/3} \cong \frac{(\bar{v}M_c)\left(1 - \frac{2M_c}{M}\right)\left(\frac{1}{2} - X_1\right)}{V_1} \quad (1)$$

where :

q_m = equilibrium swelling ratio

\bar{v} = specific volume of the polymer

M_c = molecular weight per crosslinked unit

M = molecular weight of the polymer network

X_1 = polymer-solvent interaction parameter

V_1 = molar volume of the solvent

The swelling ratio, q , is equal to the ratio of the volumes of the swollen (V) and unswollen (V_o) structures. The subscript m indicates maximum, or equilibrium swelling. Equation (1) shows that the swelling ratio depends on the degree of crosslinking and the compatibility of the solvent and polymer, as expressed by X_1 . In a good solvent, the equilibrium swelling ratio decreases with an increase of crosslinking due to the decrease in the average molecular weight of a crosslinked unit, M_c . The second term, $(1-2M_c/M)$, is the correction for network imperfection resulting from chain ends. The equilibrium swelling ratio also decreases with the increase in the primary molecular weight, M .

2.5.2 Swelling of Ionic Polymer

In addition to the degree of crosslinking and the solvent's compatibility with the polymer, the swelling of polymer with ionizable functional groups also depends on the number of charges on the polymer backbone. The swelling of ionic polymers has been described by Flory [75] as:

$$q_m^{5/3} \cong \frac{\left(\frac{i}{2V_u \sqrt{S}} \right)^2 + \frac{\left(\frac{1}{2} - X_1 \right)}{V_1}}{\frac{v_e}{V_o}} \quad (2)$$

where,

q_m = equilibrium swelling ratio

i = number of electronic charges per polymer unit

V_u = molecular volume of polymer repeating unit

S = molar ionic strength

X_1 = interaction parameter

V_1 = molecular volume of solvent

v_e = effective number of chains in network

V_o = volume of unswollen polymer network

It can be seen that the equilibrium swelling ratio depends on both the electrostatic repulsion of charges on the polymer backbone, as shown in the first term, and the polymer-solvent interaction, as shown in the second term. Large charge density (i/V_u) on the polymer network or low ionic strength (S) in the solution increases the swelling ratio. High ionic strength decreases swelling because of the shielding of the charges by mobile ions.

An osmotic pressure effect is the other explanation for ionic polymer swelling [30]. If the charge density of the polymer is higher than that of surrounding solvent, the

solvent will enter the polymer and balance the difference of charge density. This increase of solvent content in polymer results in the polymer swelling.

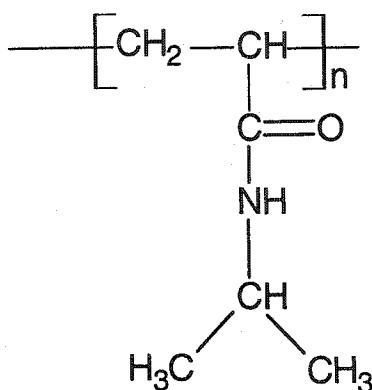
The charge density on polymer backbone is usually the most important parameter affecting ionic polymer swelling. The overall swelling degree of ionic polymers is dependent on the charge density, the solvent-polymer interaction, the level of crosslinking, and ionic strength.

2.6 Swelling Behavior of Thermosensitive Poly N-Isopropylacrylamide Polymers

Some polymers or gels can exist in two states, swollen and collapsed. The transition between these two phases is called the volume phase transition. This is an important characteristic of polymer gels and has been an exciting topic of polymer science. This transition is a coil-to-globule transition of each of the constituent polymer chains [70]. The gel volume can change up to 1000-fold [76]. Transition can be induced reversibly by external conditions such as temperature, pH, ionic strength, solvent composition, etc. because these stimuli can change the interaction of network polymer-polymer, polymer-solvent. Those interactions are classified into the van der Waals force, the hydrogen bonding, hydrophobic interaction, and electrostatic interaction [70]. Numerous stimuli make these polymer materials potentially suitable candidates for a wide variety of applications including actuators, selective membranes, and drug delivery.

Poly (N-isopropylacrylamide) (poly NIPA, 1) is a typical stimuli-sensitive polymer and has been appearing in the literature with increasing frequency over the last decade (Figure 2-5). The main application of poly NIPA has been its novel thermal behavior in aqueous media. It has become the most popular member of a class of

polymers that have inverse solubility upon heating; they are swollen at lower temperature and shrunken at high temperature. The volume change results from the coil-to-globule transition of the polymer chain driven by hydrophobic interaction. This transition from a hydrophilic to a hydrophobic structure occurs rather suddenly at a temperature which is termed the lower critical solution temperature (LCST) or simply called the transition temperature. Experimentally, the LCST of poly NIPA lies between ca. 30 and 35°C while the exact value of LCST depends on the detailed microstructure of the macromolecule [70].



(1)

Poly NIPA can be synthesized by a variety of methods. Free radical initiation of organic solutions and redox initiation in aqueous media have been the most widely used techniques to prepare poly NIPA in many forms including single chains, macroscopic gels, microgels, latexes, thin films, membranes, coatings, and fibers [70]. In this dissertation two types of initiators have been used to make poly NIPA microspheres via suspension and dispersion polymerization.

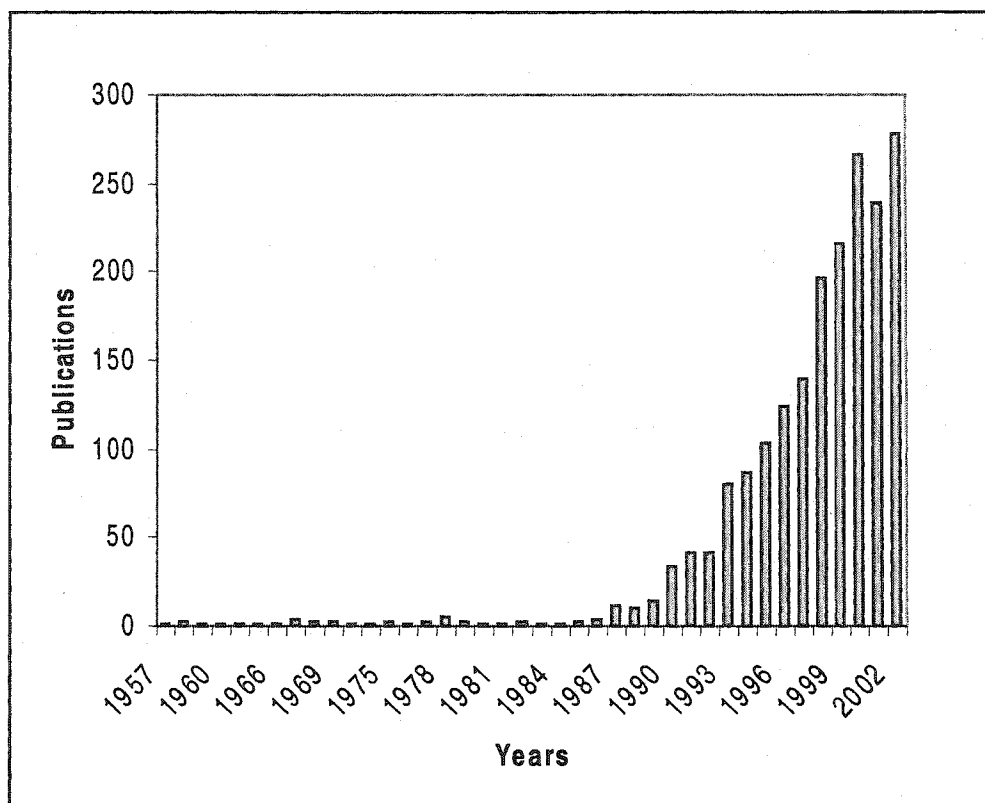


Figure 2-5. Publications of poly NIPA from Scifinder search results.

It has been demonstrated that chemical structure dramatically affects the polymer swelling behavior and the LCST values. For instance, in the case of thermosensitive polymers, the presence of ionic groups in the polymer structure can lead to a discontinuous phase transition and increase in the LCST; the ratio of hydrophobic to hydrophilic units in the polymer or side chains also play an important role in adjusting the LCST of thermo-sensitive systems. Seker investigated the swelling properties of a series of N-alkylacrylamide hydrogels for which the alkyl substituent was methyl, ethyl, isopropyl, n-propyl, and t-butyl [76]. It was shown that lengthening the side chain can strongly affect the transition temperature of polymer gels. In general, larger alkyl chains produced a dramatic decrease in polymer transition temperature. The transition

temperature for ethyl, iso-propyl, and n-propyl N-alkylacrylamide polymers are around 80, 36, 25°C, respectively. Methyl and t-butyl N-alkylacrylamide polymers were found to have no obvious phase transition while increasing the temperature from 20 to 80°C. In this dissertation, copolymers have been synthesized by mixing small amounts of n-propyl or t-butyl N-alkylacrylamide monomer with NIPA to decrease the transition temperature of resulting polymers so that our sensor can be conveniently applied at room temperature.

2.7 Optical Measurements of Microspheres Embedded in Hydrogel Membranes

As stated in introduction, our group has been developing optically-sensitive membranes for chemical sensors. These membranes contain swellable polymer microspheres designed to sense analytes. The refractive index of the hydrogel membrane remains constant and is not sensitive to analytes. When the membrane is placed in sample solution, the microspheres will swell or shrink with changing analyte concentration. The changes in the optical properties of the membranes can be measured as reflected or scattered light or as membrane turbidity.

When light passes through a medium with suspended microspheres, reflection and scattering take place. Scattering is caused by suspended microspheres and happens only if the microspheres are smaller than $(3/2)$ wavelength and the refractive index is different from the medium. Reflection occurs at the phase boundaries if there is a refractive index difference between the medium and its surroundings. The amount of reflected light can be described by the Fresnel equation:

$$R = \frac{(n_2 - n_1)^2}{(n_2 + n_1)^2} \quad (3)$$

where,

n_1 = refractive index of material 1

n_2 = refractive index of material 2

If refractive indices are close together, there is less reflection. These occur in most of our sensor systems.

The change in refractive index is the principle parameter governing the amount of light reflected and scattered. It can be measured as a change of membrane turbidity, which is determined in our lab by measuring “absorbance” in a spectrophotometer. In this case, the decrease in transmitted light intensity is actually due to reflection/scattering rather than absorption. The intensity of transmitted light obeys the following equation:

$$I = I_o e^{-\tau b} \quad (4)$$

Where,

I = intensity of light passing through the sample

I_o = intensity of incident light

τ = turbidity

b = pathlength (cm)

Turbidity can be solved as:

$$\tau = \left(\frac{2.303}{b} \right) \log \frac{I_o}{I} \quad (5)$$

This equation is similar to Beer's law. In this dissertation turbidity ("absorbance") was used to measure the extent of polymer swelling and shrinking.

2.8 Molecularly Imprinted Polymers

The concept of molecular imprinting came from Pauling's theories about antibodies in which an antigen is used as a template to form the antibody polypeptide chains to get a configuration that complements the antigen molecule [50, 77]. As a consequence of these theories, chemists conceived the idea that the same concept could be used to form a templated synthetic matrix (analogues of antibodies) that can recognize target molecules (analogues of antigens) with high selectivity. A variety of attempts were made in the following decades and now molecular imprinting is recognized as a powerful and promising technique for the preparation of synthetic polymers with predetermined specificity.

2.8.1 Molecular Imprinting Process

The molecular imprinting process can be described as a way of making artificial "locks" for "molecular keys". Figure 2-6 illustrates the principle of the imprinting, which involves four main steps:

- a. The selected template molecule is in the first step mixed with functional monomers.

- b. Complex formation of the template (print) molecule with the functional monomers (rearrangement steps)
- c. Polymerization of the resulting printing complex with an excess of cross-linking agent in an inert solvent to form a rigid polymer.
- d. Removal of the template molecule by hydrolysis or extraction.

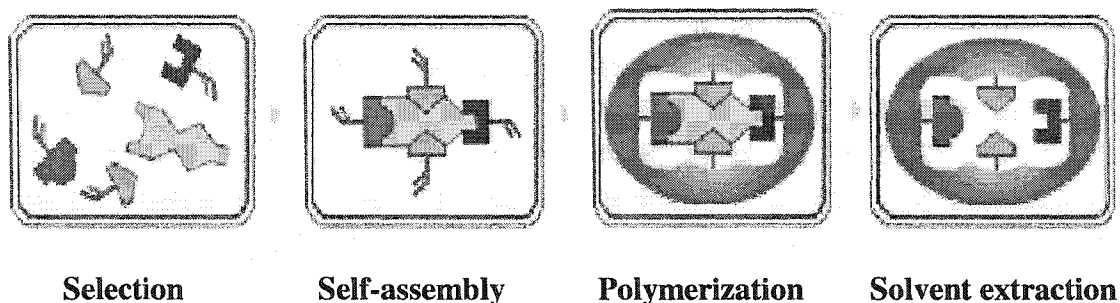


Figure 2-6. Schematic representation of the molecular imprinting principle

According to the chemical bonding involved in molecular imprinting, this technique can be classified into two systems: covalent bonding-based and noncovalent bonding-based molecular imprinting [44, 45, 48, 50].

Covalent Imprinting

Covalent molecular imprinting, also called pre-organized imprinting, was suggested and has been intensively studied by Wulff and co-workers [43]. Their pioneering work has led to further development of novel molecular imprinting systems. In covalent imprinting process, reversible covalent bonds are formed between template

and functional monomer. These covalent bonds include ester, acetal/ketal, Schiff-base, metal coordination, etc [44]. These bonds are relatively strong and can keep template-monomer complexes stable during the imprinting process resulting in high specific and homogeneous binding sites. However, there are several disadvantages for this technique, such as slow binding kinetics that may not be suitable for chromatographic separation and sensor, and lack of suitable covalent bonds which can be cleaved easily and re-bound.

Noncovalent Imprinting

Noncovalent (self-assembly) molecular imprinting, pioneered by Mosbach and co-workers, is the simplest approach for producing polymers with specific bonding properties. Monomer species first self-assemble around the template and then interact with the template via hydrogen bonding, electrostatic interactions, hydrophobic interactions, etc [44, 50]. The advantages of noncovalent imprinting are: (1) the procedure is simple and easy to perform; (2) the choice of functional monomer is more flexible; (3) the template is easy to remove from resulting polymer under mild conditions. However, the interactions in this process are not strong enough to maintain template-monomer complexes. Hence, an excess of functional monomers is usually used for complete complexation and to keep the complex stable during polymerization. Noncovalent molecular imprinting is more attractive because self-assembly and interactions between template and monomer are similar to biological systems so that this approach can be used to make biomimetic materials.

2.8.2 Polymer Composition

Templates

Since the binding strength and specificity of the MIP is dependent upon the template structure properties, such as the number and type of interaction sites and the template shape, ideal templates must satisfy with several requirements [50]: (1) multiple sites of interactions with the functional monomer. These are likely to yield binding sites with higher specificity and affinity for the template; (2) higher basicity to enhance the hydrogen bonding between the base and acid (if template is acid or base) so that there is a notable increase in affinity and selectivity; (3) sufficient shape and size to create steric complementarity for efficient discrimination between two molecules; (4) rigid conformation that can fit in the cavity of the polymer with minimal change during polymerization. This will increase the affinity and selectivity of recognition, because there will be minimal loss in entropy due to conformation changes in the site and in the template after binding if templates fit perfectly into the site [78].

In addition to template structure properties, the ratio of the template to the functional monomer is also very important for the specificity and sensitivity in the imprinted polymer. Usually an excess of monomer is used to produce more favorable results.

Type of Monomers

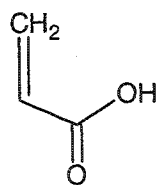
The type of functional monomer is very important for making a useful MIP because it is the component that interacts with template. In order to form recognition sites in the polymer matrix, the functional monomer is required to interact strongly with the

template. Generally, if analytes contain basic functional groups, monomers containing acidic functional groups are best for imprinting, and vice versa. Figure 2-7 illustrates the structures of common functional monomers used for MIPs [50]. Methacrylic acid is one of the most widely used monomers. It can interact via acid-base interaction with the amine group or via hydrogen bonding with a variety of polar functionalities such as RCOOH, RCOOR, NH₂COOR, etc [79].

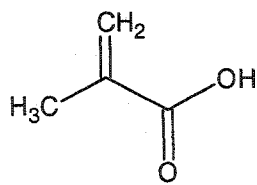
Type of Crosslinker

In the imprinting process, the percent crosslinking is a critical variable. Usually a very high degree of cross-linking is used to achieve high specificity and selectivity. This is because high rigidity can maintain functional groups in a stable arrangement complementary to the template after the template is removed [50].

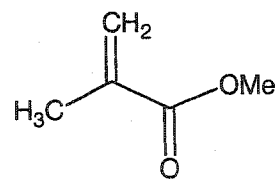
N,N'-Methylene-bisacrylamide (MBA) and ethylene glycol dimethacrylate (EDMA) have been widely used as crosslinkers in noncovalent molecular imprinting [60, 79]. New crosslinkers have also been studied. For example, trimethyl propane trimethyl acrylate (TRIM) has been used to prepare a MIP with high load capacity and excellent resolving capacity [79, 80].



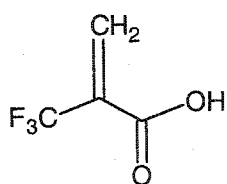
Acrylic acid



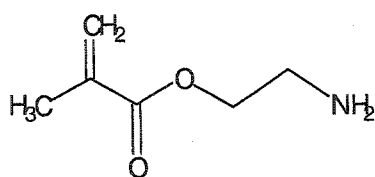
Methacrylic acid



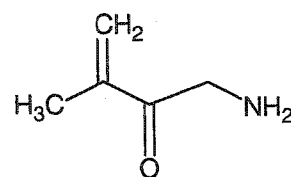
Methyl methacrylate



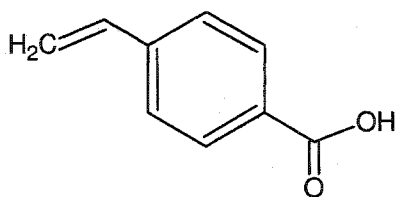
Trifluoromethacrylic acid



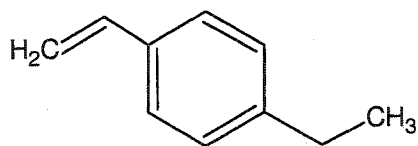
Diethylaminethyl methacrylate



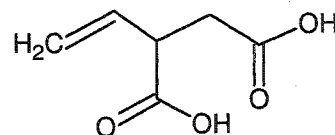
Allylamine



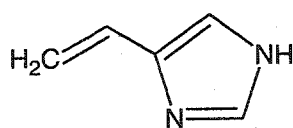
p-Vinylbenzoic acid



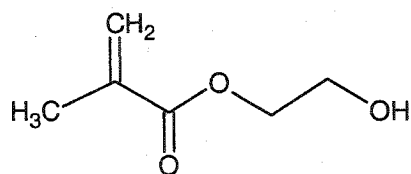
4-Ethylstyrene



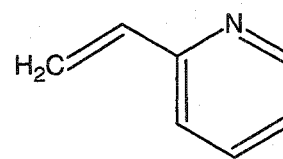
Itaconic acid



4-Vinylimidazole



2-Hydroxyethyl methacrylate



2-Vinylpyridine

Figure 2-7. Common functional monomers for MIP production.

The Effect of Temperature and Pressure

Temperature and pressure are very important experimental variables during polymerization of MIPs. At low temperature, the monomer-template complexes are more stable due to more favorable entropy leading to efficient imprints in the resulting polymer. In this dissertation, norephedrine templated poly NIPA-AAc microspheres were prepared via suspension polymerization at room temperature using an oxide initiator.

It was reported that the affinity and selectivity was 30% higher in a MIP prepared at 100 bar compared with one at a pressure of 1 bar [81]. This is because pressure can stabilize the monomer-template assemblies during polymerization. In this work, theophylline templated poly NIPA-MAA microspheres were prepared via dispersion polymerization at 70°C in a sealed flask (high pressure).

2.8.3 MIP Microspheres

MIPs can be prepared in several formats. The most common approach is to synthesize the MIP in bulk to form a macroporous monolith that is then ground and sieved to obtain the particles with the desired size range. This method is simple and the optimization of imprinting conditions is relatively straightforward. However, the grinding and sieving process is tedious and time-consuming, and only a part of polymer can be recovered as useful particles. The ground particles are not uniform but polydisperse both in shape and size, which is not ideal, especially for chromatographic application. The grinding process may also damage some of the binding sites. More uniform MIP microspheres are highly preferred for many applications such as competitive ligand binding assay, solid-phase microextraction (SPME), sensor, and chromatography.

Emulsion and seeded emulsion polymerization in aqueous media [82] and suspension polymerization in perfluorocarbon [83] have been introduced to solve some of above issues and prepare particles that are monodisperse in size and shape. However, the former methods require an aqueous phase, which can interfere with the imprinting process while the latter method is not straightforward and requires a special dispersing phase and fluorinated surfactant, which is difficult to remove from the surface of micrpspheres. Precipitation polymerization has also been used to prepare MIP microspheres [80]. Very high level of crosslinker (EDMA or TRIM) were used to obtain polymer microspheres without using any surfactant.

In all reported methods for preparing MIP microspheres, a very high degree of crosslinking is used. It is the necessary to obtain high specificity and selectivity. This also leads to high rigidity that prevents from swelling. However, swellable MIP microspheres are required for our sensor systems. A medium level of crosslinker was used to obtain uniform microspheres and also ensure high specificity and sensitivity.

CHAPTER 3

EXPERIMENTAL

3.1 Reagents

Aldrich Chemical Company, Inc., Milwaukee, WI 53233

2, 2'-Azobisisobutyronitrile (AIBN), 98%, F.W. 164.21, m.p. 103-105 °C

Poly(vinyl alcohol) (PVA), 100% hydrolyzed, average MW 14,000

Poly(vinyl alcohol) (PVA), 87-89% hydrolyzed, average MW 85,000-146,000

N-Isopropylacrylamide (NIPA), 97%, F.W. 113.16, m.p. 60-63 °C, b.p. 89-92 °C

N-tert-Butylacrylamide (NTBA), 97%, F.W. 127.19, m.p. 128-129 °C

Acrylic acid (AAc), 99%, F.W. 70.06, b.p. 139 °C

Dioxane, anhydrous, 99.8%, F.W. 88.11, b.p. 100-102 °C

Tris (hydroxymethyl) propane trimethacrylate (TRIM), F.W. 338.40

Chloroform, 99.8%, HPLC grade, F.W. 119.39, b.p. 60.5-61.5 °C. It was passed down a basic alumina column to remove ethanol and stored over molecular sieves for use as a solvent to make polymeric surfactants.

(1R, 2S)-(+)-Norephedrine hydrochloride, 99%, F.W. 187.67, m.p. 174-176 °C

Benzoyl peroxide (BPO), 97%, F.W. 242.23, m.p. 104-106 °C

Methacrylic acid (MAA), 99%, F.W. 86.09, b.p. 163 °C

Theophylline (THO), 99%, F.W. 180.2, m.p. 271-273 °C

Caffeine, 99%, F.W. 194.19, m.p. 234-236.5 °C

Acetonitrile, anhydrous, 99.8%, F.W. 41.05, b.p. 81-82 °C

Methyl sulfoxide (DMSO), 99.9%, F.W. 78.13, b.p. 189 °C

Sodium acetate, 99%, F.W. 82.03,

Sodium phosphate: NaH_2PO_4 , Na_2HPO_4

Sodium hydroxide, 97%, F.W. 40.00

Sodium chloride, 99%, F.W. 58.44

Acetic acid, glacial, 99.99%, F.W. 60.05, b.p. 117-118 °C

Methanol, 99%, F.W. 32.04, b.p. 64.7 °C

Ethanol, 95%, F.W. 46.07

Hydrochloric acid, 36.5-38.0%, F.W. 36.46

Sigma Chemical Company, PO BOX 14508, St. Louis, MO 63178

(±) Epinephrine (adrenaline), F.W. 219.7.

Bio-Rad Laboratories, 32nd & Griffin Ave., Richmond, CA 94894

N,N'-Methylene-bis-acrylamide (MBA)

Monomer-Polymer & Dajac Labs, Inc.

N-(n-Propyl) acrylamide

Polysciences, Inc., Warrington, PA

Poly(ethylene glycol) 1000 monomethyl ether monomethacrylate (PEG
1000MME monomethacrylate)

Oakwood Products, Inc.

Acryloyl 2-(N-Ethylperfluoroalkylsulfonamide)ethanol (Acryloyl PFA-1)

SP² Scientific Polymer Products, Inc.

Styrene/acrylonitrile copolymer, pellets, 30% acrylonitrile.

Fisher Scientific Company, Fair Lawn, NJ 07410

Glutaraldehyde, 50% aqueous solution

Acetone, F.W. 58.08, b.p. 56.01C

HYMEDIX International, Inc. Dayton, NJ 08540

HYPAN HN 50, HN68, and HN80 Structural Hydrogels

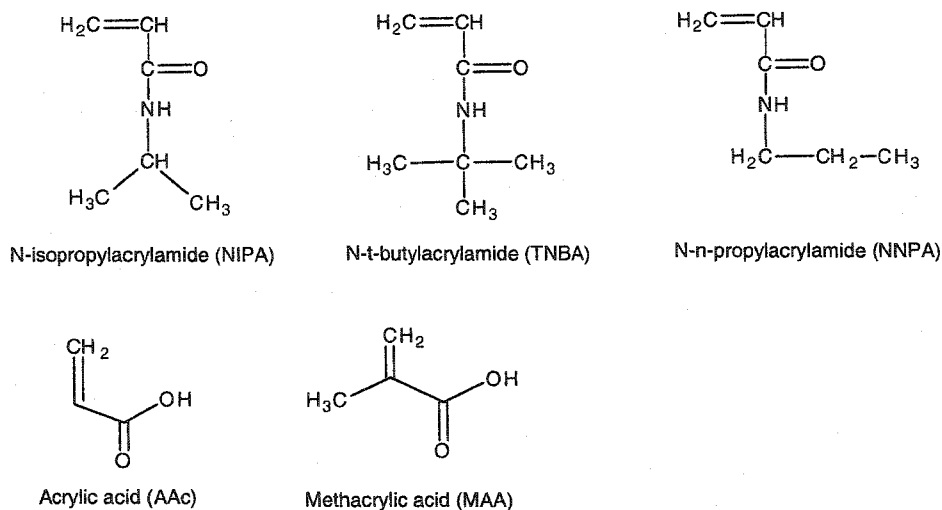
Bayer Corporation, Pittsburgh, PA

Bayhydrol 110 waterborne polyurethane

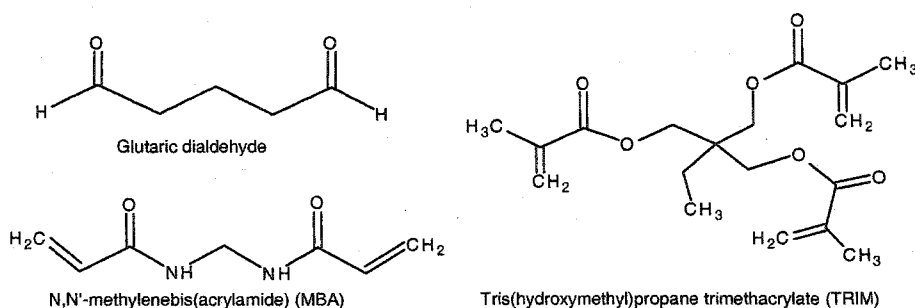
Unless otherwise specified, all buffers were prepared at 0.1 M buffer concentration and adjusted to 0.1 M ionic strength with sodium chloride. Aqueous solutions were prepared from doubly deionized distilled water prepared from a Corning Mega-Pure distillation apparatus.

Figure 3-1 illustrates the structures of major reagents used for preparation of molecularly imprinted polymer microspheres and hydrogel membranes.

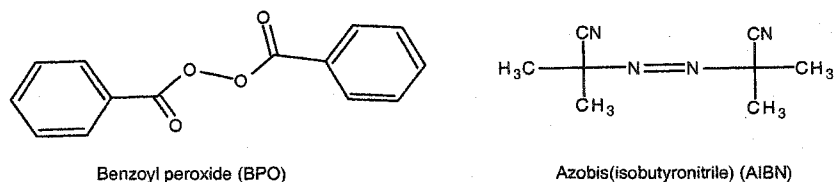
MONOMERS



CROSSLINKERS



INITIATORS



HYDROGEL POLYMERS

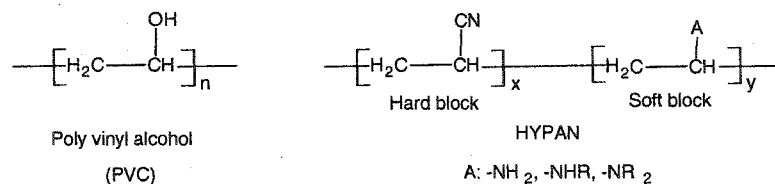


Figure 3-1. Structures of monomers, crosslinkers, initiators and polymers used for preparation of microspheres and hydrogel membranes.

3.2 Apparatus

A Cary 5 UV/Vis/NIR spectrophotometer was used for turbidity measurements, spectral scanning, kinetic studies and temperature scanning; A Fisher laboratory centrifuge (3400 rpm) and an RC5C superspeed refrigerated centrifuge from Beckman (Palo Alto, CA) were used to separate and wash polymer microspheres; A Branson model 1210 sonicator was used for cleaning microspheres or suspending microspheres in solvent; An Amray 3300FE scanning electron microscope (SEM) was used to determine microsphere diameters; A Bausch and Lomb Abbe refractometer was used to measure refractive index; A Fisher Scientific microscope was used to observe emulsified droplets and microspheres and a Carl Zeiss KS200 microscope was used to measure particle size and distribution; An Orion 901 digital analyzer with an Orion 91/55 combination pH meter was used to monitor pH during buffer preparation. A VWR 1217 reciprocal shaker bath and 5831 vacuum heater were used to synthesize and dry fluorinated surfactant.

All glassware, 150 mL three neck reaction vessels, stirring apparatus, hot plates were purchased from VWR.

3.3 Procedures

3.3.1 Preparation of Norephedrine Templated Poly NIPA-AAc Polymer Fibers by Solution Polymerization [69]

Thermosensitive copolymer fibrous gels consisting of NIPA and acrylic acid (AAc) have been prepared in the presence and absence of norephedrine template molecule. NIPA is the monomer for forming thermosensitive polymer and AAc is the functional monomer which interacts with the template molecule, norephedrine, via

hydrogen bonding. Figure 3-2 illustrates the polymerization reaction and Table 3-1 shows a typical formulation for a 15 mL batch size. Sixteen mmole of NIPA, 4 mmole of AAc, 1 mmole of N,N-methylene-bis-(acrylamide) (MBA), and 0.08 mmole of benzoyl peroxide (BPO) were dissolved in 15 mL 1,4-dioxane. *dl*-Norephedrine hydrochloride (2 mmole) was added into the solution. Some of the template molecule remained undissolved due to limited solubility. The resulting mixture was degassed and purged with nitrogen for 5 min. N, N-Dimethylaniline was then added under a constant stream of nitrogen to speed up the rate of decomposition of BPO. This initiates redox polymerization so that heating is not needed. Polymerization was carried out for 12 hour at 25 C in a sealed 100 mL round bottom flask in which glass capillaries with inner diameter of 150 μ m were immersed in solution before initiation. The turbid gels phase separated from the solution as they formed during polymerization. Fibrous gels were taken out from the capillaries and washed with water/acetic acid mixture (9/1 in volume) to extract norephedrine from gels and then washed with water several times. The clean MIP fibers were kept in water for use. The untemplated polymer gels were also prepared by the same procedure without template. Adrenaline templated fibrous gels were also prepared in the same way and used to examine the specificity of MIP gels.

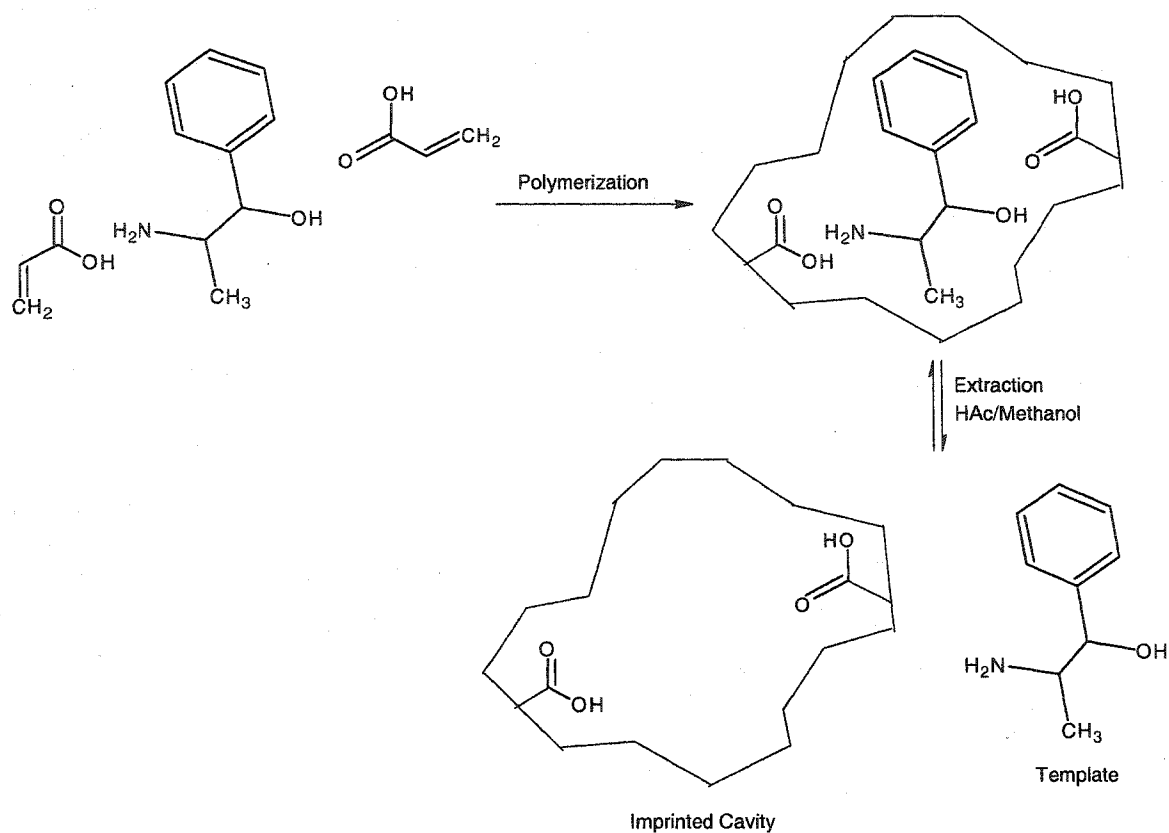


Figure 3-2. Polymerization reaction used to prepare MIPs selective for norephedrine.

Table 3-1. A typical formulation of synthesis of norephedrine templated poly NIPA-AAc polymer fibers.

Reagent	Amount
NIPA	1.81g (16 mmole)
AAc	0.288g (4 mmole)
MBA	0.154g (1 mmole)
BPO	0.018g (0.08 mmole)
DMA	10 uL (0.08 mmole)
Norephedrine	0.375g (2 mmole)
1,4-Dioxane	15 mL

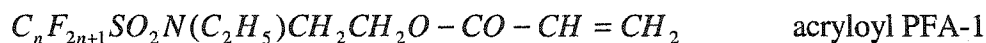
3.3.2 Preparation of Norephedrine Templated Poly NIPA-AAc Microspheres by Suspension Polymerization Using a Liquid Perfluorocarbon as Dispersing Phase

Synthesis of polymeric surfactants

To create reasonably stable emulsion droplets containing monomers, crosslinker, template molecules for suspension polymerization, a suitable surfactant must be used as a stabilizer. Two polymeric surfactants were prepared for our suspension system [83].

1. Poly (acryloyl PFA-1)

Acryloyl PFA-1 (8g, 14.4 mmole) and AIBN (0.024g, 0.146 mmole) were dissolved in 10 mL of chloroform. Dissolved oxygen was removed by nitrogen sparging for 5 min. The flask was then sealed and polymerized at 60°C for 48 hour in a shaking water bath. The resulting solution was slightly turbid and became much more turbid on cooling. Sample was placed in a vacuum dryer at 30°C under reduced pressure (20 PSI, to avoid foaming) over night to remove most of the solvent by slow evaporation. The remaining solvent was removed under reduced pressure at 60°C. The resulting polymer was a sticky pale yellow paste, which was used without further treatment. The structure of poly (acryloyl PFA-1) and its precursor monomer are shown in Figure 3-3.



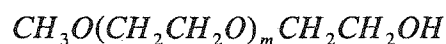
(where n averages 7.5)



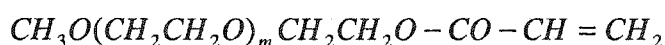
Figure 3-3. Structure of polymeric surfactant poly(acryloyl PFA-1) and the structure of acrylate precursors.

2. Poly (acryloyl PFA-1)-co-(acryloyl PEG1000MME) (termed PFPS)

A copolymer of acryloyl PFA-1 and acryloyl PEG1000MME (mole ratio 20:1) was prepared using the same procedure as poly(acryloyl PFA-1). PEG1000MME introduces hydrophilic side units to the polymer chain so that it can be easily removed from polymer surface after polymerization. Figure 3-4 shows the structure of PFPS and its precursor monomer.

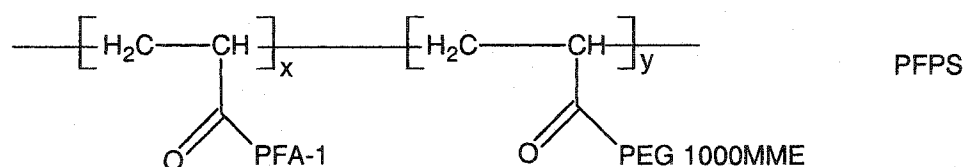


PEG1000MME



acryloyl PEG1000MME

(where m averages approximately 43)



(where x averages 19 and y averages 1)

Figure 3-4. The structures of PFPS and its precursor monomer.

Suspension polymerizations

Suspension polymerization involves two steps: emulsification and polymerization. Conventional suspension polymerization was first used to make molecularly imprinted particles using the above surfactants. Coagulated particles were always obtained until we started to carry out the polymerization in an ultrasonic bath as described in the following procedure.

PFPS surfactant (250mg) were added into 6 mL of dioxane in a 100 mL round bottom flask. Heat was needed to dissolve PFPS completely in dioxane. After cooling, monomer NIPA, functional monomer AAc, crosslinker MBA, and template norephedrine

were added and dissolved by stirring. PMC (20 mL) was then added and the mixture was degassed and emulsified in an ultrasonic bath for 5 min. BPO and DMA were added to initiate redox polymerization and the solution was purged with nitrogen for 15 min. Polymerization was carried out at room temperature under a gentle nitrogen stream for 12 hours. The resulting polymer particles were filtered on a sintered glass funnel, and the PMC was recovered. The particles were washed extensively with acetone to remove the surfactants and sonicated to break up loose aggregates of particles. Template molecule, norephedrine, was then removed by extraction using water/acetic acid (9:1 v/v) followed by washing with water several times. Particles were suspended in water for use in the following experiments. Table 3-2 shows a typical formulation for this suspension polymerization.

Table 3-2. Formulation for suspension polymerization of norephedrine templated poly NIPA-AAc MIP particles.

Phase	Components	Amounts
Suspension phase (Imprinting mixture)	NIPA	0.905g (8 mmole)
	AAc	0.144g (2 mmole)
	MBA	0.077g (0.5 mmole)
	Norephedrine	0.188g (1 mmole)
	PFPS	0.250g
	BPO	0.009g (0.04 mmole)
	DMA	5 uL (0.04 mmole)
	1,4-Dioxane	6 mL
Dispersing phase	PMC	20 mL

3.3.3 Preparation of Theophylline (THO) Templated Poly NIPA-MAA Microspheres by Dispersion Polymerization

Stabilizer (poly styrene-co-acrylonitrile, 20% w/v) was first dissolved in 50 mL of anhydrous acetonitrile in a 100 mL round-bottom flask by stirring. Template molecule (THO) was then dissolved (heat was needed to completely dissolve THO due to the low solubility of THO in acetonitrile). After cooling to room temperature, monomer (NIPA), functional monomer (MAA), crosslinker (MBA or TRIM) and initiator (AIBN) were added. The mixture was degassed for 5 min and purged with nitrogen for another 10 min. Then the flask was sealed under nitrogen. Polymerization was induced by placing the flask in a $70\pm 1^{\circ}\text{C}$ water bath and continued for 16 hours. The resulting MIP microspheres were collected by centrifugation at 10000 rpm for 10 min using an RC5C superspeed refrigerated centrifuge from Beckman. The template molecule was extracted by washing repeatedly with 20 mL methanol/acetic acid (9:1, v/v) for 5 x 1 hour, then with 20 mL acetone 3 x 1 hour to remove the stabilizer, followed by a final wash with the same volume of water. As a control, the untemplated microspheres were prepared and treated in exactly the same way, except that the template molecule was omitted from the polymerization stage. Figure 3-5 shows the polymerization reaction and Table 3-3 shows a typical formulation for this dispersion polymerization.

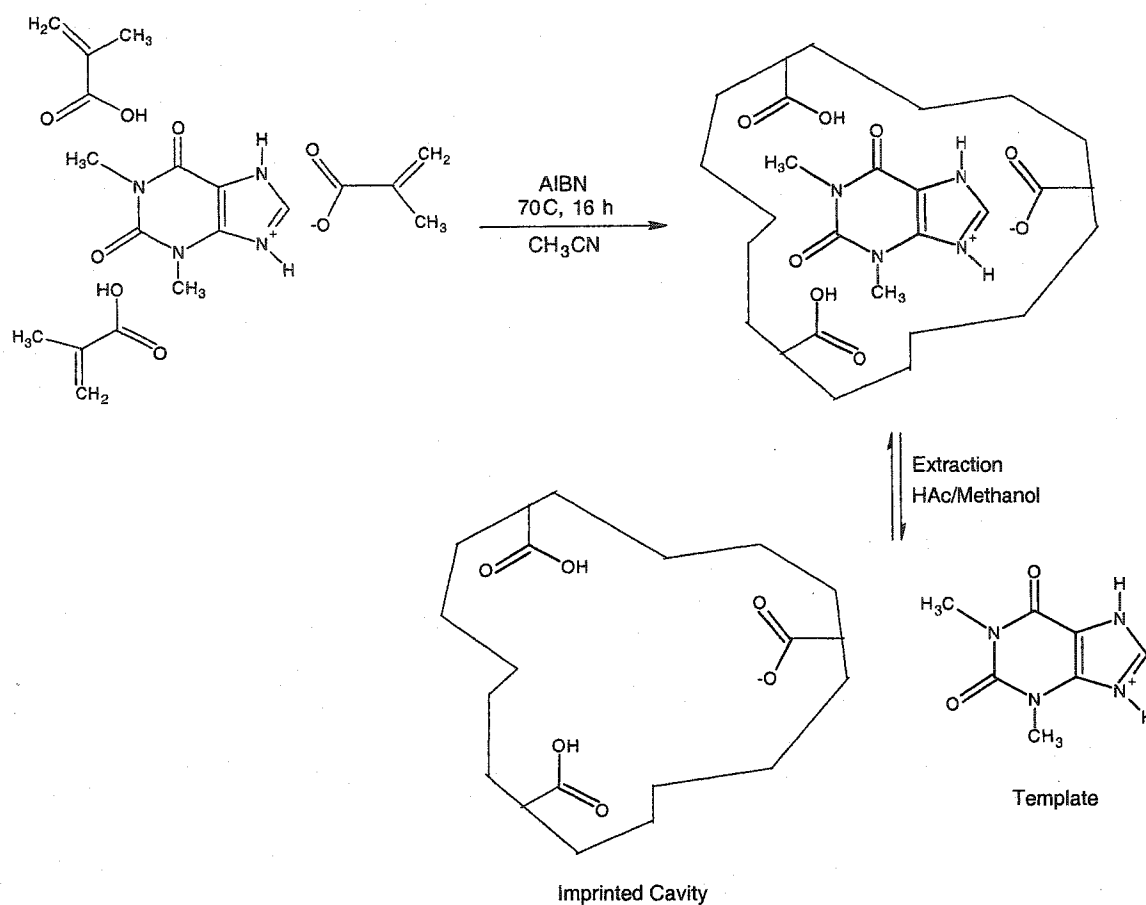


Figure 3-5. Polymerization reaction used to prepare MIPs selective for THO.

Table 3-3. A typical formulation for dispersion polymerization for THO templated poly NIPA-MAA microspheres.

Component	Amount
NIPA	1.923g (17 mmole)
MAA	0.172g (2 mmole)
MBA	0.154g (1 mmole)
THO	0.180g (1 mmole)
AIBN	0.045g (2% w/w)
Stabilizer	0.450g (20% w/w)
Acetonitrile	100 mL

Templated poly NIPA-NTBA-MAA, poly NNPA-MAA microspheres were also prepared in the same way, except that a portion or all of NIPA was replaced by NTBA or NNPA.

3.3.4 Preparation of Thermo-sensitive Poly NIPA Microspheres by Dispersion Polymerization

Polymerizations were carried out in a 100 mL round-bottom flask with a magnetic stirring bar and a condenser. NIPA and MBA were dissolved in 50 mL distilled water in the flask. After degassing for 5 minutes, the initiator KPS was introduced into solution while stirring. The mixture was purged with nitrogen for 15 minutes and then polymerized at 70 °C for 12 hour. Detailed recipes for this dispersion polymerization are given in Table 3-4. The resulting polymer microspheres were cleaned by repetitive centrifugations and dispersions using distilled water to remove free electrolytes and water-soluble polymer.

Table 3-4. Recipe for preparation of poly NIPA thermosensitive microspheres

Component	Amount
NIPA	2.036 g (18 mmole)
MBA	0.062 g (0.4 mmole)
KPS	0.042 g (2% w/w)
Water	100 mL

3.3.5 Preparation of Hydrogel Membranes

In our group, various hydrogel materials have been used for preparing membranes to embed the swellable microspheres for convenient turbidity measurements. Three of them were used and investigated in this work: poly vinyl alcohol (PVA), HYPAN, and polyurethane (PU). They have different characteristics (such as refractive index, water content, hydrophilicity, etc) and different methods of preparation (e.g. physical, chemical, radiation, etc). The ideal membranes for our sensors should have such characteristics as (1) low crosslinking (not too opaque), (2) intertness to analyte (e.g. pH, template molecule), (3) optical transparency, (4) sufficient mechanical strength, and (5) different refractive index from microspheres.

Poly(vinyl alcohol) membranes

Poly-vinyl alcohol (PVA) is a hydrophilic, water-soluble polymer with different degrees of hydration and molecular weight. PVA polymers with high hydration (e.g. over 90%) and low molecular weight (ca. 10,000-30,000) are suitable for preparing hydrogel membranes. The concentration of PVA solution affects the mechanical strength of membranes. PVA stock solution with lower concentrations results in membranes with poor mechanical strength. However, higher concentrations of PVA solutions are difficult to prepare and suspend polymer microspheres due to their high viscosity. 10%(w/w) stock PVA solutions were used in this work.

A 10% (w/w) solution of PVA (MW 13,000) was prepared. 20g of PVA were added to 180 mL distilled water in a beaker. A magnetic stir bar was used to stir the solution until PVA completely dissolved. It was then stored in a plastic bottle. A 10%

glutaraldehyde solution was prepared from a 50% stock solution and stored in a brown bottle in the refrigerator. A 4M HCl solution was used as the initiator. Below is a typical preparation procedure for PVA membranes [84].

1. 50 μ L of 10% (w/w) solution of microspheres were added to a small glass vial.
2. 10% PVA solution was added to bring the total mass to 1.0 grams.
3. Microspheres and PVA was then mixed using sonication to give a homogeneous suspension, which looks cloudy.
4. 25 μ L of 10% glutaraldehyde solution were added and the mixture was continually sonicated for about 5 minutes to ensure the homogeneous distribution of crosslinker.
5. 50 μ L of 4M HCl solution were added and sonicated or stirred but not longer than 1 minute. Otherwise, solution will polymerize before making a membrane.
6. A portion of the mixture was dropped onto a microscope slide with a 76 μ m thick Teflon spacer applied around the edges. The other microscope slide was placed on top as a cover. Both slides were tightened with clamps.
7. After gelation for at least one hour, the membrane was removed from the slides followed by washing. It was stored in distilled water for characterization and evaluation.

The thickness of the resulting membrane was controlled by the thickness of Teflon spacer applied to the microscope slides. The thickness of membranes is 76 μ m in following experiments, unless otherwise specified.

HYPAN polymer membranes [84]

HYPAN is a trade name for hydrophilic acrylate polymers with a unique multiblock copolymer structure. The polymer chain has sequences of units with hydrophilic pendant (soft block) and sequences of units with nitrile pendant (hard block) (see Figure 3-1). HYPAN polymers with various water uptake capacities were bought from HYMEDIX international, Inc. HYPAN HN68, HYPAN HN80 were used in this dissertation to prepared hydrogel membranes. The HN# indicates the water uptake capacity (% w/w) of polymer membrane when fully hydrated. Water content will affect some physical properties of the membranes, such as mechanical strength and refractive index. HYPAN does not need any crosslinker and initiator to form a gel, but crosslinks itself via the interactions between nitrile blocks when the polymer is placed in aqueous medium.

A 10% HYPAN (w/w) was prepared in DMSO by stirring. The appropriate amount of MIP microspheres was then added into 2 grams of HYPAN solution. HYPAN solution has a high viscosity. Usually a longer time stirring and an elevated temperature (~40-50 C) were needed to suspend microspheres and form a homogeneous mixture. The air bubbles produced by stirring must be removed by ultrasonification before making membranes. A small portion of the mixture was dropped on a glass slide with a 76 μm thick Teflon spacer around edges. Another glass slid was used like a squeegee to squeeze the viscous solution down across the slide to form a layer. The slide was then placed in a Petri dish with a small amount of water, but not immersed in water. The Petri dish was covered to create high humidity inside, which can hydrate the microspheres suspension in HYPAN solution. After gelation, the slide with the membrane was placed into water to extract DMSO. The membrane was then removed from the slide and washed with excess

water to removing the remaining DMSO. The cleaned membranes were stored in distilled water.

Polyurethane membranes

The Hydromed D series of polyurethane polymers with various water contents (68%, 80%) were obtained from Cardiotech International, Inc. For membrane preparation, a 10% solution of polyurethane was prepared in ethanol. The rest of the procedure is similar to the preparation of HYPAN membranes. It is easy to suspend polymer microspheres in polyurethane ethanol solution to give a homogenous suspension. Unlike PVA membranes, polyurethane membranes have a very good mechanical strength and are easy to handle, especially for thermo-sensor applications in biological medium.

3.4 Characterization

3.4.1 Scanning Electron Microscopy (SEM)

An Amray 3300FE Scanning Electron Microscope (SEM) was used to take the picture and measure the size of microspheres. For sample preparation, a drop of the microsphere suspension was placed onto a graphite SEM platform and left it to air dry. Under vacuum, a thin layer of a gold/palladium alloy was then coated on the sample layer to a thickness of about 300 Å.

3.4.2 Particle Size and Distribution

The particle size can be exactly measured from SEM graphs. An average diameter can be calculated from the number of particles in a particular distance (e.g. 10 µm) on the

SEM graphs. Carl Zeiss Microscope coupled with KS200 software was also a good tool to measure particle size, especially statistical analysis such as size distribution, mean value, relative standard deviation, etc.

3.4.3 Optical Microscopy Measurements

The size and distribution of the emulsified droplets during or after emulsification were observed using a Fisher Scientific optical microscope. This was used as a screening process to select an efficient stabilizer and suitable continuous phase for suspension polymerization. It is also useful to determine a sonication time to produce an appropriate size of emulsion droplets.

3.4.4 Refractive Index Measurements

The refractive indexes of hydrogel membranes with/without MIP microspheres were obtained by an Abbe refractometer. The refractive indexes of various solutions were also determined by a refractometer.

3.4.5 Turbidity Measurements

Homemade plastic holders were used to hold membranes in the cuvettes for membrane turbidity measurements (Figure 3-6). The membranes with template or untemplated MIP microspheres were secured in plastic holders. The holders fit inside a standard cuvette and allow the membrane to be easily handled and analyzed. A blank membrane without microspheres was also secured in the same kind of plastic holder and placed in a cuvette. This was used as the reference and filled with the appropriate buffer

solution. A Cary 500 UV/Vis standard spectrophotometer was used to measure the membrane turbidities when changing the concentration of analyte. The turbidity spectra were obtained by scanning from 400 to 1000 nm. The data presented in this dissertation refer to the turbidity at 500 nm, unless otherwise specified.

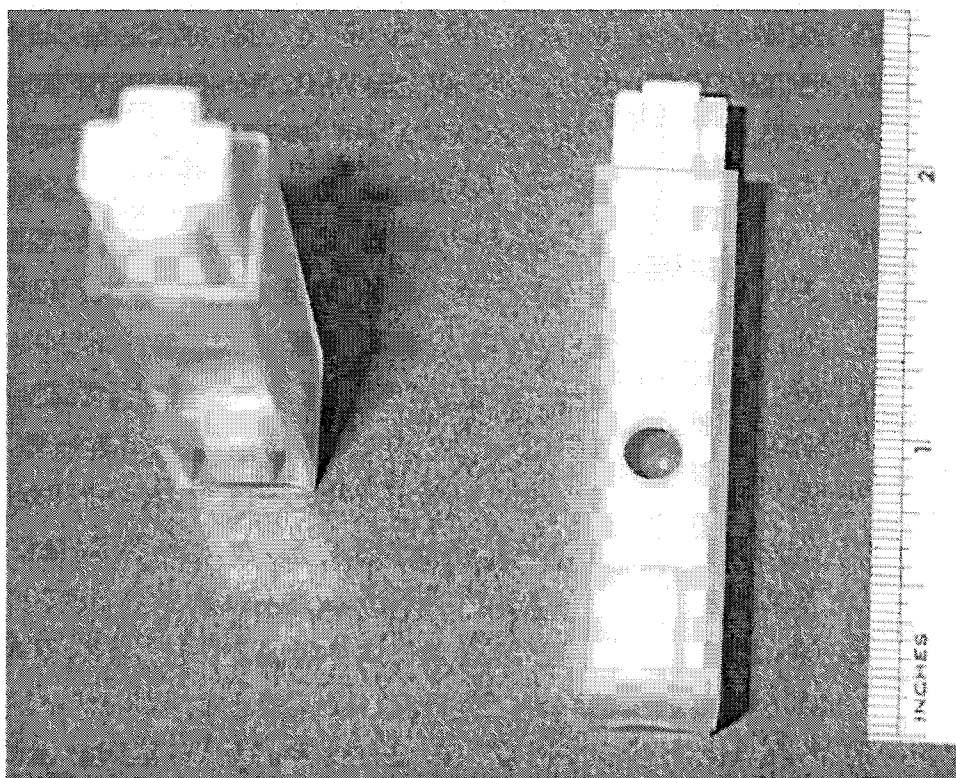


Figure 3-6. Membrane holder for turbidity measurements.

3.4.6 Transition Temperature Measurements

A Cary 500 UV/Vis standard spectrophotometer was used to measure the transition temperature of poly NIPA copolymer microspheres in membranes or solutions. The turbidity of the sample was scanned via temperature from 20 to 60 °C. Below the transition temperature, poly NIPA is in swollen state and turbidity is low without obvious

change. Turbidity increases sharply at the transition temperature. There is no further change in turbidity with increasing temperature. The resulting curve is similar to a titration curve and the transition temperature is the temperature at the “end point”. Fixed wavelength such as 500nm has been employed. Heating rate is typically 1 °C/min.

3.4.7. Response Time Measurements

The response time is defined as the time from adding analyte to reaching 90% of maximum signal. For our MIP-based sensors, the response time is determined by the association rate of template interacting with MIP, which can be obtained from kinetic scanning using UV-Vis spectrophotometer at a particular wavelength (e.g. 500 nm). It is the time when turbidity reaches the 90% of maximum.

3.4.8 Factorial Design Experiment

MIP dispersion polymerization system is more complicated than normal dispersion polymerization. More variables are involved and affect not only properties of microspheres (e.g. size, monophor, swelling, etc.), but also the recognition and sensitivity of MIP to analyte. Among these variables, the percentage of crosslinker, template to monomer ratio, and percentage of functional monomer are most important and were investigated by a factorial design experiment which provides not only the effect of the main factors no polymerization but also the interactions between factors. In this experiment, the percentage of crosslinker was investigated at three levels while the template to monomer ratio, and the percentage of functional monomer were studied at two levels. There are 12 reactions which were run in random order. Table 3-5 gives the

design of experiment and the levels of each variable. The percentage of crosslinker was set at 2%, 5%, and 8%; the ratio of template to functional monomer was set at 1/2 and 1/5; the percentage of functional monomer was set at 10% and 20%. Other variables such as initiator, stabilizer, and temperature were kept constant in these experiments.

Table 3-5. Fractional Design for Reaction Variables for THO templated poly NIPA-MAA Dispersion Polymerization.

Formulation Number	Crosslinker (MBA) (mole %)	Template/Functional Monomer (THO/MAA)	Functional Monomer MAA (mole %)
1	2	1/2	10
2	2	1/2	20
3	2	1/5	10
4	2	1/5	20
5	5	1/2	10
6	5	1/2	20
7	5	1/5	10
8	5	1/5	20
9	8	1/2	10
10	8	1/2	20
11	8	1/5	10
12	8	1/5	20

CHAPTER 4

PRELIMINARY DATA AND PREPARATION OF SWELLABLE MOLECULAR IMPRINTED POLYMER PARTICLES FOR CHEMICAL SENSING

4.1 Introduction

Biosensors have attracted considerable attention because of their outstanding specificity and sensitivity. However, biosensors often lack storage and operational stability because they are based on a fragile biological recognition element: an enzyme, antibody or receptor. It can also be difficulties to generate the affinity sensing phase and achieve the specificity toward the desired target molecule. For example, continuous immunosensors have promising applications in monitoring therapeutic drug and metabolism. But the big problem is that the sensor response times are impractically long because of the very slow rate of antibody-antigen dissociation. Also they only can be used in a small number of sensing cycles due to their limited stability and degradation. Due to these disadvantages, biosensors have not achieved the commercial success as expected in the early development phase.

Molecular imprinting has emerged providing as an alternative approach to biosensors [48, 52]. These polymers have some clear advantages over actual antibodies for sensor technology. The main advantage is that they are much more stable and can be used in extreme environments, such as in the presence of acids or bases, organic solvents or high temperatures and pressures [48].

It has been proven that polymerization in aqueous medium is not suitable for molecular imprinting because the hydrogen bonding interaction of solvent with functional monomer or template molecule will dramatically affect the assembly and interaction between template and functional monomer. As a result, almost all molecular imprinting polymers have been prepared by bulk polymerization in a single non-polar medium followed by grinding and sieving to make particles. This approach is tedious and may also damage some of the binding sites. Hence, beaded polymers would be preferable in most case, especially chromatography and sensor applications. Another problem with MIP sensor is the long response time (15-60 min) [48] because of very slow mass transfer in rigid polymers. Using smaller polymer particles with lower level of cross-linker should improve diffusion rates and lower response times. In this dissertation, methods were developed to prepare swellable molecular imprinting microspheres with a suitable size for optical sensing of the template molecule. So far, there has no such sensor reported in the literature. In this chapter, our first work was to produce the swellable MIP fibrous gels and investigate its molecular specific swelling properties based on literature. Then a few attempts that we made to produce beaded polymers will be described.

4.2 Molecular Specific Swelling of Molecular Imprinted Polymer

Usually most molecular imprinted polymers are prepared with high crosslinking to ensure a high specific capacity. As a result, there is no significant swelling when they bind with template. However, a recent study of swellable MIPs has been reported by Watanabe and coworkers [69]. Copolymer gels consisting of N-isopropylacrylamide and acrylic acid have been prepared in the presence and absence of template molecules. The

polymer was prepared as fibrous gels in capillary tubes. The resulting MIP gels show molecular specific swelling at high temperatures. However, many issues were not clear in this report. For example, they have not done the experiment where they hold the temperature constant and vary the template concentration. Also the authors did not mention any pH effect. But as we know, there is actually an acid-base interaction between the template and acrylic acid. In order to confirm the molecular specific swelling property of this kind of MIPs and to investigate selectivity, and pH effects, we first prepared norephedrine templated copolymers of NIPA, AAc and a crosslinker (MBA) in dioxane in capillary tubes [69]. The resulting polymer gels are $\sim 450\ \mu\text{m}$ in diameter. This small diameter of the polymer fiber allowed it to rapidly equilibrate with external template solution. The degree of swelling could be easily determined by measuring the length of the fiber.

4.2.1 Template selective swelling property

The fibrous gels were cut into small pieces ($\sim 2\ \text{mm}$ in length) and placed in water or template solution to measure the volume changes with increasing temperature. The length changes of gels were determined using an optical microscope and were expressed by the swelling ratios (V/V_0), where V is the volume of the gels under a certain condition, and V_0 is the volume of the gels at $15\ ^\circ\text{C}$. Figure 4-1 shows the swelling and shrinking of templated and untemplated gels in aqueous solution of given norephedrine concentration. It is clear that both templated and untemplated gels are temperature sensitive. They are swollen at low temperature and shrunken at high temperature due to the thermal-sensitivity of poly NIPA. However, the swelling ratio is different at high temperature for

the two gels. This indicates that there is molecular recognition at high temperatures. At low temperatures, the polymer is solvated. This overcomes its interaction with the template so that there is no molecular recognition at low temperatures. When temperature is increased, the polymer starts shrinking and its volume decreases reaching a constant value at higher temperature. The difference in the final volumes is because template holds monomer units in place so that the polymer can't completely collapse upon itself. This ensured that there is a molecular specific swelling of this kind of MIPs.

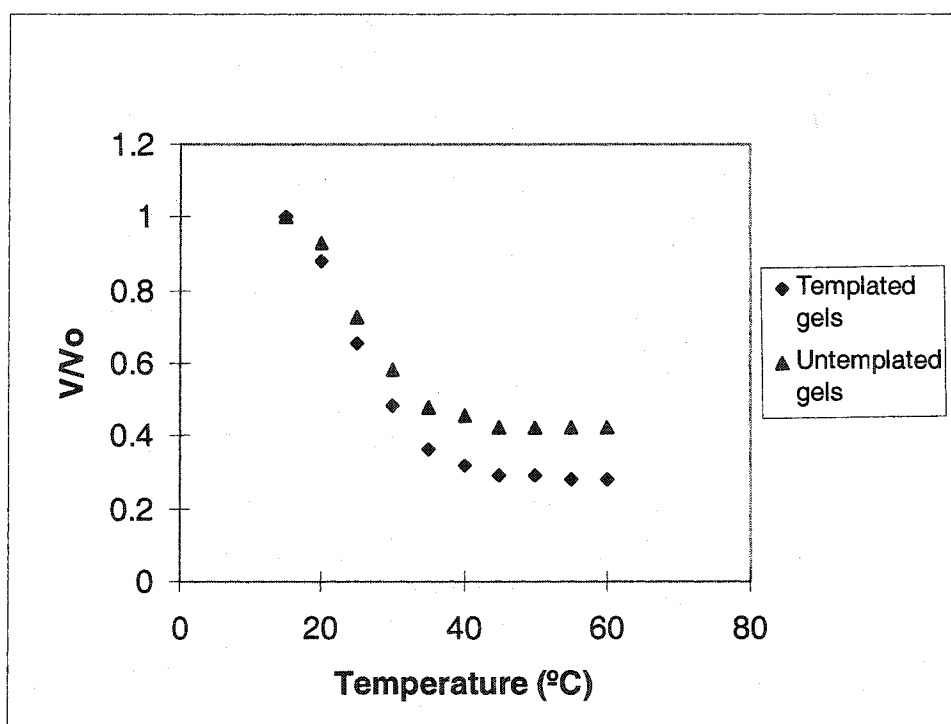


Figure 4-1. Swelling ratio (relative volume of gels, V/V_0) as a function of temperature for untemplated and templated gels in 0.1 M norephedrine solution.

At constant temperature (e.g. 30°C, or 50°C), the volume changes were measured when gels were placed in various norephedrine concentrations to investigate the gel response to norephedrine (Figure 4-3, 4-4). It can be seen that it is more sensitive at high

temperature than low temperature because the gels in shrunken states are more readily to recognize the template molecule. However, based on our observations, it took a longer time to reach association equilibrium at high temperature due to the slower mass diffusion of template into rigid polymer gels.

4.2.2 Specificity

To examine the molecular specificity of the volume change, adrenaline was selected as another template molecule, which has a similar structure to norephedrine (see figure 4-2). Norephedrine templated gels were placed in solutions with various concentrations of andrenaline. The volume changes were then measured at constant temperatures. Figure 4-3, 4-4 show the swelling ratios of norephedrine templated gels as a function of concentration of either norephedrine or adrenaline at 30, 50°C, respectively. It can be seen that norephedrine templated gel is sensitive to norephedrine and insensitive to adrenaline.

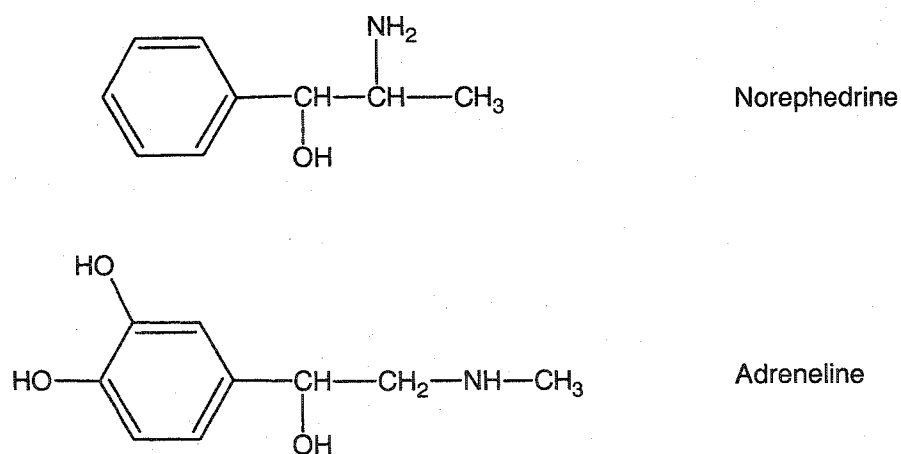


Figure 4-2. Structures of templates, norephedrine, adrenaline.

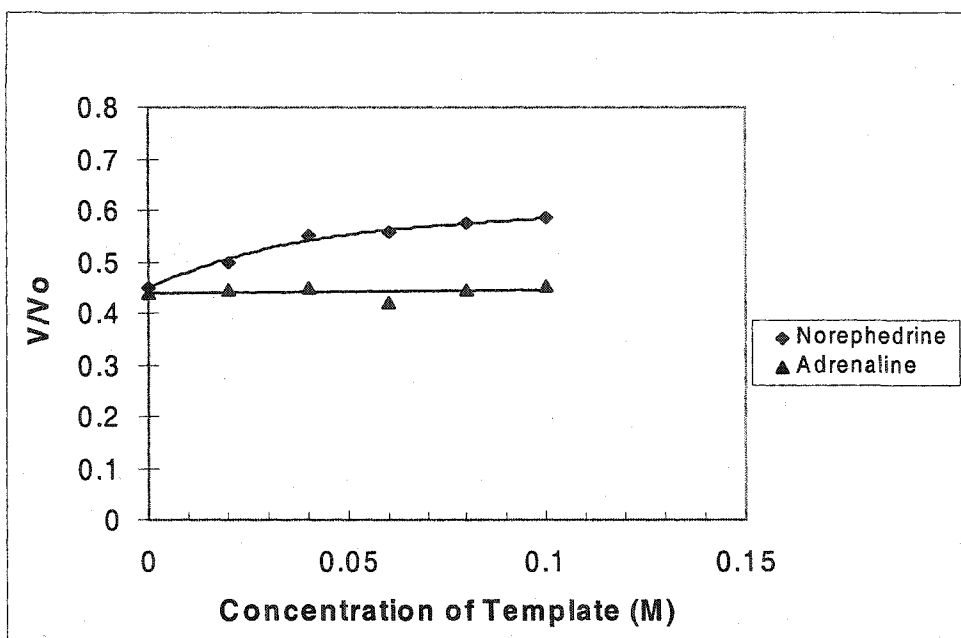


Figure 4-3. The swelling ratio for norephedrine templated gels as a function of either norephedrine or adrenaline concentration at 30°C.

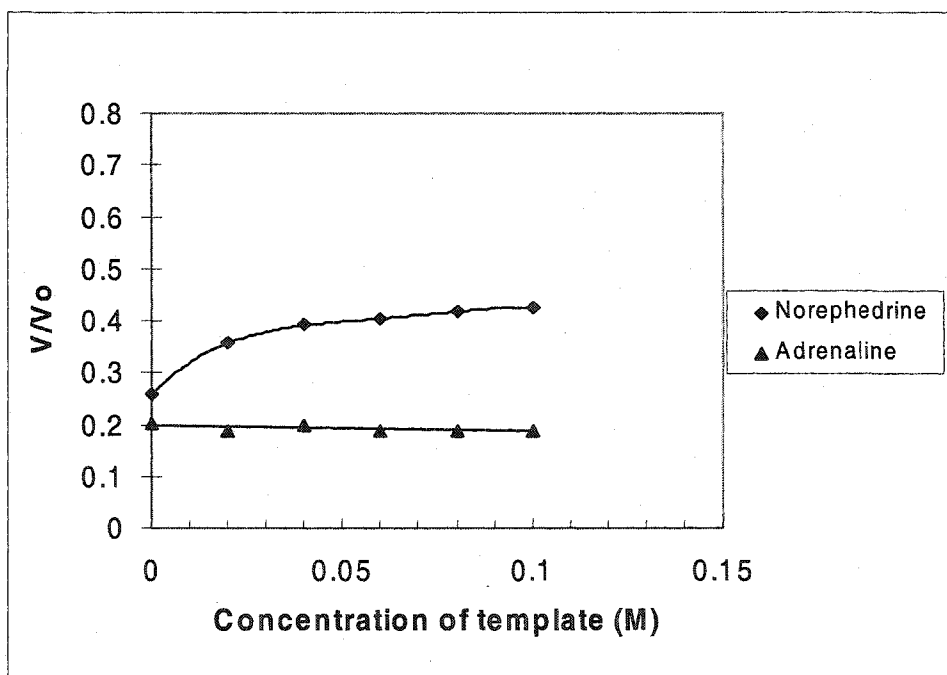


Figure 4-4. The swelling ratio for norephedrine templated gels as a function of either norephedrine or adrenaline concentration at 50°C.

4.2.3. pH dependence of swelling ratio

Figure 4-5 shows the effect of pH on the swelling ratios of norephedrine templated gels as a function of temperature. At a constant temperature (e.g. 30°C or 50°C), the swelling ratio decreased with decreasing of pH. This is because acrylic acid ($pK_a = 4.25$) introduces carboxyl groups on polymer backbone. These will be protonated at low pH and deprotonated at high pH. Deprotonation (e.g. at pH 7.0) results in negative charge on the polymer backbone. The charge repulsion causes less shrinking at higher temperatures. Thus, pH is a very important variable for swelling and shrinking of this MIPs. This will be discussed in detail in Chapter 5 and 6.

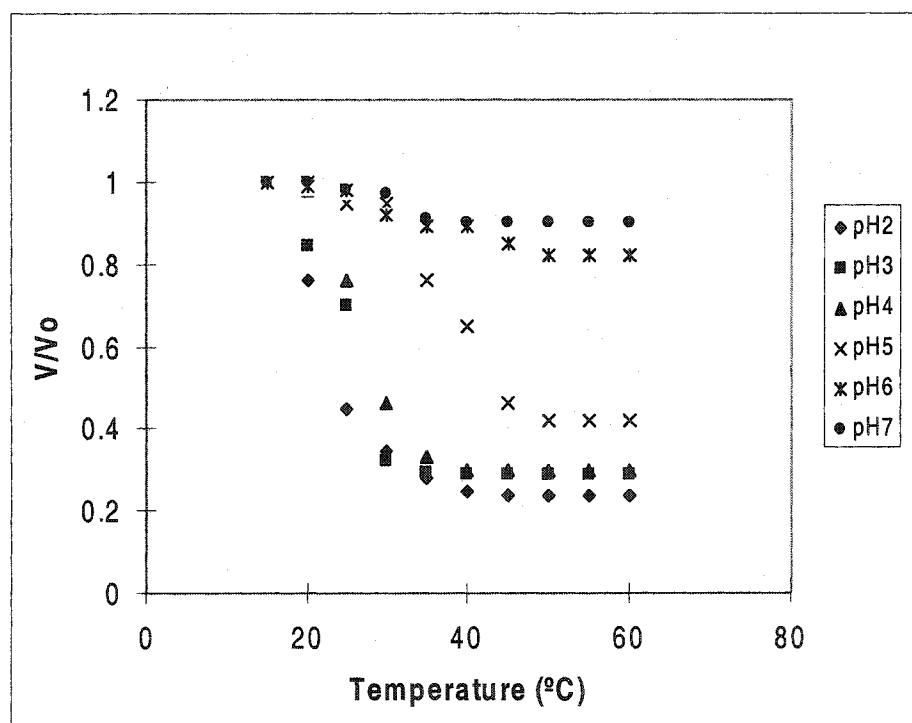


Figure 4-5. Swelling ratio for norephedrine templated gels at different pHs as a function of temperature.

4.3. Sensor Design Based on Swellable MIP Microspheres in a Hydrogel

The above results show that poly NIPA-AAc MIP gels can undergo template sensitive swelling at high temperatures with high specificity. These observations encouraged us to investigate the possibility for optical chemical sensing based on polymer swelling and shrinking. Figure 4-6 shows our sensor design. The swellable MIP microspheres are to be embedded in a hydrogel membrane. These thermal sensitive microspheres swell at low temperature, shrink at high temperature. The shrinking extent depends on template concentration. Less shrinking at higher concentration of template is due to interaction of the template with the polymer. This leads to a lower refractive index of microspheres. The turbidity changes of the hydrogel membrane can be used to measure the concentration of template.

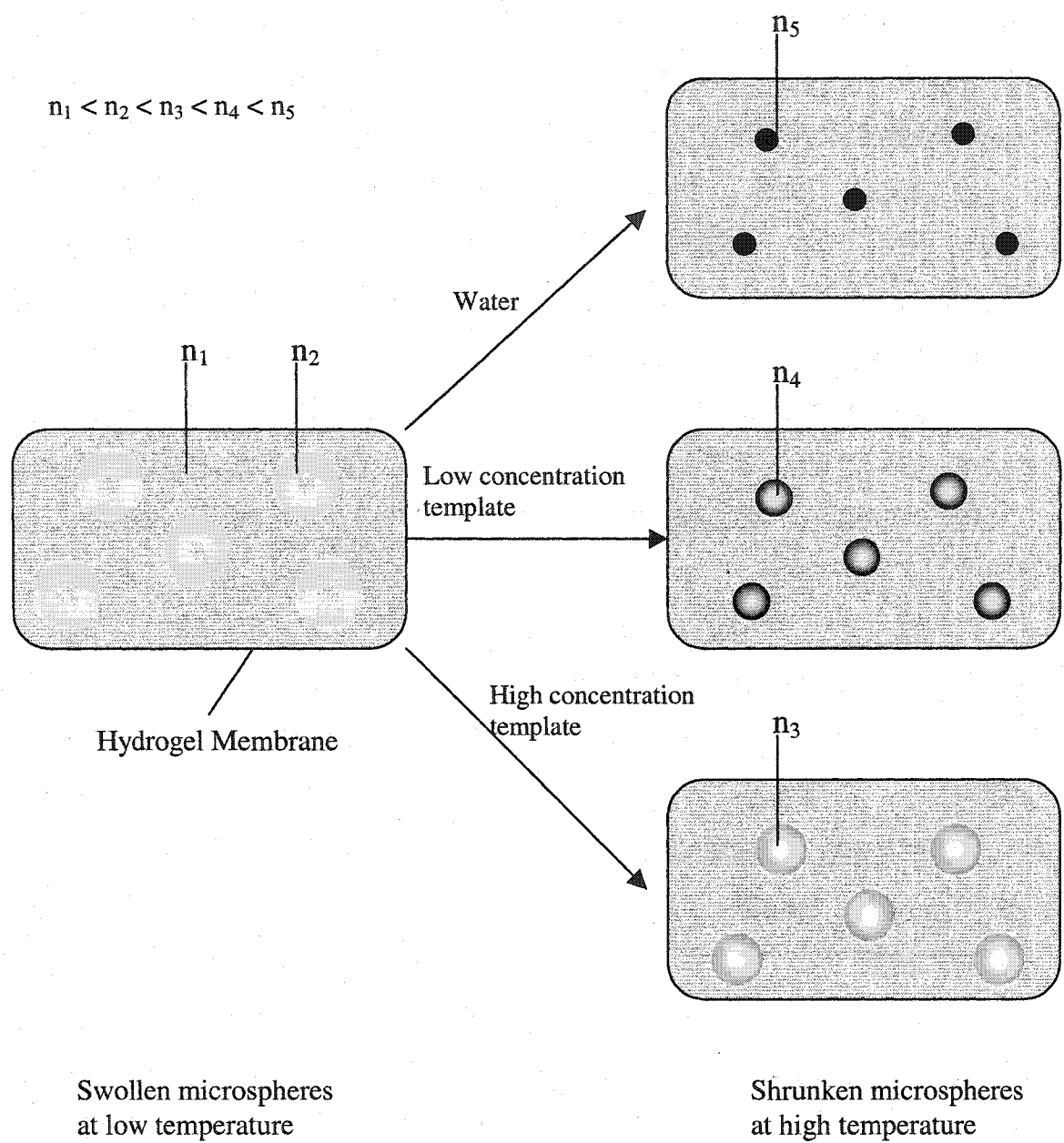


Figure 4-6. Model of chemical sensing based on swellable MIP microspheres in a hydrogel.

4.4 Preparation of Swellable MIP Particles Using Suspension Polymerization

In principle, suspension and dispersion polymerization methods can be used to produce polymer beads. These approaches offer a very attractive alternative to bulk polymerization because they can produce a high yield of particles with a suitable size. In almost all cases, water or a highly polar organic solvent is used as the continuous phase for the relatively hydrophobic monomers. On the other hand, noncovalent imprinting approach involves the interaction between monomer and template via hydrogen bonding, electrostatic interactions, hydrophobic interactions, etc. The functional monomer and templates are usually high polar organic molecules. So common suspension polymerization approaches in aqueous medium are generally unsuitable for preparing molecularly imprinted polymers due to the competition between functional monomer and solvent for specific interaction with the template molecule. In addition, random copolymerization of monomers and crosslinker will not be obtained because acidic monomers are highly soluble in water. Also water-soluble template molecules would prefer to stay in the polar solvent rather than polymer during polymerization. This will lead to very poor recognition if we try to make molecularly imprinted polymer particles by suspension polymerization in aqueous medium.

4.4.1 Suspension polymerization using liquid perfluorocarbon as continuous phase

Suspension polymerization in perfluorocarbon liquid continuous phases has been introduced to prepare MIP microspheres for HPLC stationary phase [83]. Perfluorocarbons are largely immiscible with most organic compounds. They can form an appropriate inert phase and do not interfere with the interactions between functional

monomers and template molecules during molecular imprinting. Chloroform was used as a solvent to prepare imprinting mixture.

Based on this report, we attempted to develop a suspension polymerization method for our molecular imprinting system. Perfluoro(methyl-cyclohexane) (PMC) was used as the dispersing phase. Dioxane was used as the solvent (suspension phase) to dissolve all imprinting components. It has been shown that it is very difficult to make a stable emulsion of an imprinting mixture in a liquid PMC [83]. This is because the high density of the PMC will cause rapid “creaming” of the emulsion, resulting in coalescence of dispersed droplets. Thus, surfactant must be used to stabilize emulsion droplets before and during polymerization. Commercial fluorinated surfactants (Fluorad FC135) was first tried, followed by a synthetic homopolymer of acryoyl PFA-1, and graft copolymers of acryoyl PFA-1 and acryoyl PEG1000MME (termed PFPS). Table 4-1 shows the surfactant effect on suspension polymerization. FC135 did not stabilize emulsion droplets. Furthermore, FC135 contains 15% water which will also interfere the molecular imprinting. Poly (acryoly PFA-1) yielded relatively stable emulsions for suspension polymerization resulting in some irregular aggregated particles with sizes ca. 7.0 μm . However, poly (acryoly PFA-1) has poor solubility so that it is very difficult to remove from the surface of particles after polymerization, resulting in extremely hydrophobic surfaces. PFPS was shown to give stable emulsion and could be removed from the surface of particles due to pendant hydrophilic group PEG on the polymer chain. However, the resulting particles were still coagulated [83]. The amount of surfactant and stirring rate during emulsion and polymerization are two critical variables that affect particle properties in suspension polymerization, especially using perfluorocarbon

dispersing phases. Several reactions were carried out using different amounts of surfactant and different stirring rates. Unfortunately coagulated particles were still produced. They were not easily separated.

Table 4-1. Surfactant effect on suspension polymerization.

Surfactant	Emulsion	Particle
FC135	Ineffective	---
Poly (acryoyl PFA-1)	Stable	>7 μm , aggregated
PFPS	Stable	>10 μm , coagulated

4.4.2 Membrane Emulsification

A new emulsification technique known as Shirasu Porous Glass (SPG) Membrane Emulsification has been reported recently [85-87] (Figure 4-6). This method uses the surface chemistry of a microporous membrane to disperse one of two immiscible liquids (the dispersion phase) into another liquid (the continuous phase) by applying pressure to cause the dispersion phase to permeate through the membrane. This method can continuously produce not only oil in water (O/W) or water in oil (W/O) emulsion of uniform particle size, but also O/W/O or W/O W type double emulsions.

Figure 4-7 shows the major components of the SPG membrane emulsification apparatus. The dispersion phase (mixture of monomers, crosslinker, initiator and solvent) is stored in a monomer tank and allowed to permeate through a membrane module under appropriate pressure into a circulating flow of continuous phase. The pressure from gas

tank is controlled by gauges and very important for droplet formation. The droplets are suspended in the continuous phase (aqueous solution of stabilizers and surfactants). The resulting suspension is stored in the emulsion tank with a gradual increase of droplet concentration.

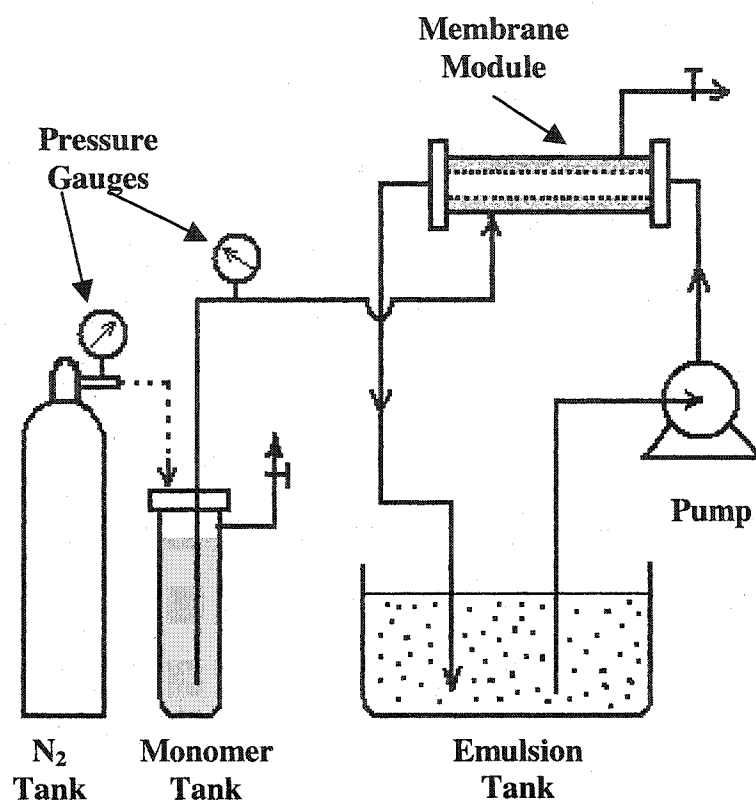


Figure 4-7. SPG Membrane emulsification apparatus [85-87].

The three requirements given below must be met absolutely for the successful preparation of such emulsions by membrane emulsification.

- (1) The microporous membrane must provide uniform pore size distribution as well as reasonable mechanical strength.
- (2) The membrane must be wetted with the continuous phase prior to contact with

the dispersion phase. Membrane wetting with the dispersion phase must be avoided. Table 4- shows the ideal medium for different membranes of SPG.

- (3) To stabilize the emulsion, a surfactant must be added to both the dispersion phase and the continuous phase or to the latter.

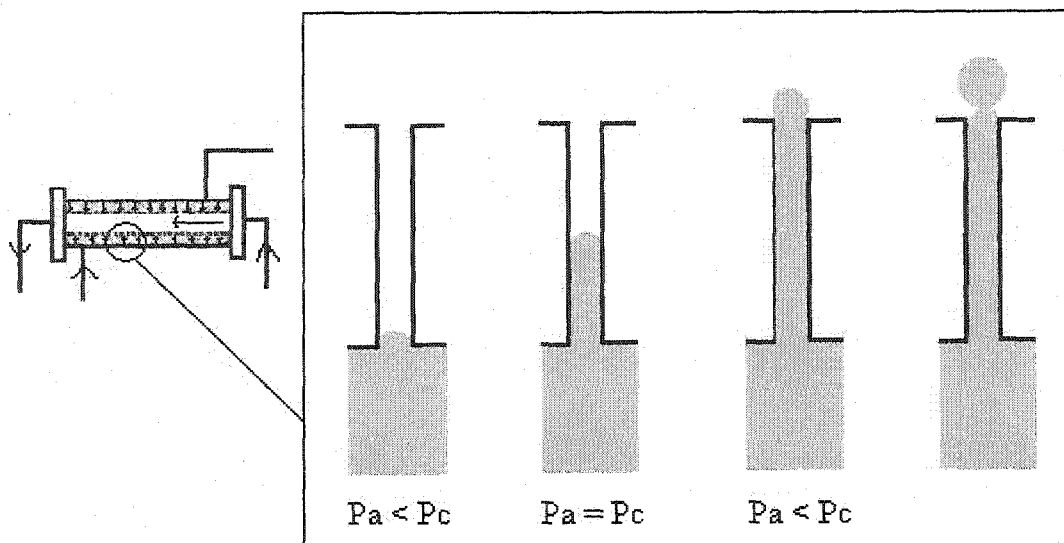
Table 4-2. The requirements of medium properties for SPG Emulsification

Medium	SPG Membrane
Ideal dispersion phase	Not wetted
Ideal continuous phase	Wetted

The formation of droplets by membrane emulsification (Figure 4-8) can be explained as follows. When the dispersion phase is pressurized and penetrates into the micropores, the following equation is derived from the pressure p_c and the micropore size D_m .

$$p_c = 4\gamma_{ow} \cdot \cos\theta / D_m \quad (4-1)$$

Where, γ_{ow} represents the interfacial tension of the O/W interface and θ represents the oil contact angle with the water surface.



P_a : Applied pressure; P_c : Critical pressure

Figure 4-8. Relationship between the applied pressure and droplet formation

As shown in the above figure, the dispersion phase does not permeate through the membrane when the pressure P is lower than P_c . However, at the moment when P has exceeded P_c , it is able to pass through the micropores for the first time, then creating a dispersion of droplets into the continuous phase. Thus, P_c is the minimum pressure where one can observe the flux of the dispersion phase. It has a special meaning in the membrane emulsification process and is called the critical pressure. Equation (4-1) also reveals that higher pressure is required as the micropore size (D_m) of the membrane becomes smaller and that the critical pressure can be reduced by a reduction in the interfacial tension.

The size of emulsion droplets from this SPG technique is far smaller than that from conventional suspension polymerization. This inspired us to use the SPG technique for our imprinting system and make smaller (e.g. $\sim 1 \mu\text{m}$), spherical MIP microspheres. In

this case, the dispersion phase is the imprinting mixture in dioxane while PMC can be a continuous phase. Usually the volume of continuous phase should be 250-500 mL so that it can be cycled through the SPG apparatus. However, PMC is very expensive and quite volatile so that it is not practical to use as continuous phase. We have to find another medium that meets the following requirements: (1) must wet the SPG membrane; (2) immiscible with dispersion phase, dioxane; (3) must be inert and not affect molecular imprinting; (4) can dissolve surfactant. (5) inexpensive and easily handled.

Concentrated salt solutions as continuous phase

Dioxane is miscible with water. However, it will no longer be miscible when salt is added in water at a critical concentration. This will not only ensure an efficient emulsion but also eliminate the solvent effect on molecular imprinting because in highly concentrated salt solutions, water molecules will prefer to interact with salt molecules instead of forming hydrogen binds with template and monomer molecules. Calcium chloride, a very soluble salt, was used to prepare salt solutions with different concentration. Then dioxane was mixed with these salt solutions to test how immiscible they are (see Table 4-3). Dioxane is immiscible with CaCl_2 solution when the concentration is higher than 80%. This solution together with stabilizer was used as the continuous phase in SPG emulsification. The imprinting mixture (NIPA, AAc, MBA, BPO, norephedrine in dioxane) was the dispersion phase.

Table 4-3. Immiscibility of dioxane with salt solutions.

Concentration of salt (%CaCl ₂ , w/w)	Immiscibility (%)
10	0
20	0
30	32
40	45
50	57
60	68
70	85
80	100

Three different stabilizers (0.1 % sodium dodecyl sulfate (SDS), 1.0% PVA, 1.0 %Triton-X-100) were added to the continuous phase to make an emulsion. Unfortunately, all of these attempts resulted in foaming and failed to produce beads after polymerization.

Mineral Oil / Decalin as Continuous Phase

A non-polar organic solvent can also be used as continuous phase in our system if it is immiscible with dioxane. After screening many organics, we found that only mineral oil is completely immiscible with dioxane. However, it was difficult to use as a continuous phase due to its high viscosity. Decalin (C₁₀H₁₈) is partly immiscible with dioxane. Different amounts of decalin were added to mineral oil to decrease the viscosity while maintaining immiscibility with dioxane. Finally 1:1 mineral oil/decalin gave the best result.

We first tried to make particles in mineral oil/decalin (1:1, v/v, 0.5 % Triton X-100 as stabilizer) using conventional suspension polymerization. This resulted in large coagulated particles with sizes of 100~150 μm . The particles were then placed in 0.5 M norephedrine solution to test the volume change. The templated particles were a little more swollen than untemplated, which means these particles swell selectively. We then tried to make smaller particles using the SPG Emulsification technique. The resulting particles were almost the same as with the conventional technique (~100 μm in size). The reason is that the SPG membrane with hydrophilic pores was not wetted by organic continuous phase but instead by the dioxane dispersion phase (Table 4-4). This did not satisfy the requirements of SPG technique (Table 4-2).

Table 4-4. Compatibility of dispersion and continuous phase with SPG membranes.

Medium	Hydrophilic SPG Membrane	Hydrophobic SPG Membrane
Dioxane	Wetted	Wetted a little bit
Oil/decalin	Wetted a little bit	Wetted

From Table 4-4, we can see that hydrophobic SPG membrane is good for both dioxane dispersion phase and oil/decalin continuous phase. 0.5% Triton X-100 was used as stabilizer. Emulsion droplets were small but unstable. Huge particles were obtained after polymerization. This is due to non efficient stabilization. Several surfactants such as block copolymers, were then screened and investigated (Table 4-5).

Table 4-5. Surfactant selection for oil phase or dioxane phase in SPG.

Surfactant	Dissolve in Oil/Decalin (% , w/w)	Dissolve in Dioxane (% , w/w)	Emulsion Droplet
Triton X-100	0.5	--	Unstable
Brij 35	0.25	--	Unstable
Styrene/isoprene	0.5	--	No droplets
Styrene/acrylonitrile(25%)	Insoluble	1.0	Precipitate
Styrene/butylmethacrylate	Insoluble	1.0	Stable one day
N-vinylpyrrolidone/ vinyl acetate	Insoluble	0.5	No droplets
Vinyl alcohol/ vinyl butyral	Insoluble	0.5	No droplets
Methyl vinyl ether/ maleic acid	Insoluble	0.5	Unstable
Polyethylene/ poly(ethylene glycol)	Insoluble	1.0	unstable
Span 80	0.5	--	unstable

It can be seen that styrene/butyl methacrylate (50%) is the best stabilizer for the oil/decalin-dioxane system we used for SPG emulsification. It was dissolved in the dioxane dispersion phase. 0.5% of Triton X-100 was still used in the oil/decalin continuous phase. The resulting particles were spherical but still relatively large, ~25 μm and there was some coagulation. The oil/decalin continuous phase is viscous and not easily handled in the flow system. It also takes considerable time to clean the SPG system, especially the glass membrane after emulsification.

Based on the above results, we concluded that SPG Emulsification technique is not suitable for emulsifying the imprinting system, especially when continuous and dispersion phases are all non polar organics, which is required for molecular imprinting.

We then moved back to the perfluorocarbon suspension system and carried out polymerization in an ultrasonic bath instead of stirring (procedure see chapter 3). This is an unconventional free-radical emulsion polymerization. The ultrasonic bath kept the droplets/particles in suspension during polymerization and allowed us to synthesize polymer that was not coagulated. It was observed that the particles obtained by this approach are smaller than those by conventional suspension polymerization. The size and distribution of particles depend upon the energy input and its distribution in the ultrasonic bath. Initially the reaction was carried out at room temperature. Ice was added frequently to the bath to keep the temperature from rising. As a result, the temperature may not be kept constant during polymerization. All of these resulted in relatively larger (ca. 6 μm) and amorphous particles (Figure 4-8). However, they were good enough to make membranes and investigate the sensing response to norephedrine. Membrane turbidity as a function of temperature decreased with the increasing of template, norephedrine. The sensing response will be discussed more detail in chapter 5.

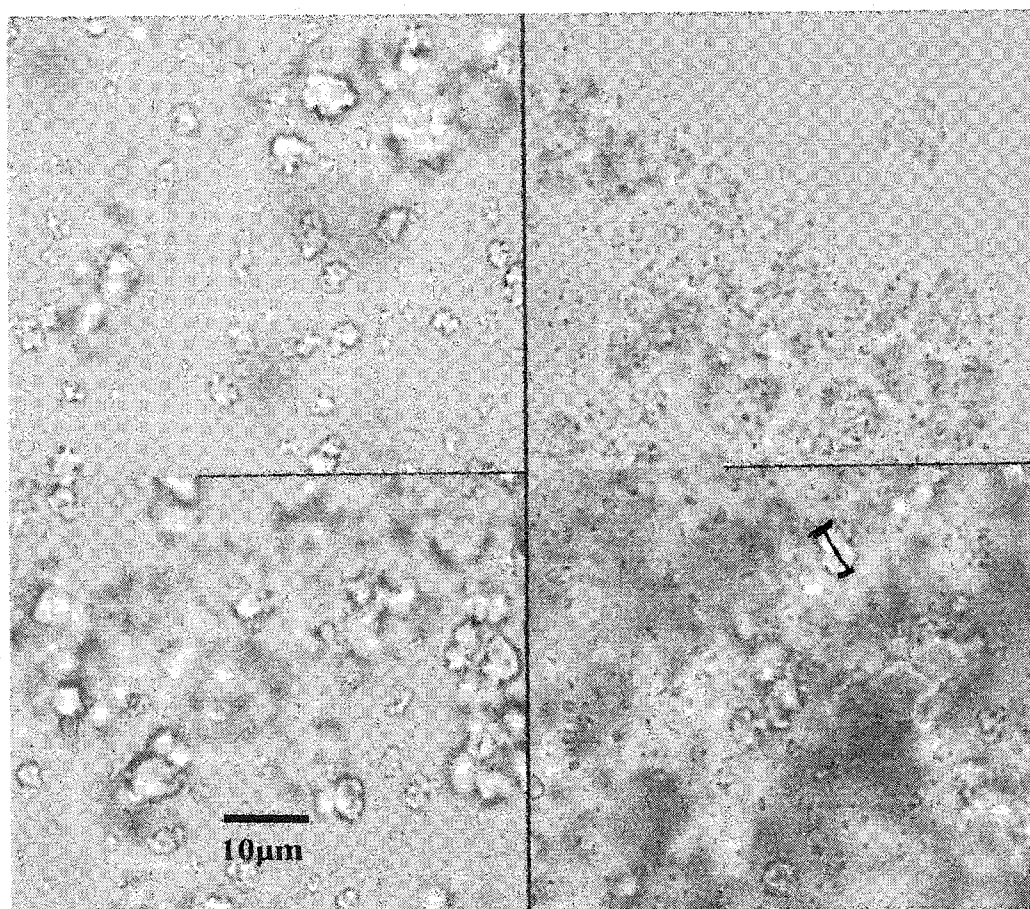


Figure 4-9. Micrographs of norephedrine imprinted poly NIPA-AAc-MBA particles prepared by perflourocarbon suspension polymerization in an ultrasonic bath.

4.5 Preparation of Swellable MIP Microspheres Using Dispersion Polymerization

When we switched to theophylline as our template, we were unable to make MIP microspheres by perfluorocarbon suspension polymerization in an ultrasonic bath. It seems that theophylline affects polymerization in this system.

Mosbach and co-workers have developed a method for preparing theophylline imprinted microspheres using dispersion polymerization in acetonitrile [80]. In their work, methacrylic acid was used as the functional monomer to interact with template. TRIM was used as crosslinker. As a solvent, acetonitrile is only a weak hydrogen bond acceptor and not a hydrogen bond donor so that its interaction with theophylline is not as strong as that with methacrylic acid. As a result, theophylline interacts with the polymer rather than the solvent during polymerization. Using a very high percentage (30% mol) of crosslinker, rigid microspheres with a high capacity for theophylline were prepared without using stabilizer.

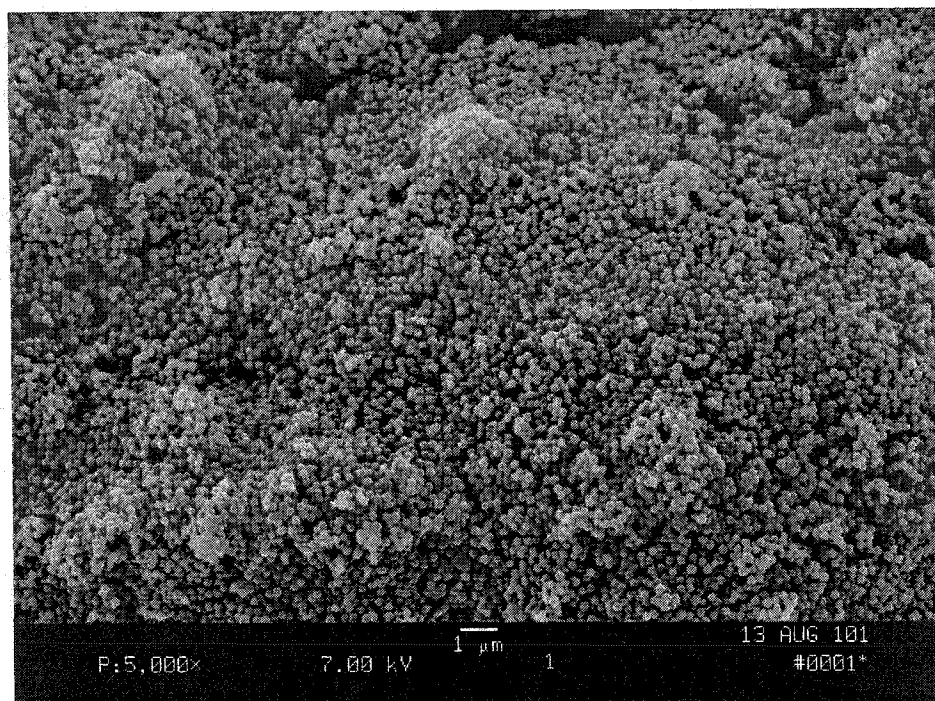
Based on this report we decided to prepare microspheres by dispersion polymerization. In initial experiments, untemplated microspheres were prepared with 12% TRIM crosslinker, 29% methacrylic acid and 59% NIPA. The resulting microspheres were uniform and 0.2 micrometer in diameter (Figure 4-9). However, in the presence of template, the resulting particles were aggregated (Figure 4-10). The presence of theophylline has affected the particle size distribution and morphology. The aggregated particles were suspended in a hydrogel membrane and evaluated. The turbidity change with temperature was small and there was no response to theophylline except at high concentration, $1.0 \times 10^{-3} \text{M}$. This is because it is very difficult for these rigid particles to swell. Therefore, much lower level of crosslinker (5% mol) was used to prepare

swellable microspheres. Figure 4-11 and Figure 4-12 show scanning electron micrographs of particles prepared using 5% of TRIM and MBA, respectively. These particles were aggregates of much smaller particles, ca. 0.1 ~ 0.2 μm in diameter. This is because no stabilizer was used to prevent coagulation. In the literature, they used a very high level of crosslinker resulting in rigid beads that do not stick together. In this case, stabilizer is not necessary and can be eliminated. However, in our system, we have to use a much lower level crosslinker to get swellable microspheres. So a suitable stabilizer was selected and the polymerization formulation was then optimized considering several factors such as particle size and distribution, high sensitivity to temperature, high response to template, etc. (see more detail description in chapter 6). Finally separated MIP microspheres with uniform size of ca. 1.0 μm were successfully prepared in acetonitrile using 20% w/w of poly(styrene-co-acrylonitrile) as the stabilizer, 5% of MBA as crosslinker (Figure 4-13). These swellable molecular imprinted microspheres respond with the selectivity and sensitivity for theophylline. More detailed discussion will be described in chapter 6.

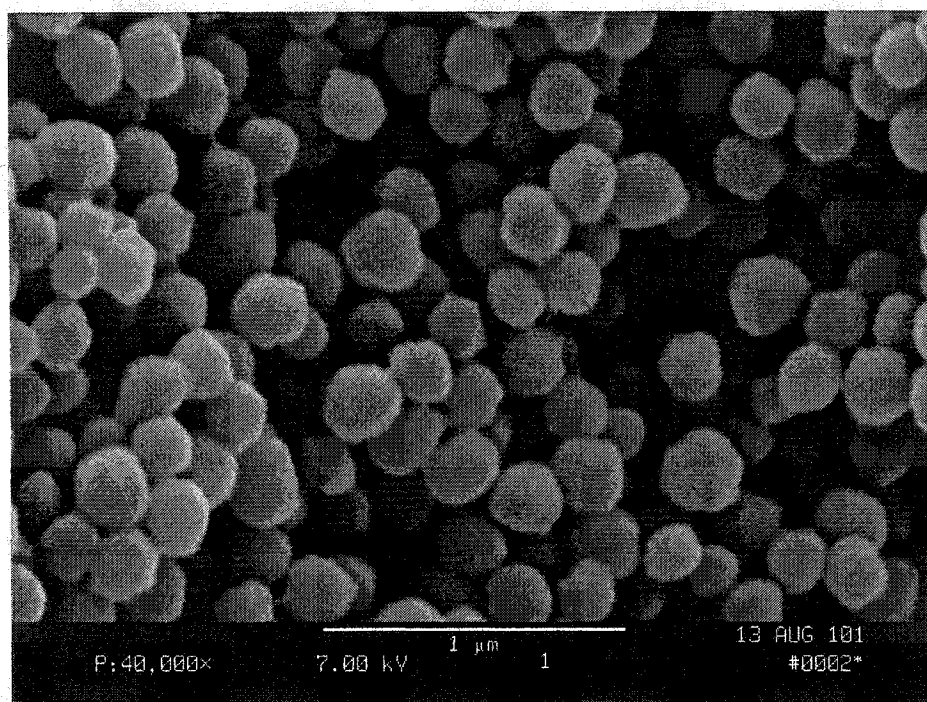
4.6 Conclusion

Norephedrine imprinted poly NIPA-AAc-MBA polymer fibers were prepared by bulk polymerization and evaluated. Their molecular specific swelling proved the potential application of these materials to optical sensing based on polymer swelling. Several attempts were made to prepare these materials as microspheres. A new method was developed to prepare particles by perfluorocarbon suspension polymerization in an ultrasonic bath which keeps emulsion droplets and particles in suspension. The resulting

particles were smaller than those prepared by conventional suspension polymerization although they were amorphorous and not uniform. Molecularly specific swelling was observed from these particles. A method of dispersion polymerization in acetonitrile was developed to prepare theophylline imprinted poly NIPA-MMA-MBA microspheres. 5% crosslinker was used to allow swelling with molecular specificity. Poly styrene-acrylonitrile was used as a stabilizer to give separated spherical particles. These imprinted microspheres were uniform, ca.1.0 μm in diameter and readily obtained via this dispersion polymerization. This is the first method for preparing swellable molecularly imprinted microspheres.

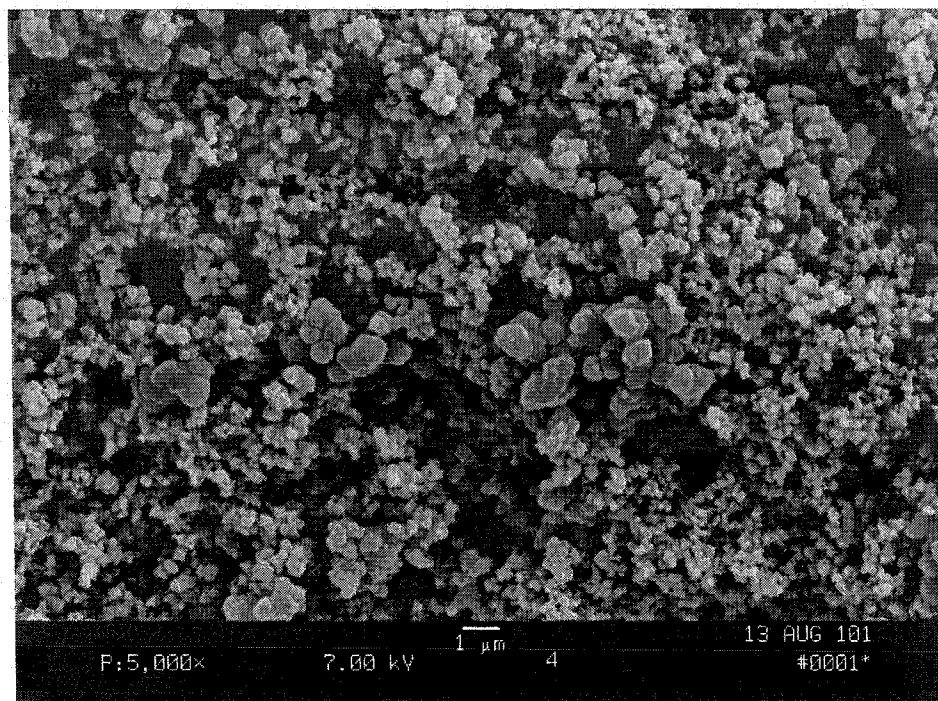


(A)

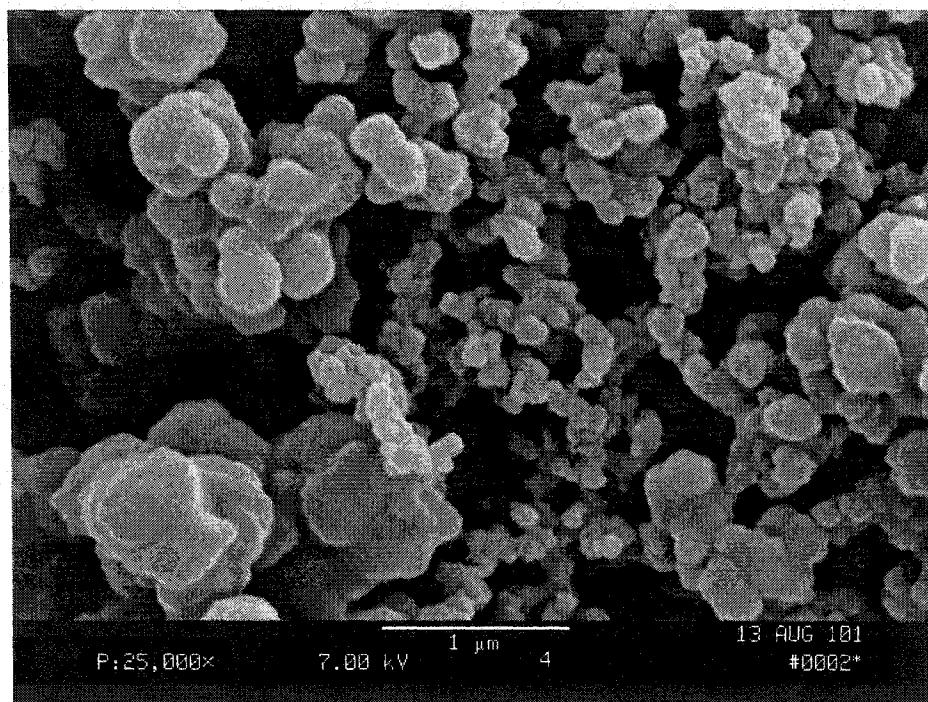


(B)

Figure 4-10. Scanning electron micrographs of untemplated poly NIPA-MAA-TRIM microspheres prepared by dispersion polymerization (59% NIPA, 29% MAA, 12% mole TRIM). A: x 5,000; B: x 40,000.

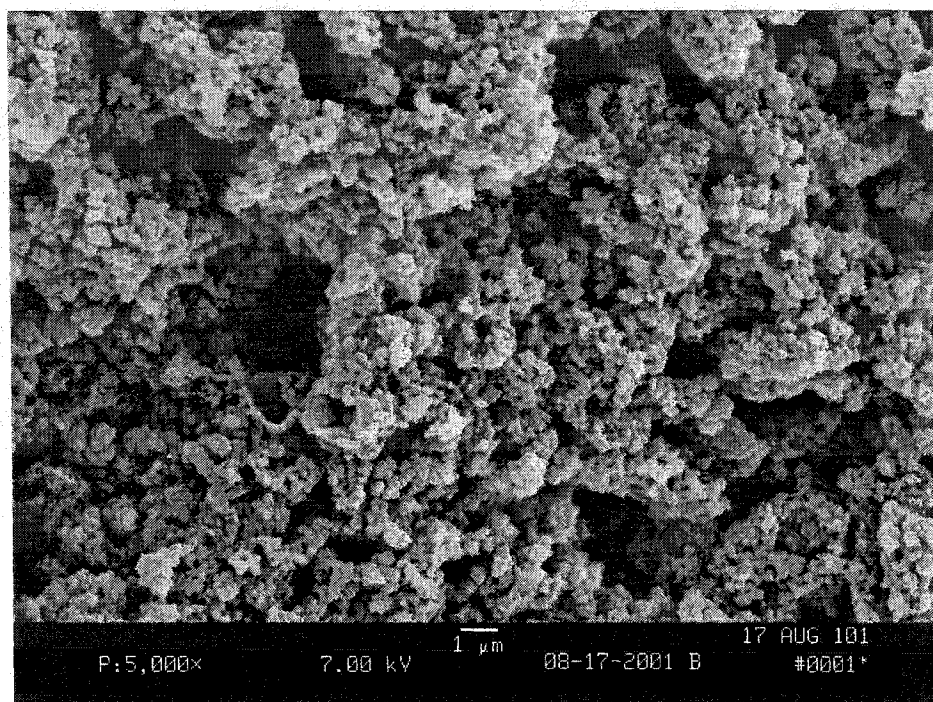


(A)

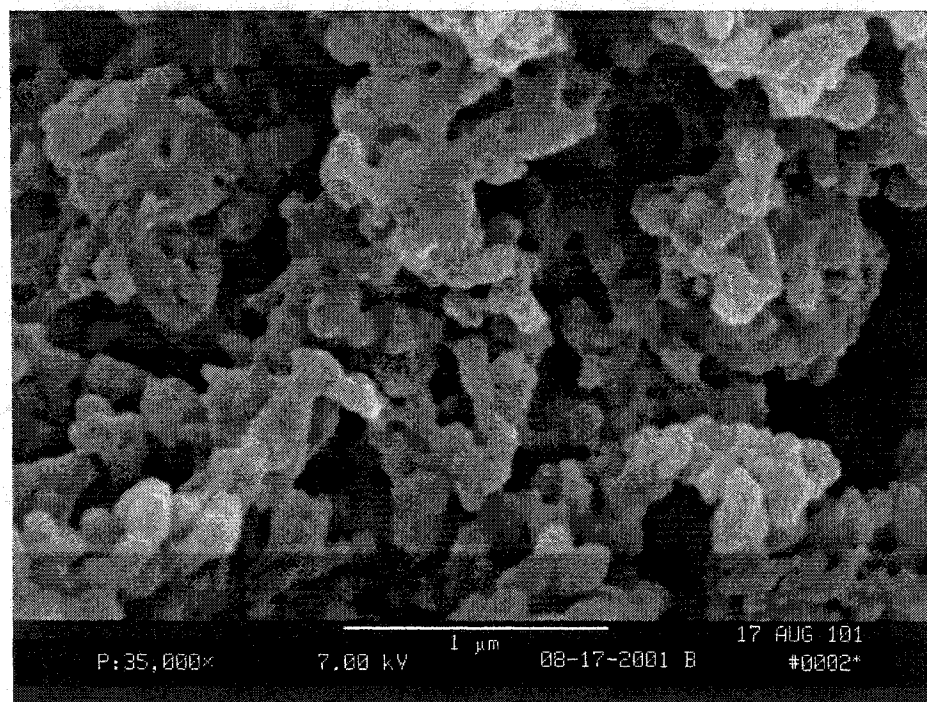


(B)

Figure 4-11. Scanning electron micrographs of theophylline templated poly NIPA-MAA-TRIM microspheres prepared by dispersion polymerization (59% NIPA, 29% MAA, 12% mole TRIM). A: x 5,000; B: x 25,000.

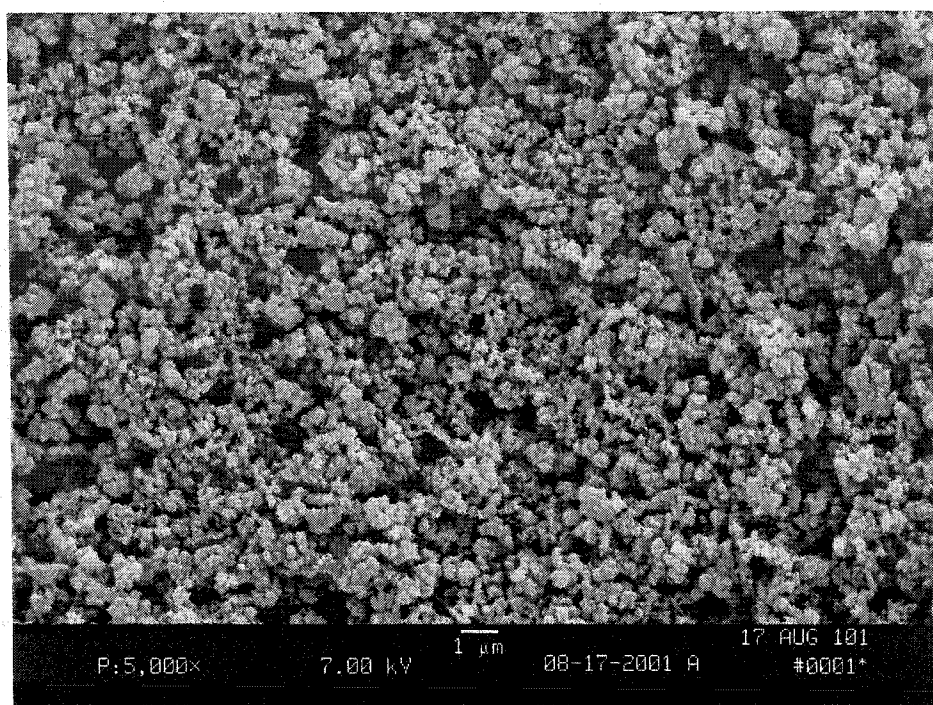


(A)

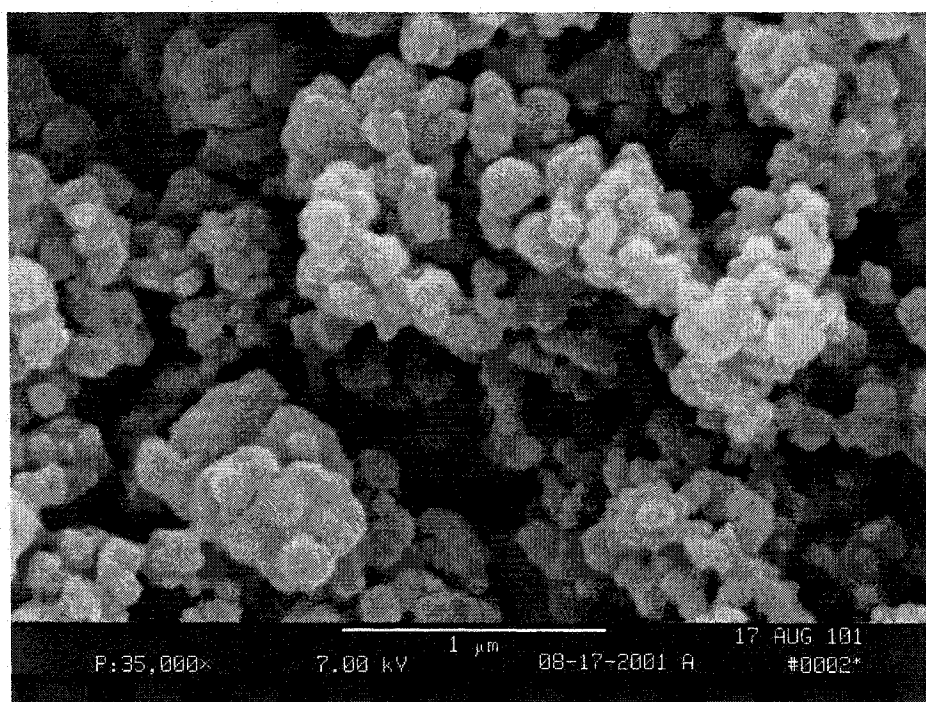


(B)

Figure 4-12. Scanning electron micrographs of theophylline templated poly NIPA-MAA-TRIM microspheres prepared by dispersion polymerization (79% NIPA, 19% MAA, 5% mole TRIM). A: x 5,000; B: x 35,000.



(A)



(B)

Figure 4-13. Scanning electron micrographs of theophylline templated poly NIPA-MAA-MBA microspheres prepared by dispersion polymerization (79% NIPA, 19% MAA, 5% mole MBA). A: x 5,000; B: x 35,000

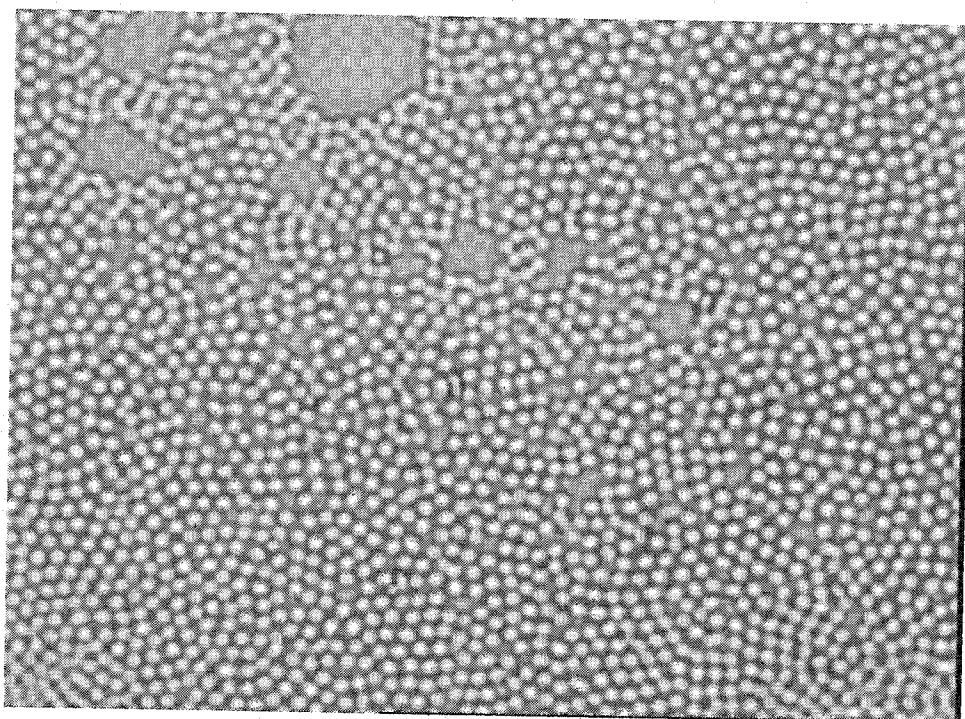


Figure 4-14. Micrograph of untemplated poly NIPA-NTBA-MAA microspheres prepared by dispersion polymerization (52.5% NIPA, 22.5 % NTBA, 20% MAA, 5% mole MBA)

CHAPTER 5

HYDROGEL MEMBRANES CONTAINING SUSPENSION POLYMERIZED MOLECULARLY IMPRINTED POLYMER PARTICLES FOR NOREPHEDRINE SENSING

5.1 Introduction

Phenylethylamine compounds, referred to as Ephedra alkaloids, comprise a group of sympathomimetic agents including (-)-ephedrine, (+)-norephedrine, (+)-pseudoephedrine, (+)-norpseudoephedrine, etc. They are found together in the herb, Ephedra (also called Mahuang, a traditional Chinese medicine) [88] and commercially available as raw materials and in pharmaceutical dosage forms [89]. These sympathomimetic or adrenergic drugs play important roles as neurotransmitters in the central and peripheral autonomic nervous systems and as hormones exerting endocrine and exocrine effects [90]. They have a stimulating effect on several systems of the body, mainly the central nervous, the respiratory and the vasomotor systems. They are used clinically in the United States. As one of sympathomimetic agents with relatively weaker actions, norephedrine is used as an ingredient of some commercially obtainable medicines [91]. It promotes bronchodilation by activating β -adrenergic receptors in the lungs, and it is used for this purpose in patients with asthma. Adverse reactions to this compound include anxiety and restlessness, toxicity incidents, irregular heartbeat, tachycardia, hypertension, and skin eruptions, etc. [88]

Products containing these phenylethylamines alone, or in combination with other ingredients, are marked as dietary supplements in the United States [88]. This is another interest in these Ephedrine-type alkaloids based on their “thermogenic” (calorie burning) effect provided by a mixture of Ephedrine, Caffeine and Aspirin (ECA), which has been used for many years. A new mixture, Norephedrine, Caffeine, and Aspirin (NCA) is used now and reaches the next plateau in fat burning. Instead of ephedrine, NCA uses norephedrine, specifically 1R, 2S-norephedrine. Norephedrine is better than ephedrine because it passes the blood-brain barrier much less than ephedrine, therefore stimulating certain parts of the brain much less. Norephedrine is about half as potent at causing the wired feeling as ephedrine. It has ideal stimulatory properties just enough to burn fat but not so much as to cause the person to feel badly. As a result norephedrine is the ideal fat loss agent, extremely thermogenic, highly anorectic, and very kind on the nervous system. Severe adverse reactions associated with consumption of dietary supplements that contain these agents are similar to those described above and often due to overdose.

Since norephedrine has a stimulating effect on several systems of the body, it is also used as an energy booster to enhance athletic performance. Therefore, it is included in the doping list of pharmacological forbidden substances indicated by the Medical Commission of the International Olympics Committee (IOC) [90, 92]. As it is widely available in asthma, ophthalmic, cold and allergy products and is found in more than 100 pharmaceutical formulations, the Commission has defined a concentration above which it is considered positive. The maximum amount allowed is $5\mu\text{g/mL}$ in urine [90].

For all of these reasons the determination of norephedrine is necessary and very important in pharmaceutical preparation, and biological fluids for monitoring therapeutic

effects in clinic use, side effects in dietary, and determining intake during athletic performance, etc.

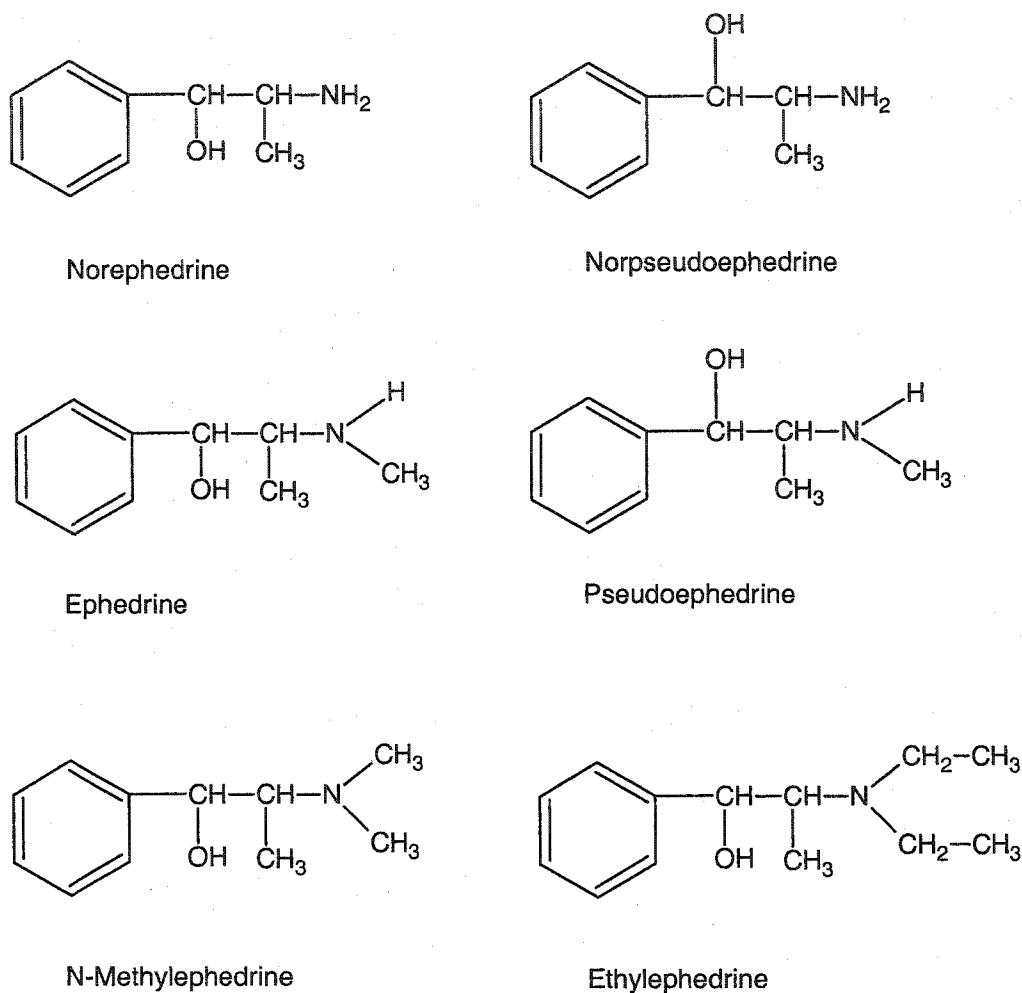


Figure 5-1. Chemical structures of sympathomimetic drugs.

A variety of analytical methods, including thin layer chromatography (TLC) [93], gas chromatography coupled with mass spectrometry (GC-MS) [88], high performance liquid chromatography (HPLC) [92, 94-96], capillary electrophoresis (CE) [97, 98], amperometric [90] and nuclear magnetic resonance spectroscopic methods (NMR) [89],

etc. have been proposed to detect the levels of norephedrine and ephedrine in pharmaceutical samples [89, 93-95] or biological fluids, such as blood plasma [96], urine [91, 92, 97], dietary supplements [88], etc. The most commonly used technique for such determinations is liquid chromatography coupled with various detectors including UV, fluorescence, and chemiluminescence. In this event a pretreatment (extraction, enrichment and purification, etc.) and a pre- or post-column selective derivatization is needed to enhance sensitivity and to resolve naturally occurring diastereomeric pairs, but the reproducibility obtained is not always sufficient because more than one derivative may be obtained for the same compound. The cleanup and resolution of these diastereomeric pairs are still two big problems in the analysis of sympathomimetic agents. Also it takes a long time (usually over 30 minutes) to perform one HPLC analysis.

In this chapter, we attempted to develop a simple, selective MIP-based sensor without any previous derivatization process for the determination of norephedrine. It is the first chemical sensor based on swellable molecular imprinted polymer particles. Hydrogel membranes containing norephedrine templated polymer particles were evaluated. The membrane's turbidity is studied as a function of particle concentration. The effect of heating rate, pH and buffer composite on turbidance and transition temperature of membranes is investigated. Finally, the use of these particles for norephedrine sensing in water and buffer is explored.

5.2 Results and Discussion

5.2.1 Preparation of norephedrine imprinted poly NIPA-AAc particles

As described in chapter 4, it was difficult to prepare imprinted poly NIPA-AAc particles by suspension polymerization in perfluorocarbon using stirring emulsion method although we increased the stirring rate and the amounts of surfactant. Coagulation was the usual result until we started to carry out the polymerization in an ultrasonic bath. This can keep droplets/particles suspension in perfluorocarbon during polymerization. The surfactant PFPS was also needed in this emulsion method and its amount affected the outcome of polymerization. Table 5-1 summarizes surfactant effect on the size and distributions of untemplated poly NIPA-AAc particles. The aggregate polymer was obtained using lower amounts of PFPS. Relatively large particles were produced with 10% PFPS. Using 20% PFPS gave small particles. Figure 5-2 is a microscope picture of untemplated poly NIPA-AAc particles prepared by perfluorocarbon suspension polymerization using ultrasonic emulsion. These particles are small and relatively uniform. The size was 1~3 micrometer which is good for embedding in a hydrogel membrane for optical sensing. 20% PFPS was used in the following experiment. However, it failed to yield uniform particles in the presence of norephedrine at the same conditions. Larger aggregates and only a few particles were present instead. It seems that the template, norephedrine, affected the polymerization. To eliminate this effect, imprinting mixture without template (NIPA, AAc, MBA, BPO, PFPS, and dioxane) was first added in system and mixed. Norephedrine dioxane solution was then added with a syringe while emulsifying. With this technique, separate particles were produced (see Figure 4-8 in chapter). These particles were amorphous and not uniform. One reason is

that temperature during polymerization was not kept constant but varied very much when we added ice to prevent the temperature from increasing during sonication. It was reported that temperature also affected the outcome of perfluorocarbon suspension polymerization [83]. Higher temperatures give small irregular particles while very low temperature (4°C) leads to aggregation. To reduce the particles size, a higher concentration of PFPS was also tried. However, this was limited by PFPS solubility in dioxane.

Table 5-1. Surfactant effect on polymer size and distribution by suspension polymerization in perfluorocarbon in sonicator.

PFPS (% w/w)	Untemplated polymer particles
< 8	Aggregate
10	> 10 μm , separated, not uniform
20	1~3 μm , a little uniform

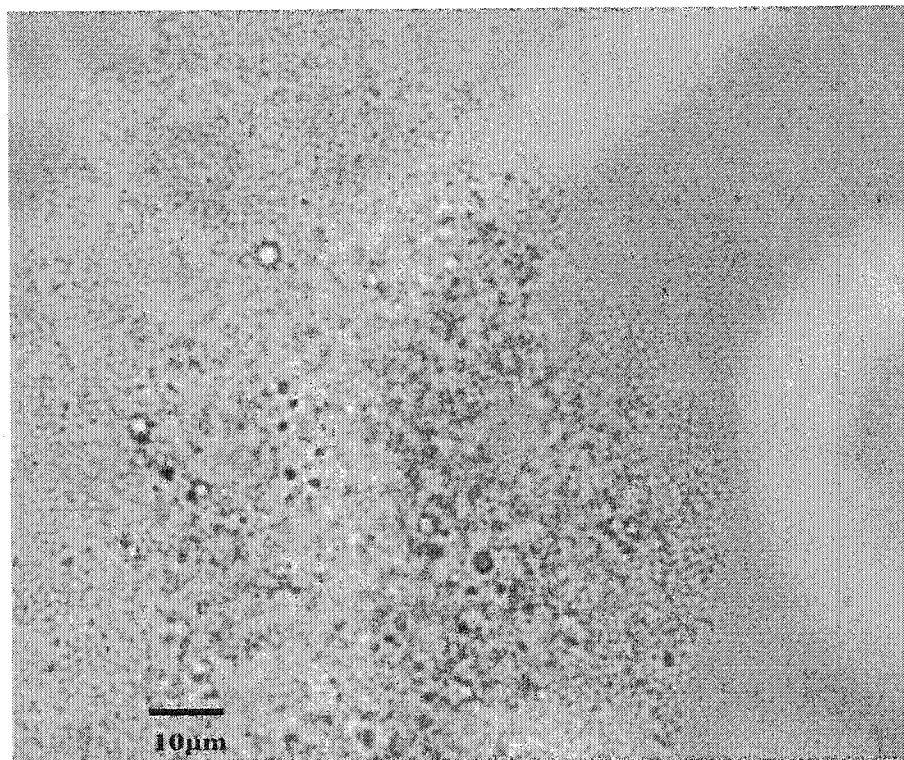


Figure 5-2. Untemplated poly NIPA-AAc particles prepared by perfluorocarbon suspension polymerization.

5.2.2 Turbidity of norephedrine imprinted poly NIPA-AAc particles in hydrogels

In our system, hydrogel membranes were prepared containing norephedrine imprinted particles. The signal comes from the scattering of light at the particle-hydrogel interface due to the refractive index differences between the particles and the hydrogel. Different hydrogels have different physical and optical properties such as refractive index, hydrophilicity, degree of swelling, etc. Both turbidity spectra and turbidity intensity can differ for different membranes. HYPAN was first chosen as the hydrogel because it is mechanically strong and has a relatively low refractive index. We investigated two different types of HYPAN hydrogels, HN80 and HN68. The HN# indicates the weight percent water content of the hydrogel in its fully hydrated form. Figure 5-3 shows the turbidity spectra of particles embedded in these two HYPAN hydrogels. It can be seen that turbidity increases slightly as the wavelength of incident light decreases for both membranes but does not otherwise depend on wavelength. The reason is that the membranes are scattering light, not absorbing a particular wavelength. This is one of the advantages of our sensor, which can use a light source in the near IR region that is used for fiber optic telecommunications. It also shows that the turbidity increases with decreasing membrane water content and that this is more significant at shorter wavelengths. This indicates that the refractive index of our poly NIPA-AAc particles is close to the refractive index of HYPAN 80 ($n=1.36$). The refractive index difference between the particles and HYPAN80 is smaller than that between particles and HYPAN68 ($n=1.38$).

The dependence on particle concentration is shown in Figure 5-4. Higher concentrations of particles in membrane result in higher turbidity, especially at shorter

wavelength. However, high particle concentration will also increase background turbidity. It has to be optimized to obtain the high sensitivity. The high viscosity of HYPAN solution results in a poor suspension for concentrated particles. Approximately 0.5% (w/w) of particles was used to prepare membranes for further study unless otherwise specified.

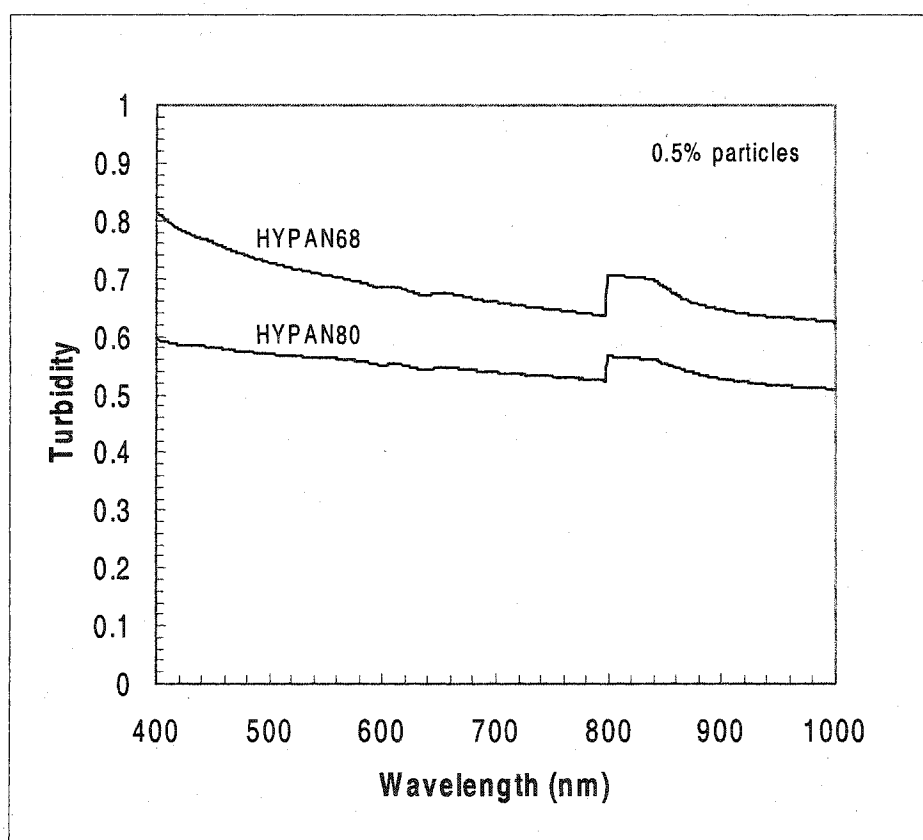


Figure 5-3. Turbidity spectra for norephedrine imprinted poly NIPA-AAc particles embedded in HYPAN membranes. (The glitch at 800 nm is where the instrument changes detectors; it is not the response of the membranes.)

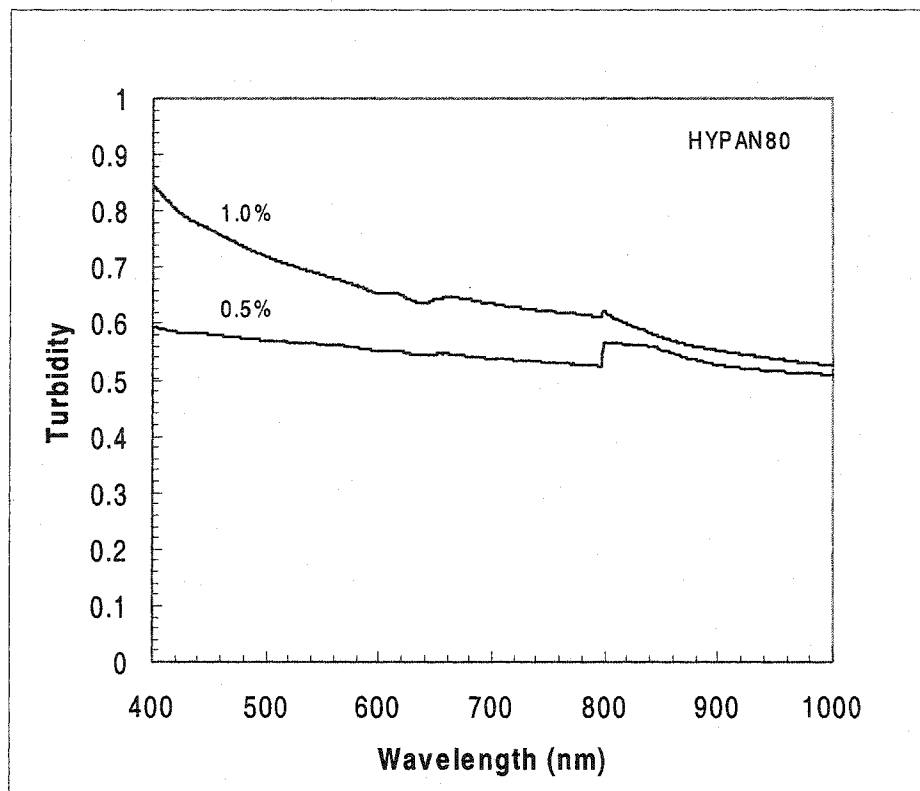


Figure 5-4. Dependence of turbidity on particles concentration (w/w) in HYPAN membranes

5.2.3 Turbidity changes as a function of temperature and phase transition

The molecularly imprinted polymer particles in our sensors are temperature sensitive because of the thermal properties of poly NIPA. Poly NIPA undergoes a temperature dependent phase transition. At low temperatures it is solvated by water and swollen. At high temperatures, it shrinks and comes out of solution. For pure poly NIPA aqueous solution, the phase transition occurs over a narrow temperature range around 32°C [70]. Comonomers and additives affect the transition temperature of poly NIPA. The exact value depends on polymer composition, molecular weight or crosslinker. The transition temperature can be simply estimated by visual observation of the phase separation upon heating or exactly quantified by using a standard UV-Vis spectrophotometer [70]. Fixed wavelength such as 500 nm or 600 nm can be employed. Figure 5-5 shows a typical phase transition of norephedrine imprinted poly NIPA-AAc polymer particles in PVA membrane. The turbidity was measured as absorbance at 500 nm in a Cary 5 spectrophotometer with the ability to vary temperature. The heating rate is 1°C/min. The addition of comonomers (AAc) and crosslinker (MBA) causes the phase transition to occur more gradually over a wider temperature range (32~44°C). The transition temperature is 39°C which is higher than that of pure poly NIPA.

As described in chapter 4, our sensor is based on the swelling response of shrunken state of particles. In this case, membranes with the lower transition temperature allow the sensor to be applied at low temperature. Also large turbidity change at a shrunken state is necessary for a high sensitivity. Figure 5-6 shows turbidity changes of poly NIPA-AAc particles as a function of temperature in different hydrogel membranes. The turbidity contrast shown in Figure 5-6 was calculated from the following equation:

$$\text{Contrast} = \frac{\text{Turbidity at } 60^{\circ}\text{C} - \text{Turbidity at } 22^{\circ}\text{C}}{\text{Turbidity at } 22^{\circ}\text{C}} \quad (5-1)$$

It is clear that PVA membrane is better than HYPAN80 due to the lower transition temperature (39°C) and the high turbidity contrast (3.0). The reason is that the refractive index of particles is closer to refractive index of PVA ($n=1.34$). The membrane has high turbidity when particles are shrunken.

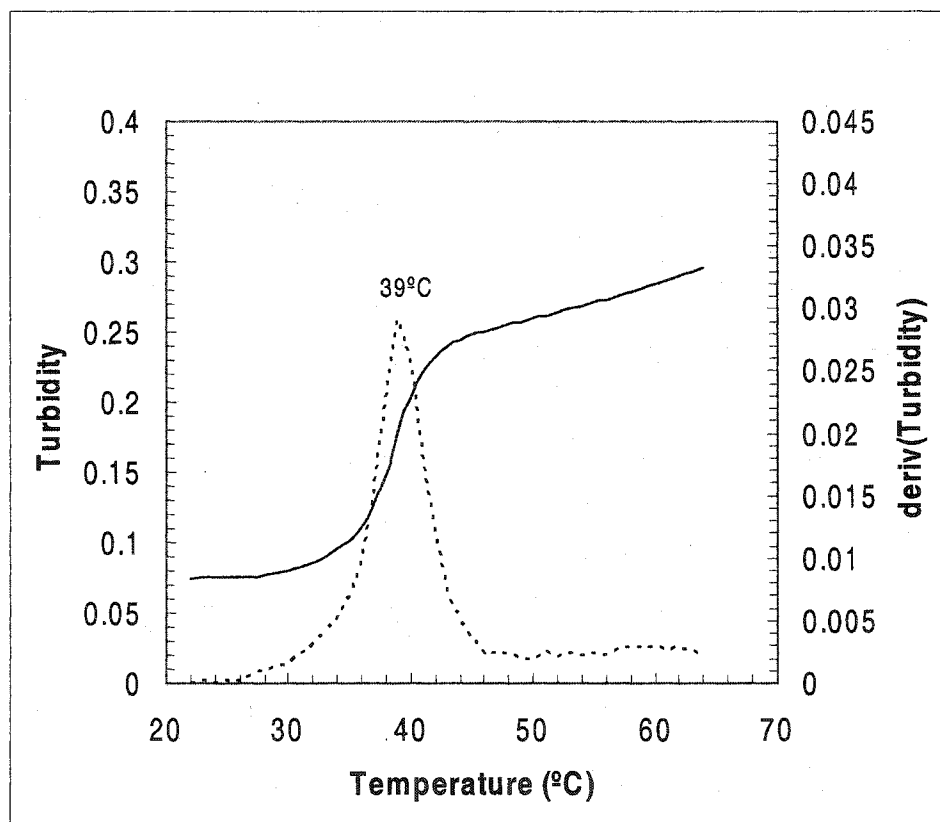


Figure 5-5. Turbidity of poly NIIA-AAc particles embedded in PVA membrane as a function of temperature and the determination of transition temperature. (Wavelength: 500 nm, heating rate: 1°C/min.)

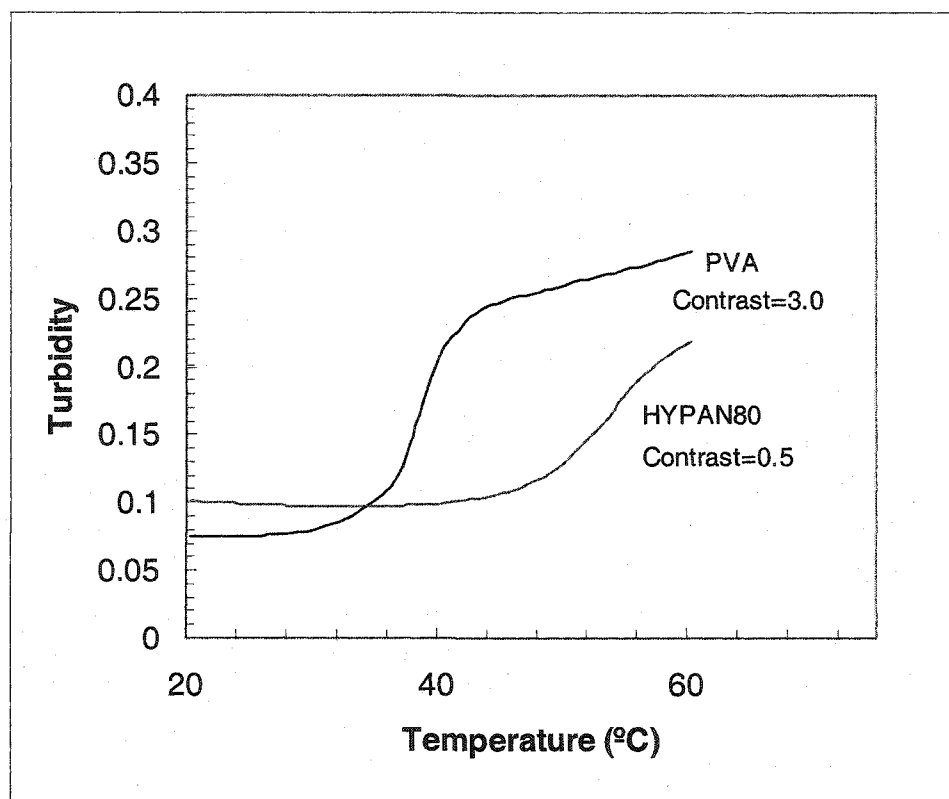


Figure 5-6. Comparison of swelling properties and transition temperatures of poly NIIA-AAc particle embedded in HYPAN80 and PVA membranes in water. (Wavelength: 500 nm, heating rate: 1°C/min.)

5.2.4 pH effect on turbidity measurements and transition temperature

Figure 5-7 shows deprotonation of the polymer back bone of poly NIPA-AAc particles. The carboxyl group of acrylic acid on polymer backbone can be deprotonated at high pH. Figure 5-8 shows the turbidity changes of the norephedrine imprinted poly NIPA-AAc particles in PVA membrane as a function of pH and temperature. Turbidity was measured as absorbance at 500 nm. The temperature scan rate was 1°C/min. The sample membrane was prepared from suspension 0.5% particles in 10% PVA solution. The reference was a particle free PVA hydrogel membrane. AAc ($pK_a \sim 4.25$) is protonated at low pH, and there is no charge on polymer backbone. At low pH, phase transition will take place at low temperature because there is no charge repulsion; On the other hand, at high pH, the deprotonation of AAc induces negative charge onto polymer backbone causing phase transition to shift to higher temperature. When pH is larger than 6, there is no apparent phase transition up to 62°C due to complete deprotonation of AAc.

Figure 5-9 is the pH effect on turbidity changes of imprinted poly NIPA-AAc particles in HYPAN80 membrane at the same conditions use for the PVA membrane. The reference was a particle free HYPAN80 hydrogel membrane. It can be seen that the effect trend is almost the same. However, the turbidity contrast in the shrunken state is smaller and the transition temperature at pH 5 is higher than that of PVA membrane. This is consistent with the result in water. Therefore, PVA membrane was suitable for our particles and used for further work.

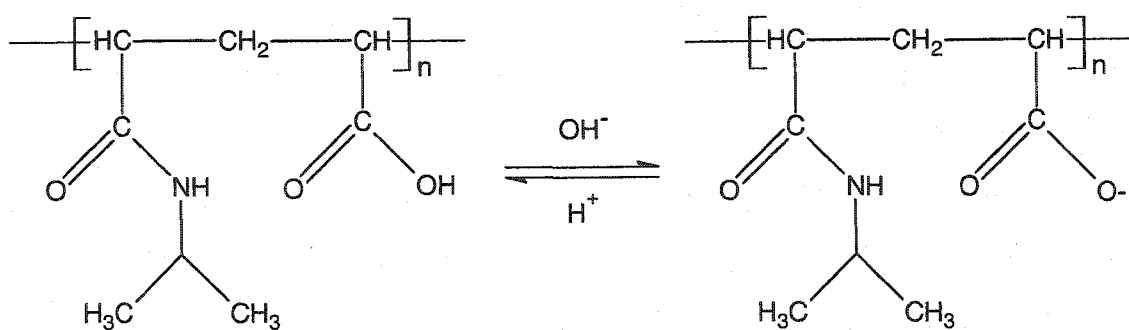


Figure 5-7. Deprotonation of the poly NIPA-AAc particles.

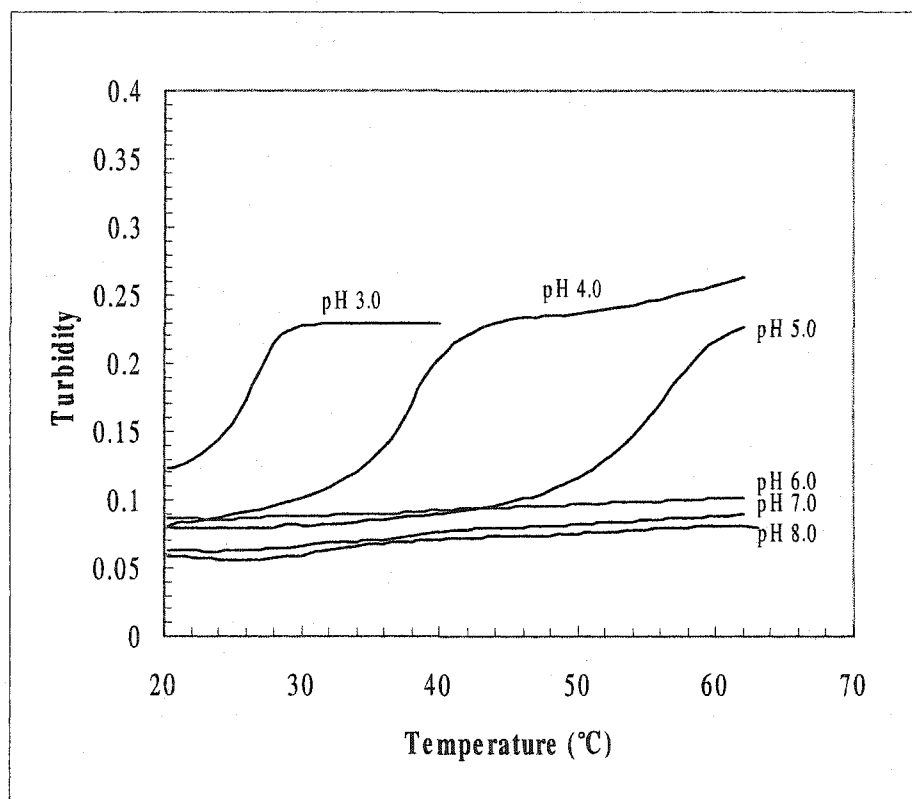


Figure 5-8. pH effect on turbidity of poly NIPA-AAc particles in PVA membrane as a function of temperature. (Wavelength: 500 nm, heating rate: 1°C/min.)

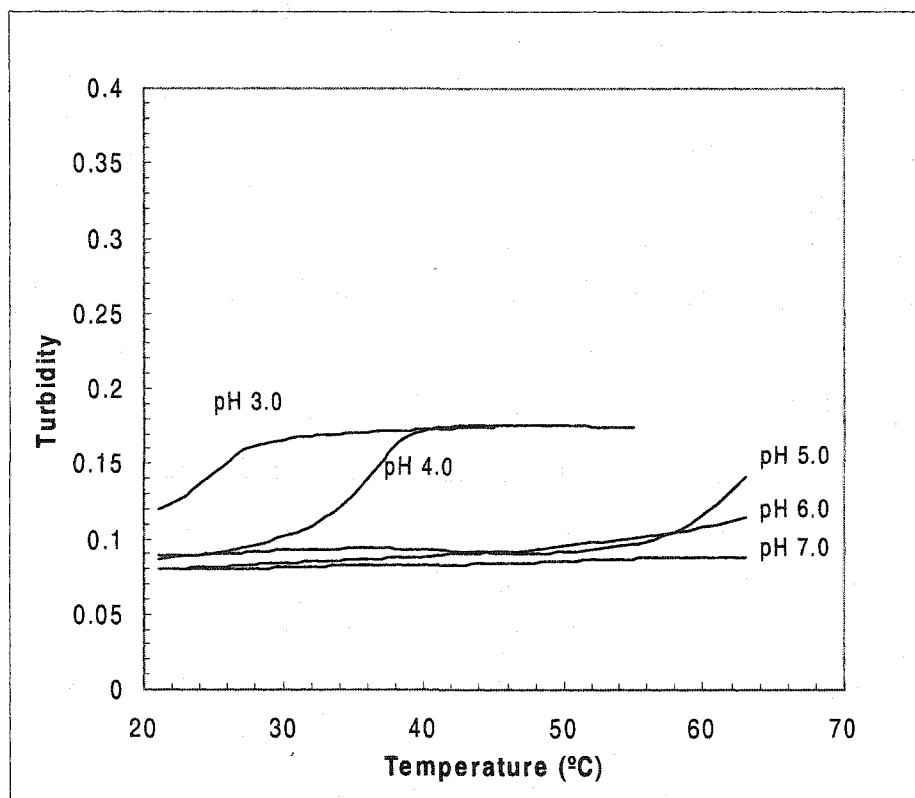


Figure 5-9. pH effect on turbidity of poly NIPA-AAc particles in HYPAN80 membrane as a function of temperature. (Wavelength: 500 nm, heating rate: 1°C/min.)

5.2.5 Heating rate effect on transition temperature

The transition temperature of poly NIPA-AAc particles is very important for our sensor because the measurements will be taken at shrunken state (see Figure 4-1, 4-5). The lower transition temperature can allow our sensor to be conveniently used at room temperature. Most of our experiments were to measure the turbidity changes in the presence of template with increasing temperature. During these experiments, we found that heating rate affected transitions very much. Figure 5-10 shows the heating rate effect at pH 4.0 buffer. It can be seen that the transitions depend on heating rate at $\geq 1^\circ\text{C}/\text{min}$. It can be expected that the transition temperature will be independent and accurately measured at very slow heating rates. However, measurements will be very time consuming at such slow heating rate. As a compromise between accuracy and time, $1^\circ\text{C}/\text{min}$ heating rate was used in further study unless otherwise specified.

5.2.6 Buffer composite effect on turbidity measurements and phase transition

From Flory's polymer swelling equation, the ionic strength of the buffer will have an effect on the swelling of ionic polymer. If the polymer is charged in buffer, the degree of swelling decreases with increasing ionic strength levels due to the shielding of the fixed charges by mobile ions. Figure 5-11 shows the effect of buffer composite on the turbidity of a PVA membrane containing poly NIPA-AAc particles in pH 4.0. Three concentrations of buffer were investigated, 0.001, 0.01, 0.1 M. It can be seen that the magnitude of the turbidity change is not affected by ionic strength results were conversed with Flory's equation. The reason is that, in our case, poly NIPA-AAc is protonated at pH 4.0 and there are no charges on polymer backbone. The shift in transition temperature

with increasing ionic strength comes from the hydrogen bonding interaction between the buffer and polymer. A higher temperature is required to overcome the hydrogen binding interaction and cause the polymer to shrink.

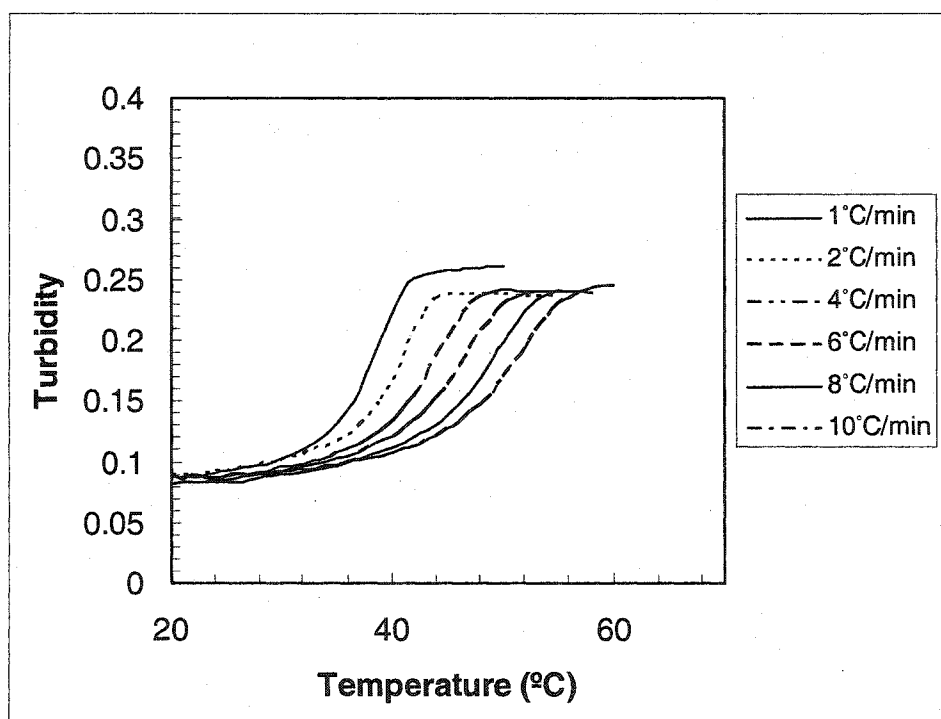


Figure 5-10. Heating rate effect on transition temperature of poly NIPA-AAc particles in PVA membrane in pH 4.0 acetate buffer. Wavelength = 500 nm.

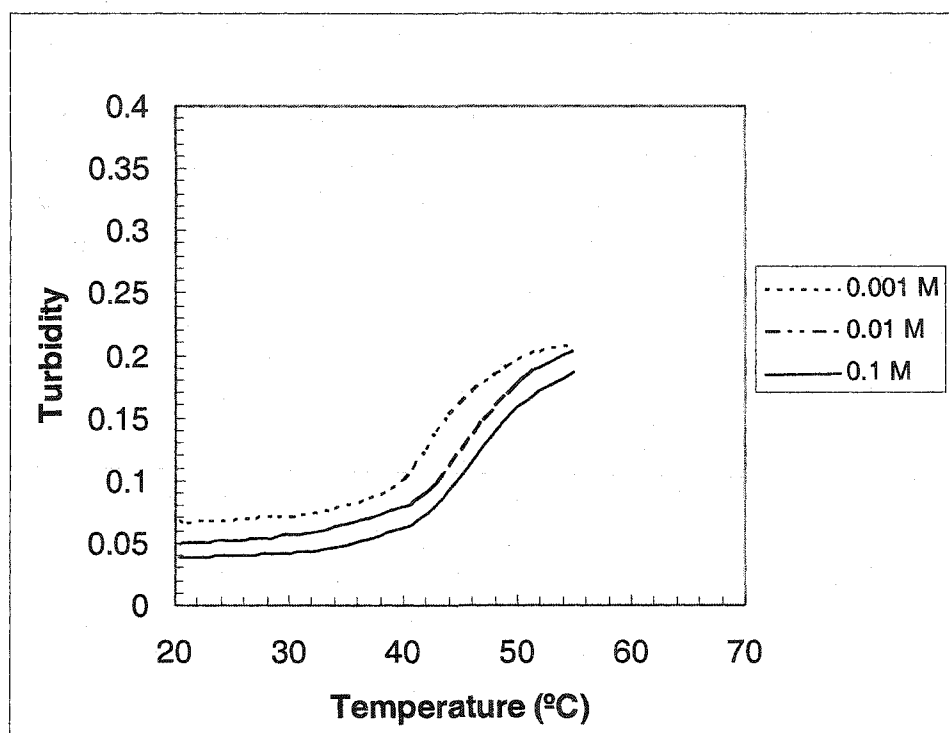


Figure 5-11. Buffer composite effect on turbidity and transition temperature of poly NIPA-AAc particles in PVA membrane at pH 4.0.

5.2.7 Norephedrine measurements

Figure 5-12 shows the turbidity of templated poly NIPA-AAc particles in PVA membrane as a function of temperature at varying concentrations of norephedrine in water. The turbidity was measured as absorbance at 500 nm wavelength and 1°C/min heating rate. We can see that in all cases there is an increase in turbidity with temperature. This is due to the poly NIPA phase transition with temperature. The addition of as little as 1.0×10^{-7} M norephedrine is sufficient to cause a large decrease in turbidity. This indicates that norephedrine causes polymer to swell resulting in lower refractive index. Higher concentrations of norephedrine produce a further decrease in turbidity. The magnitude of the change in turbidity is greater at higher temperatures where the polymer has a lower affinity for water. The unexpected phenomenon is that there is a shift of transition temperature with increasing norephedrine concentration. This effect is associated with the norephedrine-polymer interaction. Figure 5-13 shows the turbidity vs. $-\log$ of the norephedrine concentration at 55°C in Figure 5-12.

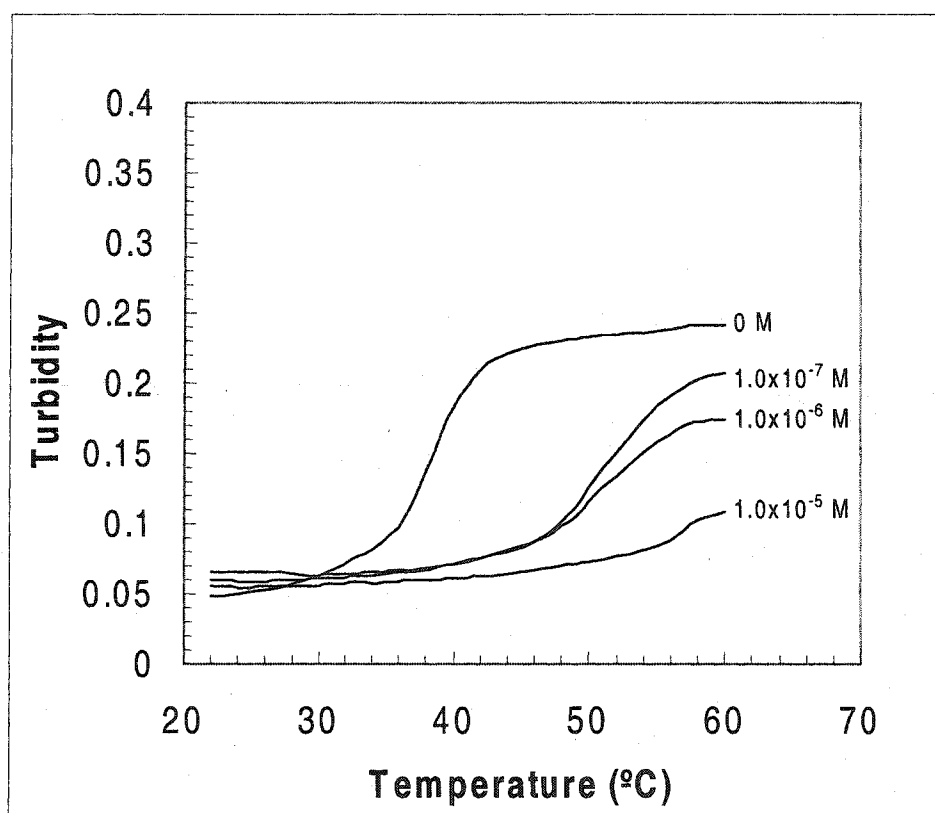


Figure 5-12. Turbidity of norephedrine templated poly NIPA-AAc particles in PVA membrane as a function of temperature and concentration of norephedrine. (Heating rate is 1°C/min). Turbidity was measured as absorbance at 500 nm.

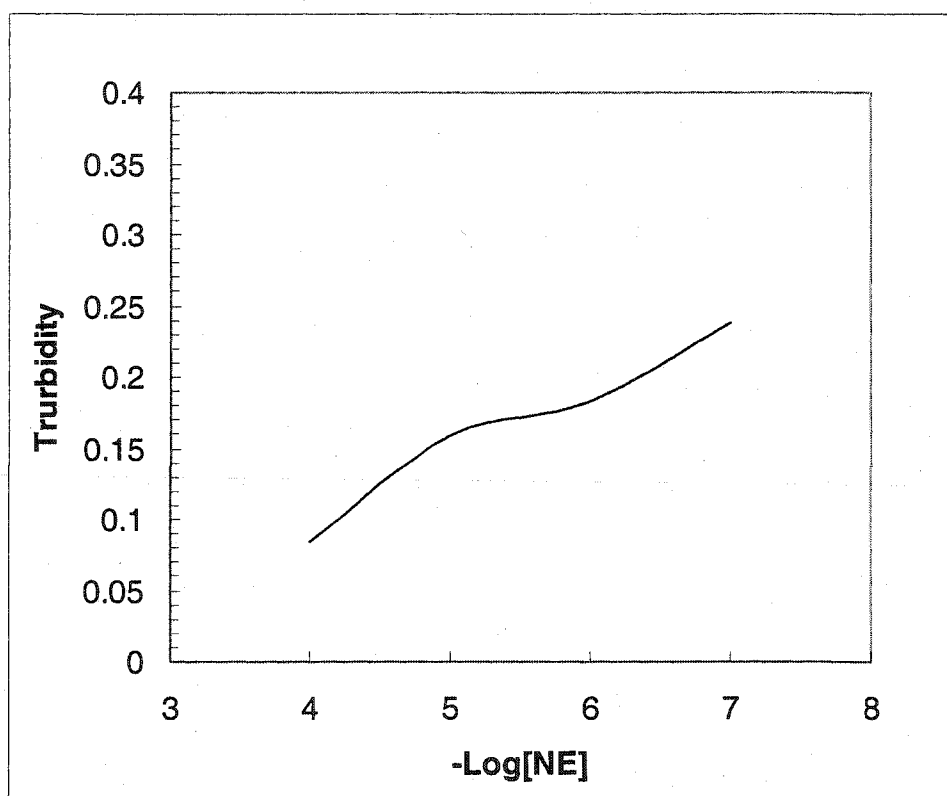


Figure 5-13. Norephedrine (NE) response of templated poly NIPA-AAc particles in PVA membrane in water at 55°C.

5.2.8 Specificity

Figure 5-14 shows the turbidity of untemplated poly NIPA-AAc particles in a PVA membrane as a function of temperature and norephedrine concentration. There is a shift in transition temperature with increasing norephedrine concentration. The possible reason for this shift is that norephedrine interacts with untemplated polymer via unspecific hydrogen binding, but not at multiple sites as with templated polymer (Figure 3-2, 5-12). The same turbidity at the fully shrunken state further indicates that there is no specific interaction and no recognition for norephedrine at this state.

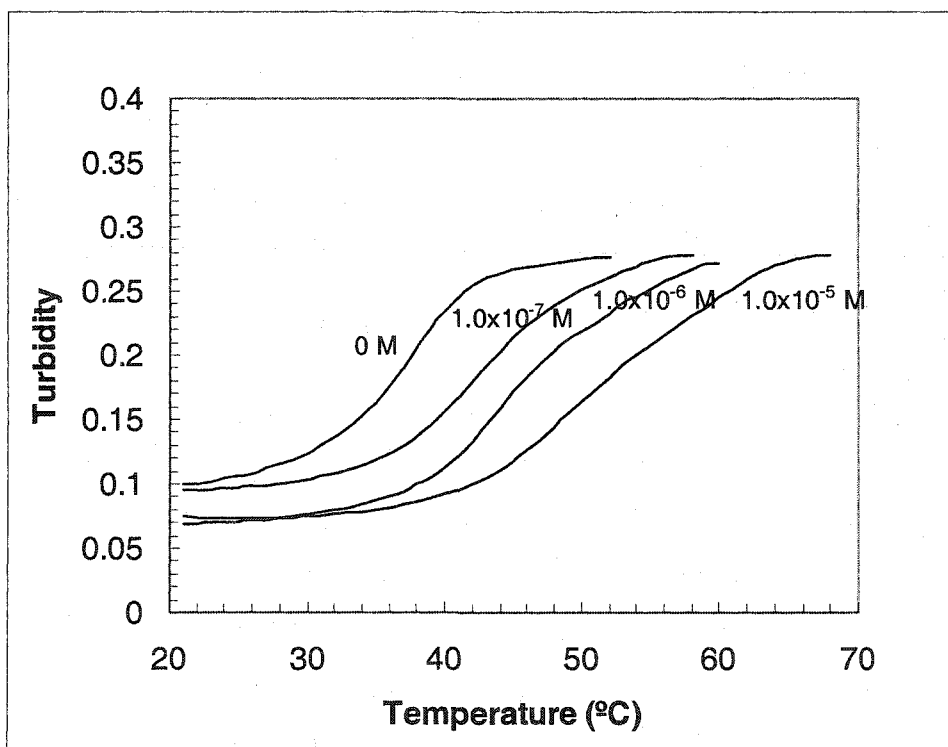


Figure 5-14. Turbidity of untemplated poly NIPA-AAc particles in PVA membrane as a function of temperature and concentration of norephedrine. (Heating rate is 1°C/min). Turbidity was measured as absorbance at 500 nm.

5.2.9 Response time and reversibility

The response time of the membrane containing templated particles was measured by monitoring turbidity as a function of time. The temperature must be kept at a constant for this experiment. Figure 5-15 shows the turbidity of particles as a function of time for 1.0×10^{-6} M norephedrine added to water at 50°C. The response occurs within five minutes. There are many factors that affect the response time such as particle size, functional group density, particle morphology, temperature, thickness of membrane, etc. All of these factors cumulatively affect analyte molecule diffusion in and out of the particles.

After measuring response at higher concentrations of norephedrine (Figure 5-12 5-14), the membrane was exposed to water and the turbidity went back up. This indicates that the membrane responds reversibly to norephedrine.

5.2.10 Norephedrine response in buffer medium

From above results, we know that norephedrine affected the transition temperature when it was measured in water so that all measurements have to be done at high temperature. In order to eliminate norephedrine effect, buffer was used to prepare norephedrine solutions. Figure 5-16 shows the response of templated particles for norephedrine at pH 4.0. pH 4.0 was selected because poly NIPA-AAc particles show a lower transition temperature at this pH. There is no effect on transition temperature. Figure 5-17 shows the norephedrine response at 45°C and pH 4.0. The response is much smaller than in water (Figure 5-13). It indicates that the interaction of polymer-buffer is stronger than the interaction of polymer-norephedrine.

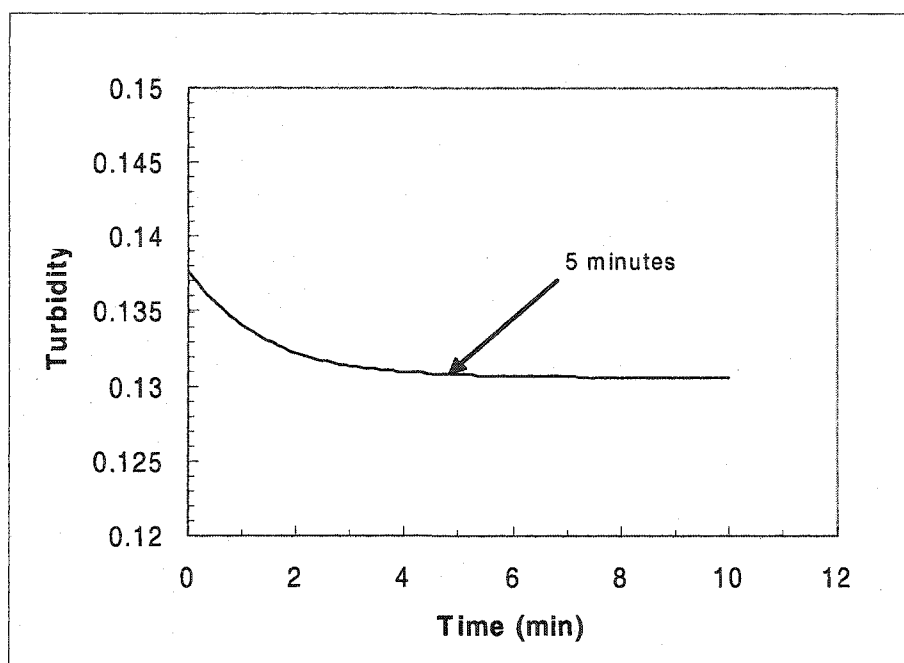


Figure 5-15. Response vs. time for templated poly NIPA-AAc particles in PVA membrane upon adding 1×10^{-6} M norephedrine at 50°C .

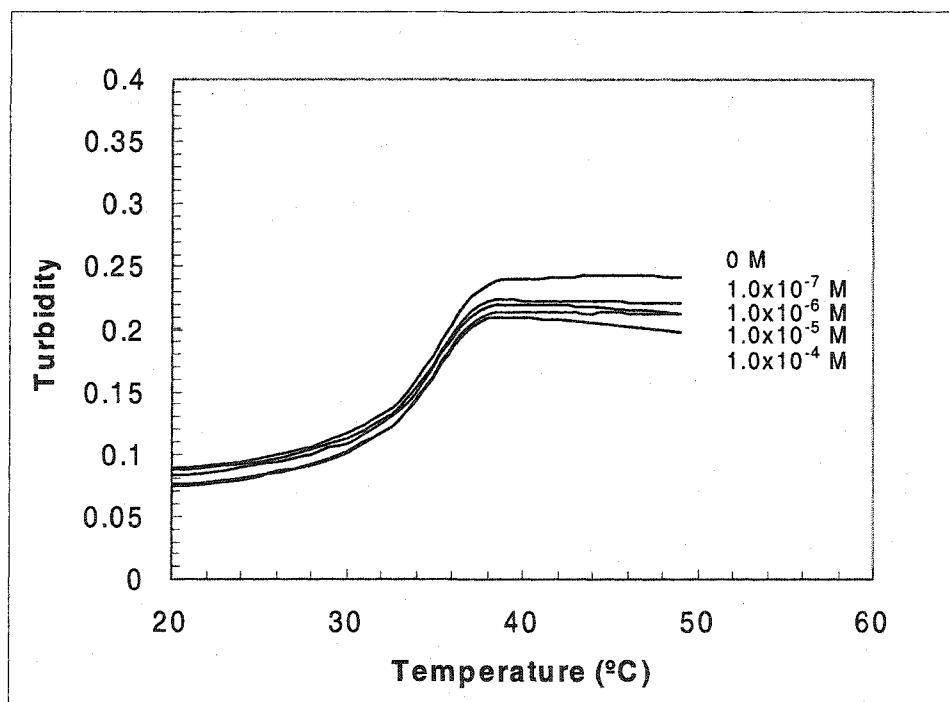


Figure 5-16. Turbidity of norephedrine templated poly NIPA-AAc particles in PVA membrane as a function of temperature and concentration of norephedrine in pH4.0. (Heating rate is $1^{\circ}\text{C}/\text{min}$). Turbidity was measured as absorbance at 500 nm.

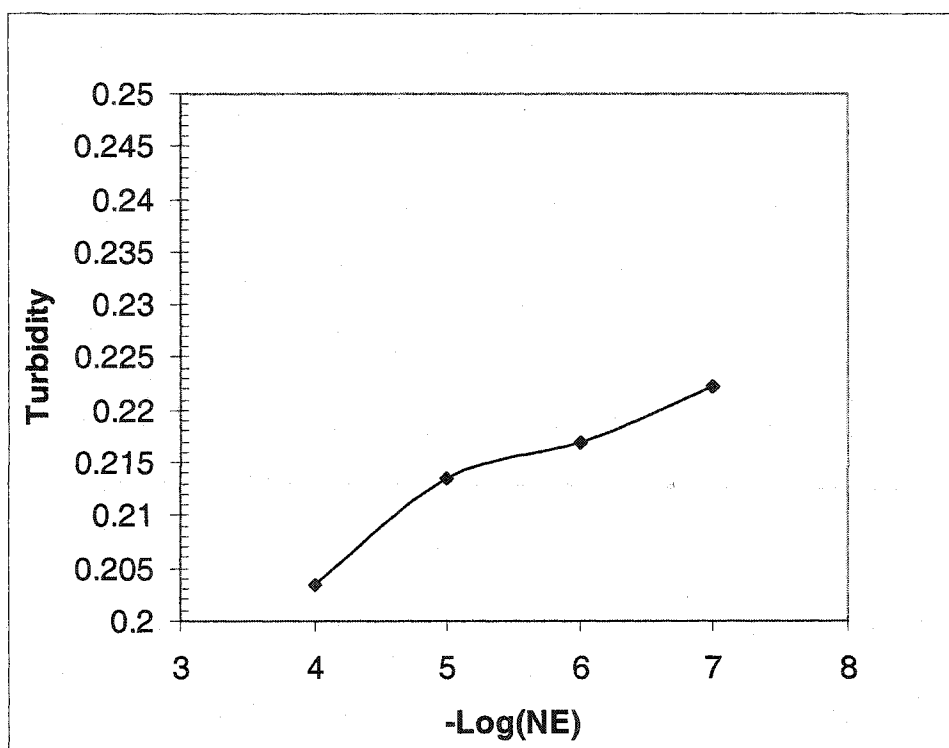


Figure 5-17. Turbidity vs. log norephedrine for a PVA membrane containing templated poly NIPA-AAc particles at pH 4.0 and 45°C.

5.3 Conclusion

Poly NIPA-AAc polymer particles were prepared in the presence and absence of template, norephedrine, by suspension polymerization in perfluorocarbon using ultrasonic emulsion technique. The polymerization formulation was optimized. 20% of PFPS surfactant was used for the preparation of both templated and untemplated polymer particles. Untemplated particles were spherical with diameter from 1 to 3 micrometer. Norephedrine was titrated into the reaction system to eliminate its effect on polymerization of templated particles resulting in relatively large particles (average ca. 6 μm).

HYPAN and PVA hydrogel polymers were used to prepare sensing membranes containing norephedrine templated poly NIPA-AAc particles. Their optical properties and thermal sensitivities were evaluated using UV-Vis spectrophotometer. Particles suspended in PVA membrane produced a larger turbidity change with increasing temperature than in HYPAN. Lower transition temperature of particles in PVA and lower background also encouraged us to use PVA as the sensing membrane although it has a relatively weak mechanical strength.

The transition temperature is dependent upon heating rate. In order to obtain consistent results and lower transition temperature, the heating rate $1^{\circ}\text{C}/\text{min}$ was applied in all experiments. The turbidity-temperature profile is also affected by pH. At high pH, deprotonation of acrylic acid induces negative charges onto polymer backbone. Charge repulsion causes the polymer to swell leading to phase transitions at higher temperatures. The norephedrine response of poly NIPA-AAc particles in pH 4.0 is very small due to the stronger interaction of polymer with buffer. The response of norephedrine in water seems

dramatic. When membrane was exposed in $1.0 \times 10^{-7} \text{M}$ norephedrine at 50°C , turbidity changed by 15%. The same membrane shows no response to adrenaline. The response time is about 5 minutes.

The results show that our swellable norephedrine imprinted poly NIPA-AAc particles respond selectively, sensitively, reversibly to norephedrine.

CHAPTER 6

HYDROGEL MEMBRANES CONTAINING DISPERSION POLYMERIZED SWELLABLE MOLECULARLY IMPRINTED POLYMER MICROSPHERES FOR THEOPHYLLINE SENSING

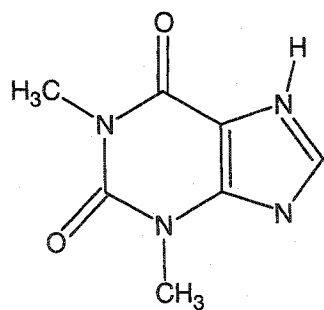
6.1 Introduction

Theophylline is one of most commonly prescribed pharmaceuticals. Physiological conditions such as heart failure, liver disease, infection and obesity can reduce theophylline elimination. Theophylline is a drug used in the treatment of asthma and chronic bronchitis, pathological conditions affecting the trachea and bronchi. They cause the narrowing of the airways. A continuous theophylline therapy can greatly reduce these symptoms [99]. Values for therapeutic serum concentrations are reported between 6-20 mg/L [99]. Toxic effects of theophylline are related to its concentration in the plasma. The symptoms include vomiting, nausea, headache, nervousness, and irritability. High concentrations can produce life threatening toxicity [99]. To prevent this fatal toxicity, frequent measurements or monitoring of theophylline in plasma are very important clinically.

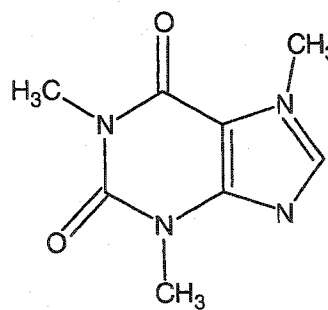
There are a variety of analytical methods for determining theophylline such as spectrophotometry [100], HPLC [19, 101-103], HPLC-MS [104], HPTLC [105, 106], GC [107], GC-MS [108], CE [109, 110], and various immunoassays [111, 112]. However, HPLC methods are lengthy and require sample pretreatments such as extraction [102] or filtration [103]. In addition, there are interferences for HPLC methods if other drugs in

the serum are extracted together with theophylline. The main shortcoming of immunoassays is the potential cross-reactivity of structurally similar compounds such as caffeine and other metabolites [111, 112]. Molecularly imprinted polymers (MIPs) were demonstrated to provide selective affinity for theophylline [80] and various other drugs [46, 69]. Recently, Mullett and Lai developed an on-line method that used a MIP column for the selective solid-phase extraction of theophylline in serum, followed by pulsed elution of the bound theophylline with several 20 μ L aliquots of polar solvent for direct UV detection [113].

The objective of this chapter is to develop a new theophylline optical sensor based on swellable molecularly imprinted polymer microspheres in a hydrogel. In Chapter 5, we prepared norephedrine-sensitive polymer that responded to norephedrine in water. However, there is only small response at pH 4.0 (which is not a practical medium) and no response at higher pH, such as pH 7.0, a biological medium. This is because the buffer-polymer interaction is stronger than the template-polymer interaction. However, for theophylline sensing, the theophylline-polymer interaction will be stronger so that theophylline-templated MIP polymers can be used in buffer for theophylline sensing. This is because theophylline has three basic nitrogens rather than one as in norephedrine. Caffeine has the same structure except for a methyl group in place of hydrogen (Figure 6-1). Therefore, it was used to evaluate the selectivity of theophylline templated MIPs.



Theophylline (THO)



Caffeine (CAF)

Figure 6-1. The structures of theophylline and caffeine.

In this chapter, first swellable THO templated poly NIPA-MAA microspheres were prepared by dispersion polymerization. The swelling and optical properties of a hydrogel membrane containing these microspheres were evaluated and investigated. The THO sensor based on this material was shown to respond in water at high temperature and in buffer at biological temperature. In order to conveniently apply the sensor at room temperature or biological temperature, the temperature transition of poly NIPA-MAA was lowered by replacing part of NIPA with N-t-butylacrylamide (NTBA) or all of the NIPA with N-n-propylacrylamide (NNPA). THO templated poly NIPA-NTBA-MAA and poly NNPA-MAA microspheres were prepared and characterized. The resulting THO sensors based on these two materials can then be successfully used at room temperature.

6.2 Results and Discussion

6.2.1 Preparation of theophylline templated poly NIPA-MAA microspheres

Initially, we attempted to make microspheres by suspension polymerization in perfluorocarbon as we described in Chapter 5 to prepare norephedrine templated MIP

particles. This was completely unsuccessful due to the very low solubility of theophylline in dioxane and the effect of theophylline itself on polymerization. Then we decided to prepare microspheres by dispersion polymerization based on the work of Mosbach and co-workers [80]. Methacrylic acid was used as a functional monomer that interacts with template along with TRIM as a crosslinker. First we successfully prepared untemplated poly NIPA-MAA microspheres with 12% TRIM. The resulting particles were separated, spherical, and uniform (Figure 4-9). The templated polymer, unfortunately, was aggregated (Figure 4-10). Further evaluation of these templated particles showed that there was no response to theophylline. This is because the particles were too rigid to swell with such high crosslinking. We then evaluated a formulation containing lower crosslinker (5%) which is the same concentration used in original literature [69] and in chapter 5. Figure 4-11, 4-12 show the scanning electron micrographs of resulting particles using 5% TRIM and MBA as crosslinkers, respectively. The particles were then cast into a 75 μm thick PVA membrane. The membrane contained approximately 0.5% by weight particles. The optical properties of these membranes were evaluated using standard spectrophotometer. Figure 6-2 shows the turbidity of these membranes as a function of temperature. The contrast shown in Figure 6-2 was calculated from the following equation:

$$\text{Contrast} = \frac{\text{Turbidity at } 60^\circ\text{C} - \text{Turbidity at } 22^\circ\text{C}}{\text{Turbidity at } 22^\circ\text{C}} \quad (6-1)$$

It can be seen that particles using MBA as crosslinker have a larger turbidity change with increasing temperature than those using TRIM as crosslinker. The reason is that TRIM

has one more vinyl group than MBA and therefore has a higher cross-linking efficiency. This will result in more backbone rigid if using the same percentage as MBA. Therefore, MBA was used as the crosslinker in following experiments.

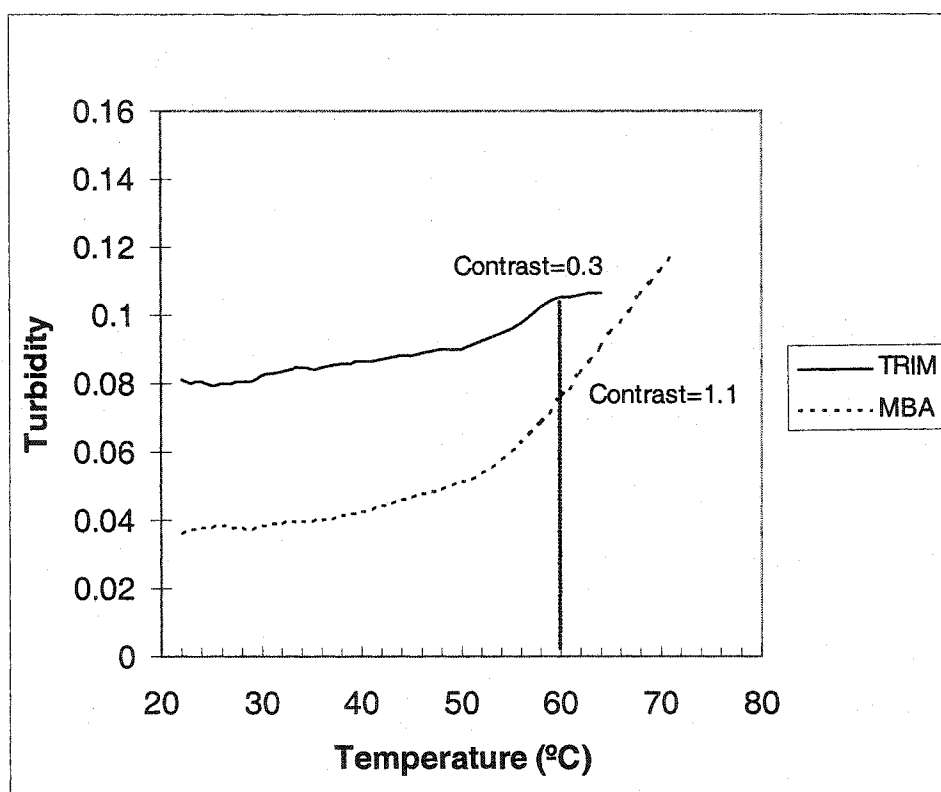


Figure 6-2. Turbidity changes as a function of temperature for poly NIPA-MAA microspheres with 5% MBA or TRIM as a crosslinker. (76 μ m PVA membrane; Wavelength: 500 nm; Heating rate: 1°C/min)

As shown in Figure 4-11, 4-12, we failed to get separated particles. This is because we were not using a stabilizer to prevent coagulation. As reported in literature for the preparation of imprinted microspheres [80], a stabilizer is not needed when using high levels of crosslinker, because this results in rigid beads that do not stick to each other. However, because level of crosslinker in our formulation is much lower, a suitable stabilizer is needed. Most stabilizers are uncrosslinked polymers so we need to consider their solubility in the solvent, acetonitrile. Poly (acrylonitrile) or copolymers containing poly (acrylonitrile) segments were expected to be stabilizers since the monomer units are similar to the solvent acetonitrile. After screening of these polymers or copolymers, poly (acrylonitrile-co-styrene) (containing 30% acrylonitrile) was the best one for our imprinting system. 20% (w/w) of this stabilizer is the optimum amount to produce separated, spherical, and uniform polymer beads with diameters ca. 1.0 μm (Figure 4-13)..

6.2.2 Effect of formulation variables on polymer properties

Table 6-1 shows the results of the factorial experiment described in chapter 3. There were no results for formulations #1-6 because the resulting polymer particles stick to each other forming a big block during extraction and washing. They were very difficult to separate. However we can still get information about how main variables affect polymer properties from #7-12. The turbidity contrast value in Table 6-1 were calculated based from the data at 60°C in Figure 6-3, which shows the turbidity change of polymer #7-12 as a function of temperature. We are interested in the turbidity contrast at shrunken state, which affects sensor sensitivity.

The results of the analysis of variance (ANOVA) Table 6-2, shows all of the main effects and the interacting effects. The main squares (MS) are actual variance estimates and are used to calculate the F ratio. The MS Factor is the combined variance estimate of the treatment and error variance. The MS Error estimates the error variance alone. The ratio of (MS Factor/MS Error) allows one to reject or retain the null hypothesis. The F_{critical} value for this experiment is 18.51, which means if any F ratio is larger than F_{critical} , the null hypothesis may be rejected. When this situation is met, one may conclude that the independent variable has affected the system. The p value represents the probability of incorrectly rejecting the null hypothesis.

The results of ANOVA for this experiment show that no effects are statistically significant at the 95% confidence level. This unexpected result is because all turbidities are small even though there is relatively big difference between results of individual formulations. Since we did not obtain data for formulation #1-6, the ANOVA also can not produce statistical results for all interactions. However, by comparing the F ratios for three main effects in Table 6-2, we still can see that the factors with the larger effects on swelling property are NIPA percentage and crosslinker percentage. The average effects of the three factors are shown in Figure 6-4. Each point represents the average of two formulations for the variables at each level.

Table 6-1. Results of factorial experiment for reaction variables.

Formulation Number	Turbidity Contrast (60°C)	% Crosslinker	THO/MAA	% NIPA
7	0.914	5	1/5	90
8	0.225	5	1/5	80
9	0.687	8	1/2	90
10	0.207	8	1/2	80
11	0.370	8	1/5	90
12	0.264	8	1/5	80

Table 6-2. Results of Analysis of Variance for turbidity contrast.

<i>Source</i>	<i>SS</i>	<i>Df</i>	<i>MS</i>	<i>F</i>	<i>p</i>
MAIN EFFECTS					
A: % Crosslinker	0.0469	1	0.0469	1.07	0.4097
B: THO/MAA	0.0169	1	0.0169	0.39	0.5980
C: % NIPA	0.2711	1	0.2711	6.18	0.1307
INTERACTIONS					
A*B	---		---	---	---
A*C	---		---	---	---
A*B*C	---		---	---	---
Error	0.0877	2	0.0438		
Total	0.4226	5			

Where:

SS = Sum of Squares

Df = Degrees of freedom

MS = Mean Squares

F = F-Ratio (MS factor)/(MS Error)

p = probability of incorrectly rejecting full hypothesis

F_{critical} = 18.51 at 95% confidence level, df = 2.

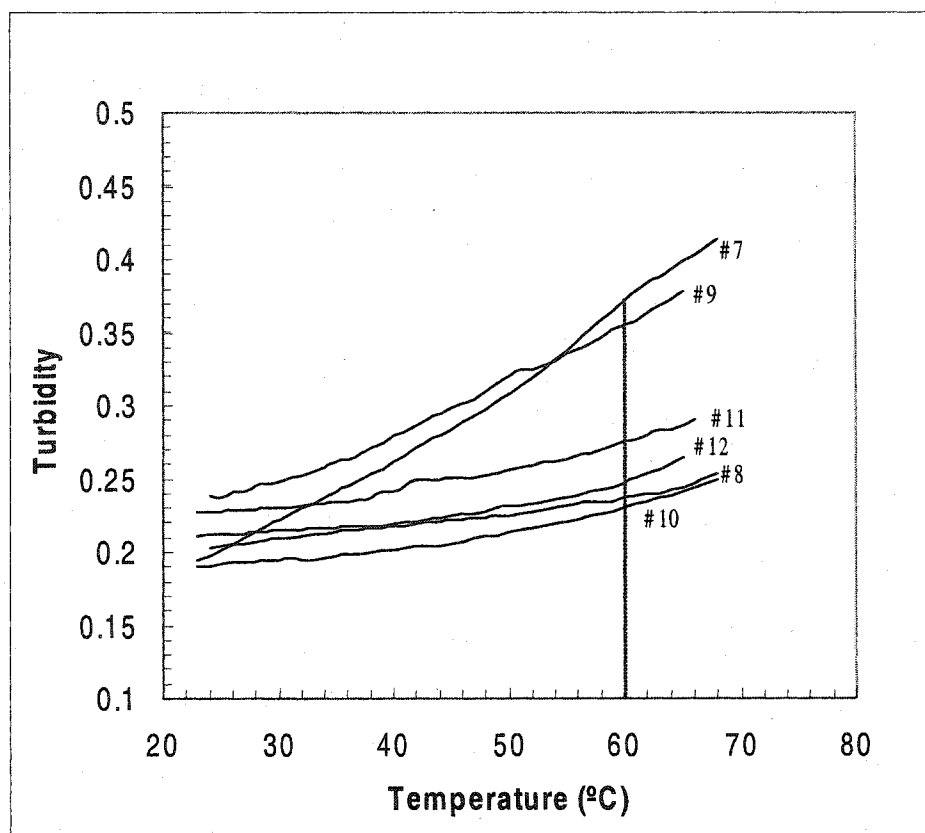


Figure 6-3. Turbidity change of poly NIPA-MAA formulation #7-12 as a function of temperature.

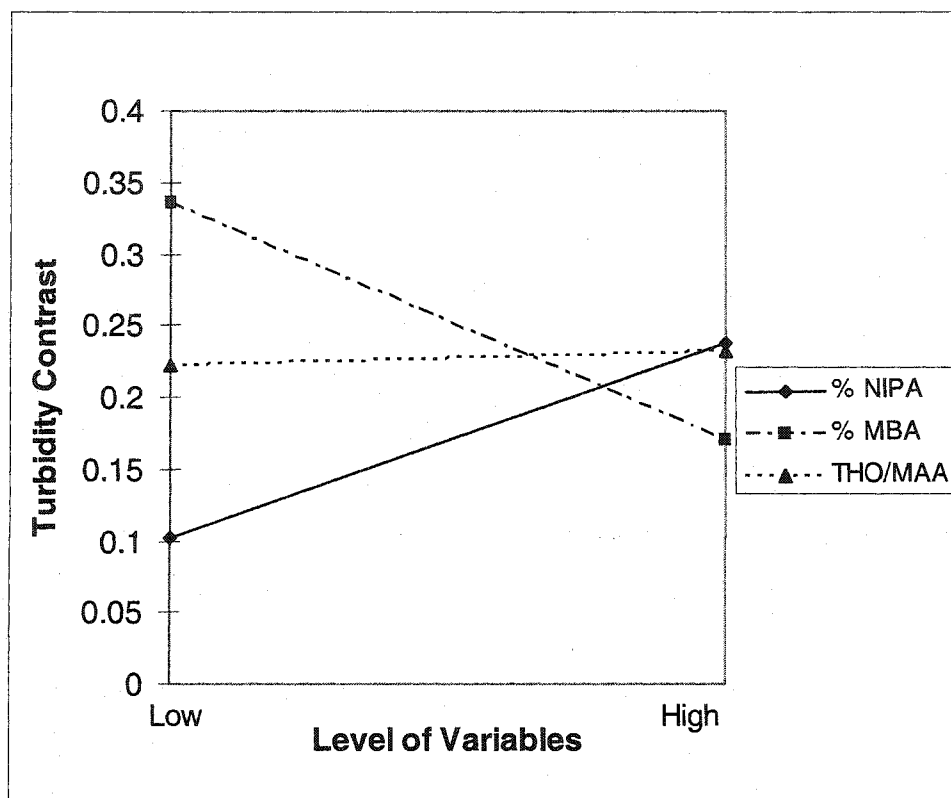


Figure 6-4. The average effect on turbidity contrast upon changing the level of the main variables. The points are average values of the microspheres produced with formulations containing either high or low levels of a particular factor.

6.2.2.1 The effect of NIPA

The percentage of NIPA is a critical variable and has the largest effect on turbidity contrast, Figure 6-4. Our sensor responds at the shrunken state of poly NIPA-MAA microspheres. A large percentage of NIPA is necessary for the swelling and shrinking. However, increasing percentage of NIPA will decrease the percentage of functional monomer. This results in fewer recognition sites in the polymer leading to lower sensitivity

6.2.2.2 The effect of crosslinker

The percentage of crosslinker (MBA) also has a very large effect on turbidity contrast, Figure 6-4. Lower crosslinking results in more flexible microspheres and larger swelling and shrinking. However, it is difficult to form separated, spherical microspheres with lower crosslinking (e.g. formulation #1 to #6). Lower crosslinking will also decrease selectivity and sensitivity. Higher crosslinking might enhance selectivity by imprinting stronger shape-memory to the polymer, but it results in more rigid microspheres that swell and shrink less.

6.2.2.3 The effect of ratio of template to functional monomer

From Figure 6-4, the effect of the ratio of template to functional monomer on turbidity contrast is less dramatic than that of the %NIPA and %crosslinker. The higher ratio of THO to MAA (eg. 1/2) results in higher turbidity contrast than the lower ratio of THO to MAA. The increase in the ratio of THO to MAA leads to more extra THO in the mixture during imprinting. This results in more recognition cavities in the polymer,

which results in more swelling and shrinking. However, a larger effect of the ratio of THO to MAA on sensitivity was expected and will be discussed in section 6.2.3.

6.2.2.4 Interactions

The interactions of the variables provide additional information on how these factors can affect swelling properties. Although we can not obtain the effects of all interactions from ANOVA table 6-2, we can still discuss two interactions based on the data of formulations #7-12.

The interaction between percentage of NIPA and ratio of THO/MAA shows that the high THO/MAA ratio increases turbidity contrast to a greater extent at a high percentage of NIPA than that at a low percentage, Figure 6-5. At the high THO/MAA ratio, extra THO can form more complex, template-functional monomer complexes, during the self-assembly step. This results in more recognition cavities after polymerization and extraction. This also leads to high shrinking with increasing temperature.

The interaction between the percentage of NIPA and the percentage of crosslinker shows that increasing NIPA content increases turbidity contrast to a greater extent at a low percentage of crosslinker than at the high one, Figure 6-6. Our polymer consists predominantly of NIPA and MAA. If we decrease the percentage of one monomer, we actually increase the percentage of the other one. At low level of crosslinker, increasing %NIPA will decrease %MAA resulting in high shrinking at high temperature.

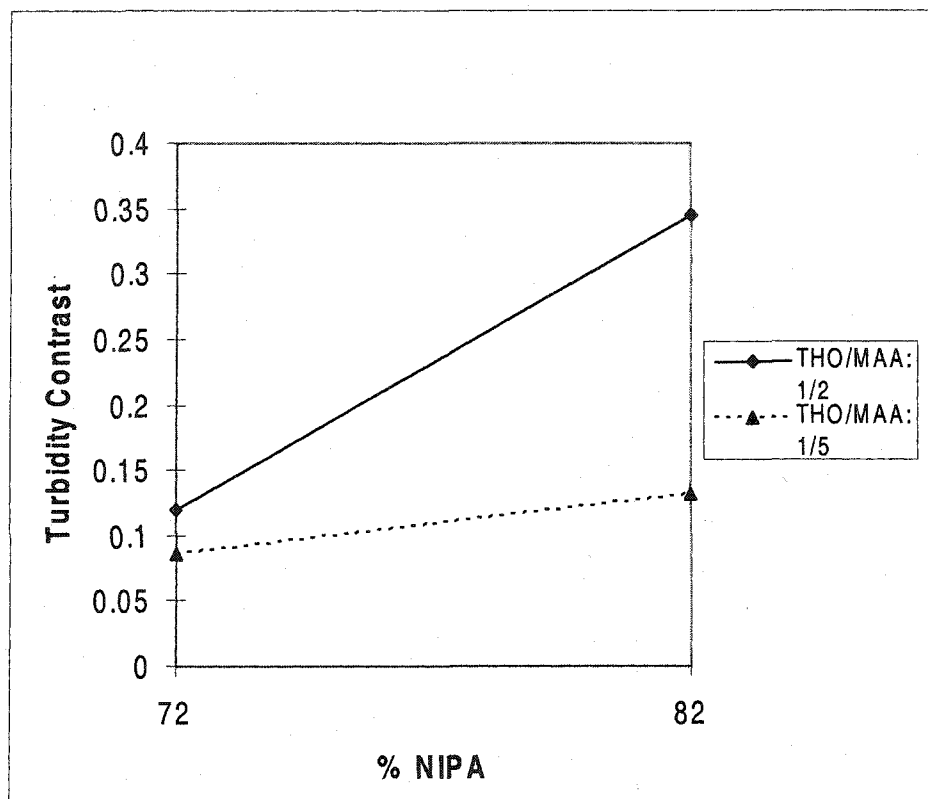


Figure 6-5. The effect of the NIPA*THO/MAA interaction on turbidity contrast.

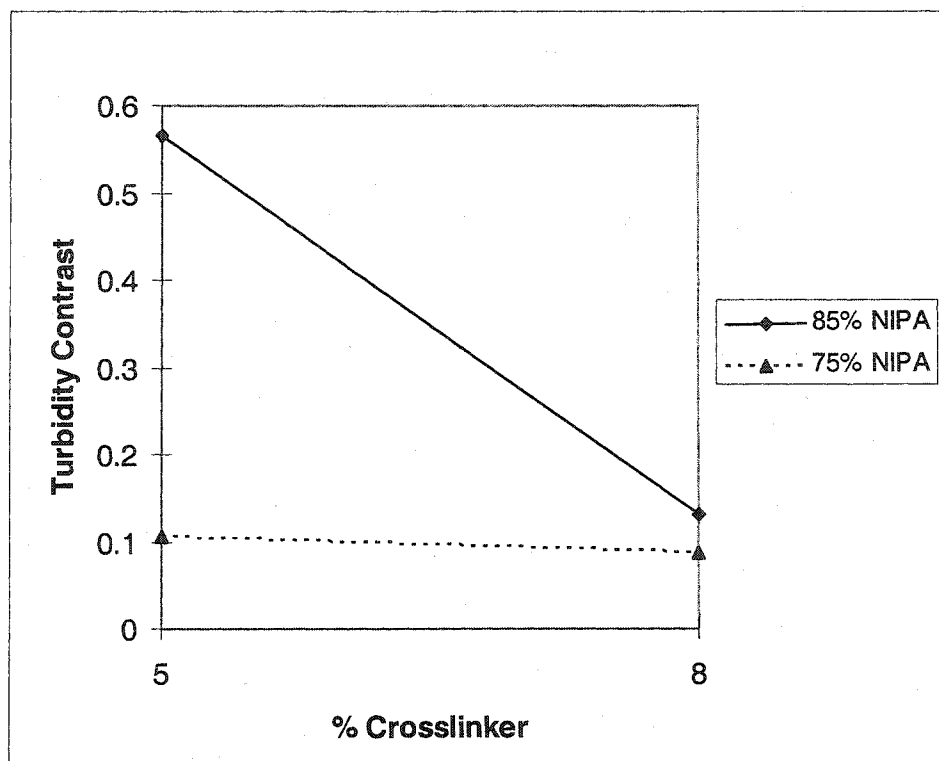


Figure 6-6. The effect of the Crosslinker*NIPA interaction on turbidity contrast.

6.2.3 Effect of formulation variables on sensor response and specificity

The effects of main formulation variables on sensor response and specificity were also investigated. Figure 6-7a to 6-7f show the turbidity changes of THO templated microspheres as function of temperature and concentration of template, theophylline. After comparing Figure 6-7a and 6-7e (same levels of NIPA, THO/MAA but different level of crosslinker, 5% and 8%, respectively), we can see that the sensitivity is already very good with 5% crosslinker. 8% crosslinking results in more rigid microspheres with relatively low sensitivity.

We expect that the ratio of NIPA to recognition monomer MAA will also affect sensitivity to a considerable extent. When the percentage of NIPA is increased, the

percentage of MAA will be decreased. A high level of MAA is expected to form more recognition sites leading to high sensitivity, but it also causes less swelling due to the lower percentage of NIPA. From data in chapter 5 and Figure 6-7, it can be seen that 20% MAA is sufficient for high sensitivity.

The ratio of template to recognition monomer is also important for sensitivity. Ideally, one recognition molecule should bind to one active site on the template. So the stoichiometric ratio is 1/3 for THO to MAA, since THO has one nitrogen and two oxygens that act as hydrogen bond acceptors. We tried two ratios, 1/2 and 1/5, in formulation # 7~12. From Figure 6-7c and 6-7e, we can see that the ratio of one theophylline for two recognition monomer results in high sensitivity. In generally, optimum imprinting is obtained when the ratio of template to recognition monomer is slightly greater than stoichiometric.

Figure 6-8a ~ 6-8f show the turbidity changes of THO templated microspheres as function of temperature and concentration of caffeine. Formulation variables have less effect on selectivity. Relatively higher selectivity was obtained when using higher level of recognition monomer (20%) and higher level of crosslinking (8%) (see Figure 6-8d and 6-8f). A high level of recognition monomer ensures the maximum number of complementary interactions to be developed during polymerization. A high level of crosslinker helps to shape the functional groups in a stable arrangement complementary to the template. However, the selectivity is already good with 5% crosslinking.

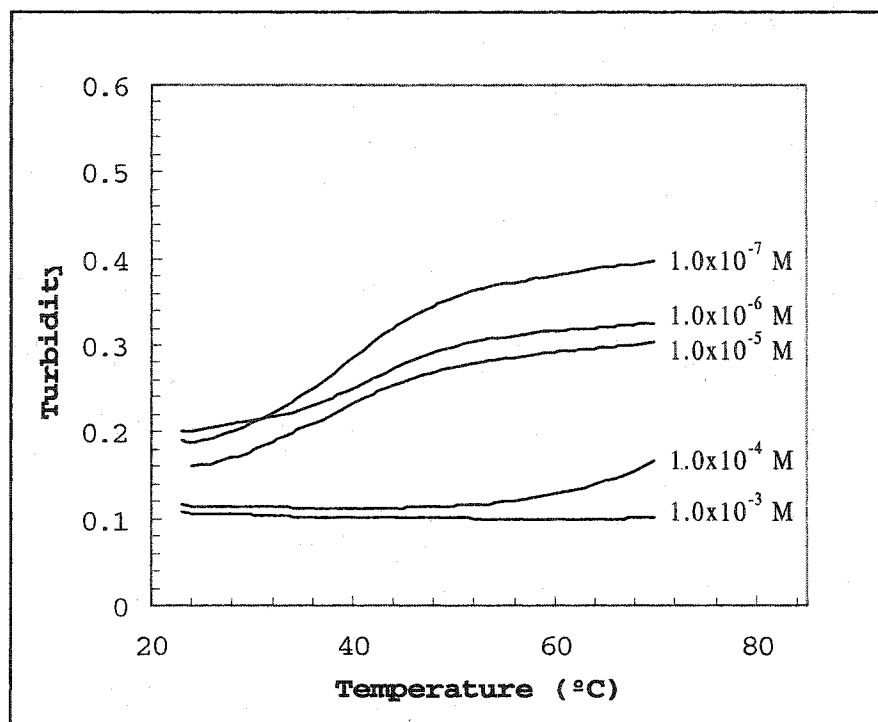
The preferred level of main formulation variables for the preparation of poly NIPA-MAA microspheres by dispersion polymerization was chosen: 75% NIPA, 20%MAA, 5% mol MBA, and a ratio of one THO for two MAA.

6.2.4 THO response and selectivity of templated poly NIPA-MAA in water

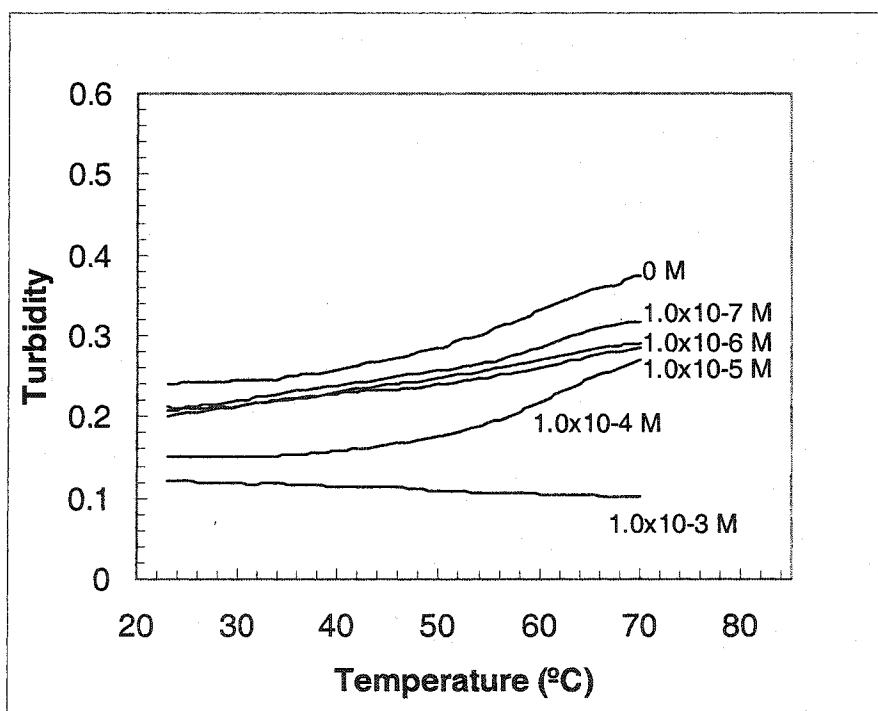
Figures 6-7 and Figures 6-8 show the turbidity of templated poly NIPA-MAA as a function of temperature at varying concentration of theophylline and caffeine in water. The results are dramatic. The addition of as little as 1.0×10^{-7} M theophylline is sufficient to cause a large decrease in turbidity. This indicates that THO is causing microspheres to swell lowering the refractive index. Higher concentrations of theophylline further decrease turbidity. The extent of the change in turbidity is greater at higher temperatures where the polymer has a lower affinity for water. This is consistent with the original literature description [69] and our results in chapter 5 for norephedrine templated polymer.

In all of Figure 6-7a to 6-7f, the response difference for 1.0×10^{-6} and 1.0×10^{-5} M theophylline is very small. The one possible explanation is that the polymer may have two populations of recognition sites, one with a high affinity for theophylline and another with a much lower affinity.

As shown in Figure 6-8, these MIP microspheres have almost no response to caffeine with the concentration as high as 1.0×10^{-4} M indicating that our swellable poly NIPA-MAA microspheres are highly selective.

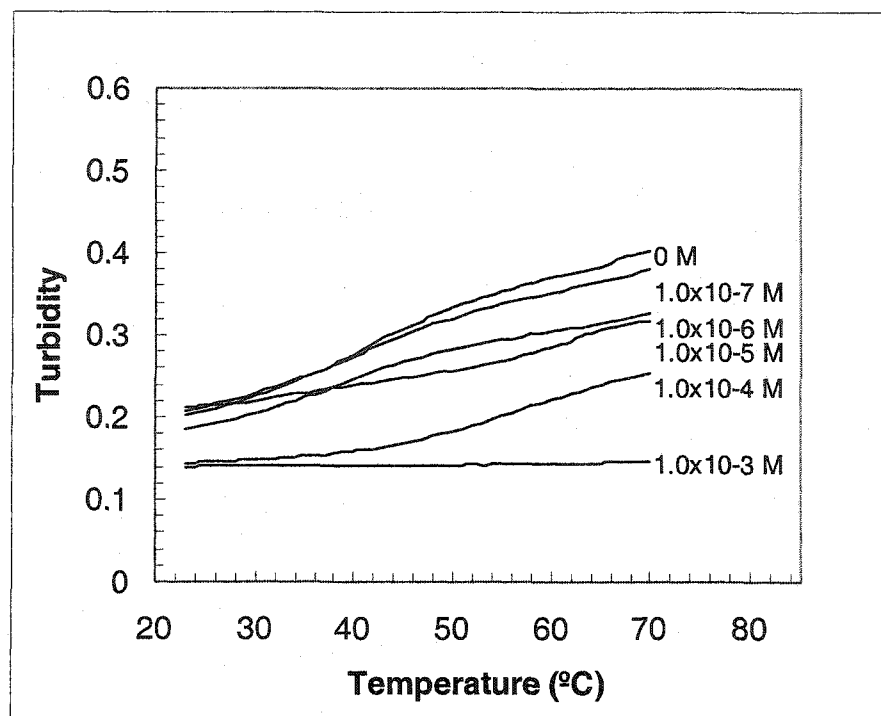


(a)

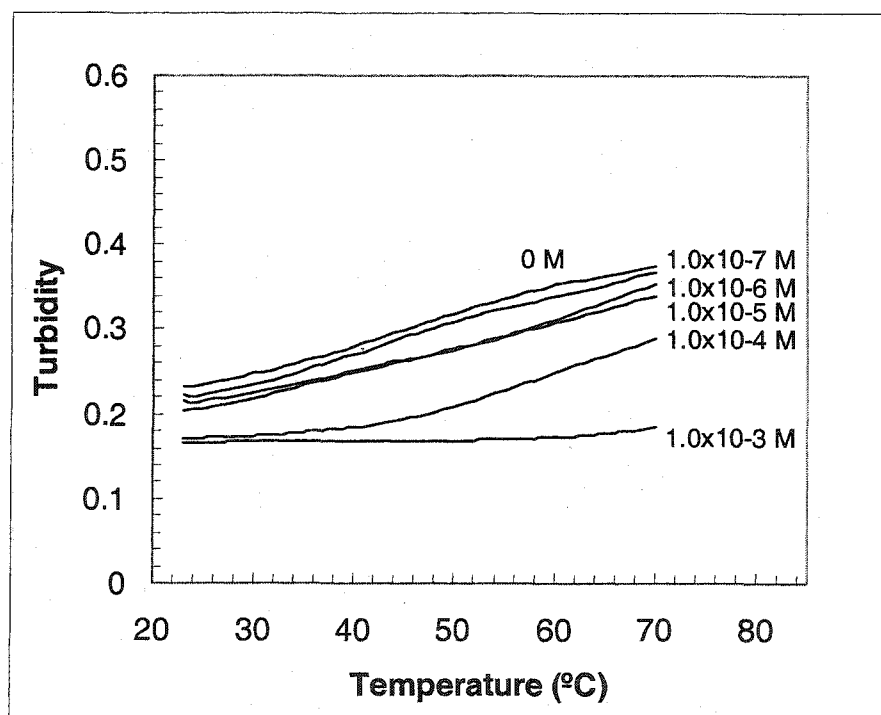


(b)

Figure 6-7. Turbidity of templated poly NIPA-MAA microspheres as a function of temperature and THO concentration. (a). formulation #7, (b). formulation #8.

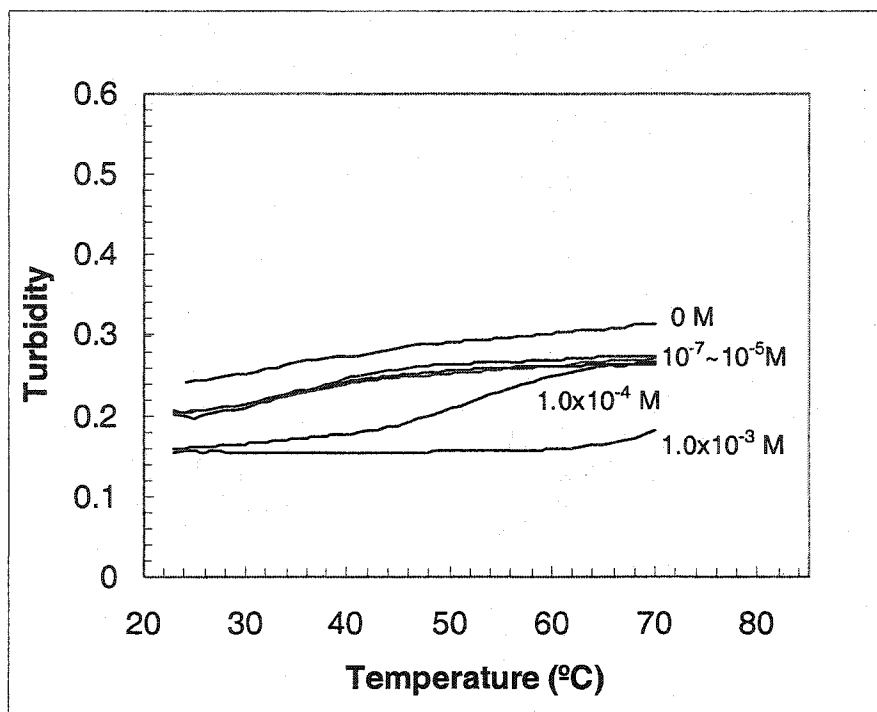


(c)

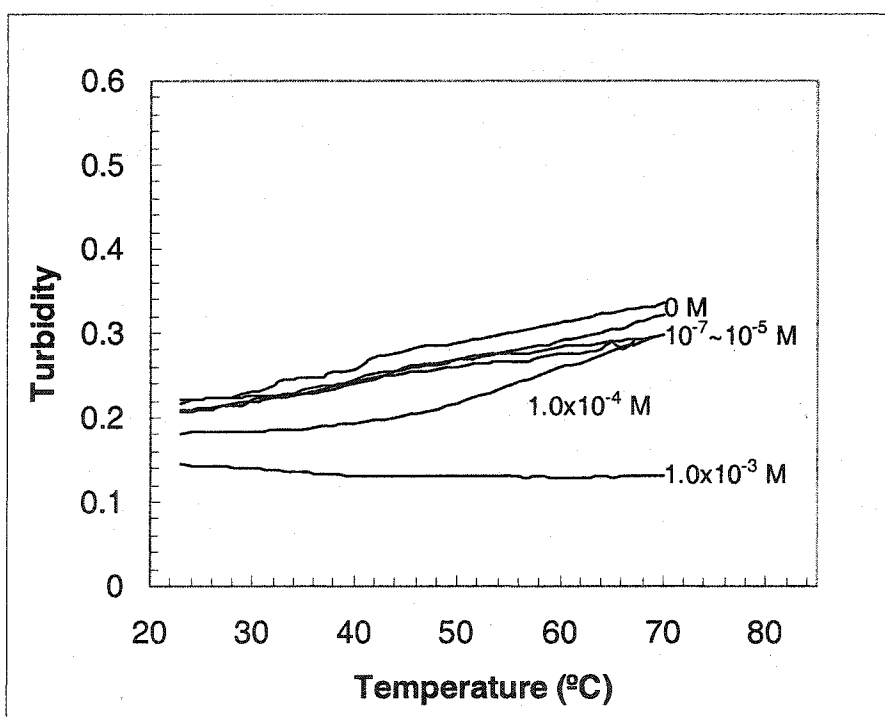


(d)

Figure 6-7 (continued). Turbidity of templated poly NIPA-MAA microspheres as a function of temperature and THO concentration. (c). formulation #9, (d). formulation #10.

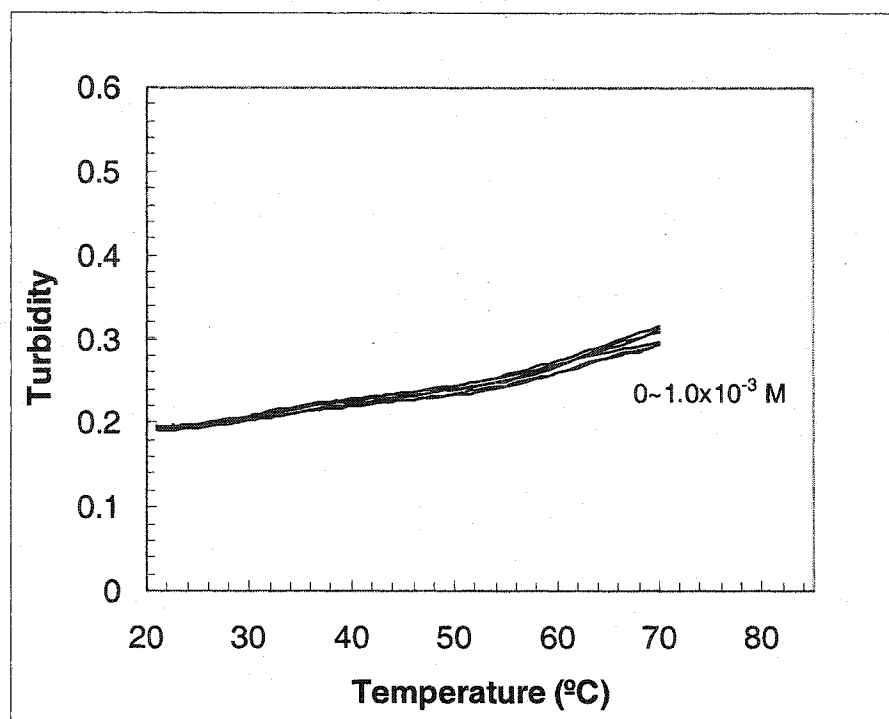


(e)

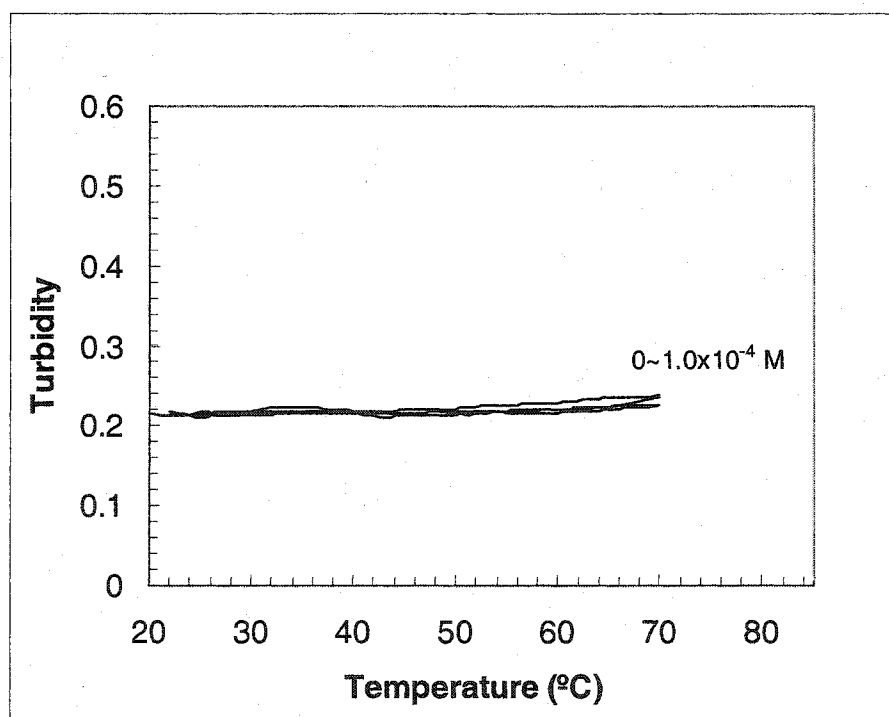


(f)

Figure 6-7 (continued). Turbidity of templated poly NIPA-MAA microspheres as a function of temperature and THO concentration. (e). formulation #11, (f). formulation #12.

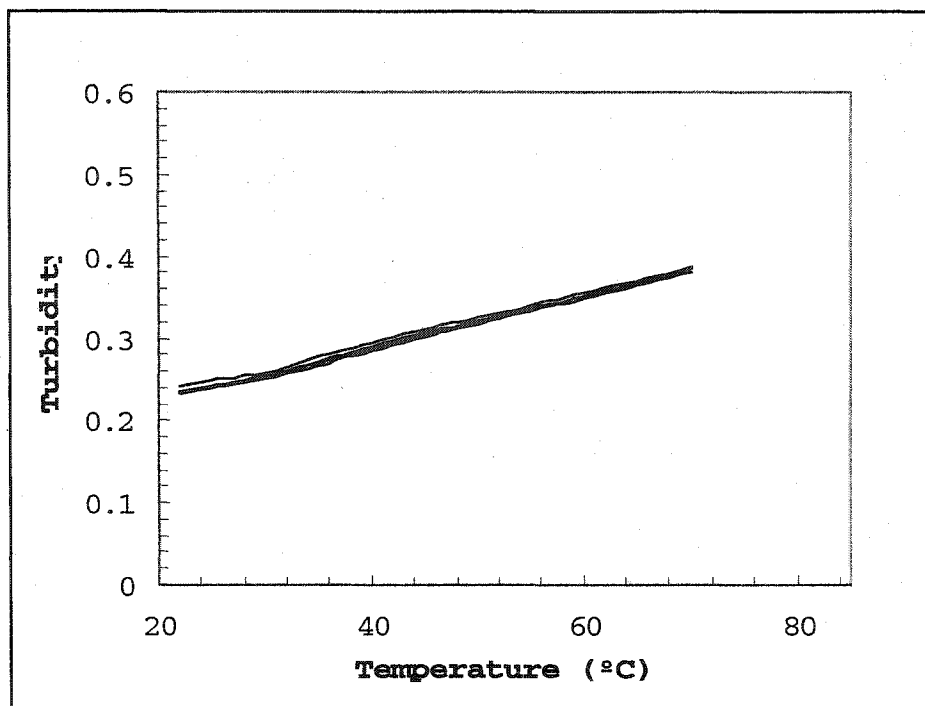


(a)

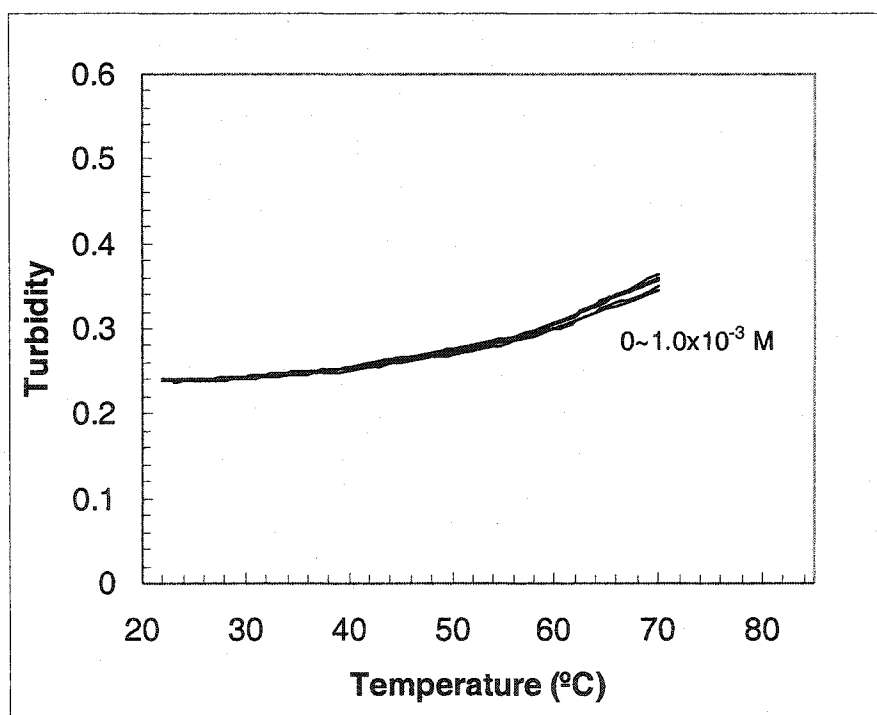


(b)

Figure 6-8. Turbidity of templated poly NIPA-MAA microspheres as a function of temperature and CAF concentration. (a). formulation #7, (b) formulation #8.

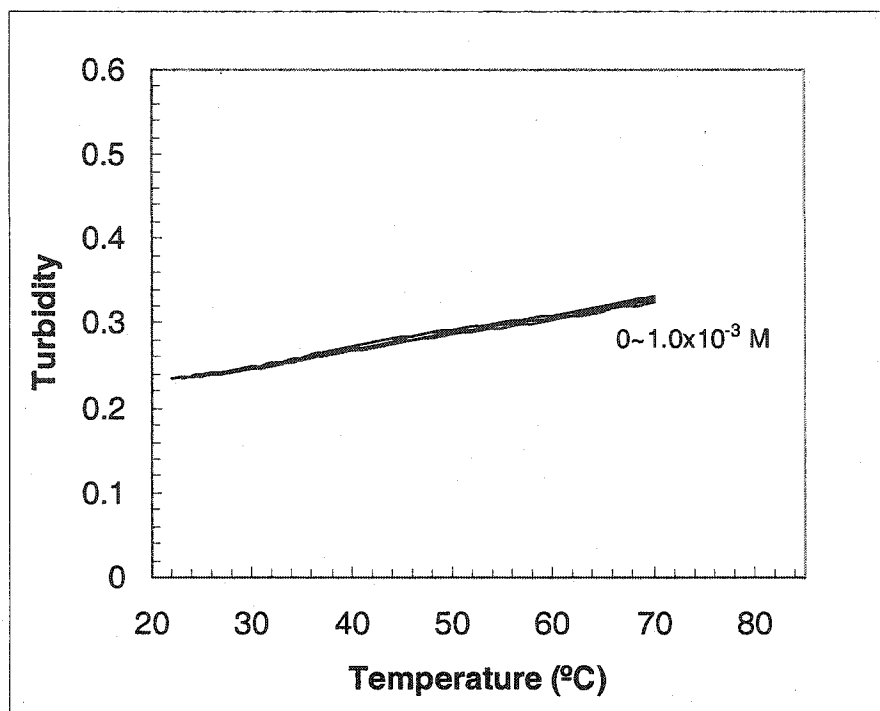


(c)

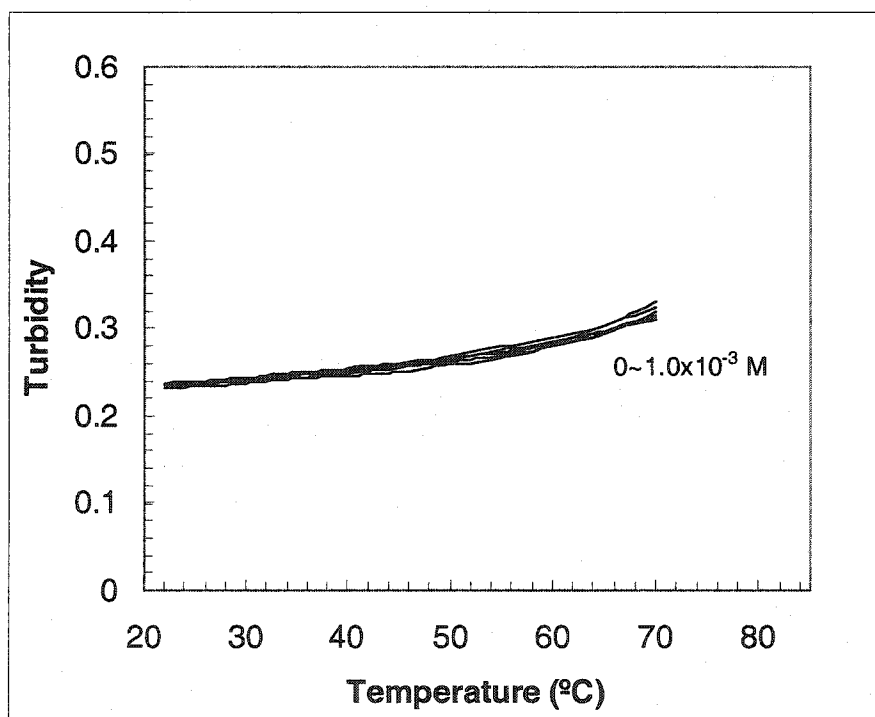


(d)

Figure 6-8 (continued). Turbidity of templated poly NIPA-MAA microspheres as a function of temperature and CAF concentration. (c). formulation #9, (d) formulation #10.



(e)



(f)

Figure 6-8 (continued). Turbidity of templated poly NIPA-MAA microspheres as a function of temperature and CAF concentration. (e). formulation #11, (f) formulation #12.

6.2.5 pH effect on turbidity and transition of poly NIPA-MAA microspheres

Figure 6-9 shows deprotonation of the polymer back bone of poly NIPA-MAA microspheres. The carboxyl group of methacrylic acid on polymer backbone can be deprotonated at high pH. Figure 6-10 shows the turbidity changes of untemplated and templated poly NIPA-MAA microspheres in a PVA membrane as a function of pH and temperature. These results are similar with those in chapter 5 for poly NIPA-AAc particles. MAA ($pK_a \sim 4.7$) is protonated at low pH and there is no charge on the polymer backbone. Its phase transition will take place at low temperature due to lack of charge repulsion. The deprotonation of MAA at high pH introduces negative charge onto the polymer backbone and causes the phase transition to shift to higher temperature. When pH is larger than 6, there is no phase transition due to complete deprotonation of MAA.

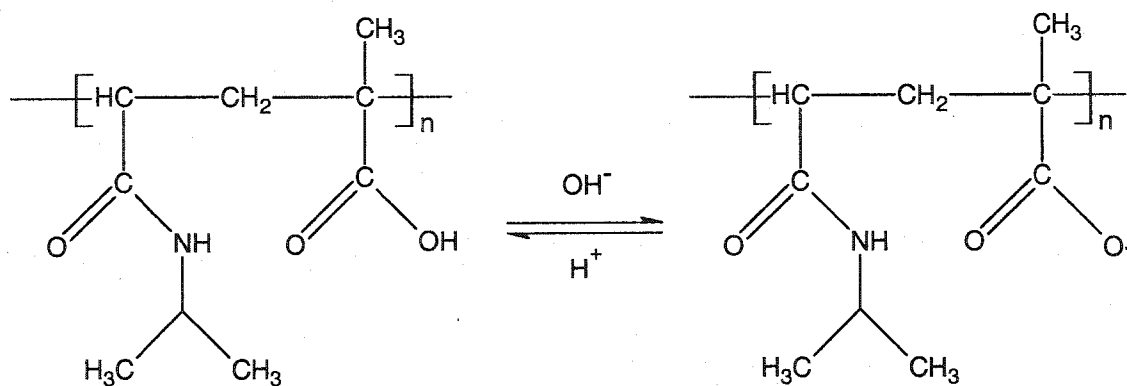
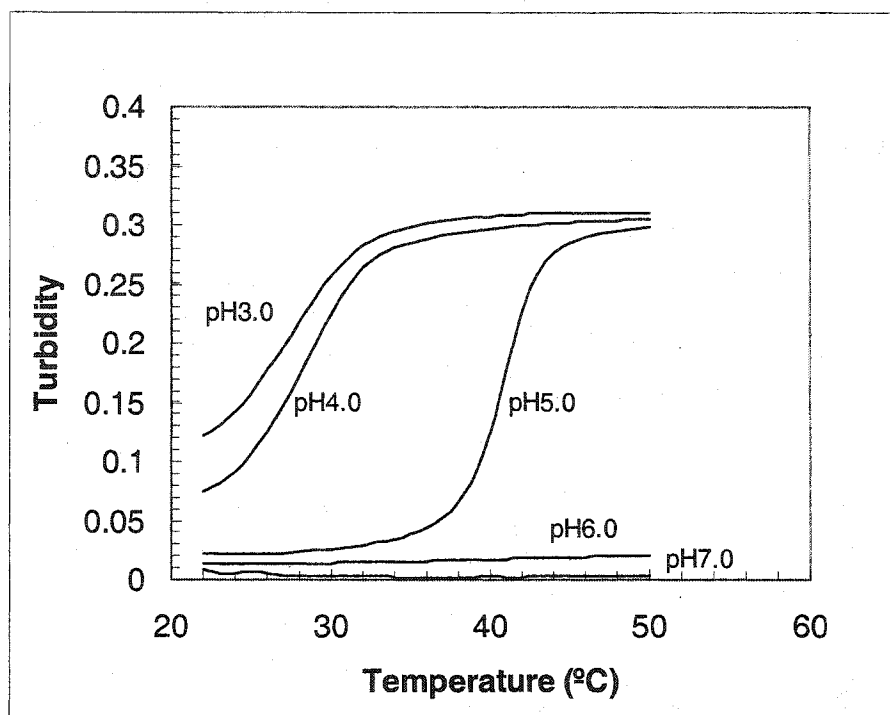
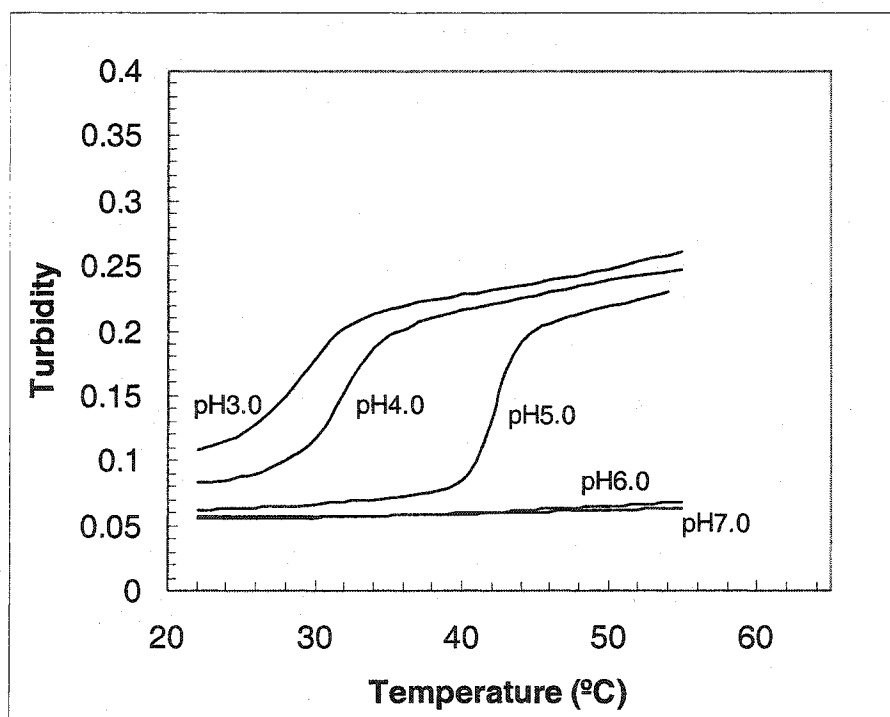


Figure 6-9. Deprotonation of the poly NIPA-MAA microspheres.



(a)



(b)

Figure 6-10. pH effect on transition temperature and turbidity change as a function of temperature. (a). Untemplated poly NIPA-MAA, (b). Templated poly NIPA-MAA

6.2.6 Response and selectivity of poly NIPA-MAA in buffer

If theophylline is prepared in buffer solution with high pH (>6), the neutralized theophylline ($pK_a \sim 5.2$) will interact with specific sites and take the cavity position before deprotonation of MAA. There is a competition between template-polymer interaction and buffer-polymer interaction. The template-polymer interaction will decrease deprotonation of polymer decreasing the net charge on the polymer. Polymer will be more shrunken in theophylline/buffer than in buffer itself. Figure 6-11 shows turbidity change of poly NIPA-MAA microspheres in PVA membrane as a function of temperature in 1.0×10^{-3} M theophylline/buffer solutions. It can be seen that the presence of theophylline is causing the polymer to shrink in buffer. The higher the pH, the more deprotonation resulting in less shrinking. There is no significant difference in response for pH 6, 7, and 8. So pH 7.0 was used to prepare theophylline solutions for the following experiments.

Figure 6-12 shows the turbidity of poly NIPA-MAA as a function of temperature and concentration of theophylline in pH 7.0. We can see that our MIP microspheres respond to theophylline concentration as low as 1.0×10^{-8} M in pH 7.0. Higher concentrations of theophylline cause the polymer to shrink (increasing refractive index) resulting in higher turbidity. This reverses the sensing mechanism in water. It is interesting to note that there is a phase transition when the membrane was placed in relatively high concentration of theophylline buffer solutions. The transition temperature is around 33°C so that our membrane can be used at biological temperatures. We can also see that the difference in response for 1×10^{-6} and 1×10^{-5} M THO is very small. Again this suggests that the polymer may have two populations of binding sites. One population of sites has a high affinity for THO and another population of sites has a lower affinity.

Figure 6-13 shows the response to theophylline in buffer at 37°C. The turbidity is correlated to the concentration of THO.

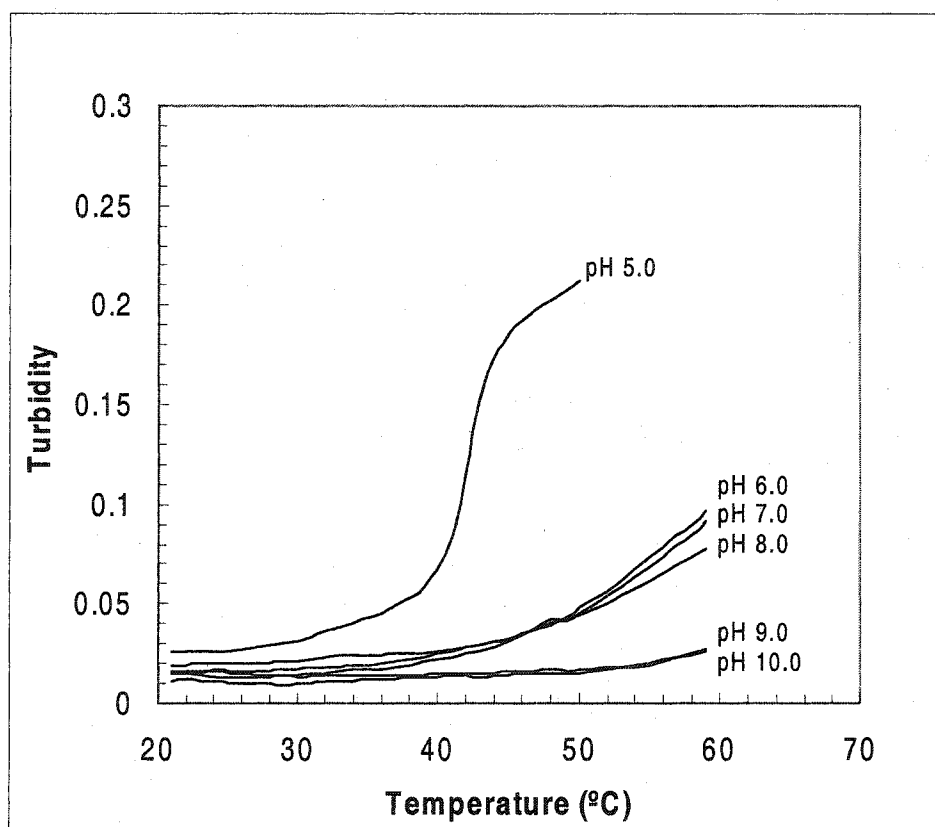


Figure 6-11. Turbidity of templated poly NIPA-MAA microspheres in PVA membrane as function of temperature and pH in the presence of 1×10^{-3} M THO. (Phosphate buffer concentration is 0.1 M)

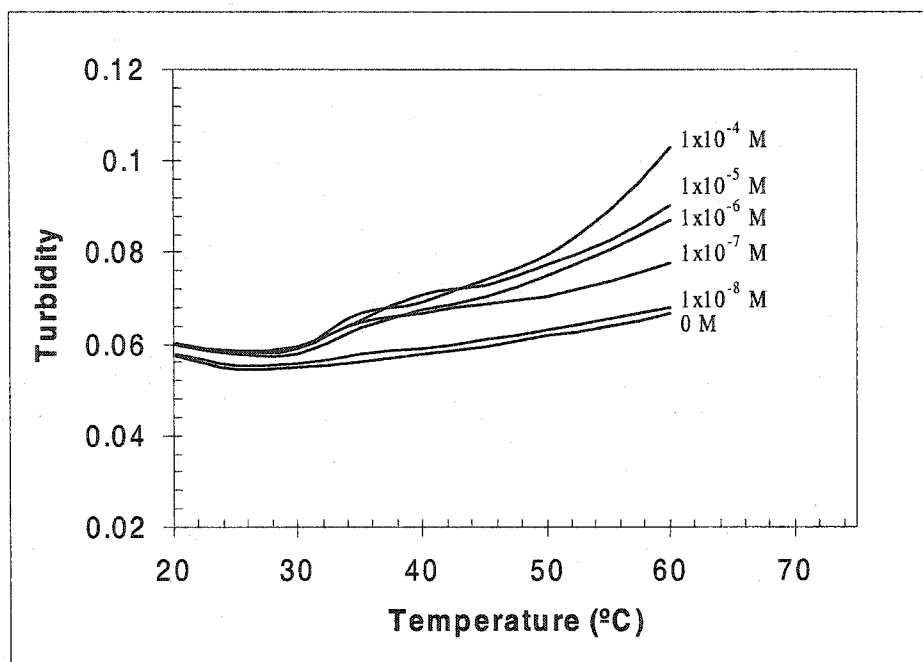


Figure 6-12. Turbidity change of templated poly NIPA-MAA microspheres as function of temperature and concentration of theophylline in pH 7.0 buffer.

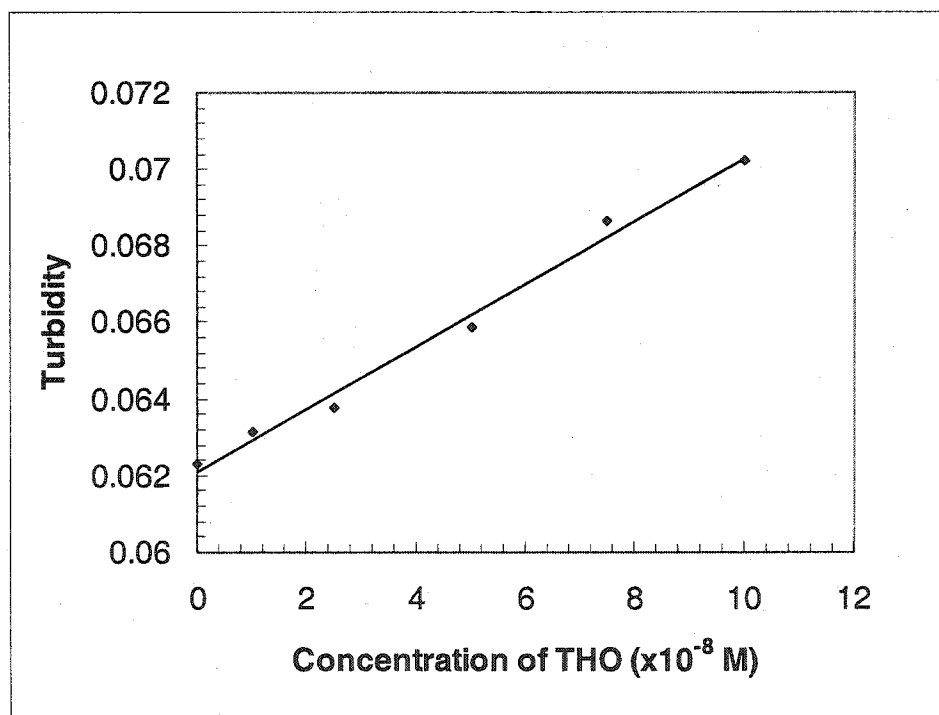


Figure 6-13. THO response of templated poly NIPA-MAA in pH 7.0 buffer at 37°C.

Figure 6-14 shows the turbidity of untemplated poly NIPA-MAA as a function of temperature and concentration of theophylline in pH 7.0. This indicates that the reference MIP has no response to theophylline at concentrations as high as 1.0×10^{-4} M. To examine the molecular specificity of our polymer, caffeine was selected as another template.

Figure 6-15 shows turbidity change of THO templated poly NIPA-MAA as function of temperature and concentration of caffeine in pH 7.0. There is no significant response to caffeine concentrations as high as 1.0×10^{-4} M demonstrating the high selectivity of our polymer.

All the above results show that our swellable imprinted poly NIPA-MAA microspheres respond with the sensitivity and selectivity required for biological sensing applications.

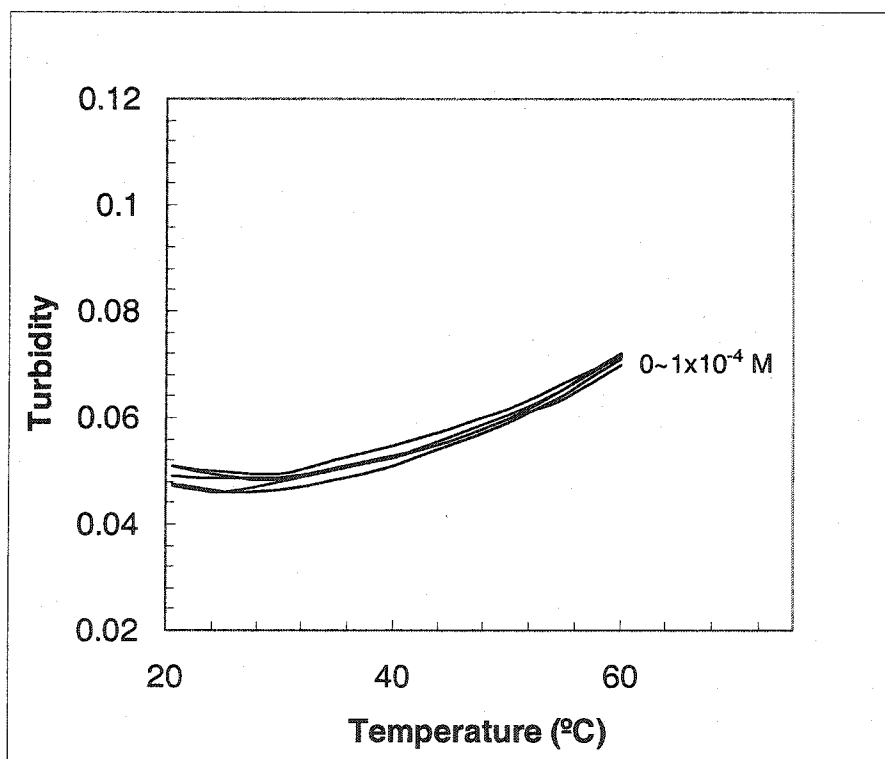


Figure 6-14. Turbidity of untemplated poly NIPA-MAA microspheres as a function of temperature and concentration of theophylline in pH 7.0 buffer.

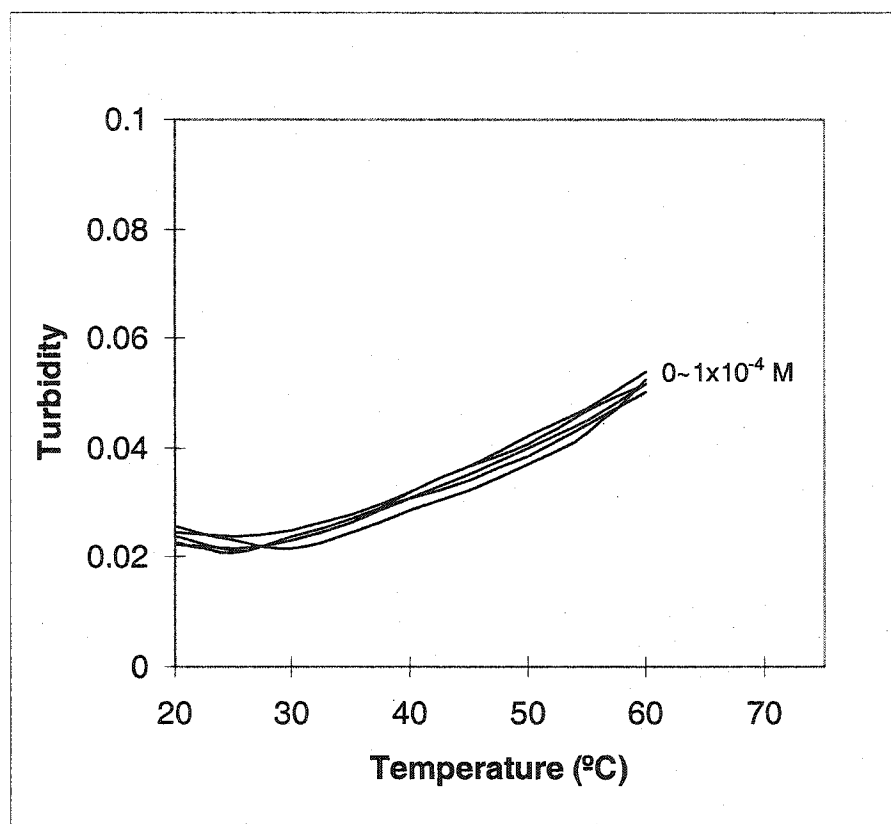


Figure 6-15. Turbidity of THO templated poly NIPA-MAA microspheres as a function of temperature and concentration of caffeine in pH 7.0 buffer.

6.2.7 Varying the polymer transition temperature

So far, poly NIPA-MAA microspheres can be successfully used in water at high temperature (e.g. 50°C) and in buffer at 37°C. They have high sensitivity and selectivity. However, the maximum sensitivity is at fairly high temperatures, ca. 50°C in water. Sensors for other applications should conveniently respond at room temperature. This issue can be solved by changing the polymer transition temperature.

The effect of the alkyl group substituent on the swelling behavior of N-alkylacrylamide hydrogels has been reported [76]. It was found that the alkyl groups have a pronounced effect on the features of gel swelling. Generally, larger alkyl chains produced a large decrease in gel transition temperature (Table 6-2). The transition temperature of poly ethylacrylamide and poly N-isopropylacrylamide were 80°C and 32°C, respectively. Poly methylacrylamide is always swollen even at high temperature, 90°C, while poly N-t-butylacrylamide (poly NTBA) is always shrunken at all temperatures. The transition temperature of isomeric propyl derivatives were found to differ by 12°C, with n-propyl exhibiting the lower value because n-propyl group has a greater dynamic volume owing to its longer chain.

To shift response to lower temperatures we need to replace part of the NIPA in the preliminary data formulation with N-t-butylacrylamide. The copolymer poly NIPA-NTBA is expected to have a lower transition temperature than poly NIPA. The exact value will depend on the ratio of NIPA to NTBA. Poly NIPA-NTBA microspheres with different percentages of NTBA were prepared by dispersion polymerization in aqueous medium at 70°C. 2% MBA was used as crosslinker and 2% potassium persulfate (KPS) was used as initiator. The appropriate amounts of the resulting microspheres were

suspended in water. The transition temperatures were measured by the method described in chapter 3. Figure 6-16 shows the swelling behavior of poly NIPA-NTBA with increasing of temperature as a function of the percentage of NTBA. When the amount of NTBA was 0% to 10%, 20%, 30%, and 40% of total acrylamide monomers, the transition temperature decreased from 32.5 to 25.4, 16.4, 9.5, and 3.3°C, respectively. These transition temperatures are inversely proportional to the percentage of NTBA. A quantitative correlation was found between the gel transition temperatures and the ratio of NTBA in copolymer gels (Figure 6-17.). We can see that the transition temperature of copolymer with higher than 20% of NTBA is low enough for our sensor which can be used at room temperature or physiological temperature. This formulation was used to prepare molecularly imprinted poly NIPA-NTBA-MAA microspheres.

Table 6-3. Effect of alkyl side group on transition temperature of N-alkylacrylamide hydrogel [76].

Alkyl Side Group	Transition Temperature (°C)
Methyl	208 (predicted)
Ethyl	80
cyclo-propyl	48
iso-Propyl	37
n-Propyl	25
tert-Butyl	None (shrunken at all temperature)

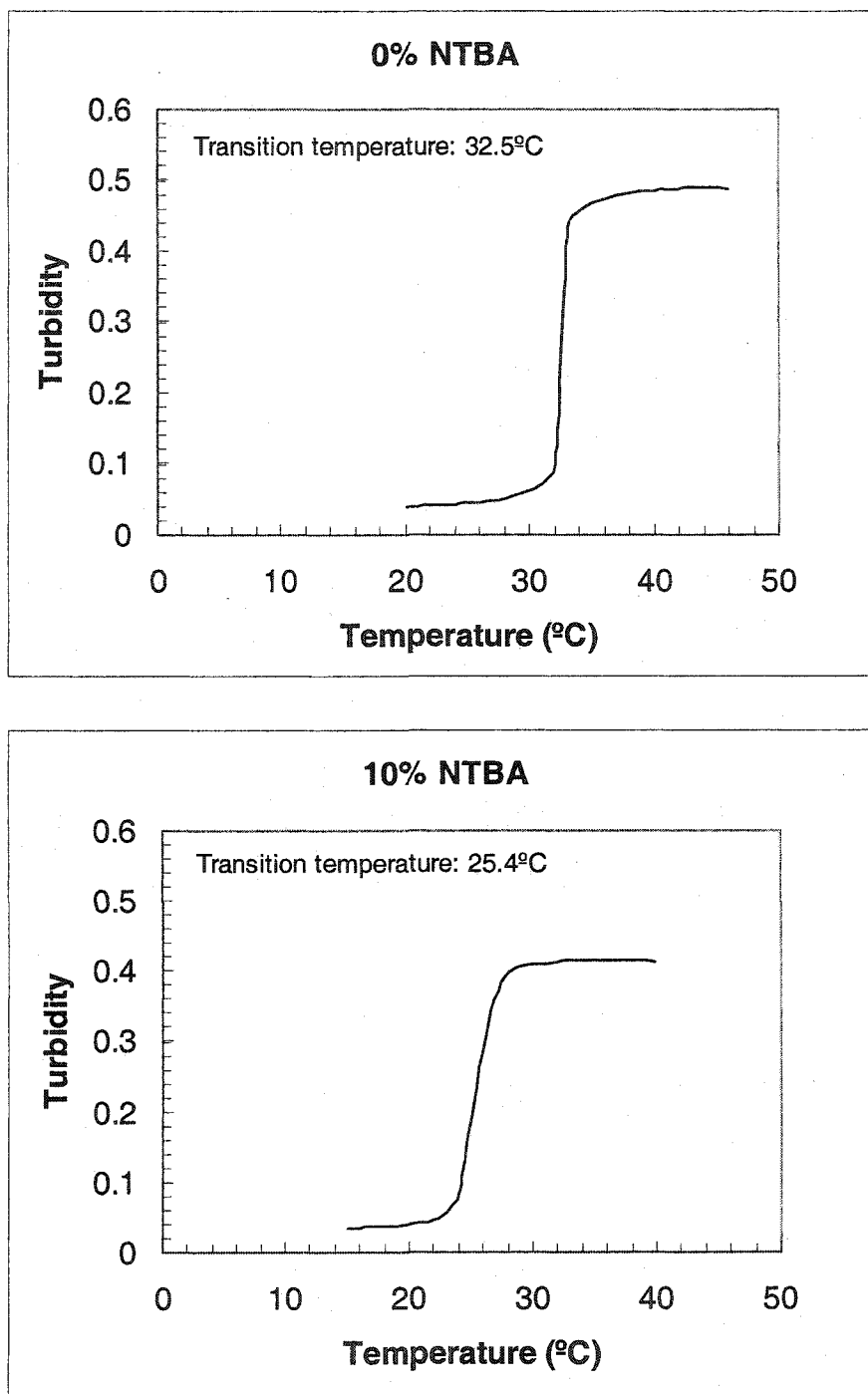


Figure 6-16. Turbidity of poly NIPA-NTBA-MAA microspheres as a function of temperature and percentage of NTBA.

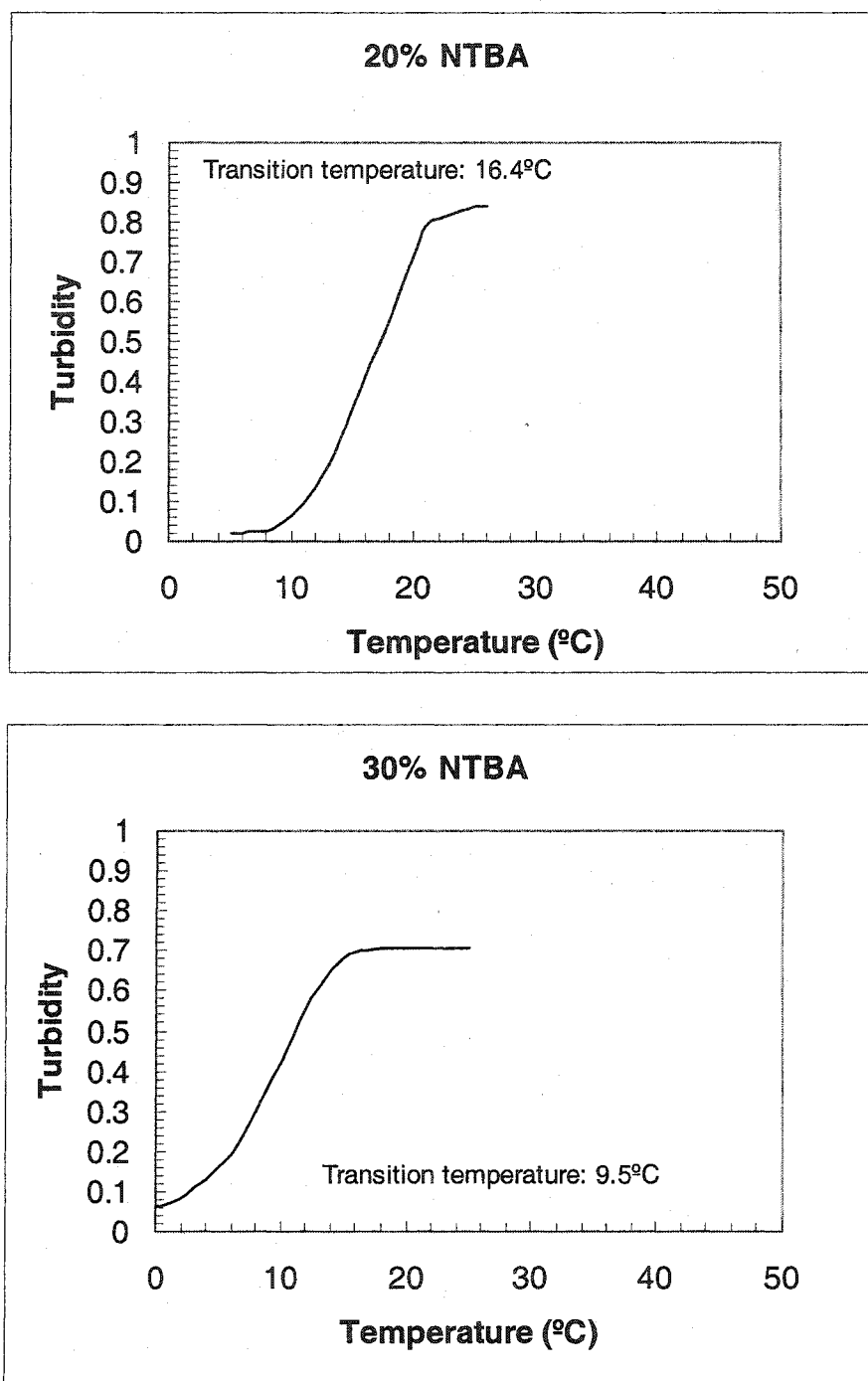


Figure 6-16 (continued). Turbidity of poly NIPA-NTBA-MAA microspheres as a function of temperature and percentage of NTBA.

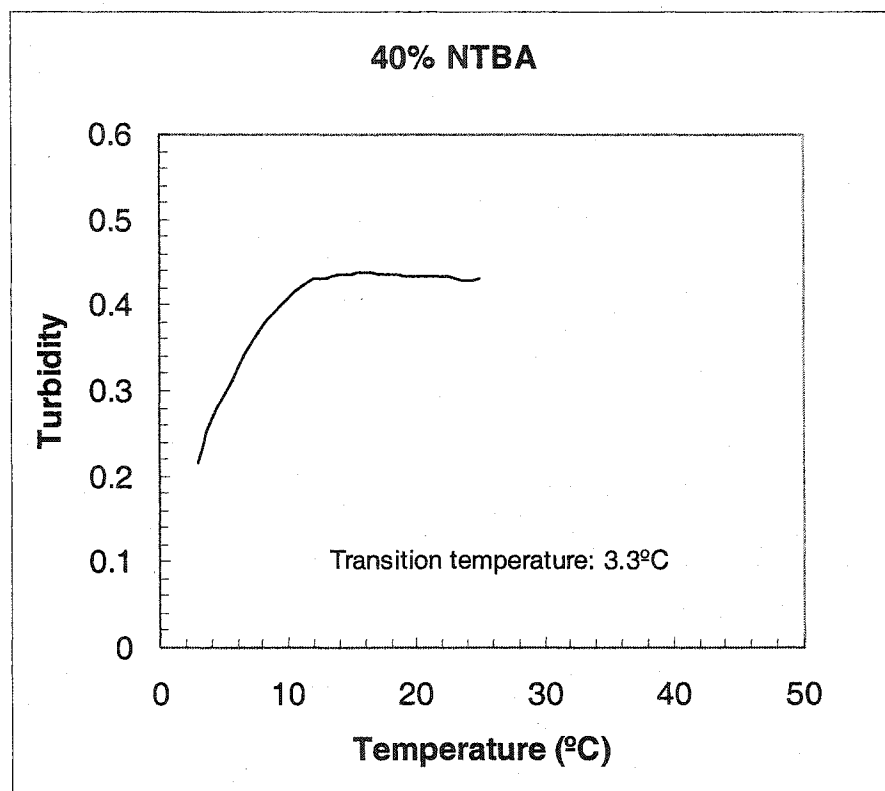


Figure 6-16 (continued). Turbidity of poly NIPA-NTBA-MAA microspheres as a function of temperature and percentage of NTBA.

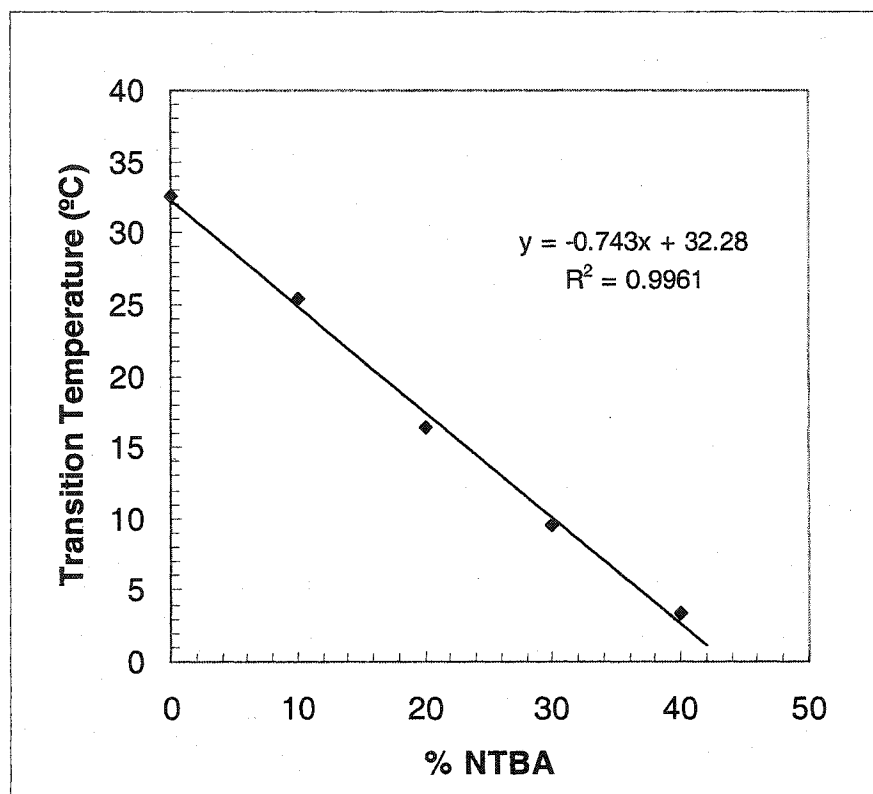


Figure 6-17. Transition temperature of poly NIPA-NTBA-MAA microspheres as a function of percentage of NTBA.

6.2.8 Response and specificity of poly NIPA-NTBA-MAA microspheres

6.2.8.1 Preparation of poly NIPA-NTBA-MAA microspheres

Figure 6-18 and Figure 6-19 show light micrographs and size distribution of poly NIPA-NTBA-MAA microspheres by replacing 30%, and 20% of NIPA with NTBA, respectively. 20% poly acrylonitrile-co-styrene was used as the stabilizer in dispersion polymerization in acetonitrile. The resulting microspheres are very uniform and spherical with diameters ca. 1.0 μm . The standard derivation in the diameters is less than 0.19. To examine the swelling property of these microspheres, they were cast in 76 μm PVA membranes. Figure 6-20 shows the turbidity change of these membranes as a function of temperature in water. Microspheres containing 30% NTBA has a lower turbidity contrast in the shrunken state, though transition temperature is as low as 10°C. Microspheres containing 20% NTBA have a higher turbidity contrast and the transition temperature (~12°C) is also low enough. It can be used for sensing at any temperature higher than 17°C. The turbidity contrast difference for these two polymers is due to the difference percentage of NIPA. So, the optimum formulation for poly NIPA-NTBA-MAA is 60% NIPA, 15% NTBA, and 5% MBA. Figure 6-21 shows the light micrographs of theophylline templated poly NIPA-NTBA-MAA microspheres. They have a similar size distribution as the untemplated polymer. They were used in following experiments.

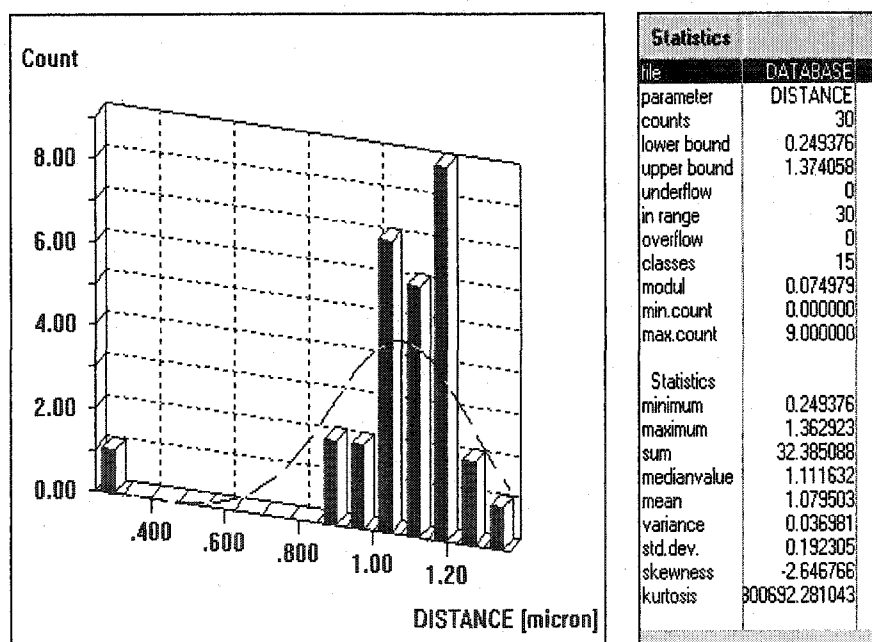
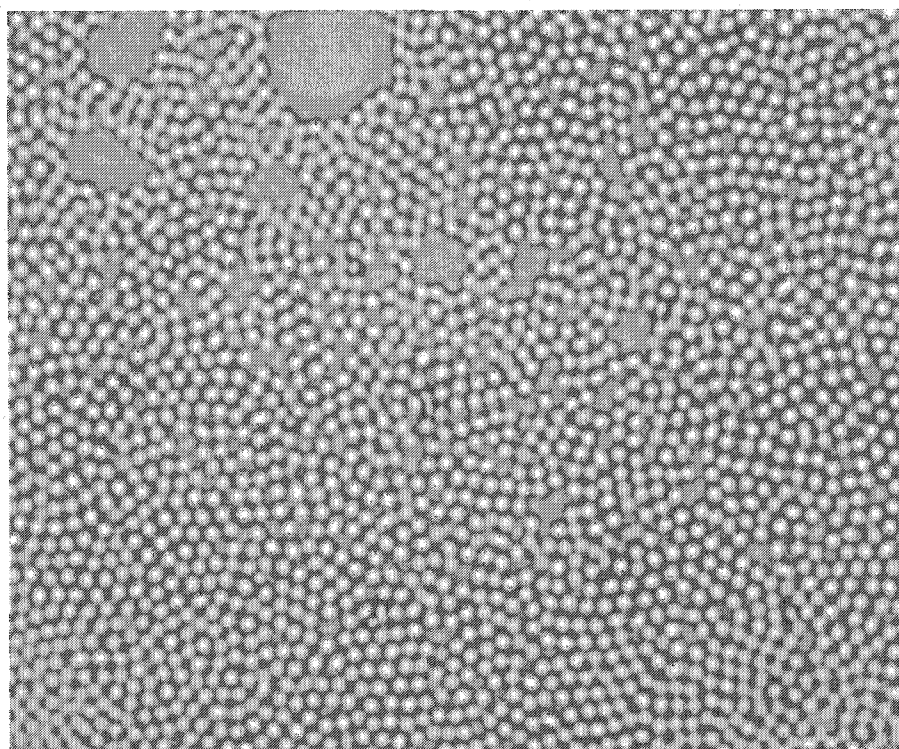


Figure 6-18. Micrograph and size distribution of untemplated poly NIPA-NTBA-MAA microspheres prepared by dispersion polymerization. (52.5%NIPA, 22.5%NTBA, 20%MAA, 5%MBA)

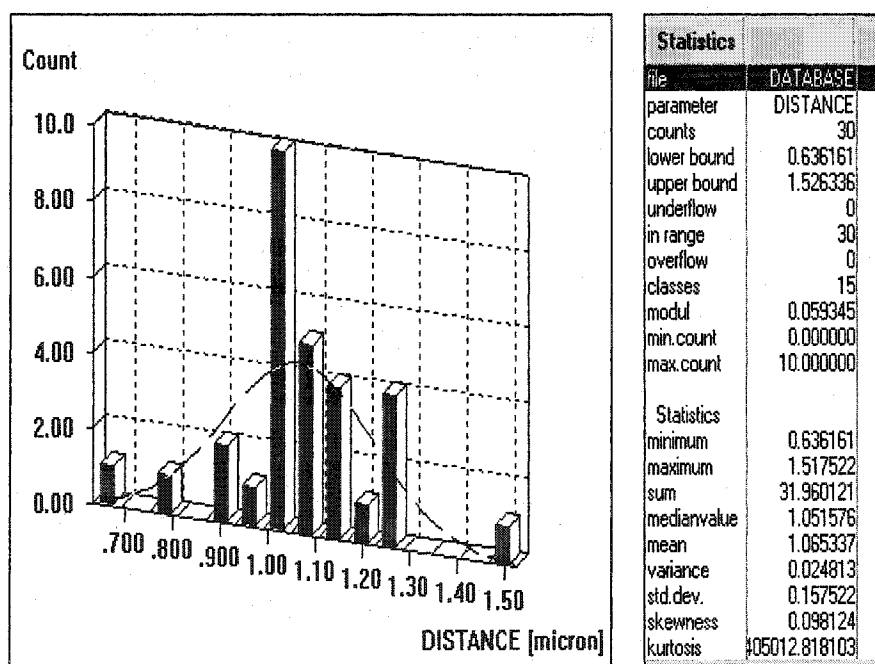
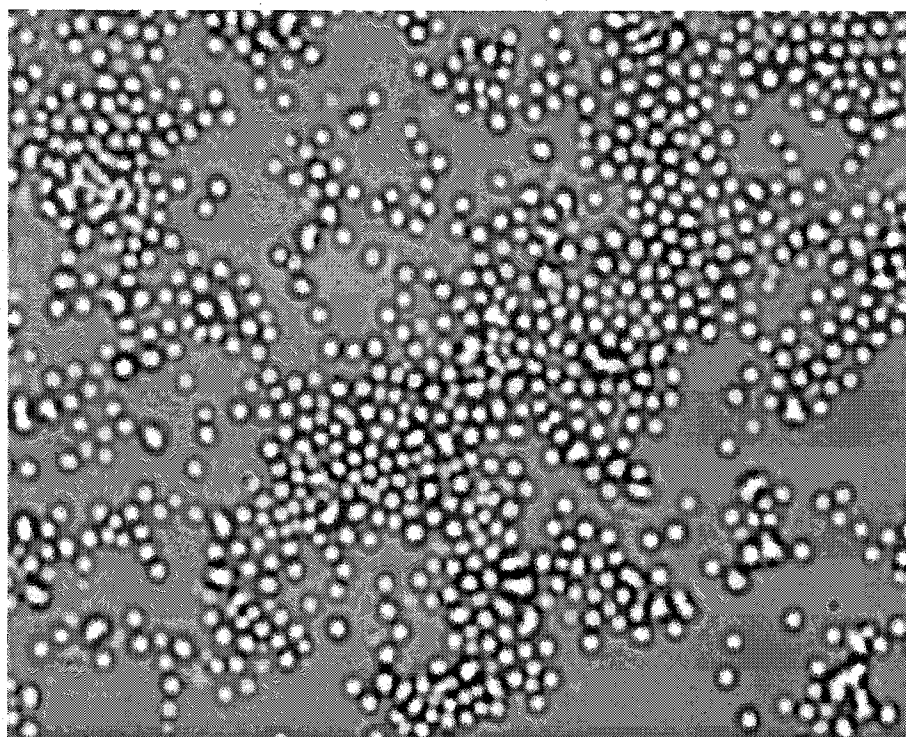


Figure 6-19. Micrograph and size distribution of untemplated poly NIPA-NTBA-MAA microspheres prepared by dispersion polymerization. (60%NIPA, 15%NTBA, 20%MAA, 5%MBA)

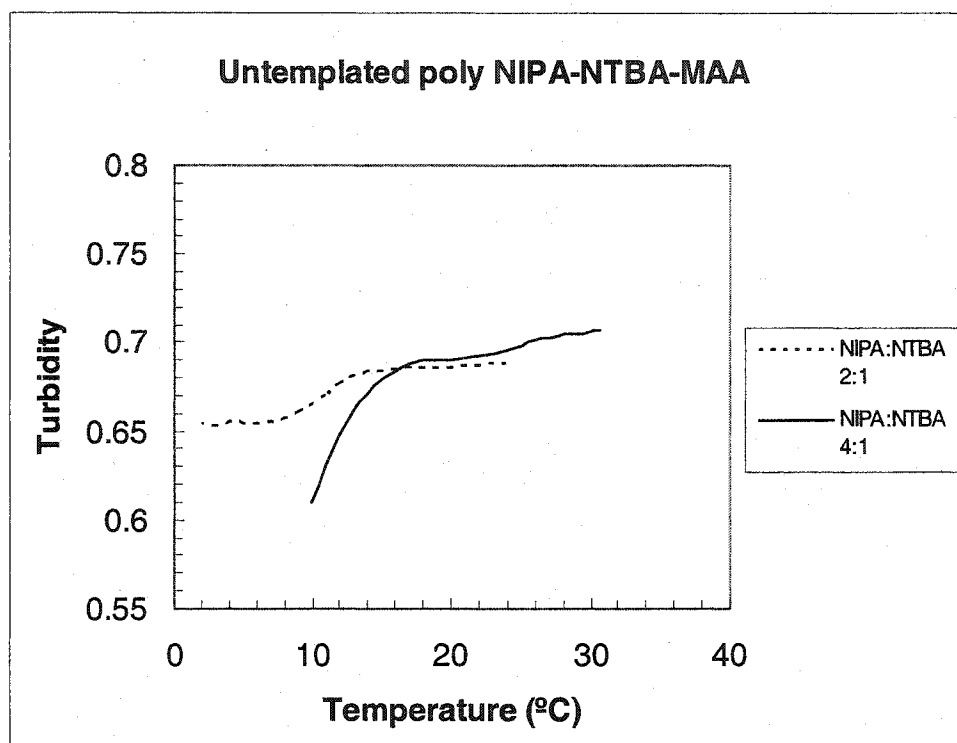


Figure 6-20. Turbidity changes and phase transition of poly NIPA-NTBA-MAA microspheres containing different percentages of NTBA

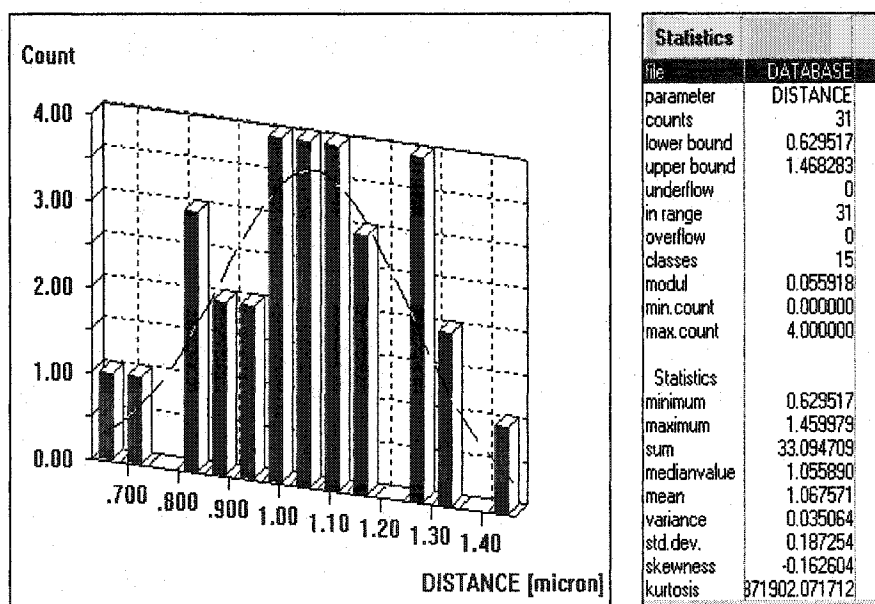
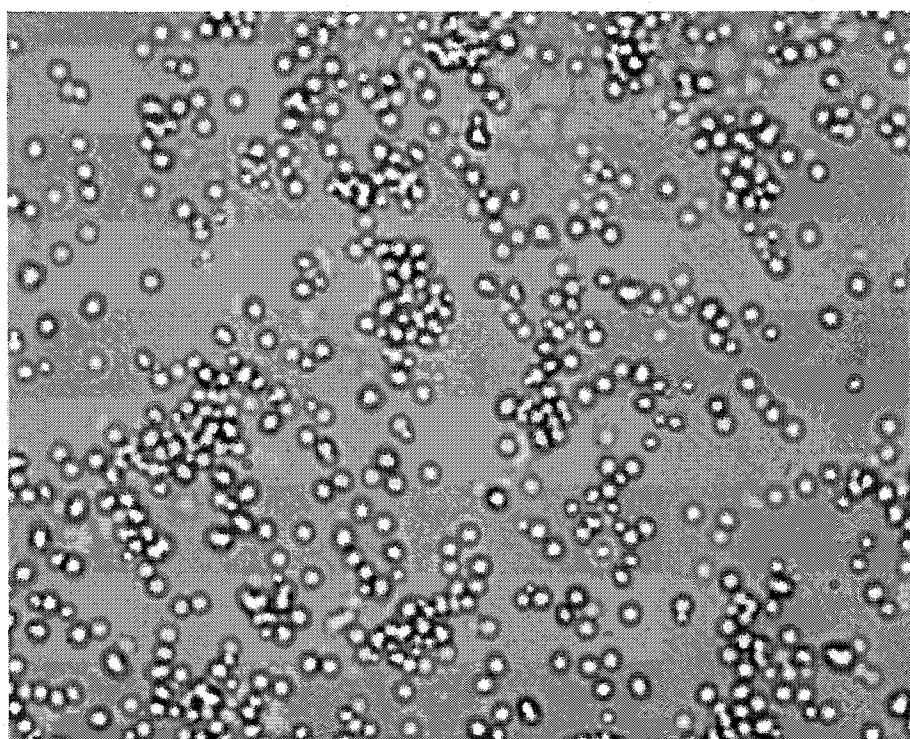


Figure 6-21. Micrograph and size distribution of THO templated poly NIPA-NTBA-MAA microspheres prepared by dispersion polymerization. (60%NIPA, 15%NTBA, 20%MAA, 5%MBA)

6.2.8.2 Sensor response and selectivity in water

As shown in Figure 6-20, the transition temperature of poly NIPA-NTBA-MAA was lowered to 12°C. Therefore, these MIP microspheres can be used at any temperature higher than 17°C. Figure 6-22 and 6-23 show turbidity vs. log [theophylline] concentration for a PVA membrane containing templated and untemplated poly NIPA-NTBA-MAA microspheres at 30°C, respectively. We can see that templated membrane responds to theophylline concentrations as low as 1.0×10^{-7} M, while the untemplated membrane does not respond to theophylline at concentrations as high as 1.0×10^{-2} M. This proves that templated membrane has high molecular specificity.

The high selectivity of THO templated membrane is shown in Figure 6-24. There is no response to caffeine at concentrations as high as 1.0×10^{-2} M.

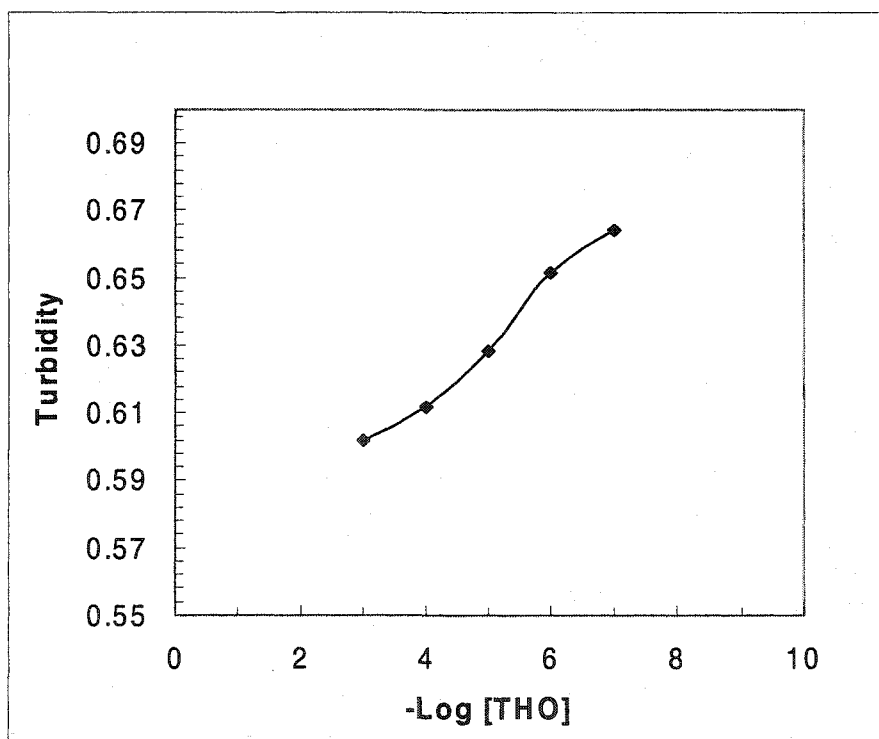


Figure 6-22. THO response of templated NIPA-NTBA-MAA microspheres in a PVA membrane at 30°C.

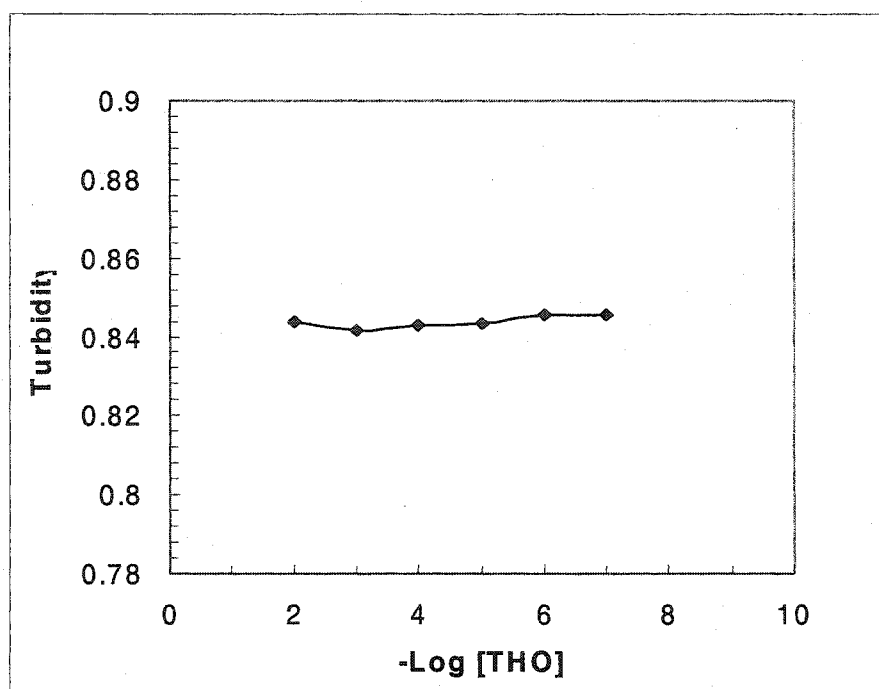


Figure 6-23. THO response of untemplated NIPA-NTBA-MAA microspheres in a PVA membrane at 30°C

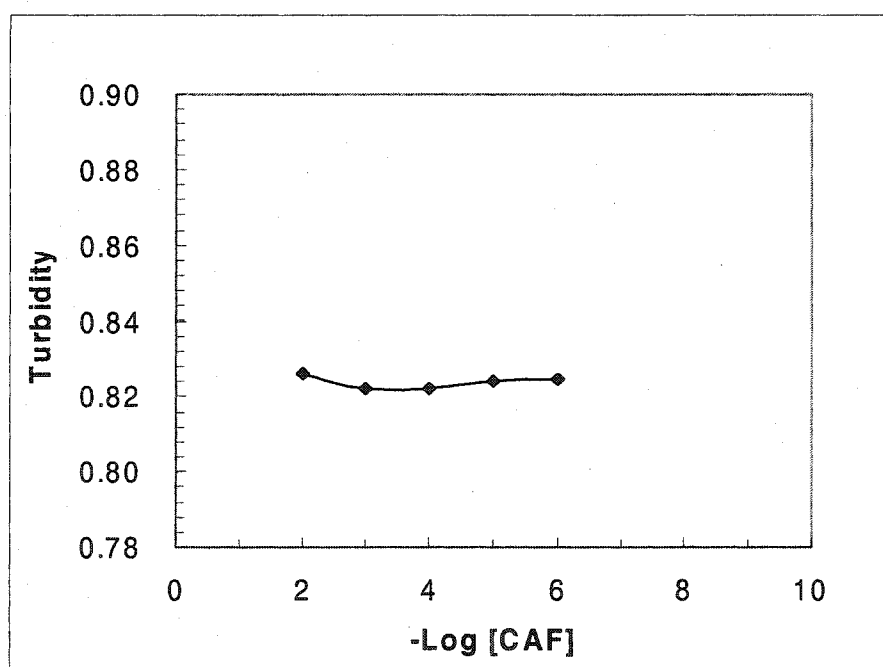


Figure 6-24. CAF response of THO templated NIPA-NTBA-MAA microspheres in a PVA membrane at 30°C.

6.2.8.3 pH effect on turbidity and phase transition of poly NIPA-NTBA-MAA

Figure 6-25 shows turbidity of THO templated poly NIPA-NTBA-MAA microspheres in a PVA membrane as a function of temperature and pH. The data are similar to those we observed for poly NIPA-MAA microspheres except for a larger decrease in turbidity in buffers at high pH. There is no phase transition at pH 6, 7, and 8, which is good for sensor response in buffer. This is because the sensing mechanism here is the same as that for poly NIPA-MMA microspheres. The addition of theophylline in buffer will decrease the buffer-polymer interaction. Less charge repulsion causes the polymer to shrink resulting in a higher turbidity. We did not examine the detailed response of this membrane in buffer because we think it should be the same as that of poly NIPA-MAA which has a more simple formulation than poly NIPA-NTBA-MAA.

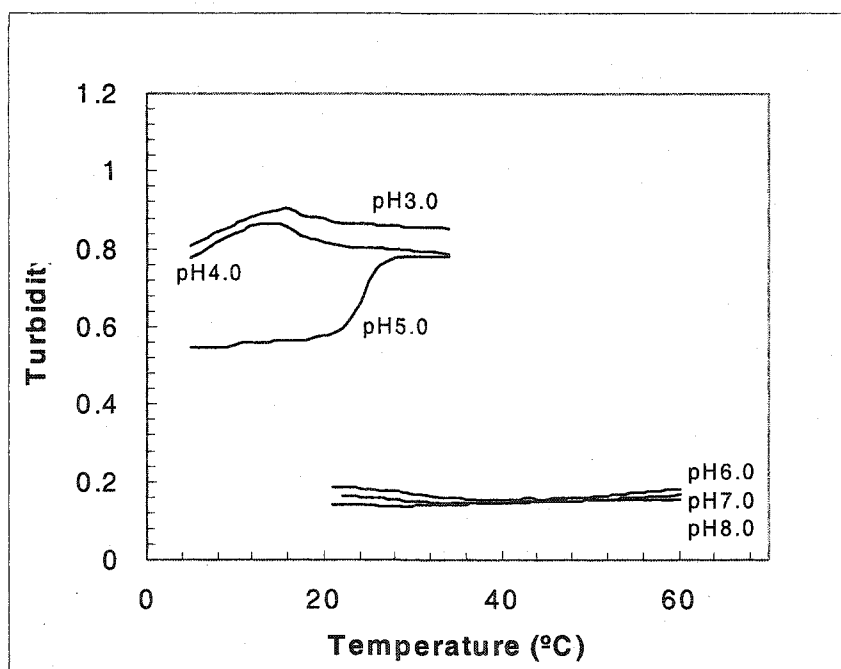


Figure 6-25. Turbidity of templated poly NIPA-NTBA-MAA microspheres in PVA membrane as a function of temperature and pH.

6.2.9 THO Response and specificity of poly NNPA-MAA microspheres

6.2.9.1 Preparation of poly NNPA-MAA microspheres

It was reported that N-n-propylacrylamide (NNPA) has a phase transition at ca. 25°C [76]. Poly NNPA-MAA microspheres were prepared by dispersion polymerization following the same formulation as that of poly NIPA-MAA except that all of the NIPA was replaced with NNPA. Figure 6-26 and 6-27 show the microscope pictures and size distribution of untemplated and THO templated poly NNPA-MAA microspheres. The resulting microspheres are uniform (Std. dev. <0.16), spherical with a diameter ca. 1.0 μm . 5% (w/w) of these microspheres were then embedded in PVA membranes to evaluate optical properties, sensitivity and specificity.

Figure 6-28*a* and *b* show the turbidity of untemplated and templated microspheres with increasing temperature. We can see that these copolymers have a phase transition at ~15°C and can be conveniently used at room temperature for THO sensing in water.

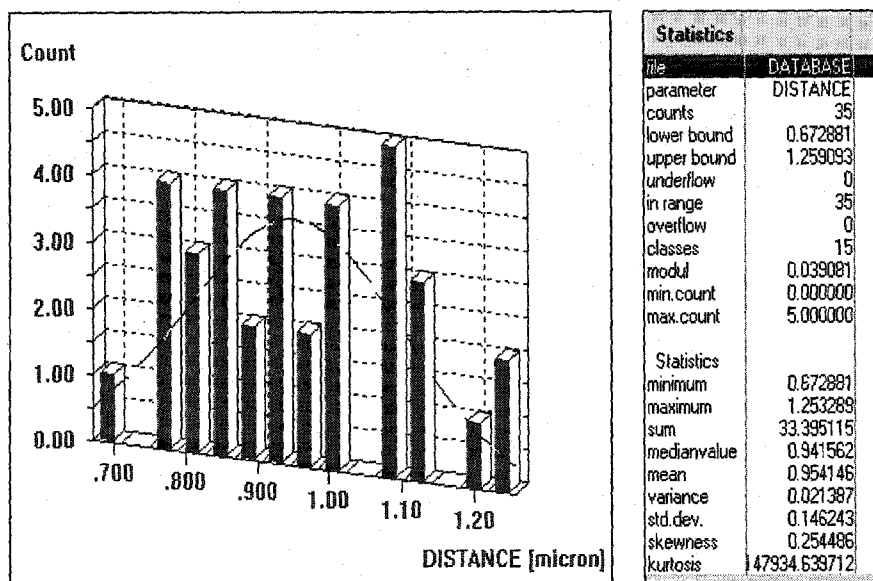
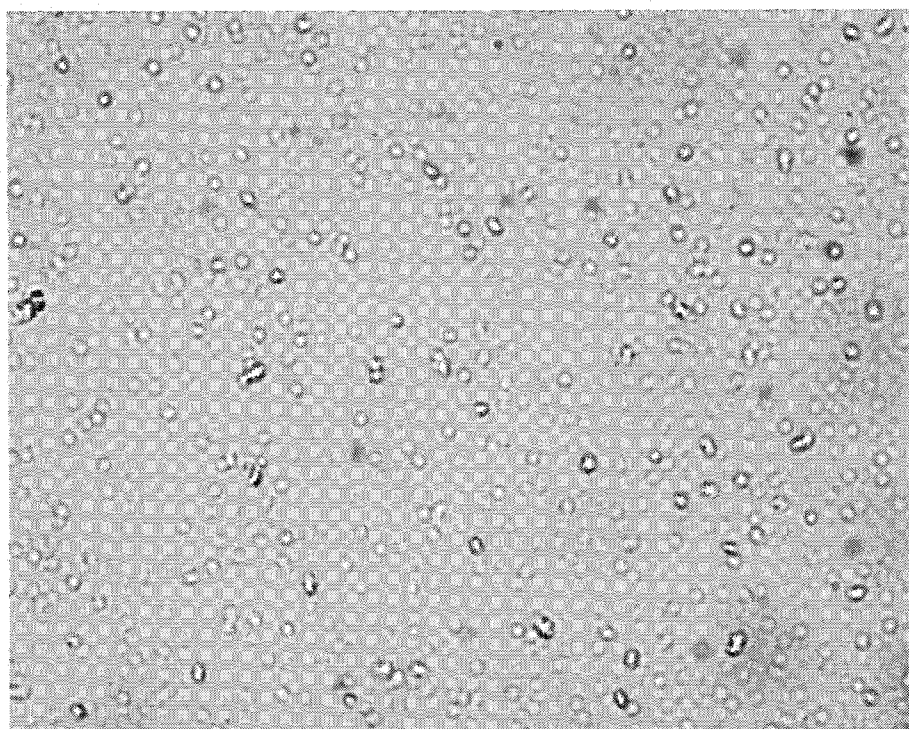


Figure 6-26. Micrograph and size distribution of untemplated poly NNPA-MAA microspheres prepared by dispersion polymerization

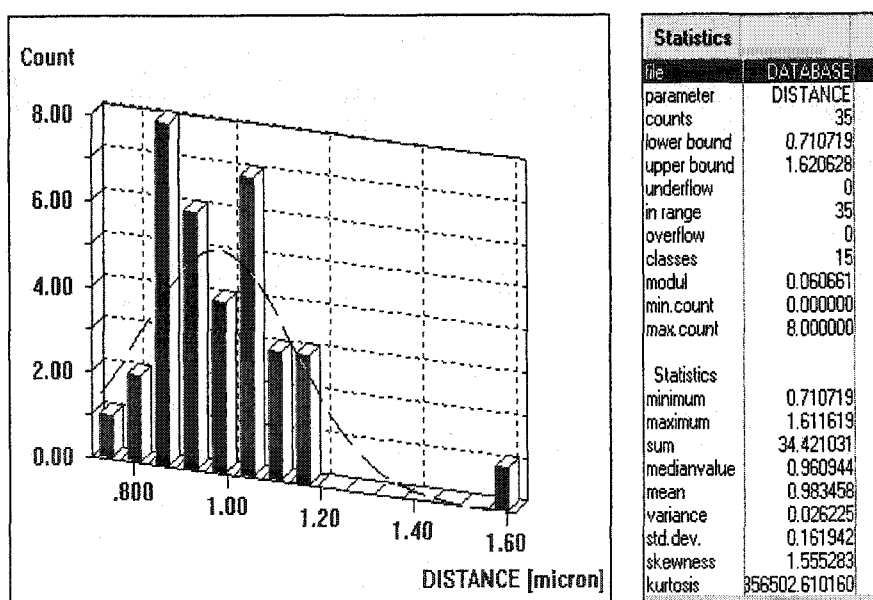
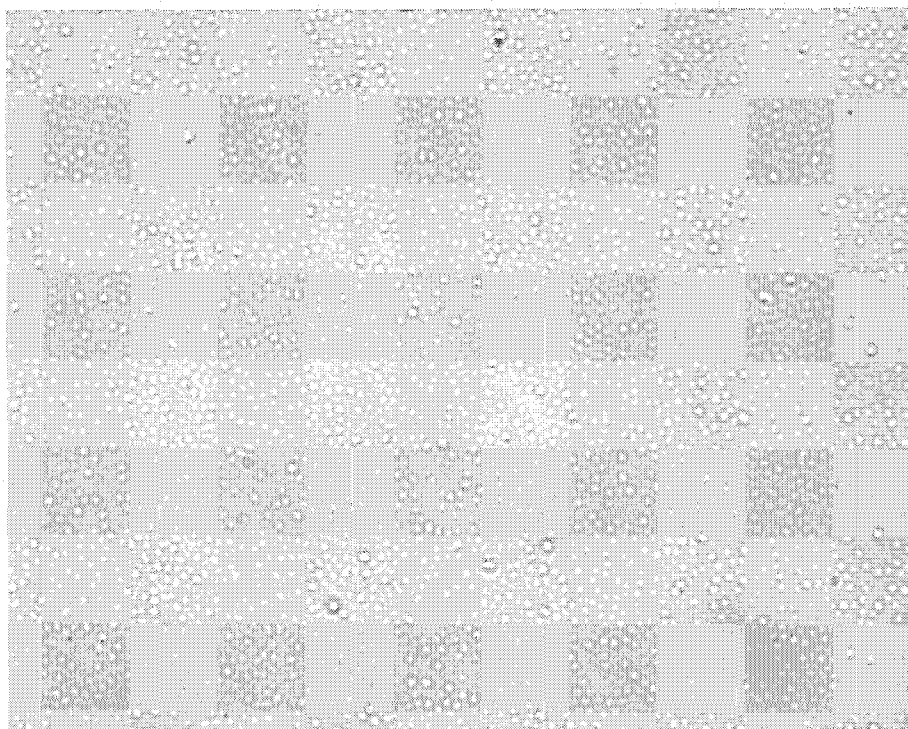


Figure 6-27. Micrograph and size distribution of templated poly NNPA-MAA microspheres prepared by dispersion polymerization.

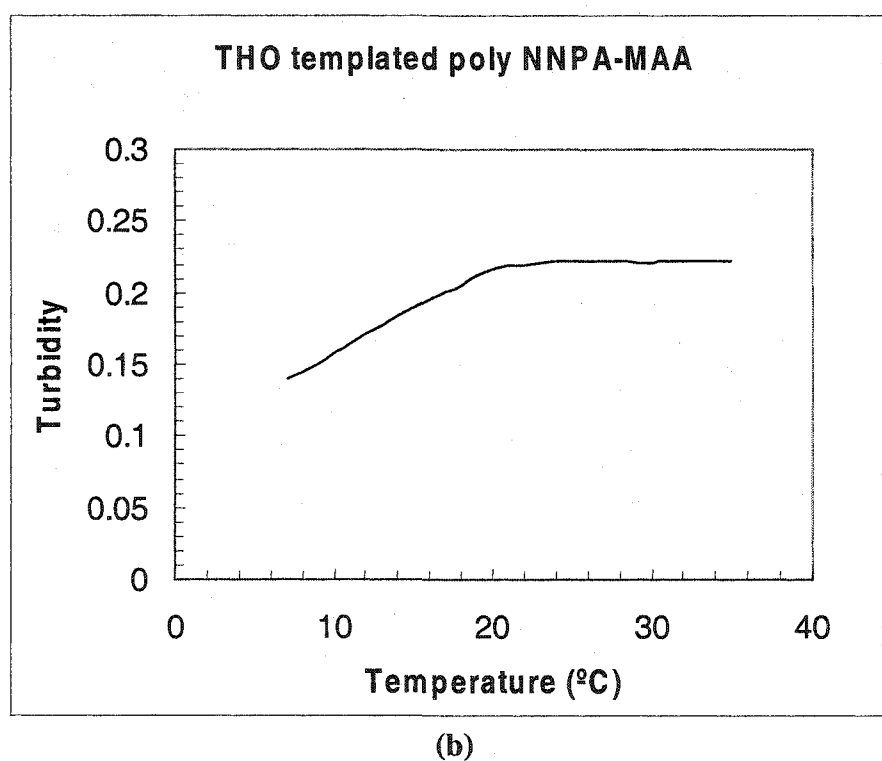
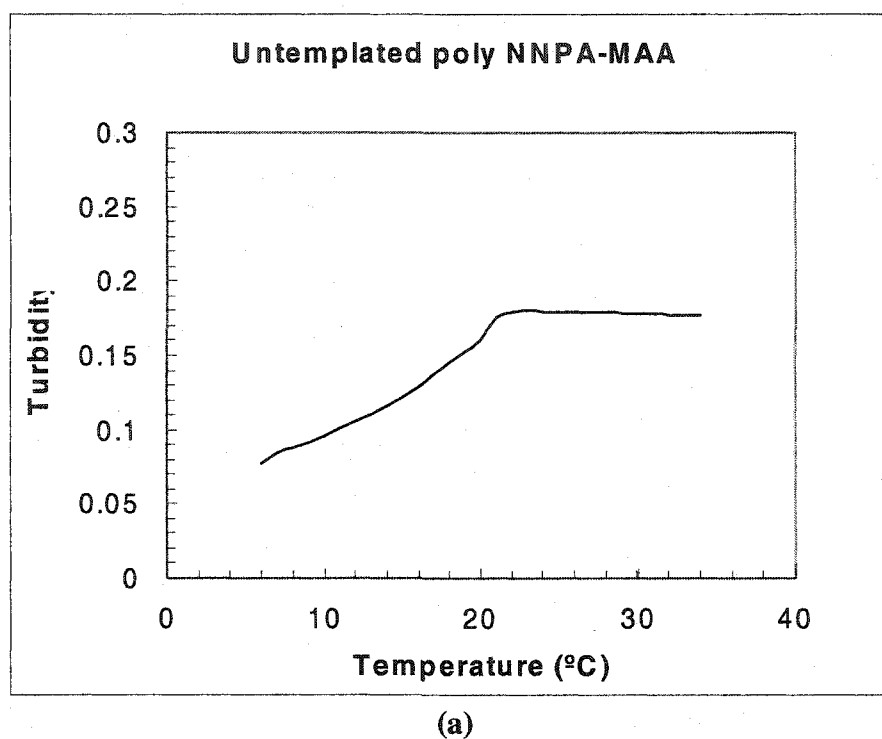


Figure 6-28. Turbidity of untemplated and templated poly NIPA-MAA microspheres as a function of temperature. (a). untemplated, (b) templated.

6.2.9.2 Response and selectivity of poly NNPA-MAA in water

With low phase transition temperature, poly NNPA-MAA microspheres can be used for THO sensing in water at room temperature. Figure 6-29 shows turbidity vs. time measurements for different concentrations of theophylline at 25°C. Most of the response occurs within 5~10 minutes. However, response doesn't level off completely, indicating that there is a slow component to the response time. One possible explanation is that the polymer is in completely shrunken state in water at 25°C. This leads to slower mass transfer of theophylline into and out of the recognition cavities.

Figure 6-30 shows THO response of a membrane containing templated poly NNPA-MAA microspheres at 10 minute and 25°C. It is sensitive to THO concentration in the range from 1.0×10^{-7} to 1.0×10^{-4} M.

Figure 6-31 shows the turbidity change of untemplated microspheres in theophylline solutions. There is no response to theophylline up to 1.0×10^{-3} M. Figure 6-32 and 6-33 show the high selectivity of templated poly NNPA-MAA. It is completely insensitive to caffeine at concentrations as high as 1.0×10^{-3} M.

Figure 6-34 shows that when the membrane was placed in theophylline solution at constant temperature, the turbidity went down due to swelling and went back up when the membrane was exposed to water and theophylline molecules diffused out from the membrane. This confirms that the membrane responds reversibly to theophylline.

All of these results indicate that our swellable imprinted poly NNPA-MAA microspheres can be conveniently used for theophylline sensing in water at room temperature with high sensitivity, selectivity, and reversibility.

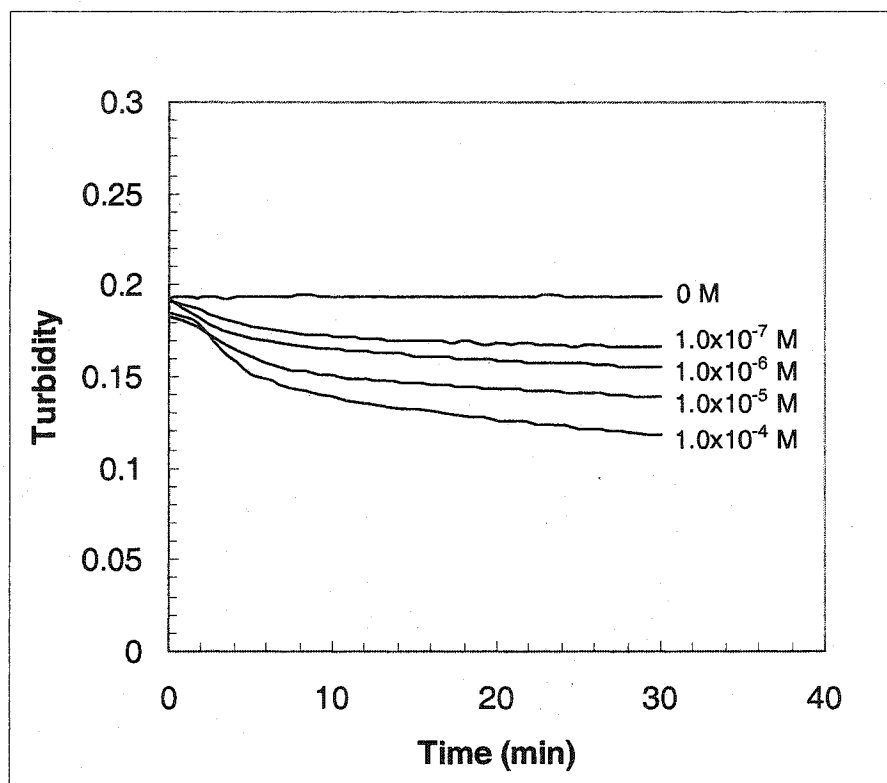


Figure 6-29. Turbidity of PVA membrane containing templated poly NNPA-MAA microspheres as a function of theophylline concentration at 25°C.

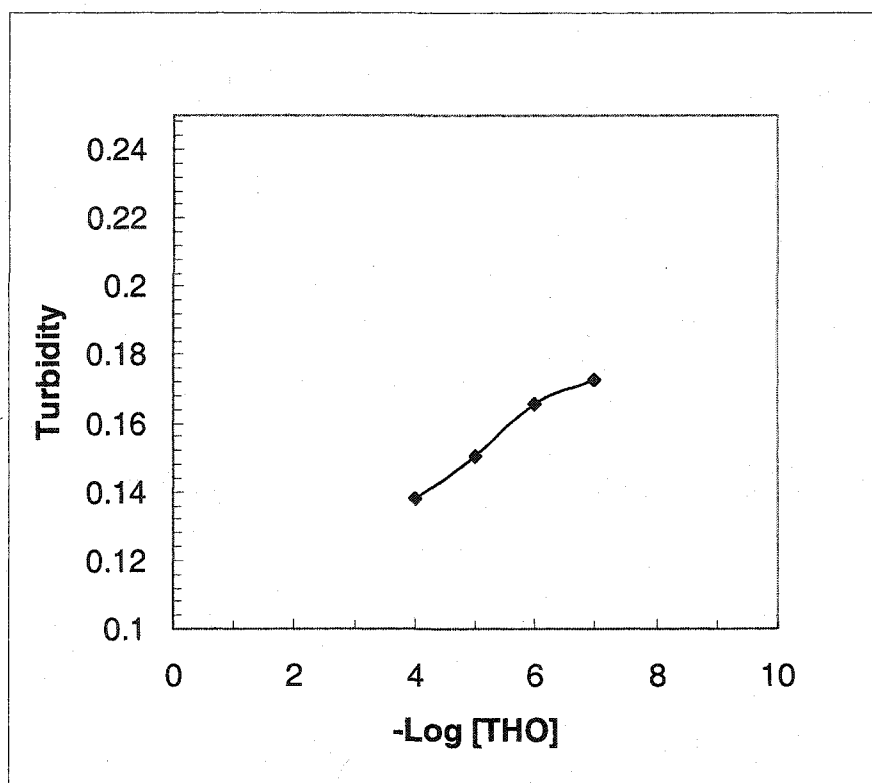


Figure 6-30. Turbidity vs. log THO concentration for a PVA membrane containing templated poly NNPA-MAA microspheres at 25°C. Turbidity was measured 10 minutes after changing the THO concentration.

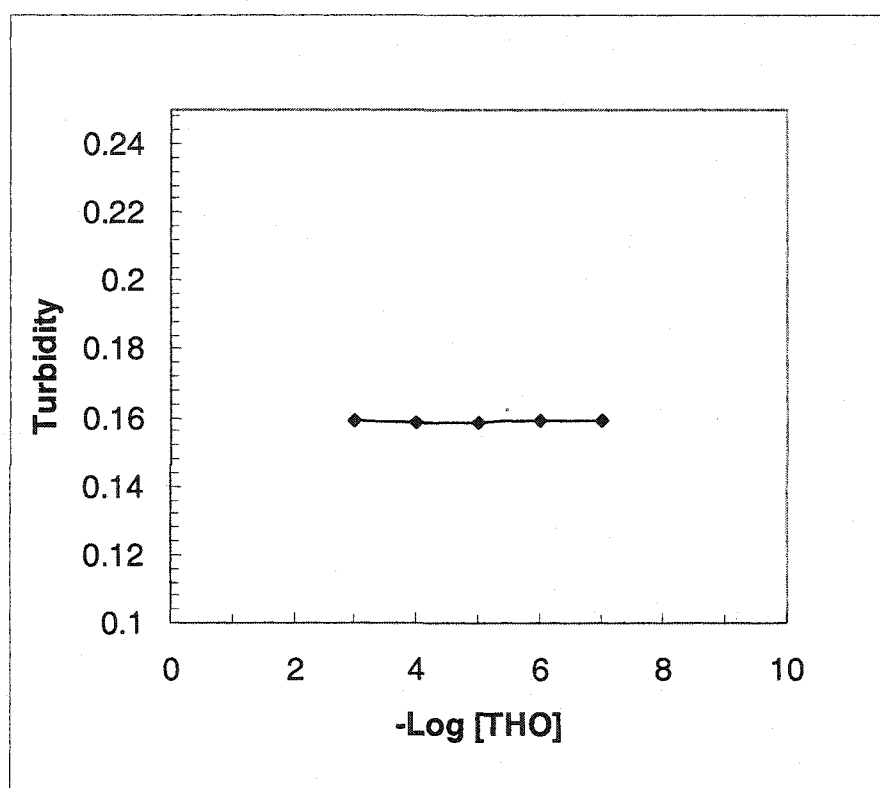


Figure 6-31. Turbidity vs. log THO concentration for PVA membrane containing untemplated poly NNPA-MAA microspheres at 25°C.

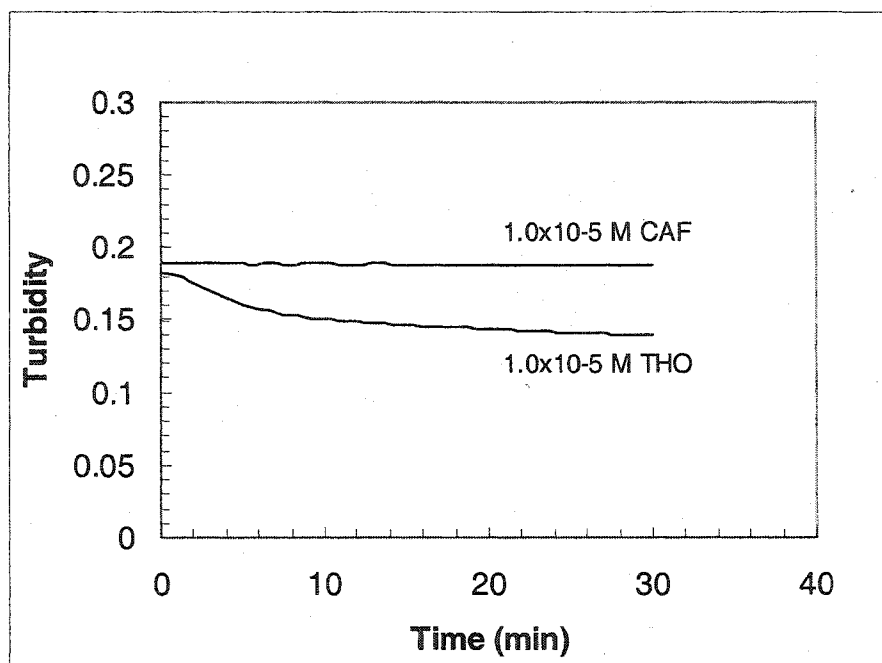


Figure 6-32. Response vs. time for templated poly NNPA-MAA polymers responding to theophylline and caffeine at 25°C.

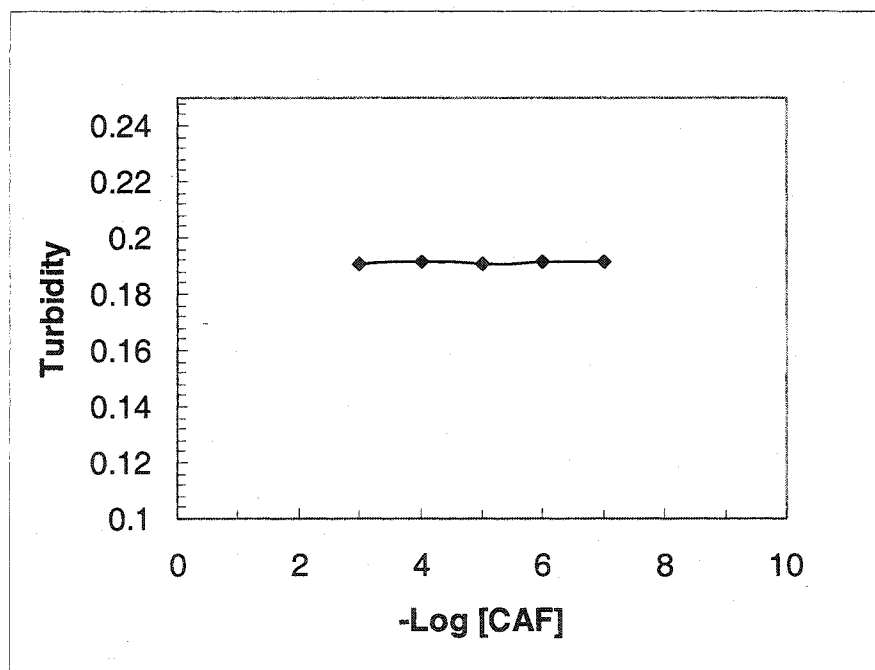


Figure 6-33. Turbidity vs. log caffeine concentration for a PVA membrane containing THO templated poly NNPA-MAA microspheres at 25°C

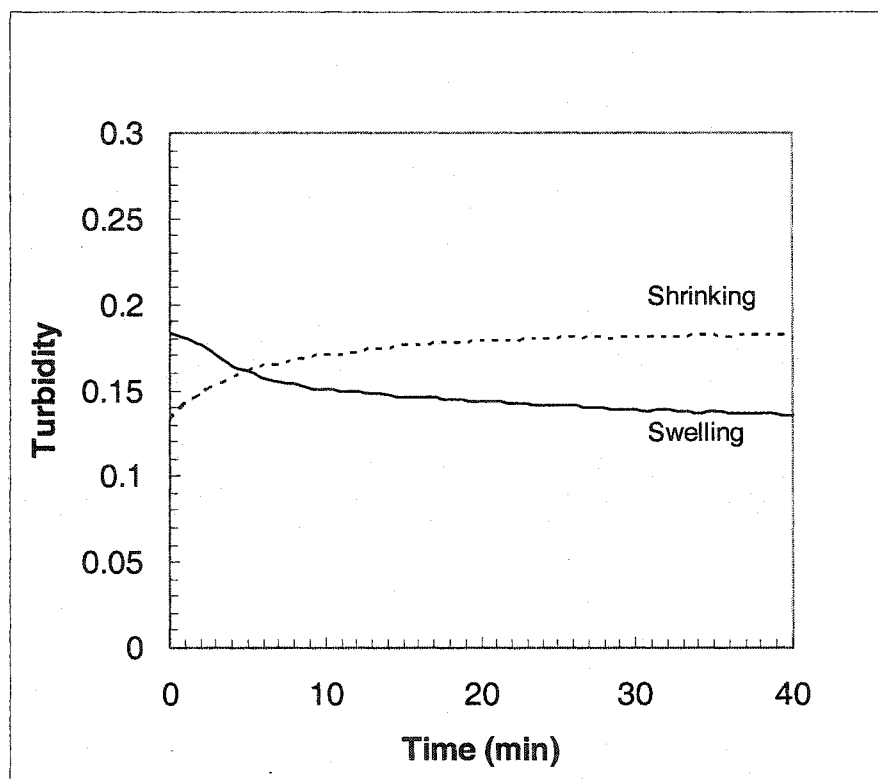


Figure 6-34. Turbidity vs. time for a membrane containing templated poly NNPA-MAA microspheres in 1.0×10^{-5} M THO solution and water at 25°C.

6.2.9.3 pH effect on THO templated poly NNPA-MAA microspheres

Figure 6-35 shows the pH effect on turbidity and phase transition of THO templated poly NNPA-MAA microspheres in PVA membrane. The result is similar to those we obtained before for poly NIPA-MAA and poly NIPA-NTBA-MAA polymers due to the deprotonation of methacrylic acid. At pH 7.0 and 8.0, the turbidity levels off with increasing temperature. Figure 6-36 and 6-37 show the turbidity of templated polymer as a function of temperature in 1.0×10^{-3} M THO/buffer solutions. At high temperature, the turbidity went up in pH 7.0 and 8.0 due to the presence of theophylline in buffers and there is also a response at biological temperature, which is the same behavior that we observed before. So, swellable imprinted poly NNPA-MAA microspheres can be used for biological sensing applications.

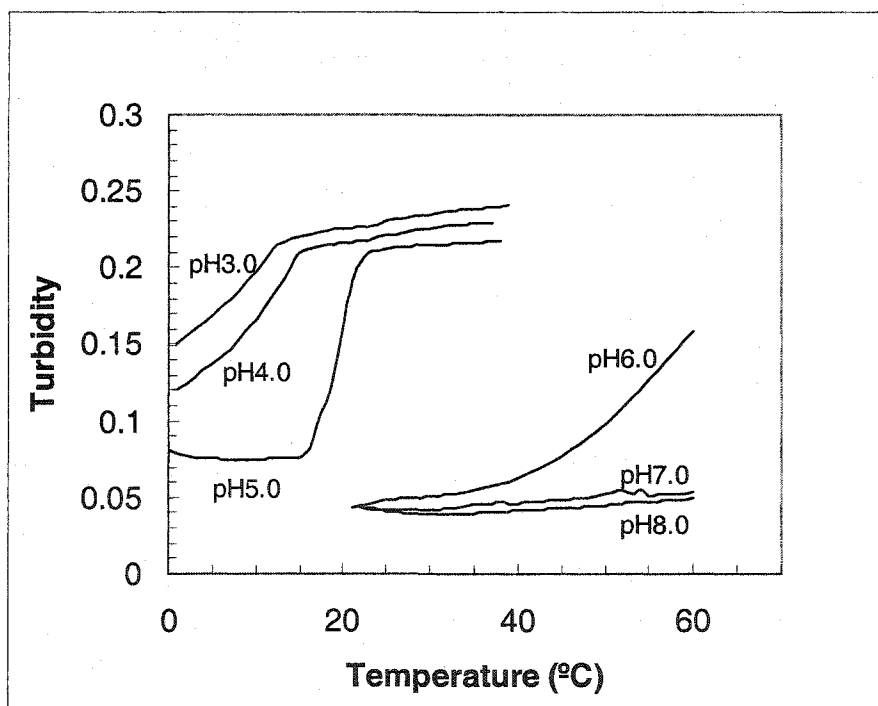


Figure 6-35. Turbidity of THO templated poly NNPA-MAA microspheres as function of temperature and pH. (Wavelength=500 nm, Heating rate=1°C/min.)

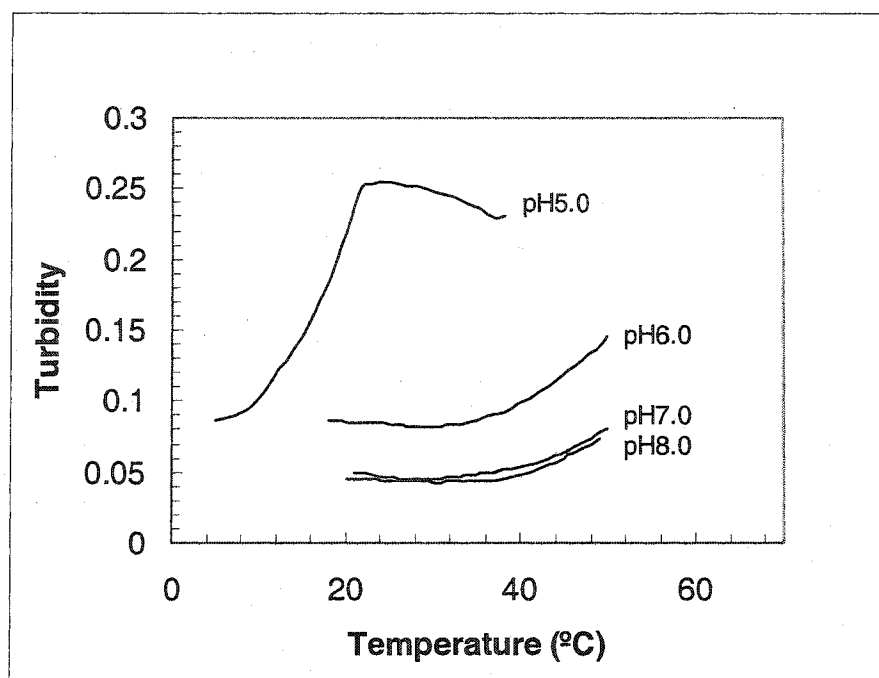


Figure 6-36. Turbidity of THO templated poly NNPA-MAA microspheres as a function of temperature and pH for 1×10^{-3} M THO solutions.

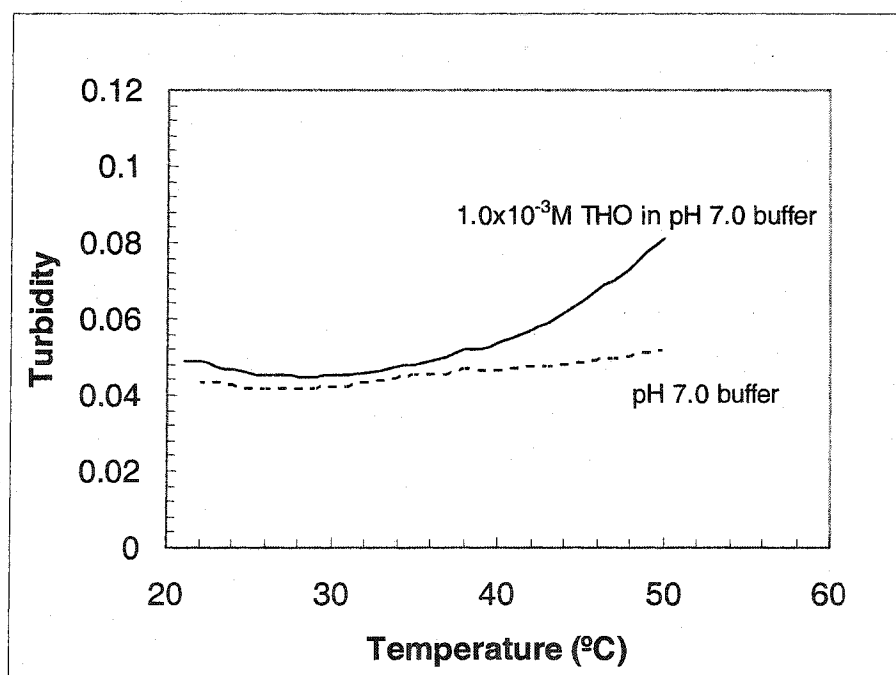


Figure 6-37. Turbidity of THO templated poly NNA-MAA microspheres as a function of temperature in 1.0×10^{-3} M THO buffer solution.

6.3 Conclusion

Swellable molecularly imprinted poly NIPA-MAA microspheres were prepared by dispersion polymerization in acetonitrile. 20% poly (acrylonitrile-co-styrene) was used as a stabilizer resulting in fairly uniform and spherical beads with diameter ca. 1.0 μm . There are a variety of factors that affect polymer properties. The most important factors affecting polymer swelling are the percentages of NIPA and crosslinker. Increased NIPA level and decreased crosslinker level led to larger swelling and shrinking. However, decreased NIPA (increased functional monomer, MAA) and increased crosslinker resulted in high selectivity. A high ratio of template to functional monomer led to more recognition sites in the polymer, but a large amount of template was shown to affect polymerization. The optimum formulation was 75% NIPA, 20%MAA, 5% crosslinker, and 2/1 of MAA to template.

PVA membranes containing templated poly NIPA-MAA microspheres were used to evaluate response and selectivity. They can be used for sensing theophylline in water (50°C) and biological medium (37°C) at concentrations as low as 1.0×10^{-8} M THO. There was no response to caffeine up to 1.0×10^{-3} M showing high selectivity.

In order to use our sensor at room temperature in water, the phase transition of poly NIPA-MAA was shifted to low temperature by replacing part of NIPA with NTBA or all of NIPA with NNPA. The optimum formulation for poly NIPA-NTBA-MAA microspheres was 60% NIPA, 15% NTBA, 20% MAA, 5%MBA, and 2/1 of MAA to THO. The phase transition was decreased to $\sim 12^\circ\text{C}$. The optimum formulation of poly NNPA-MAA is 75% NNPA, 20% MAA, 5% MBA, and 2/1 of MAA to THO. The transition of this polymer is $\sim 15^\circ\text{C}$. Both of these polymer microspheres were quite

uniform, spherical, and $\sim 1.0\ \mu\text{m}$ in diameter and successfully used at room temperature.

They were sensitive to theophylline concentration as low as $1.0 \times 10^{-7}\ \text{M}$ and did not respond to caffeine as high as $1.0 \times 10^{-3}\ \text{M}$.

CHAPTER 7

PRELIMINARY EVALUATION OF POLY NIPA MICROSPHERES FOR TEMPERATURE SENSING

7.1 Introduction

Due to their potential use in various applications, especially in the biomedical field, environment-sensitive polymers (hydrogels) have attracted increasing interest in the past decade [70]. One major reason is that these water-swollen polymers provide a biocompatible environment for biomolecules such as proteins and nucleic acid probes. These polymers can be conveniently classified by the type of stimuli including pH-sensitive, temperature-sensitive, electric signal-sensitive, light-sensitive, ionic strength-sensitive, and so on. Temperature-sensitive hydrogels are the most commonly studied class of environment-sensitive polymer systems. Among the many temperature-sensitive polymers, poly(N-isopropylacrylamide) (poly NIPA) is probably the most popular one and has been investigated extensively both fundamentally and for various applications. It possesses inverse solubility in water, which is a property contrary to the thermal behavior of most polymers in organic solvents. Its phase transition from a hydrophilic to a hydrophobic structure occurs abruptly (see Figure 6-16 on page 133) at the temperature known as the lower critical solution temperature (LCST).

Most polymers increase their water-solubility as the temperature increases. Polymers with a LCST, however, decrease their water-solubility as the temperature increases. They

shrink as the temperature increases above the LCST. This type of swelling behavior is known as inverse (or negative) temperature-dependence. These inverse temperature-dependent polymer chains have either moderately hydrophobic groups or a mixture of hydrophilic and hydrophobic segments. At lower temperatures, hydrogen bonding between hydrophilic segments and water molecules is the dominant interaction, leading to dissolution in water. As the temperature increases, however, hydrophobic interactions between hydrophobic segments become stronger, while hydrogen bonding becomes weaker. The net result is shrinking of the polymers due to hydrophobic interactions. Generally, as the polymer contains more hydrophobic constituent, the LCST becomes lower [70, 76]. So, the LCST can be changed by adjusting the ratio of hydrophilic and hydrophobic segments of the polymer [76] or by making copolymers of hydrophobic (e.g. NIPA) and hydrophilic (e.g. acrylic acid) monomers [Figure 5-5]. Copolymers of NIPA can also be made using other monomers, e.g. N-n-propylacrylate (NNPA), to alter the LCST (Figure 6-28).

A variety of work has been reported on the applications of poly NIPA hydrogels including separation and purification of proteins, drug delivery, control of enzyme activity, etc.[70] These applications were also found to be attractive with microgels and latices prepared by precipitation polymerization in water in the presence of crosslinker [70, 114]. Increasing temperature above the LCST, the particles exhibited thermosensitive properties reflected in a dramatic change in particle size, colloidal stability, etc.

This chapter investigates the possible use of crosslinked poly NIPA microspheres embedded in hydrogel membranes for temperature sensing. Poly NIPA microspheres

were prepared by dispersion polymerization in water in the presence of a crosslinker (MBA). The thermal behavior of resulting microspheres in buffer was studied. The ionic strength effect on turbidity of the membranes containing these microspheres was investigated. Finally, the temperature response and reversibility were investigated.

7.2 Synthesis of Poly NIPA Microspheres by Dispersion Polymerization

Based on the literature describing the preparation of poly(N-isopropylmethacrylamide)(poly NIPMA) latexes by precipitation polymerization with high crosslinker (12%) in water [114], thermosensitive crosslinked microspheres was prepared by dispersion polymerization of NIPA as a main monomer, MBA as a crosslinker, and potassium persulfate (KPS) as the initiator without any surfactant. Figure 7-1 shows the microscope picture and size distribution of the resulting microspheres. They are quite uniform (Std. Dev. = 0.05) with an average size of 0.99 μm . A relatively low level of crosslinking (2%) was used to ensure large swelling and shrinking. Surfactant-free microspheres were easily cleaned after polymerization.

Two hydrogels, PVA and polyurethane (PU), were used to prepare membranes containing these temperature-sensitive microspheres. It was observed that PVA is unsuitable for large swelling and shrinking due to its weak mechanical strength. It was very easily to be broken while PU has high strength so that it was used and investigated for temperature sensing. Figure 7-2 illustrates the turbidity spectra of PU membrane containing poly NIPA microspheres. Turbidity decreases rapidly from 350nm to 600nm due to the relatively small size of beads. 400 nm wavelength was selected ensuring high sensitivity.

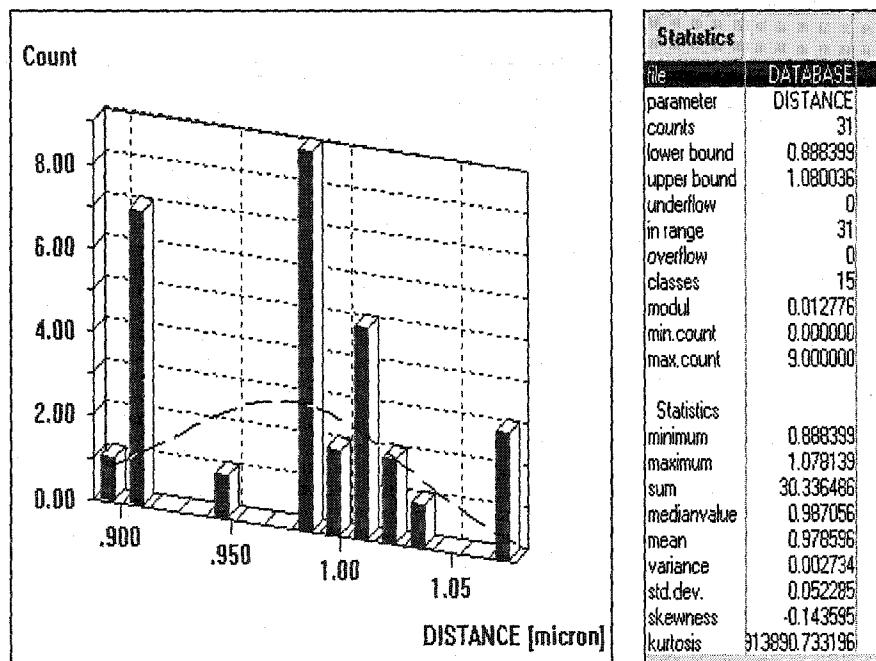
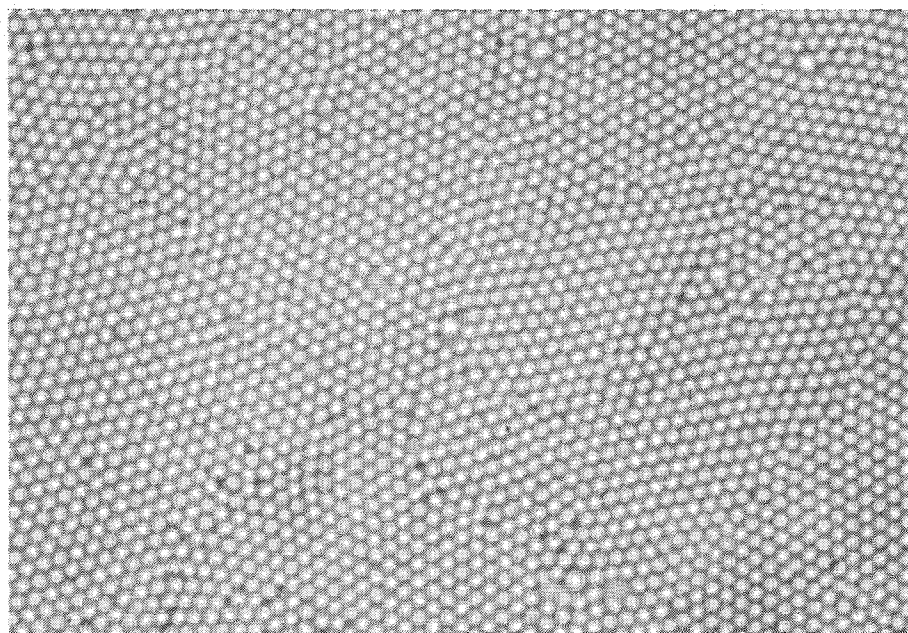


Figure 7-1. Micograph and size distribution of poly NIPA microspheres prepared by dispersion polymerization in aqueous medium.

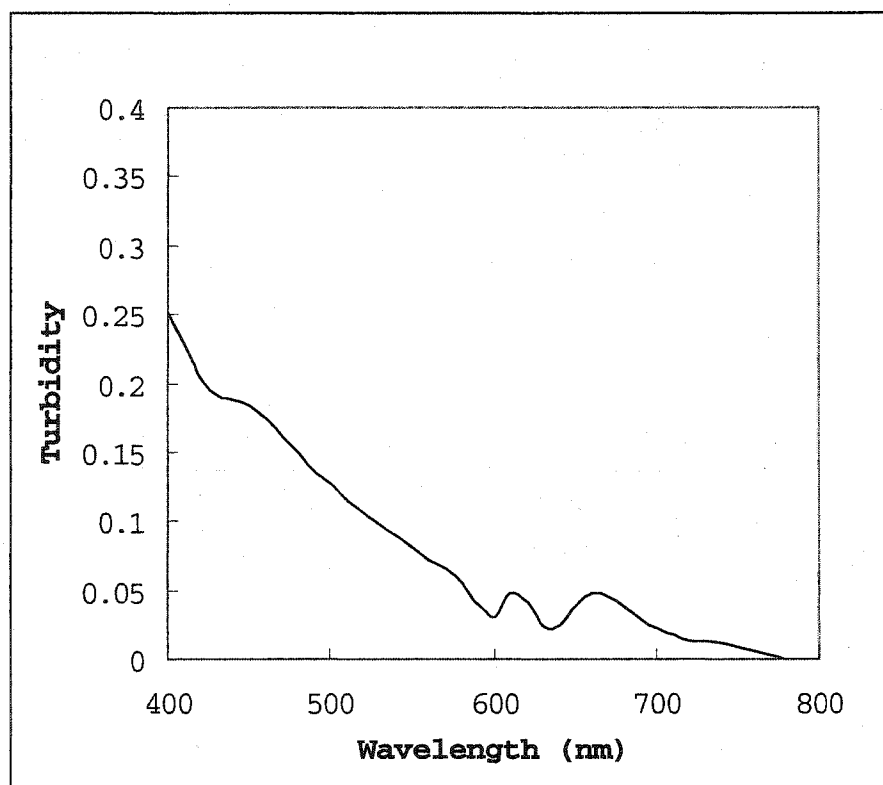


Figure 7-2. Turbidity spectra of poly NIPA-MBA microspheres embedded in polyurethane hydrogel.

7.3 pH Effect

Figure 7-3 shows the turbidity change of poly NIPA microspheres suspended in water and pH 7.0 as a function of temperature. The gradual change of turbidity was observed in buffer. The transition temperature in buffer shifts to low temperature. It is unexpected because there is no proton association/dissociation on poly NIPA backbone. One possible explanation is that NIPA or MBA is not pure and contains some basic components (e.g. amine). It is probably in the acid form in water and neutral form in pH 7.0.

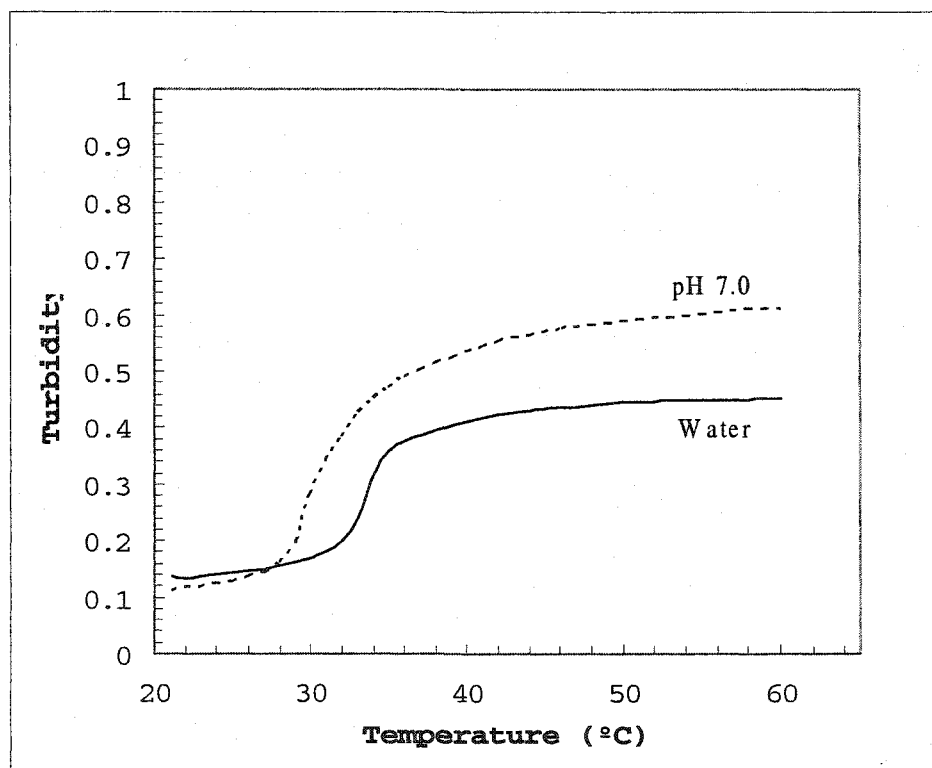


Figure 7-3. Turbidity of poly NIPA-MBA microspheres as a function of temperature in pH 7.0 and water.

7.4 Ionic Strength Effect

The effect of salt on thermo-sensitive behavior was also detected by turbidity change as a function of temperature (Figure 7-4). It shows a more gradual phase transition in 0.1 M NaCl than in water. A small shift of transition temperature was also observed. As stated in introduction of this chapter, the LCST was determined by the ratio of hydrophilic and hydrophobic segments in the polymer. As temperature above LCST, hydrophobic interaction is stronger than hydrogen bonding interaction so that polymer comes out from solution. In solution with high ionic strength, charged ions will affect or prevent hydrophobic interaction so that LCST will shift to high temperature.

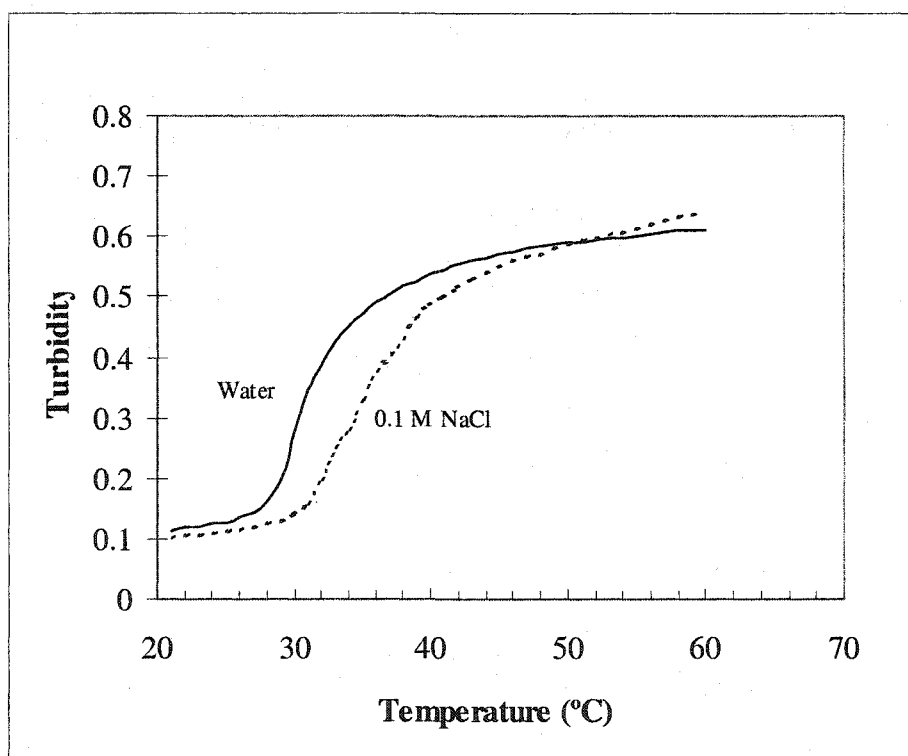


Figure 7-4. Turbidity of poly NIPA-MBA microspheres as a function of temperature in water and 0.1M NaCl.

7.5 Thermal Response

Figure 7-5 and 7-6 show the thermal response of PU membrane containing poly NIPA microspheres in water and pH 7.0 buffer, respectively. The phase transition is sharp in water, which can be used in some on-off switching sensor devices. The gradual phase transition in pH 7.0 buffer enables these membranes to be suitable for monitoring temperature changes in the range of 29~34°C in biological media. For other temperature ranges, a series of copolymer of NIPA and NTBA can be used due to their different transition temperatures.

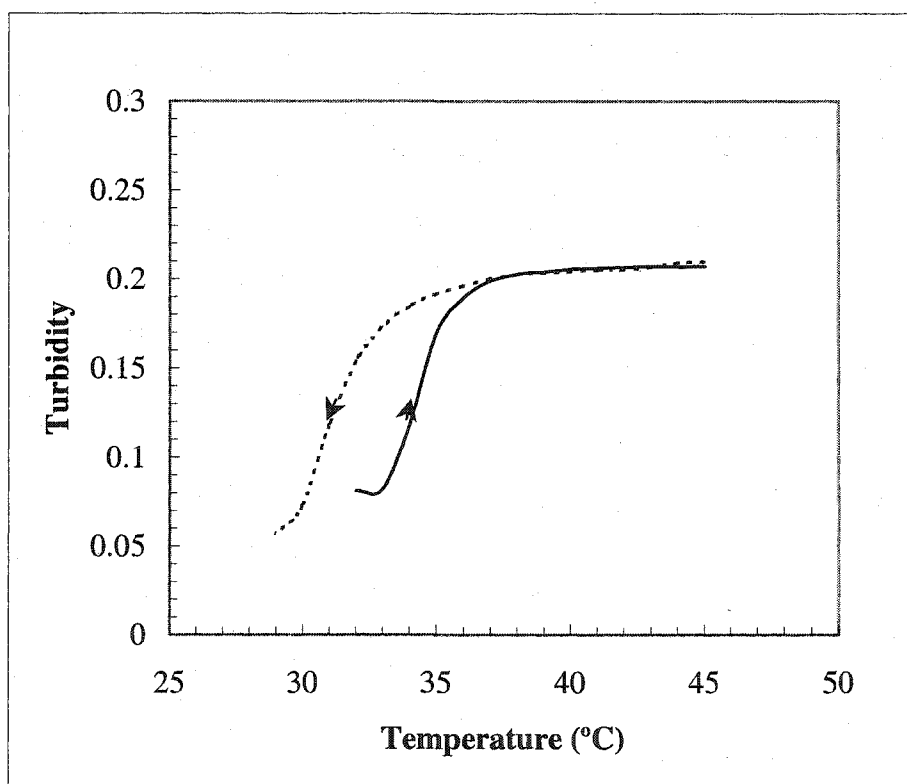


Figure 7-5. Turbidity of a polyurethane membrane containing poly NIPA-MBA microspheres as a function of temperature in water. (wavelength: 400nm, Heating rate: 1°C/min)

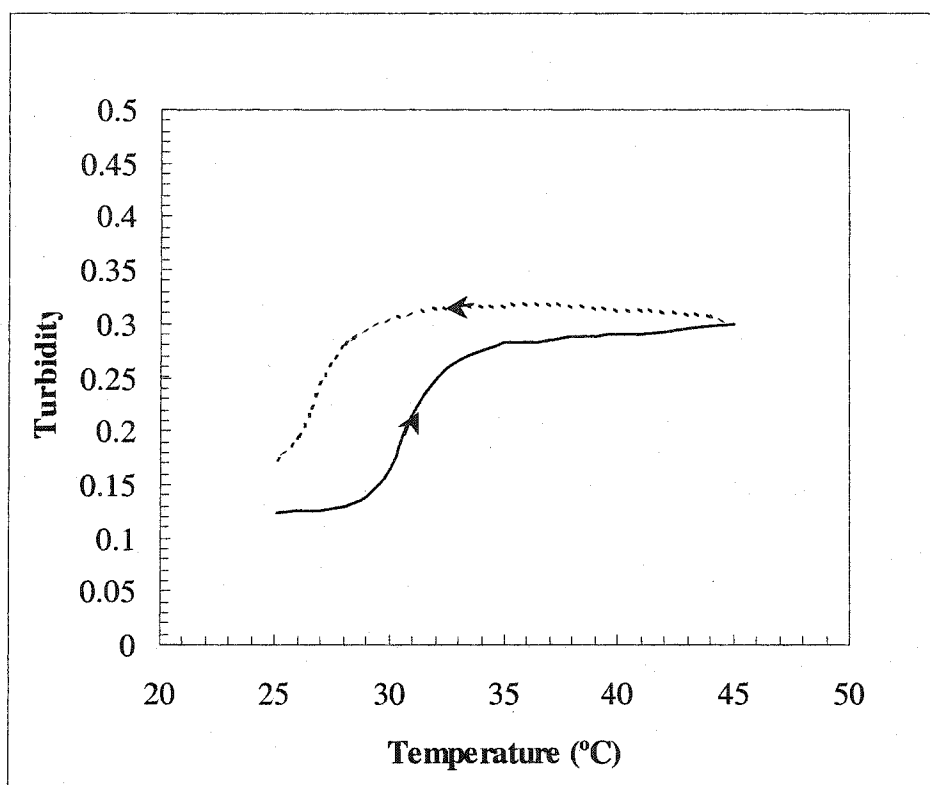


Figure 7-6. Turbidity of a polyurethane membrane containing poly NIPA-MBA microspheres as a function of temperature in pH 7.0. (wavelength: 400nm, Heating rate: 1°C/min)

7.6 Conclusion

MBA crosslinked poly NIPA microspheres were prepared by dispersion polymerization in water. The resulting microspheres are fairly uniform and spherical. The average size is around 1.0 μm which is good for our sensor system. The thermal behaviors of resulting microspheres in buffer, water, salt solution were studied. The phase transition shifts to lower temperature in buffer probably due to impurities in the NIPA monomer. The shift of phase transition temperature to higher values in salt solution is because ions decrease the hydrophobic interaction of polymer chains. The temperature response is quite sensitive and stable in buffer showing its potential application in biological media.

CHAPTER 8

CONCLUSIONS AND FUTURE WORK

8.1 Conclusions

A new method was developed for preparing swellable norephedrine templated poly NIPA-Acc particles by suspension polymerization in perfluorocarbon using ultrasonic emulsion technique. Sonication can keep emulsion droplets and particles in suspension so that they are not coagulated. The particles were crosslinked with an intermediate level of MBA (5%) in dioxane containing 20% PFPS as surfactant. The resulting particles were around 6 μm . The optical properties of HYPAN and PVA hydrogel membranes containing norephedrine templated poly NIPA-AAc particles were evaluated. The PVA membrane has higher turbidity contrast at the sensing temperature. The turbidity-temperature profile is affected by heating rate and pH. The buffer-polymer interaction is stronger than the norephedrine-polymer interaction resulting in a very small signal when it was used in buffer. However, the sensor response to norephedrine in water is dramatic showing high sensitivity (1.0×10^{-7} M) and selectivity for norephedrine. The response time is ~5 minutes.

Swellable theophylline templated poly NIPA-MMA microspheres were prepared by dispersion polymerization in acetonitrile. Poly styrene-co-acrylonitrile (20% w/w) was used as a stabilizer. The resulting microspheres were quite uniform, spherical, and ~1.0 μm in diameter. The main formulation variables were studied through a factorial

experiment. The percentages of NIPA and crosslinker are very important. The ratio of MAA to THO affects the formation of recognition sites. The optimum formulation is 75% NIPA, 20%MAA, 5% MBA, and 2/1 ratio of MAA to THO. PVA membranes containing THO templated poly NIPA-MAA microspheres were evaluated. It was successfully used for theophylline sensing in water (50°C) and biological medium (37°C) with a high sensitivity (1.0×10^{-8} M) and selectivity (no response to caffeine up to 1.0×10^{-3} M).

The phase transition of poly NIPA-MAA was shifted to low temperature by replacing part of NIPA with NTBA or all of NIPA with NNPA. The formulations of these THO templated polymers were optimized. The resulting microspheres were quite uniform, spherical, and $\sim 1.0 \mu\text{m}$ in diameter. The transition temperatures of poly NIPA-NTBA-MAA and poly NNPA-MAA are 12 and 15 °C, respectively. PVA membranes containing these microspheres were successfully used at room temperature. They were sensitive to theophylline as low as 1.0×10^{-7} M and did not respond to caffeine as high as 1.0×10^{-3} M.

Thermosensitive poly NIPA microspheres were prepared by dispersion polymerization in aqueous media. They were slightly crosslinked with MBA. Potassium persulfate was used as initiator. Polyurethane has a high mechanical strength and was used to prepare hydrogel membrane containing poly NIPA microspheres. pH and ionic effect on sensor response were investigated. Sensor was preliminarily evaluated in water and biological media. However, there are still some problems need to be solved, such as hysteresis, etc.

8.2 Future Work

The above results show that our swellable molecularly imprinted microspheres can be used to make sensor elements. They respond with the high sensitivity and selectivity required for many biological applications. High stability and reversibility were also found. Molecularly imprinted microspheres can be prepared using different functional monomers to sense different analytes.

However, when Acc or MAA was used as a functional monomer, pH will affect the mechanism of sensor response. There is a competition between polymer-buffer and polymer-template interaction. The deprotonation of carboxylic acid group increases polymer solubility in water and also interferes with the poly NIPA phase transition so that we have to adjust the phase transition by adding NTBA or NNPA. In order to avoid this pH effect, we can prepare molecularly imprinted polymers using other functional monomers that will not ionize at neutral pH. For example, vinylpyridine (VP) (Figure 2-7) is not protonated at neutral pH. Molecularly imprinted polymer with VP as the functional monomer should respond without interference in physiological media.

More biocompatible hydrogels with a higher mechanical strength can be tried to make the membrane containing our swellable molecularly imprinted microspheres. The fiber optic sensor can be developed with this membrane attached on the tip of fiber. The interaction of analyte and MIP microspheres causes microspheres to swell. The decrease in membrane turbidity will reflect less light back into the fiber. This fiber optic sensor could be used practically for biological measurements.

LIST OF REFERENCE

- (1) Murray, R. W.; Dessy, R. E.; Heineman, W. R.; Janata, J.; Seitz, W. R., Chemical Sensors and Microinstrumentation; American Chemical Society: Washington D.C, 1989.
- (2) Janata, J., Principles of Chemical Sensors; Plenum Press: New York, 1989.
- (3) Spichiger-Keller, U. E., Chemical Sensors and Biosensors for Medical and Biological Applications; Weinheim, Wiley-VCH, 1998.
- (4) Frant, M. S., *Analyst*, **1994**, *119*, 2293.
- (5) Janata, J., *Anal. Chem.*, **2001**, *73*, 150a.
- (6) Bormann, S., *Anal. Chem.*, **1981**, *53*, 1616A.
- (7) Arnold, M. A., *Anal. Chem.*, **1992**, *64*, A1015.
- (8) Lubbers, D. W., Optiz, N., *Sensors and Actuators*, **1983**, *4*, 641.
- (9) MacCraith, B. D., Principles of Chemical and Biological Sensors; Interscience Publisher: New York, 1998.
- (10) Wolfbeis, O. S., Fiber Optic Chemical Sensors and Biosensors; CRC Press: Boca Raton, FL, 1991.
- (11) Tan, W.; Shi, Z.Y.; Kopelman, R., *Anal. Chem.*, **1992**, *64*, 2985.
- (12) Seitz, W. R., *CRC Crit. Rev. Anal. Chem.*, **1988**, *19*, 135.
- (13) Janata, J.; Josowicz, M., *Anal. Chem.*, **1998**, *70*, 179R.
- (14) Bergman, I., *Nature*, **1968**, *218*, 396.
- (15) Freeman, T. M.; Seitz, W. R., *Anal. Chem.*, **1978**, *50*, 1242.
- (16) Peterson, J. I; Goldstein, S. R.; Fitzgerald, R. V.; Buckhold, D. K., *Anal. Chem.*, **1980**, *52*, 864.
- (17) Saari, L. A.; Seitz, W. R., *Anal. Chem.*, **1983**, *55*, 667.

- (18) Leiner, M. J. P., *Sensors and Actuators: B*, **1995**, 29, 169.
- (19) Ferguson, J. A.; Healey, B. G.; Bronk, K. S.; Barnard, S. M.; Walt, D. R., *Anal. Chim. Acta*, **1997**, 340, 123.
- (20) Brecht, A.; Gauglitz, G., *Sensors and Actuators, B*, **1997**, 38, 1.
- (21) Lieberman, R. A.; Wlodarczyk, M. T., *SPIE Proc.*, **1989**, 1172.
- (22) Lieberman, R. A.; Wlodarczyk, M. T., *SPIE Proc.*, **1993**, 2068.
- (23) Wolfbeis, O. S., *Anal. Chem.*, **2000**, 72, 81R.
- (24) Wolfbeis, O. S., *Anal. Chem.*, **2002**, 74, 2663.
- (25) Chudyk, W.; Kenny, J.; Jarvis, G.; Pohlig, K., *Anal. Chem.*, **1985**, 57, 1237.
- (26) Shahriari, M. R.; Ed., Grattan, K. T. V. and Meggitt, B. T., *Optical Fiber Sensor Technology*; Kluwer Academic Publisher: London, 1998.
- (27) MacCraith, B. D., *Sensors and Actuators: B*, **1993**, 11, 29.
- (28) Szunerits, S.; Walt, D. R., *ChemPhysChem*, **2003**, 4, 186.
- (29) Tanaka, T., *Phys. Rev. Lett.*, **1978**, 40, 820.
- (30) Seitz, W. R.; Rooney, M. T. V.; Miele, E. W.; Wang, H.; Kaval, N.; Zhang, L.; Doherty, S.; Milde, S.; Lenda, J., *Anal. Chim. Acta*, **1999**, 400, 55.
- (31) Qiu, Y.; Park, K., *Advanced Drug Delivery Reviews*, **2001**, 53, 321.
- (32) Sakai, Y.; Sadaoka, M.; Matsuguchi, M.; Sakai, H., *Sensors and Actuators: B*, **1995**, 24-25, 689.
- (33) Duebendorfer, J.; Kunz, R. E.; Jobst, J.; Moser, I.; Urban, G., *Sensors and Actuators: B*, **1998**, 50, 210.
- (34) Pan, S.; Conway, V.; Shakhsher, Z.; Emerson, S.; Bai, M.; Seitz, W.R.; Legg, K.D., *Anal. Chim. Acta*, **1993**, 279, 195.
- (35) Zhang, Z.; Shakhsher, Z.; Seitz, W. R., *Mikrochim. Acta*, **1995**, 121, 41.
- (36) Seitz, W. R., *Journal of Molecular Structure*, **1993**, 292, 105.
- (37) McCurley, M. F.; Seitz, W. R., *Anal. Chim. Acta*, **1991**, 249, 373.

- (38) Shkhsher, Z.; Seitz, W. R., *Anal. Chem.*, **1994**, 66, 1731.
- (39) Zhang, L.; Langmuir, M. E.; Bai, M.; Seitz, W. R., *Talanta*, **1997**, 44, 1691.
- (40) Wang, H., Nitrated poly(4-hydroxystyrene) microspheres for optical pH and potassium ion sensing based on turbidity changes accompanying polymer swelling, Dissertation, University of New Hampshire, Durham, 2000.
- (41) Kaval, N.; Seitz, W. R., *Proc. SPIE-Int. Soc. Opt. Eng.*, **1999**, 3860, 224.
- (42) Liu, H., Magnetoacoustic chemical sensors based on swellable polymer microspheres, Dissertation, University of New Hampshire, Durham, 2002.
- (43) Wulff, G., *Angew. Chem. Int. Ed. Engl.*, **1995**, 34, 1812.
- (44) Takeuchi, T.; Haginake, J., *J. Chromatogr. B*, **1999**, 728, 1.
- (45) Remcho, V. T.; Tan, Z. J., *Anal. Chem.*, **1999**, 248A.
- (46) Byrne, M.E.; Park, K.; Peppas, N.A., *Advanced Drug Delivery Reviews*, **2002**, 54, 149.
- (47) Suedee, R.; Srichana, T.; Rattananont, T., *Drug Delivery*, **2002**, 9, 19.
- (48) Kriz, D.; Ramstrom, O.; Mosbach, K., *Anal. Chem.*, **1997**, 69, 345A.
- (49) Dickert, F. L.; Hayden, O., *TrAC Trends in Anal. Chem.*, **1999**, 18, 192.
- (50) Al-Kindy, S.; Badia, R.; Suarez-Rodriguez, J. L; Diaz-Garcia, M. E., *Critical Reviews in Anal. Chem*, **2000**, 30, 291.
- (51) Piletsky, S.A.; Turner, A.P.F., *Electroanalysis*, **2002**, 14, 317.
- (52) Haupt, K.; Mosbach, K., *Chem. Rev.*, **2000**, 100, 2495.
- (53) Hedborg, E.; Winqvist, F.; Lundstroem, I.; Andersson, L. I.; Mosbach, K., *Sensors and Actuators: A*, **1993**, 37-38, 796.
- (54) Kriz, D.; Mosbach, K., *Anal. Chim. Acta*, **1995**, 300, 71.
- (55) Piletsky, S.A.; Parhometz, Y.P.; Lavryk, N.V.; Panasyuk, T.L.; El'skaya, A.V., *Sensors and Actuators: B*, **1994**, 19, 629.
- (56) Piletsky, S.A.; Piletskaya, E.V.; Elgersma, A.V.; Yano, K.; Karube, I.; Parhometz, Y.P.; El'skaya, A.V., *Biosensors & Bioelectron.*, **1995**, 10, 95.

- (57) Sergeyeva, T.A.; Piletsky S.A.; Brovko, A.A.; Slinchenko, E.A.;Sergeeva, L.M.; Panasyuk, T.L.; El'skaya, A.V., *Analyst*, **1999**, 124, 331.
- (58) Sergeyeva, T.A.; Piletsky S.A.; Brovko, A.A.; Slinchenko, E.A.;Sergeeva, L.M.; Panasyuk, T.L.; El'skaya, A.V., *Anal. Chim. Acta*, **1999**, 392, 105.
- (59) Ji, H.; McNiven, S.; Ikebukuro, K.; Harube, I., *Anal. Chim. Acta*, **1999**, 390, 93.
- (60) Chianella, I.; Piletsky, S.A.; Tothill, I.E.; Chen, B.; Turner, A.P.F., *Biosensors and Bioelectronics*, **2003**, 18, 119.
- (61) Kriz, D.; Ramstrom, O.; Svensson, A.; Mosbach, K., *Anal. Chem.*, **1995**, 67, 2142.
- (62) Matsui, J.; Tachibana, Y.; Takeuchi, T., *Anal. Commun.*, **1998**, 35, 225.
- (63) Turkewitsch, P.; Wandelt, B.; Darling, G.D.; Powell, W.S., *Anal. Chem.*, **1998**, 70, 2025.
- (64) Jenlkins, A.L.; Uy, O.M.; Murray, G.M., *Anal. Chem.*, **1999**, 71, 373.
- (65) Al-Kindy, S.; Badia, R.; Diaz-Garcia, M. E., *Anal. Lett.*, **2002**, 35, 1763.
- (66) Piletsky, S.A.; Piletskaya, E.V.; Yano, K.; Kunimiya, A.; Elgersma, A.V.; Levi, R.; Kahlow, U.; Takeuchi, T.; Karube, I., *Anal. Lett.*, **1996**, 29, 157.
- (67) Piletsky, S.A.; Piletskaya, E.V.; El'skaya, A.V., *Anal. Lett.*, **1997**, 30, 445.
- (68) Levi, R.; McNiven, S.; Piletsky, S.A.; Cheong, S.; Yano, K.; Karube, I., *Anal. Chem.*, **1997**, 69, 2017.
- (69) Watanabe, M.; Akahoshi, T.; Tabata, Y.; Nakayama, D., *J. Am. Chem. Soc.*, **1998**, 120, 5577.
- (70) Schild, H.G., *Prog. Polym. Sci.*, **1992**, 17, 163.
- (71) Stevens, M.P., *Polymer Chemistry: An Introduction*; Oxford University Press: New York, 1990.
- (72) Young, R. J., *Introduction to Polymers*; Chapman and Hall: New York, 1983.
- (73) Candau, F.; Ottewill, R. H., *Scientific Methods for the Study of Polymer Colloids and Their Applications*; Kluwer Academic Publisher: Boston, 1988.
- (74) Lovell, P.A; El-aasser, M.S., *Emulsion Polymerization and Emulsion Polymers*; John Wiley and Sons: New York, 1997.

- (75) Flory, P.J., *Principles of Polymer Chemistry*; Cornell University Press: New York, 1953.
- (76) Seker, F; Ellis, A. B., *J. Polym. Sci. Part A: Polym. Chem.*, **1998**, 36, 2095.
- (77) Pauling, L.J., *J. Am. Chem. Soc.*, **1940**, 62, 2643.
- (78) Sellergren, B., *TrAC Trends in Anal. Chem.*, **1999**, 18, 164.
- (79) Kempe, M.; Mosbach, K., *J. Chromatogr. A*, **1955**, 694, 3.
- (80) Ye, L.; Weiss, R.; Mosbach, K., *Macromolecules*, **2000**, 33, 8239.
- (81) Kempe, M., *Anal. Chem.*, **1996**, 68, 194.
- (82) Haginaka, J; Takehira, H; Hosoya, K; Tanaka, N., *J. Chromatogr. A*, **1999**, 849, 331.
- (83) Mayes, A.G.; Mosbach, K., *Anal. Chem.*, **1996**, 68, 3769.
- (84) Kaval, N., *Dissertation*, University of New Hampshire, Durham, 2002.
- (85) Omi, S.; Katami, K.; Yamamoto, A.; Iso, M., *J. Appl. Polym. Sci.*, **1994**, 51, 1.
- (86) Omi, S.; Katami, K.; Taguchi, T.; Kaneko, K.; Iso, M., *J. Appl. Polym. Sci.*, **1995**, 57, 1013.
- (87) Yuyama, H.; Watanabe, T.; Ma, G.; Nagai, M.; Omi, S., *Colloids and Surfaces A: Physicochemical and Engineering Aspects*, **2000**, 168, 159.
- (88) Betz, Joseph M.; Gay, Martha L.; Mossoba, Magdi M.; Adams, Sarah; Portz, Barbara S., *Journal of AOAC International*, **1997**, 80, 303.
- (89) Hanna, G. M., *Journal of AOAC International*, **1995**, 78, 946.
- (90) Chicharro, M.; Zapardiel, A.; Bermejo, E.; Perez, J. A.; Hernandez, L., *Anal. Chim. Acta*, **1999**, 379, 81.
- (91) Isono, H; Suzuki, T.; Nojiri, H., *J. Health Sci.*, **2000**, 46, 351.
- (92) Imaz, C.; Carreras, D.; Navajas, R.; Rodriguez, C.; Rodriguez, A. F.; Maynar, J.; Cortes, R., *J. Chromatogr.*, **1993**, 631, 201.
- (93) Lippstone, M. B.; Grath, E. K.; Sherma, J., *J. Planar Chromatogr.--Modern TLC*, 9, 456.

- (94) Sheu, S. J.; Huang, M. H., *Chromatographia*, **2001**, *54*, 117.
- (95) Okamura, N.; Miki, H.; Harada, T.; Yamashita, S.; Masaoka, Y.; Nakamoto, Y.; Tsuguma, M.; Yoshitomi, H.; Yagi, A., *J. Pharm. Biomed. Anal.*, **1999**, *20*, 363.
- (96) Kaddoumi, A.; Kubota, A. Nakashima, M. N.; Takahashi, M.; Nakashima, K., *Biomed. Chromatogr.*, **2001**, *15*, 379.
- (97) Chicharro, M.; Zapardiel, A.; Bermejo, E.; Perez, J. A.; Hernandez, L., *J. Chromatogr. Biomed. Appl.*, **1993**, 622, 103.
- (98) Hong, S.; Lee, C. S., *Electrophoresis*, **1995**, *16*, 2132.
- (99) Jourquin, G.; Kauffmann, J. M., *J. Pharm. Biomed. Anal.*, **1998**, *18*, 585.
- (100) Goicoechea, H.C.; Olivieri, A.C.; Munoz de la Pena, A., *Anal. Chim. Acta*, **1999**, *384*, 95.
- (101) Umemrui, T.; Inagaki, K., *Analyst*, **1998**, *123*, 1767.
- (102) Rasmussen, B.B.; Broesen, K., *J. Chromatogr., B: Biomed. Appl.*, **1996**, 676, 169.
- (103) Bispo, M.S.; Veloso, M.C.; Pinheiro, H.L.; Oliveira, R. F.; Reis, J.O.; Andrade, J.B., *J. Chromatogr. Sci.*, **2002**, *40*, 45.
- (104) Kanazawa, H.; Atsumi, R.; Matsushima, Y; Kizu, J., *J. Chromatogr., A*, **2000**, *870*, 87.
- (105) Mirfazaelian, A.; Goudarzi, M.; Tabatabaieifar, M.; Mahmoudian, M., *J. Pharm. Pharmaceut. Sci.*, **2002**, *5*, 131.
- (106) Devarajan, P.V.; Sule, P. N.; Parmar, D.V., *J. Chromatogr., B: Biomed. Sci. Appl.*, **1999**, 736, 289.
- (107) Lee, B. L.; Jacob, P.; Benowitz, N. L., *J. Chromatogr. A*, **1989**, 494, 109.
- (108) Desage, M.; Soubeyrand, J.; Soun, A.; Brazier, J. L.; Georges, Y., *J. Chromatogr. A*, **1984**, 336, 285.
- (109) Zhang, Z.; Fasco, M. J.; Kaminsky, L. S., *J. Chromatogr. B*, **1995**, 665, 201.
- (110) Johansson, I. M.; Gron-Rydberg, M. B.; Schmekel, B., *J. Chromatogr. A*, **1993**, 652, 487.

- (111) Malliaros, D.P.; Wong, S.S.; Wu, A. H.; Campbell, J.; Leonard, H.; Houser, S.; Berg, M.; Gornet, T.; Brown, C.; Feng, Y. J., *Therapeutic Drug Monitoring*, **1997**, *19*, 224.
- (112) Wciks, J. F. C.; Myring, A.; Wilson, J. F., *Ann. Clin. Biochem.*, **1994**, *31*, 291.
- (113) Mullett, W. M.; Lai, E. P. C., *Anal. Chem.*, **1998**, *70*, 3636.
- (114) Duracher, D.; Elaissari, A.; Pichot, C., *J. Polym. Sci. Part A: Polym. Chem.*, **1999**, *37*, 1823.